The role of the AcrB multidrug resistance efflux pump in the biology of *Salmonella enterica* serovar Typhimurium

by

Xuan Wang Kan

A thesis submitted to the University of Birmingham for the degree of

DOCTOR OF PHILOSOPHY

Antimicrobials Research Group
Institute of Microbiology and Infection
College of Medical and Dental Sciences
The University of Birmingham
September 2018

Abstract

Efflux pumps confer multidrug resistance to bacteria by exporting drugs and preventing them from reaching their target. The most abundant and best studied efflux pump in *Salmonella* Typhimurium is AcrB. The biological function of AcrB was unexplored. Therefore, the impact of loss of AcrB-mediated efflux was studied in *S.* Typhimurium, using an AcrB D408A mutant, which expressed an inactive form of AcrB.

Transcriptomic studies revealed significant differences between the AcrB D408A mutant and previously constructed Δ*acrB* and *acrB*::*aph* mutants, which did not express AcrB. The *acrB*::*aph* mutant differed in the motility phenotype from the other two mutants. However, all three mutants were multidrug hypersusceptible and were attenuated when compared against their parental wild-type strain. AcrB-mediated efflux also had a role in quorum sensing, persister formation and maintenance of the overall metabolic state of *Salmonella*. Analysis of the effluxome of AcrB in *S.* Typhimurium and *E. coli* revealed that fatty acids/alcohols are a common substrate of AcrB in both species and acylcarnitines were exclusive to *S.* Typhimurium.

This study presents a novel model to analyse the physiological role of RND efflux pumps and demonstrates that AcrB is more than just a mechanism of antibiotic resistance.

For my family, especially my grandparents

Acknowledgements

I would like to thank my supervisors, Professor Laura Piddock and Dr. Jessica Blair for giving me the opportunity to do a PhD with you and for your constant support and guidance throughout my PhD. Your scientific and moral support were invaluable to me. I would also like to thank all the past and present members of ARG, without your companionship my PhD would not have been as fun as it was.

Many thanks to Professor Sir Charles George and Arjang G. Zadeh for their philanthropic donations towards this work. This thesis would not be here without your financial support. I would also like to acknowledge CONACyT, my sponsors, for partially funding my PhD.

A big thanks to all of our collaborators, Dr. Barbara Chirullo for doing the mouse experiments, Dr. Helen Zgurskaya for providing the anti-AcrB antibodies, Professor Al Ivens for your bioinformatics expertise in analysing the raw RNA-seq data, Dr. Dan Dwyer and Sean Mack for the metabolic modelling and Dr. Warwick Dunn and Dr. Catherine Winder for your metabolomics expertise.

I would like to thank my friends and the UoB Pokémon GO community for giving me those few minutes a day to take a break and for sharing advice from your own PhD and life experiences.

And last but not least, I would like to thank my family for giving me the freedom to find my place in the world, my amazing husband for being here with me in the most difficult moments and my fantastic mother and father in-law, who have constantly looked after me for the past four years and fed me trifle and custard when I most needed it.

Table of contents

List of figures

List of tables

List of abbreviations

Abbreviation	Definition
μg	Micrograms
μL	Microliters
μM	Micromolar
3X	Three-times concentrated
ABC	ATP-binding cassette
ACR	Acriflavine
AI	Autoinducer
AI-2	Autoinducer-2
AMP	Ampicillin
AMP50	50μg/mL of ampicillin
aTET	Anhydrotetracycline
ATP	Adenosine triphosphate
bp	Base pair
BSAC	British Society for Antimicrobial Chemotherapy
CAR	Carbenicillin
CAR50	50μg/mL of carbenicillin
CAZ	Ceftazidime
CCCP	Carbonyl cyanide-m-chlorphenyl hydrazone
cDNA	Complementary deoxyribonucleic acid
CFU	Colony forming units
CHL	Chloramphenicol
CIP	Ciprofloxacin
COG	Clusters of Orthologous Groups
CTX	Ceftriaxone
DNA	Deoxyribonucleic acid
DPBS	Dulbecco's phosphate buffered saline
dsDNA	Double-stranded deoxyribonucleic acid
DTT	Dithiothreitol
E.	*Escherichia*
EBI	European Bioinformatics Institute
ENA	European Nucleotide Archive
ERY	Erythromycin
ETBR	Ethidium bromide
EUCAST	European Committee on Antimicrobial Susceptibility Testing
ExM	Exometabolome or conditioned medium
EZ	EZ Rich Defined Media
FMN	Flavin mononucleotide
FUS	Fusidic acid
g	Grams

G	Gravity
GEN	Gentamicin
H33342	Hoechst 33342
HAE	Hydrophilic and amphiphilic efflux
HME	Heavy metal efflux
HPLC-MS	High-resolution liquid chromatography mass spectrometry
HYG	Hygromycin B
HYG100	100μg/mL of hygromycin
ID	Identity
IM	Inoculation medium
iNTS	Invasive non-typhoidal *Salmonella*
IP	Intraperitoneal
KAN	Kanamycin
KAN50	50μg/mL of kanamycin
Kb	Kilobase pair
L	Litre
LAMP	Lysosomal associated membrane protein
LB	Lysogeny medium
LPS	Lipopolyssacharide
MATE	Multidrug And Toxin Extrusion
MC	Mutation cassette
MDR	Multidrug resistance
MFP	Membrane fusion protein
MFS	Major Facilitator Superfamily
mg	Miligrams
MIN	Minocycline
miRNA	Micro-RNA
mL	Millilitre
mRNA	Messenger ribonucleic acid
MS	Mass spectrometry
NAL	Nalidixic acid
nm	Nanometres
NOV	Novobiocin
NTS	Non-typhoidal *Salmonella*
OD	Optical density
OD_{540}	Optical density at 540nm
OD_{600}	Optical density at 600nm
OMF	Outer membrane factor family
OMPs	Outer membrane proteins
OXA	Oxacillin
PAβN	Phenylalanine-β-naphtylamide
PBS	Phosphate buffered saline

PCR	Polymerase Chain Reaction
PHE	Public Health England
PPAR-δ	Peroxisome proliferator-activated receptor δ
QS	Quorum sensing
RHO	Rhodamine 6G
RNA	Ribonucleic acid
RNA-seq	RNA-sequencing
RND	Resistance-Nodulation-Division
RNS	Reactive nitrogen species
ROS	Reactive oxygen species
rRNA	Ribosomal ribonucleic acid
S.	*Salmonella enterica* serovar
SCV	*Salmonella* containing vacuole
SDS	Sodium dodecyl sulphate
SIF	*Salmonella* induced filament
SIT	*Salmonella* induced tubule
SMR	Small Multidrug Resistance
SNP	Single nucleotide polymorphism
SPI	*Salmonella* Pathogenicity Island
T3SS	Type III secretion system
T3SS-1	*Salmonella* pathogenicity island 1 type III secretion system
T3SS-2	*Salmonella* pathogenicity island 2 type III secretion system
TA	Toxin-antitoxin module
TCSS	Two-component signalling system
TET	Tetracycline
Tn	Transposon
tRNA	Transfer ribonucleic acid
WHO	World Health Organisation
XLD	Xylose-lysine-deoxycholate

CHAPTER 1.

Introduction

1.1 Gram-positive and Gram-negative bacteria: Composition of the bacterial cell envelope

Bacteria are unicellular organisms capable of self-replicating. As with any other cell, they possess an envelope that surrounds their cytoplasm and genetic material. However, the composition of the bacterial cell envelope is more complex than that of mammalian cells (Silhavy *et al*., 2010).

The bacterial cell envelope is typically composed of a cytoplasmic membrane formed by a bilayer of phospholipids, followed by a layer of peptidoglycan. Peptidoglycan is a polymer formed of chains of N-acetyl glucosamine-β-1,4-N-acetyl muramic acid cross-linked by side chains of short peptides (de Pedro and Cava, 2015). It confers rigidity to the cell, determines the shape of bacteria and protects them against osmotic shock. It also determines the affinity of crystal violet-iodine for the cell envelope allowing bacteria to be classified into two groups: Gram-positive and Gram-negative. Gram-positive bacteria retain the dye complex due to their 30-100 nm thick peptidoglycan layer. Gram-negative bacteria, with 7-8 nm of peptidoglycan, do not retain the dye complex (Silhavy *et al*., 2010).

In Gram-positive bacteria, the peptidoglycan is the outermost layer of the cell envelope. In contrast, Gram-negative bacteria have an outer membrane surrounding their peptidoglycan (Figure 1.1). The outer membrane serves as a selective permeability barrier and protects Gram-negative bacteria against environmental stresses. Unlike the cytoplasmic membrane (also referred to as inner membrane in Gram-negative bacteria), the outer membrane is formed of a bilayer of glycolipids and phospholipids, with glycolipids on the outer leaflet of the bilayer, interacting with the

Figure 1.1 Cell envelope of Gram-negative bacteria.

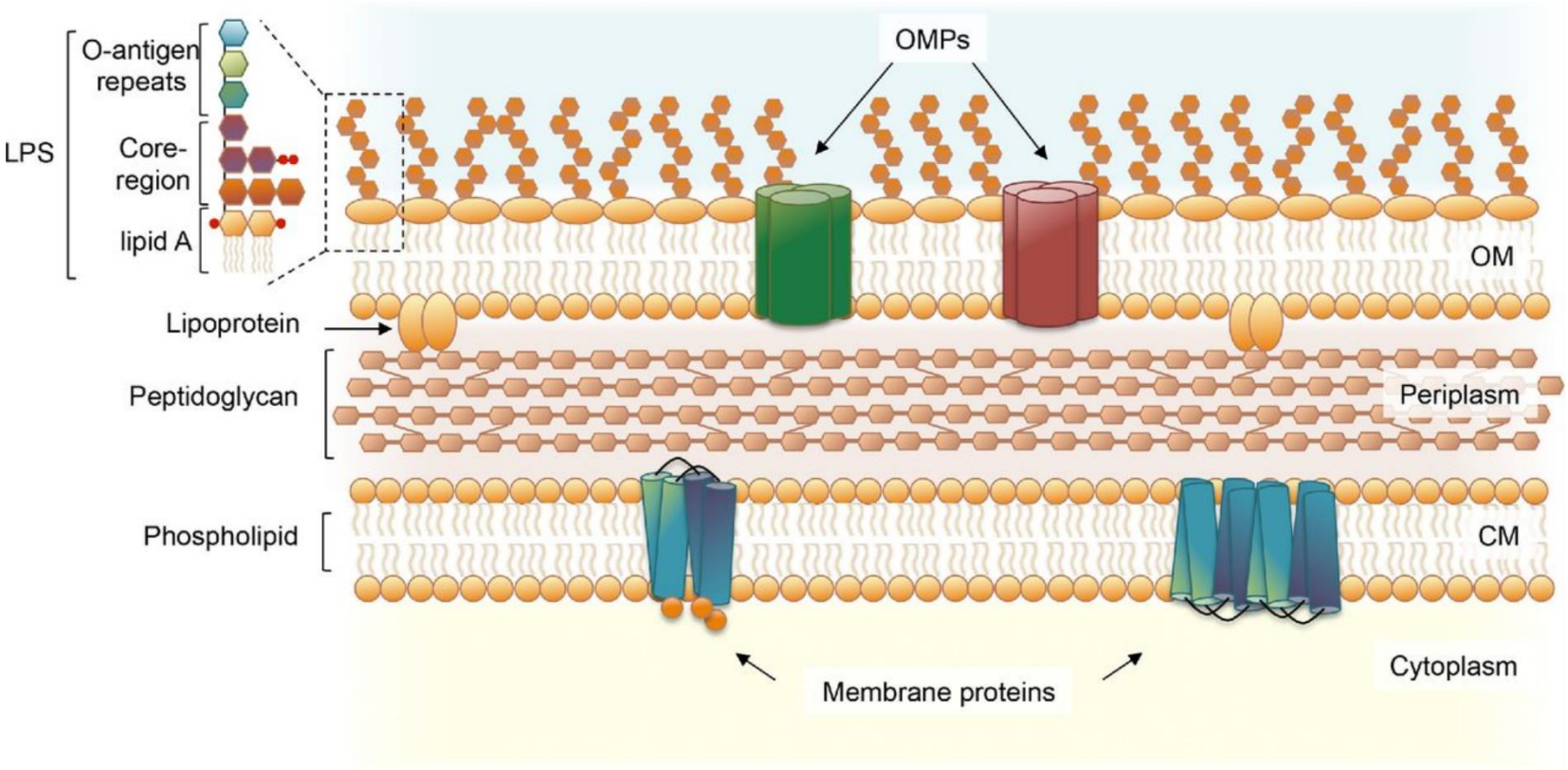

LPS, lipopolyssacharide; OMPs, outer membrane proteins; OM, outer membrane; CM, cytoplasmic or inner membrane. From Maldonado *et al*. (2016).

external environment, and phospholipids on the inner leaflet, facing the periplasmic space or periplasm (May and Silhavy, 2017). The periplasm is an aqueous compartment in between the inner membrane and outer membrane, where the peptidoglycan is found. The OM is anchored to the peptidoglycan via the Lpp lipoprotein, also called Braun's lipoprotein (Silhavy *et al*., 2010).

The most abundant glycolipid in the outer membrane is lipopolysaccharide (LPS), also known as endotoxin due to its association with toxic shock in patients with septicaemia caused by Gram-negative bacteria (Raetz and Whitfield, 2002). LPS is formed of three moieties: lipid A, core oligosaccharide and O-antigen. Lipid A is formed of a glucosamine dimer backbone, with acyl chains attached to it. This moiety anchors LPS to the outer membrane and is responsible for the reduced permeability of the outer membrane when compared to the cytoplasmic membrane. The degree of acylation of lipid A determines the degree of permeability of the outer membrane (Nikaido, 2003, Maldonado *et al*., 2016). The core of the LPS molecule is made of oligosaccharides that form a linear structure. Similar to lipid A, phosphorylation of core oligosaccharides has been shown to decrease the permeability of the outer membrane (Walsh *et al*., 2000, Nikaido, 2003). The O-antigen is an oligosaccharide formed of repeating sugar residues but, unlike the core, the O-antigen can be linear or branched. This moiety of the LPS does not contribute significantly to the outer membrane permeability (Nikaido, 2003). However, it is highly immunogenic and has a role in virulence of multiple species of Gram-negative bacteria (Maldonado *et al*., 2016). For example, *Salmonella enterica* alters its LPS to avoid or delay detection by the host's immune system, thus facilitating the infection process (Slauch *et al*., 1996, Duerr *et al*., 2009).

As the outer membrane is almost impermeable, it requires proteins to facilitate the diffusion of small molecules into the periplasm. Outer membrane proteins (OMPs) are

typically lipoproteins anchored to the lipid bilayer, formed of transmembrane β-barrels (Figure 1.1). Some of the best characterised OMPs are pore-forming proteins called porins, such as OmpC and OmpF. These form channels across the outer membrane to facilitate diffusion of small molecules into the cell (May and Silhavy, 2017).

1.2 Classification and nomenclature of *Salmonella* spp.

Salmonella spp. are Gram-negative, facultative intracellular bacilli that belong to the Enterobacteriaceae family. *Salmonella* was first isolated from pigs in 1885 by Theobald Smith and initially referred to as the 'hog cholera bacillus'. Later, it was renamed *Salmonella* after Dr. Daniel E. Salmon, an American veterinarian and colleague of Smith (Agbaje *et al*., 2011).

Bacteria from the genus *Salmonella* are easily identifiable due to their common biochemical profiles and genetic similarities, but identification at species level is more difficult. In 1966, *Salmonella* species were first assigned by Kauffmann according to their surface antigenic patterns. Genetic analyses in the 1970s reclassified all known salmonellae into two species: *S. enterica* or *S. bongori*, and the previously considered species were assigned as serovars (Agbaje *et al*., 2011). Since then, nearly 2600 serovars have been described. The correct way to refer to *Salmonella* spp. serovars is by writing the genus, followed by the species, subspecies and serovar; for example, *Salmonella enterica* subsp. e*nterica* ser. Typhimurium. For the purpose of this thesis, all *Salmonella* serovars will be abbreviated as genus followed by serovar name; for example, *Salmonella* Typhimurium or *S.* Typhimurium.

S. enterica is subdivided into six subspecies with most mammalian disease causing *Salmonella* found within *S. enterica* subsp. *enterica* (Lamas *et al*., 2018). *S. bongori* is commonly associated with infections in reptiles. However, there have been rare cases of *S. bongori* infecting humans (Andino and Hanning, 2015, Gal-Mor *et al*., 2014).

S. enterica gained importance as a human pathogen during World War II, when the Medical Research Council of Great Britain showed that an increase in cases of food poisoning was associated with the consumption of egg-derived products contaminated with *Salmonella* spp. (Steele, 1963). Further studies identified *Salmonella* as a cause of zoonotic infections, where bacteria are transmitted from animals to humans and *vice versa*. Most *S. enterica* serovars can infect a wide range of hosts; however, some serovars are restricted to a single host. For example, *S.* Typhi is a strict human pathogen with no other known reservoirs, while *S.* Typhimurium infects a wide range of animals including poultry, mice, cattle and humans.

1.3 Clinical manifestations of *Salmonella enterica* infections in humans

The typical description of an infection caused by *Salmonella* sp. is salmonellosis. Clinical manifestations of salmonellosis in humans vary depending on the serovar causing the infection as well as the patient's age and any other diseases they might have. Generally, *S.* Typhi and *S.* Paratyphi (typhoidal *Salmonella*) cause typhoid fever or enteric fever, while non-typhoidal *Salmonella* (NTS) cause acute gastroenteritis. The representative serovars of NTS are *S.* Typhimurium and *S.* Enteriditis. Patients infected with NTS develop diarrhoea, vomiting, nausea and abdominal pain after an incubation period of 6 to 72 hours (World Health Organization, 2017c); these

symptoms last up to 7 days in immunocompetent patients (Andino and Hanning, 2015). However, NTS gastroenteritis can develop into a systemic infection, characterised by bacteraemia, fever and chills among other symptoms. This form of NTS is refered to as iNTS (invasive non-typhoidal *Salmonella*) and is commonly associated to high risk populations such as infants, immunocompromised and elder patients. Complicated iNTS infections can develop into focal extraintestinal infections, where the systemic spread of the pathogen can cause further localised infections in specific organs. Examples of extraintestinal infections are meningitis, osteomyelitis, pneumonia, endovascular infections, myositis and infection of other soft tissues (Wen *et al*., 2017). Rare cases of septic arthritis caused by contaminated prosthetic joints have also been reported (Gupta *et al*., 2014).

Enteric fever is a form of invasive disease exclusive of typhoidal serovars. It is characterised by the presence of fever; other symptoms may include headache, rash and abdominal pain. Some patients have diarrhoea but this symptom is rare in typhoidal fever (Waddington *et al*., 2014). Untreated patients infected with typhoidal *Salmonella* can enter an asymptomatic chronic carrier state. This happens in 1 to 4% of patients and contributes to the epidemiology of the disease, since chronic carriers of typhoidal salmonellae shed from 10^6 to 10^{10} pathogens per gram of faecal matter for 12 months or longer (Gal-Mor *et al*., 2014, Waddington *et al*., 2014).

A chronic carrier state in NTS has not been as thoroughly studied as in typhoidal salmonellae. Studies dating back to 1987 indicate that only 0.15% of healthy adults and 3.9% of children become chronic carriers (Gunn *et al*., 2014). A study from Thailand showed that 98.8% of patients continue shedding NTS 12 days after clearance of the gastrointestinal symptoms. The same study stated that the duration of NTS excretion was around five weeks (Sirinavin *et al*., 2004). However, a recent

study from Israel showed that approximately 2.2% of all NTS gastroenteritis cases developed into a chronic carrier state where shedding of *Salmonella* continued from 30 days to 8.3 years post-infection (Marzel *et al*., 2016).

1.4 Pathogenesis and virulence factors of *Salmonella*

A typical *Salmonella* infection starts when contaminated food is ingested. The infective dose varies between 100 to 10^9 CFU depending on the serovar of NTS, the gastric acidity of the patient and the type of food consumed (Kothary and Babu, 2001, Hara-Kudo and Takatori, 2011). It is thought that foods with high protein and/or fat content such as ice cream and cheese will protect *Salmonella* from the acidic pH of the stomach favouring the infection (Kothary and Babu, 2001).

The infection can be separated into multiple stages: 1) colonisation of intestinal epithelial cells and M cells, 2) internalisation or invasion, 3) multiplication and, 4) in infections caused by iNTS and typhoidal serovars, systemic dissemination through macrophages (Wiedemann *et al*., 2014). An overview of the pathogenesis of *S. enterica*, as observed in murine infection models, is shown in Figure 1.2.

1.4.1 Colonisation of the gastrointestinal tract by *Salmonella*

The first challenge *Salmonella* spp. encounters after being ingested is the acidic pH of the stomach followed by the gut microbiome during colonisation. The microbiome of a healthy individual will provide physical resistance against colonisation. To outcompete the microbiome, *Salmonella* induces an inflammatory response, which

Figure 1.2 Pathogenesis of *Salmonella enterica* infections.

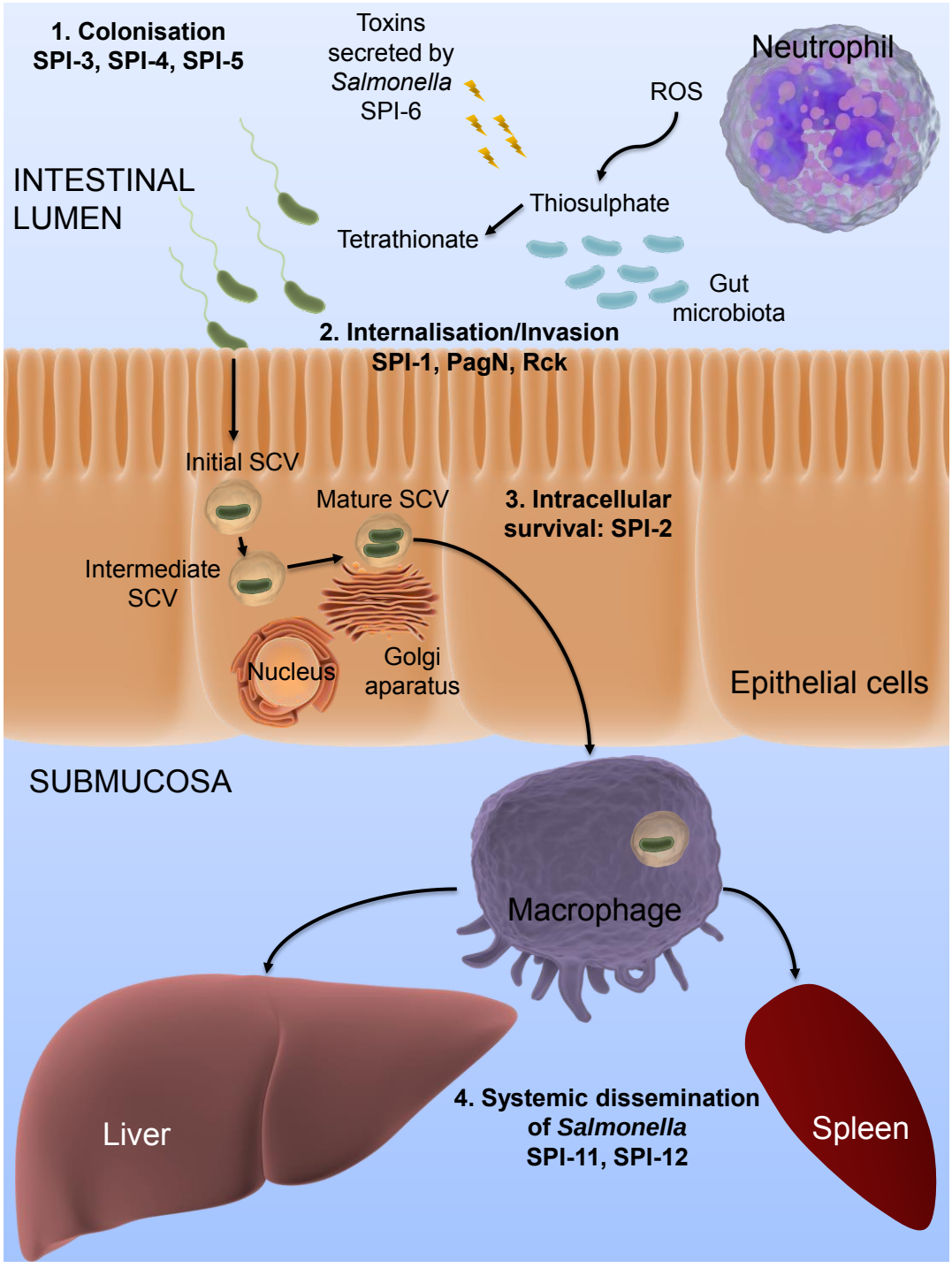

A *S. enterica* infection can be divided into four stages, these are indicated in the figure alongside the main virulence factors involved in each stage. Figure was constructed with elements from the Library of Science and Medical Illustrations.

generates reactive oxygen and nitrogen species (ROS and RNS, respectively). Most enterobacteria are unable to survive these reactive species. However, *Salmonella* can metabolise these chemical species into tetrathionate and nitrates, respectively, and use them as respiration acceptors (Ilyas *et al*., 2017).

The inflammatory response starts when *Salmonella* outer membrane components such as LPS and flagellins are recognised by the innate immune system. This causes rapid infiltration of neutrophils which are responsible for the production of the ROS and RNS (Figure 1.2). The interaction of *Salmonella* Pathogenicity Island (SPI) 1 effectors with intestinal epithelial cells favours the inflammatory response through activation of NF-κB and the release of IL-1β and IL-23 pro-inflammatory cytokines (Santos *et al*., 2009). SPI-1 effectors also favour the production of RNS by macrophages, which provides an advantage to *Salmonella* during colonisation (Cherayil *et al*., 2000). The induction of inflammation in the gut is responsible for the typical diarrhoea observed in NTS infections.

SPIs are horizontally-acquired genetic elements that encode virulence factors and are involved in multiple stages of the infection. They are highly conserved within *Salmonella* species and serovars. *S.* Typhimurium, for example, carries 17 of the 21 SPIs identified in the genus *Salmonella* (Ilyas *et al*., 2017). Among the virulence factors encoded in SPIs, the secretion systems and their effector proteins are the best studied. Secretion systems are needle-like complexes that *Salmonella* uses to inject effector proteins into eukaryotic and prokaryotic cells. SPI-1 encodes a type III secretion system (T3SS) which interacts with eukaryotic cells (see section 1.4.2). An example of SPI that targets prokaryotic cells is SPI-6, which encodes a type VI secretion system (T6SS) that secretes the Tae4 antibacterial amidase. It has been

proposed that Tae4 is used by *Salmonella* to kill commensal bacteria and subvert the gut microbiome (Sana *et al*., 2016). (Figure 1.2)

Once the microbiome has been breached, *Salmonella* colonises the mammalian gut via interaction with antigen-sampling M cells (Peyer's patch) and intestinal epithelial cells. *Salmonella* migrates to these cells through chemotaxis and flagella-dependent motility. Flagella-dependent motility can be classified in to swimming and swarming. Swimming consists of the movement of single bacterium through a liquid or semisolid environment. Swarming is characterised by groups of bacteria that intertwine their flagella to form a raft-like structure, which then moves across a solid or semisolid surface. Both types of motility are required to establish an infection, particularly during the colonisation stage. Swimming is mainly used to find an adequate niche for bacteria to infect and multiply (Friedlander *et al*., 2013), while swarming facilitates adhesion and biofilm formation, leading to persistent infections (Kearns, 2010).

Colonisation of intestinal epithelial cells occurs through two stages: an initial reversible attachment followed by a strong irreversible adhesion mediated by bacterial factors (Wiedemann *et al*., 2014). Attachment and adhesion are mediated by flagella, LPS, fimbriae and non-fimbrial adhesins such SiiE and BapA. It has been proposed that MisL, a SPI-3 encoded protein, play a role in colonisation as it binds to fibronectin, abundant on epithelial cells when the inflammatory response is activated (Ilyas *et al*., 2017). The combination of adhesins of each serovar dictates their host specificity (Wiedemann *et al*., 2014).

1.4.2 Internalisation of or invasion by *Salmonella*

Following adhesion to the host cell, internalisation of bacteria occurs. In M cells, *Salmonella* is internalised by endocytosis. However, in non-phagocytic epithelial cells, two mechanisms of invasion have been described: trigger and zipper. Both involve rearrangement of the eukaryotic host cell's cytoskeleton. The trigger mechanism is associated with the formation of 'membrane ruffles', allowing bacteria to be internalised in vacuoles. This mechanism is dependent on the expression of the SPI-1 type III secretion system (T3SS-1) (Boumart *et al*., 2014, Wiedemann *et al*., 2014) . The effectors secreted by T3SS-1 include SopB, encoded in SPI-5, which facilitates the formation of membrane ruffles. SPI-4 also favours internalisation of *Salmonella* into epithelial cells via the SiiE adhesin, which allow bacteria in close proximity to the invasion site to be engulfed by the membrane ruffle (Lorkowski *et al*., 2014).

SPI-1 expression is regulated by HilA, this protein is induced by the mild alkaline pH of the intestinal lumen as well as low oxygen content and high osmolarity (López *et al*., 2012). Interestingly, the LoiA protein encoded in SPI-14 regulates the expression of SPI-1 in response to low oxygen content. This then modulates the trigger invasion mechanism (Jiang *et al*., 2017).

The expression of SPI-1 and 2 is bistable. Bistability refers to the presence of two phenotypes in a genetically identical population. Bistability in the expression of SPIs results in a fully virulent subpopulation and a non-infective one (Stewart and Cookson, 2012). The latter is suggested to be a reservoir of live bacteria and may be a way in which *Salmonella* transmission is ensured if the infection fails (Arnoldini *et al*., 2014, Koirala *et al*., 2014).

The zipper mechanism has only been described in three NTS serovars: Typhimurium, Enteriditis and Dublin. It comprises the recognition of a specific bacterial ligand by a receptor on the host cell that leads to local accumulation of actin, observed as 'tight membrane extensions'; this last mechanism is likely to be mediated by the Rck or PagN invasins, but further studies are required (Boumart *et al*., 2014).

1.4.3 Intracellular survival and multiplication

After invasion of epithelial cells or uptake by phagocytic cells, *Salmonella* remains in vacuoles named *Salmonella* containing vacuoles (SCV). The SCV is characterised by a variety of host membrane markers. These markers are also indicators of the state of maturation of the SCV. For example, an early SCV is characterised by high levels of phosphatidyl-3-phosphate, whereas the appearance of lysosome-associated membrane proteins (LAMPs) mark the formation of a mature SCV (Knuff and Finlay, 2017).

Inside the cells, lysosomes bind to vacuoles to degrade the contents of the latter. However, *S.* Typhimurium avoids the union of the SCV to lysosomes by injecting SPI-2 effectors into the cytoplasm of the host cell via T3SS-2. SPI-2 expression is triggered by the low pH and the low magnesium ion content inside the SCV. Simultaneously, these conditions repress the expression of *hilA*, downregulating SPI-1 (Ilyas *et al*., 2017). The switch between expression of SPI-1 and SPI-2 is also mediated by a small RNA (sRNA), PinT (Westermann *et al*., 2016).

Subsequently, SPI-2 effectors are used to transport the SCV to the perinuclear region near the Golgi apparatus; this location allows *Salmonella* to capture nutrients from

transport vesicles, facilitating the maturation of the SCV (López *et al*., 2012, Wiedemann *et al*., 2014). (Figure 1.2)

Salmonella can only replicate inside a mature SCV when sufficient nutrients have been incorporated into the vacuole. This stage is characterised by the production of *Salmonella* induced-tubules (SITs), tubulovesicular extensions that are extended throughout the host cell's microtubule network (López *et al*., 2012). The most abundant type of SITs are *Salmonella*-induced filaments (SIFs). Recent studies suggest that SIFs have a role in nutrient acquisition for the SCV (Popp *et al*., 2015) and might help accommodate bacteria during replication (Knuff and Finlay, 2017); however, their function remains unclear.

S. Typhimurium is also found free in the host cell cytosol. This has been observed *in vitro* in epithelial cells, macrophages and fibroblasts. However*, S*. Typhimurium cannot replicate in the cytosol of phagocytic cells and only replicates in the cytosol of epithelial cells. Cytosolic replication occurs in approximately 20% of the infected epithelial cells (Malik-Kale *et al*., 2012, Knodler, 2015). The release of *Salmonella* into the cytosol happens as a defect in SCV maturation. Analyses of the cytosolic population revealed that it expressed mainly SPI-1 with almost negligible levels of expression of SPI-2, whereas its vacuolar counterpart expressed mainly SPI-2. As the cytosol is a richer environment than the SCV, the cytosolic population enters a hyper-replicative state. This and the expression of T3SS-1 effectors leads to pyroptosis of the host cell (Knodler, 2015). Pyroptosis is characterised by the rapid rupture of the membrane which releases inflammatory cytokines and, in this case, motile *Salmonella* expressing SPI-1 that can then spread and infect other epithelial cells.

The cytosolic population has also been observed *in vivo* in extruded enterocytes from chicks, cattle and mice, but with considerably lower numbers of bacteria than reported for *in vitro* experiments (Knodler, 2015). Cytosolic replication of *Salmonella* in macrophages is inhibited by a yet unknown mechanism. Furthermore, release of *Salmonella* from the SCV in a macrophage leads to immediate pyroptosis through activation of caspases. Free *Salmonella* are then phagocytosed by neutrophils, where it can form SCVs or perish (Jennings *et al*., 2017).

Micro-RNAs (miRNA) have been associated with *Salmonella* intracellular survival. Bacteria cannot produce miRNAs; however, *Salmonella* exploits the RNA processing machinery of the host to generate its own miRNAs. These miRNAs interfere with the eukaryotic gene expression at a posttranscriptional level, facilitating intracellular survival of *Salmonella* (Gu *et al*., 2017).

1.4.4 Systemic dissemination

Generally, NTS multiply inside intestinal epithelial cells limiting the infection to the intestines; however, iNTS and typhoidal *Salmonella* traverse the epithelial cell barrier to infect the underlying lymphoid tissues and multiply within macrophages. *Salmonella*-infected macrophages will then spread the infection to blood, liver and spleen causing a systemic infection (Gal-Mor *et al*., 2014).

Apart from surviving inside SCVs, *Salmonella* avoids detection by the immune system through surface-antigenic changes. For example, SPI-12 encodes the OafA acetylase, which alters the outer membrane O-antigen affecting its recognition by the immune system. Similarly, the SPI-11 proteins PagD, EnvE and EnvF can remodel the

membrane making it unrecognisable by the cells from the immune system (Ilyas *et al*., 2017).

1.5 Epidemiology and treatment

Salmonellosis is associated with the consumption of contaminated water and a wide range of foods. These include pork, poultry, eggs and dairy products; rare outbreaks related to the consumption of contaminated flour, nuts and chocolate have also been documented (Andino and Hanning, 2015). Fruits and vegetables that have been in contact with manure or farm animals can also transmit the infection (Gal-Mor *et al*., 2014, Wiedemann *et al*., 2014). In recent years, the exposure to exotic pets has also been deemed a risk factor in the acquisition of NTS (Barrett and Fhogartaigh, 2017).

NTS gastroenteritis was estimated to affect 78 million people and cause 59,000 deaths globally in 2010 (Havelaar *et al.*, 2015). In England and Wales alone, around 8,000 to 10,000 cases are reported each year. In low and medium income countries, NTS are considered one of the leading causes of deaths and hospitalisations (Andino and Hanning, 2015).

Salmonellosis affects all age ranges from infants to >80 year-olds. Recent surveillance information shows that the highest incidence of salmonellosis happens among children under the age of 10 (Kwambana-Adams *et al*., 2015, Public Health England, 2017), where the disease outcome is the most severe.

S. Typhimurium and *S.* Enteriditis are responsible for 80% of all human cases worldwide (Wen *et al*., 2017). These serovars alongside *S.* Dublin cause the majority of the cases of invasive disease in high and low income countries (Marks *et al*., 2017,

Haselbeck *et al*., 2017). It is estimated that iNTS infections cause around 600,000 deaths per year, most of which occur in Africa (Haselbeck *et al*., 2017), where malnourishment and co-infection with HIV and/or malaria contribute to the systemic dissemination of the disease (Feasey *et al*., 2015).

As NTS infections are generally limited to a mild gastroenteritis, patients do not require treatment. In cases of severe diarrhoea and vomiting, rehydration and electrolyte replacement are recommended. Treatment of NTS gastroenteritis with antibiotics is not recommended as it can cause patients to become asymptomatic carriers, an important factor in the spreading of the disease. However, in immunocompromised patients, infants and elderly patients, antibiotic treatment might be needed and is compulsory in cases of invasive disease (World Health Organization, 2017c).

Clinically used antibiotics against NTS include penicillins, chloramphenicol, trimethoprim-sulfamethoxazole, fluoroquinolones, azithromycin and third-generation cephalosporins (Wen *et al*., 2017). Penicillins, such as ampicillin and amoxicillin, chloramphenicol and trimethoprim-sulfamethoxazole are not recommended due to the increasing number of resistant NTS. The preferred antibiotics to treat NTS gastroenteritis are ciprofloxacin, a fluoroquinolone, and azithromycin (Barrett and Fhogartaigh, 2017). For iNTS, ciprofloxacin is the first-line treatment. Levofloxacin and moxifloxacin (alternative fluoroquinolones) as well as extended spectrum third-generation cephalosporins, ceftriaxone and cefotaxime, are used as alternatives in cases of ciprofloxacin-resistance (Kariuki *et al*., 2015). Unfortunately, NTS and iNTS resistant to ciprofloxacin and ceftriaxone are increasing. A surveillance study carried out in Australia showed that the number of ciprofloxacin-resistant NTS increased from 0.1% in 1995 to 7.8% in 2015. Resistance to third-generation cephalosporins increased from 0.1% in 2002 to 1% in 2015 (Williamson *et al*., 2017). Similarly, in the

USA, the percentage of ceftriaxone-resistant iNTS isolated from bloodstream increased from 2.7% (1997 to 2007) to 5% in recent years (2003 to 2013) (Wen *et al*., 2017).

Bacteria can be resistant to one or more antibiotics at the same time. When resistance to three or more antibiotics occur, the isolate is termed “multidrug resistant” (MDR) (Hur *et al*., 2012). MDR *Salmonella* emerged at the beginning of the 1990s. By 2013, they were identified by the World Health Organisation (WHO) as a “serious public health concern” and in 2017, fluoroquinolone-resistant *Salmonella* were classified as a high-priority microorganism in the bacterial pathogen list for research and development of the WHO (World Health Organization, 2017b).

1.6 Antibiotic resistance in bacteria

MDR bacteria are a public health threat as they reduce the effectiveness of antibiotic therapy. Antibiotic-resistant bacteria started appearing almost as soon as antibiotics were discovered. For example, Prontosil, a sulphonamide and the first antibiotic to be used in the clinical environment, became available in 1932 to treat Gram-positive infections; a few years later, in 1939, clinical isolates of *Streptococcus pneumoniae* resistant to the sulphonamide were reported (Miller and Bohnhoff, 1950). Other examples are shown in Figure 1.3.

It is generally accepted that MDR bacteria have emerged due to the widespread use of antibiotics in people, animals and the environment (World Health Organization, 2017a). However, it is important to note that drug resistance is not always

Figure 1.3 Timeline between introduction of antibiotic into clinical practice and development of antibiotic resistance.

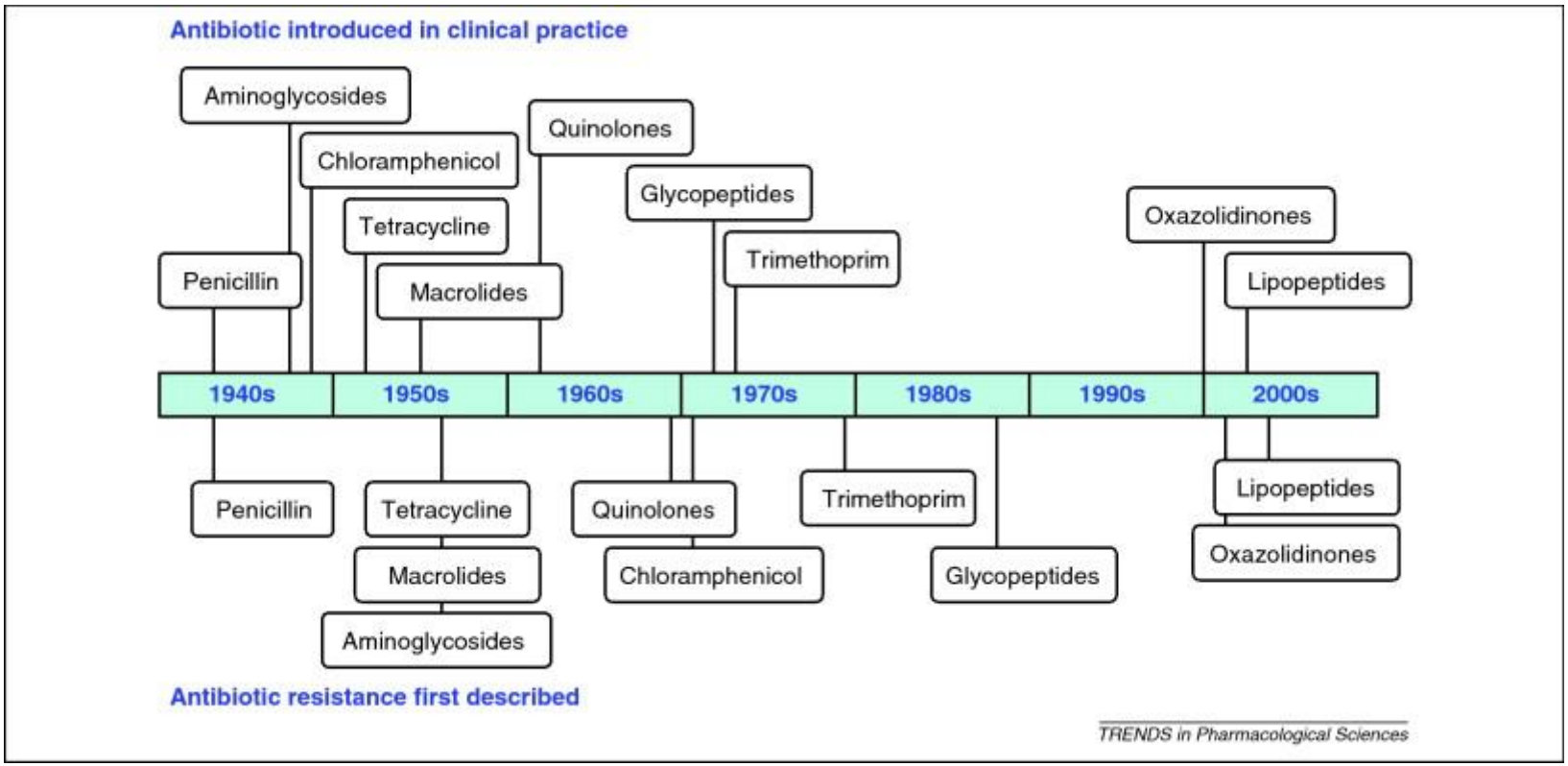

From Hogberg *et al*. (2010).

acquired as some bacteria are intrinsically resistant to some classes or specific antibiotics (Blair *et al*., 2015c). For example, Gram-negative bacteria are intrinsically resistant to vancomycin as the antibiotic cannot traverse their outer membrane (Tsuchido and Takano, 1988). On the other hand, vancomycin is fully active against Gram-positive bacteria; however, they can acquire mutations or additional genetic elements that confer resistance against the antibiotic, such as the Tn1546 transposon in *Enterococcus* spp. (Cetinkaya *et al*., 2000).

Bacteria acquire resistance to antibiotics through five main mechanisms: 1) direct modification of antibiotics, 2) modification and/or protection of drug targets, 3) reduced membrane permeability to antibiotics, 4) increased efflux (Blair *et al*., 2015c) and 5) metabolic bypass (Table 1.1).

1.7 Bacterial efflux pumps and MDR

Bacteria use efflux pumps to transport a variety of compounds from the inside to the outside of the cell. These include fatty acids, dyes, metabolites, detergents and antibiotics. Bacterial efflux pumps are classified into seven families: the major facilitator superfamily (MFS), the small multidrug resistance (SMR) family, the resistance-nodulation-division (RND) superfamily, the multidrug and toxin extrusion (MATE) family, the ATP-binding cassette (ABC) superfamily and two recently discovered families, the proteobacterial antimicrobial compound efflux (PACE) family and the AbgT family of antimetabolite transporters (Chitsaz and Brown, 2017) (Figure 1.4).

Table 1.1 Mechanisms of antibiotic resistance in bacteria.

Mechanism	Description	Examples
Direct modification of antibiotics	Bacteria secrete enzymes to hydrolyse or chemically modify antibiotics to inactivate them.	• β-lactamases hydrolyse penicillins (β-lactams). • Amynoglycoside-modyfying enzymes confer resistance to kanamycin.
Modification and/or protection of drug targets	Antibiotics generally bind to specific targets, mostly proteins, in bacteria. Mutations that change the structure of the target proteins are common as they affect the binding of the antibiotic without affecting the function of the protein. Protection of the target through overexpression of the target, methylation and addition of peptides is also common.	• Mutations in *gyrA* confer resistance to fluoroquinolones. • Methylation of the 16s rRNA through genes of the *erm* family confer resistance to aminoglycosides. • Protection of topoisomerase IV and DNA gyrase via pentapeptide repeat proteins (PRPs) confer resistance to quinolones.
Reduced membrane permeability to antibiotics	In Gram-negative bacteria, hydrophilic antibiotics diffuse through OM porins. Downregulation of porins results in decreased diffusion of antibiotics into the bacterium.	• Decreased expression of OmpC contributes towards resistance to β-lactams. • Substitution of OmpF by OmpX is associated with nalidixic acid resistance.
Increased efflux of antibiotics	Overexpression of efflux pumps prevents intracellular accumulation of antibiotics as pumps actively extrude drugs from the bacterial cell.	• Overexpression of AcrAB-TolC RND efflux complex in Enterobacteriaceae contributes towards resistance to a variety of antibiotics. • Overexpression of LmrS MFS efflux pump confers resistance to linezolid in *Staphylococcus aureus.*
Metabolic bypass	This mechanism is observed for antibiotics that target essential metabolic genes. It consists in the acquisition of genes that encode a resistant version of the target protein, but has the same function. Therefore, when the target protein is inhibited by drugs, the alternative resistant protein can function in the pathway.	• Trimethoprim-sulphamethoxazole inhibits essential proteins in the biosynthesis of folate in bacteria. Resistant versions of these proteins are encoded in transposons from the Tn21 family and are horizontally transferred between Enterobacteriaceae.

Adapted from Blair *et al*. (2015) and Munita and Arias (2016).

Figure 1.4 Bacterial multidrug resistance efflux pumps.

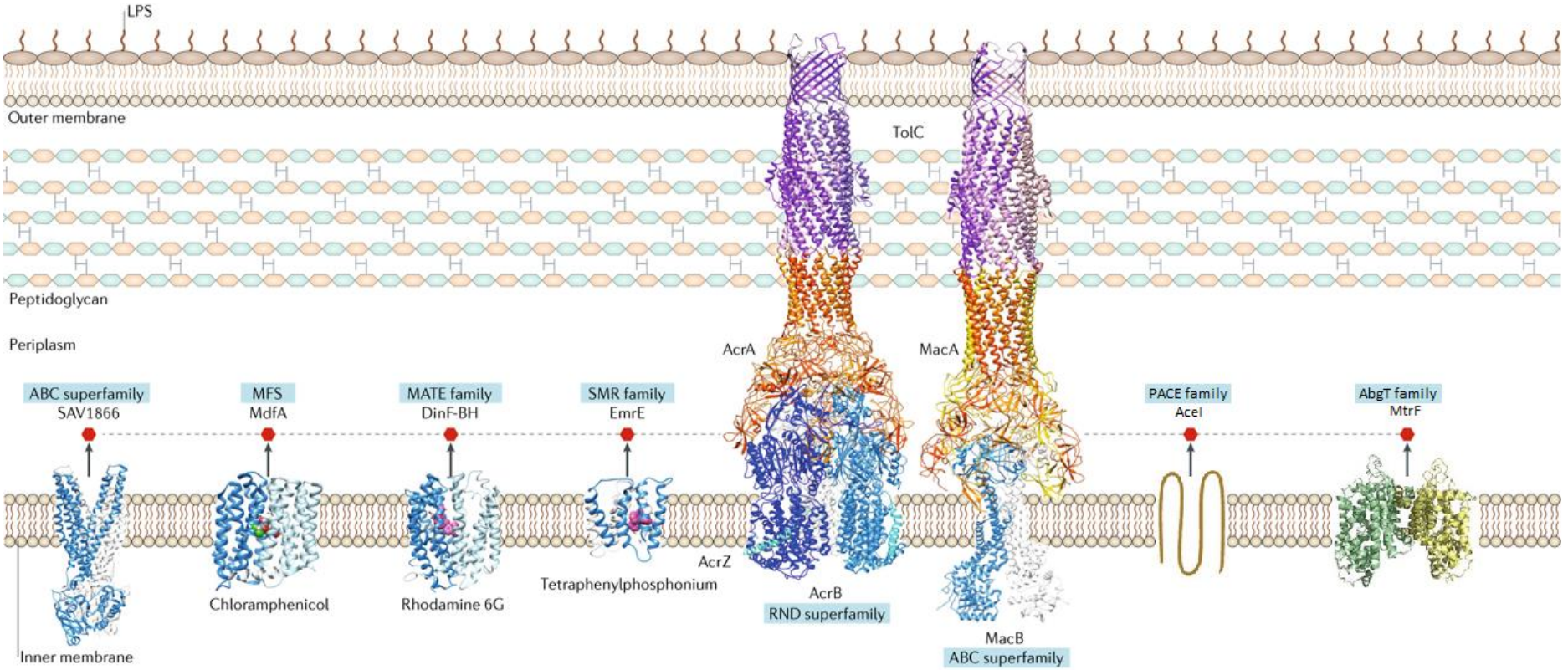

Examples of the best studied pumps in each family is shown. X-ray crystallography structures are shown where known. Adapted from Chitsaz and Brown (2017) and Du *et al*. (2018).

Transporters from the ABC and AbgT family have a dual activity as importers and exporters. The role of ABC transporters in nutrient uptake and export of cell wall precursors and toxic metabolites has been well studied (Chitsaz and Brown, 2017). In contrast, transporters from the AbgT family have only gained attention in recent years. AbgT transporters are named after the *E. coli* folic acid precursor importer AbgT. They were initially classified as importers until the MtrF protein in *Neisseria gonorrhoeae*, a homologue of AbgT, was shown to be involved in resistance towards hydrophobic antibiotics through an efflux-mediated mechanism (Veal and Shafer, 2003). AbgT-family pumps have not been identified as MDR efflux pumps in enteric bacteria (Delmar and Yu, 2016).

Efflux pumps from the PACE family were recently discovered in *Acinetobacter baumannii* after exposure to the biocide chlorhexidine. The paradigm PACE pump is AceI and homologous pumps have been found in multiple bacterial species. However, no reports have been made of PACE transporters in members of the Enterobacteriaceae family (Hassan *et al*., 2015).

Efflux pumps are classified as active transporters as they require energy to translocate their substrates. Based on the source of energy they use, pumps can be classified into primary and secondary transporters. Primary transporters use energy from hydrolysis of ATP, whereas secondary transporters obtain energy from electrochemical gradients formed through the diffusion of protons or ions through a membrane (Elbourne *et al*., 2017). Except for ABC pumps, most of the pump families are secondary transporters and their main source of energy is the proton-motive force (PMF). This is generated by the difference in pH between the environment and the inside of the cell. The PMF in Gram-negative bacteria is generated in the periplasmic space, which tends to be

more acidic than the cytoplasm. Additionally, some pumps from the MATE family use a Na^+ gradient as energy source as well as PMF (Du *et al*., 2018).

Efflux pumps are located in the cytoplasmic membrane. This means that in Gram-positive bacteria they can export drugs directly to the outside of the cell. However, in Gram-negative bacteria they need to interact with an outer membrane efflux protein from the outer membrane factor (OMF) family to extrude antibiotics and other substrates from the cell. RND pumps, such as AcrB, form complexes with the TolC OMF. These pump-OMF complexes are stabilised by membrane fusion proteins (MFP), also called periplasmic adaptor proteins. Therefore, RND pumps are normally found as tripartite complexes that span the periplasm (Murakami *et al*., 2006). Some transporters from the ABC and MFS families also form complexes with TolC, examples of these are the MacB ABC pump and the EmrB MFS pump (Chitsaz and Brown, 2017). However, most non-RND pumps do not interact with OMFs. These pumps are referred to as single-component pumps and they only efflux their substrates into the periplasm, from where the drug can diffuse back into the cytoplasm. To avoid re-entry of the drug into the cytoplasm, drugs in the periplasm are extruded from the bacterial cell via a tripartite pump, usually an RND pump (Li *et al*., 2015).

RND pumps can only transport drugs from the periplasm, unlike ABC pumps which can transport drugs from the cytoplasm. A recent study has shown that AcrB, the paradigm RND pump, has an entrance channel facing the cytoplasm. This channel is likely to be involved in uptake of substrates from the cytoplasm (Zwama *et al*., 2018).

1.8 RND efflux pumps: The paradigm AcrAB-TolC complex

According to their substrates specificity, RND efflux pumps are sub-classified into the hydrophobic and amphiphilic efflux (HAE-RND) and the heavy metal efflux (HME-RND) families (Anes *et al*., 2015). *S.* Typhimurium and *E. coli* have between 9 to 11 RND efflux pumps, most of which belong to the HAE-RND subfamily and are involved in export of multiple drugs and solvents (Elbourne *et al*., 2017). The RND pumps present in *S.* Typhimurium SL1344, a commonly used laboratory strain and the strain used in this work, are shown in Table 1.2.

Of all RND pumps in Enterobacteriaceae, AcrB is the most abundant and best studied RND pump associated with MDR. AcrB is highly conserved among Enterobacteriaceae and it is also highly similar to the MexB RND pump from *Pseudomonas aeruginosa* (Figure 1.5).

AcrB works as part of a tripartite complex with the TolC OMF and the AcrA MFP (Seeger *et al*., 2008, Symmons *et al*., 2009). AcrA, the MFP, is composed of four domains: an α-hairpin domain, a lipoyl domain, a β-barrel domain and a membrane proximal domain (Anes *et al*., 2015). The last three domains interact with AcrB, whereas the α-hairpin domain interacts with TolC. AcrA confers stability to the pump-OMF assembly and is hypothesised to be involved in substrate recognition of the pump. *acrA*-deletion mutants have altered drug-susceptibility phenotypes (Blair *et al*., 2009), but how the protein influences drug-susceptibility remains unknown.

The OMF, TolC, is formed of three β-barrel protomers embedded in the OM. TolC ends in an α-helix bundle tube inserted in the periplasm. The α-helix bundle differentiates OMFs from porins as the latter are formed exclusively of β-barrels (Zgurskaya *et al*., 2011). When TolC is not interacting with efflux pumps, it is found in

Table 1.2 RND efflux pumps encoded in the chromosome of *S.* Typhimurium SL1344.

Protein name	Gene name*	Substrate	Description*	Subtype
SL1344_0346	Not annotated	Multidrug/solvent efflux (HAE1 subfamily)	Efflux pump membrane transporter	HAE1
SL1344_0402	secD	Protein export (SecDF)	Protein translocase subunit SecD	SecDF
SL1344_0468	acrB	Multidrug/solvent efflux (HAE1 subfamily)	Efflux pump membrane transporter	HAE1
SL1344_1374	ydhJ	Multidrug efflux	Hypothetical HlyD-family protein	No Subtype
SL1344_2104	yegN/mdtB	Multidrug/solvent efflux (HAE1 subfamily)	Multidrug resistance protein MdtB	HAE1
SL1344_2105	yegO/mdtC	Multidrug/solvent efflux (HAE1 subfamily)	Multidrug resistance protein MdtC	HAE1
SL1344_2444	acrD	Multidrug/solvent efflux (HAE1 subfamily)	Efflux pump membrane transporter	HAE1
SL1344_3337	yhcQ/aaeA	Multidrug efflux	p-hydroxybenzoic acid efflux pump subunit AaeA	No Subtype
SL1344_3364	acrF	Multidrug/solvent efflux (HAE1 subfamily)	Efflux pump membrane transporter	HAE1

(*) Gene names and description were obtained by searching the protein name code in the Uniprot database. Adapted from TransportDB (Elbourne *et al*., 2017).

Figure 1.5 Protein sequence similarity of AcrB in Enterobacteriaceae and its homologue MexB in *P. aeruginosa*.

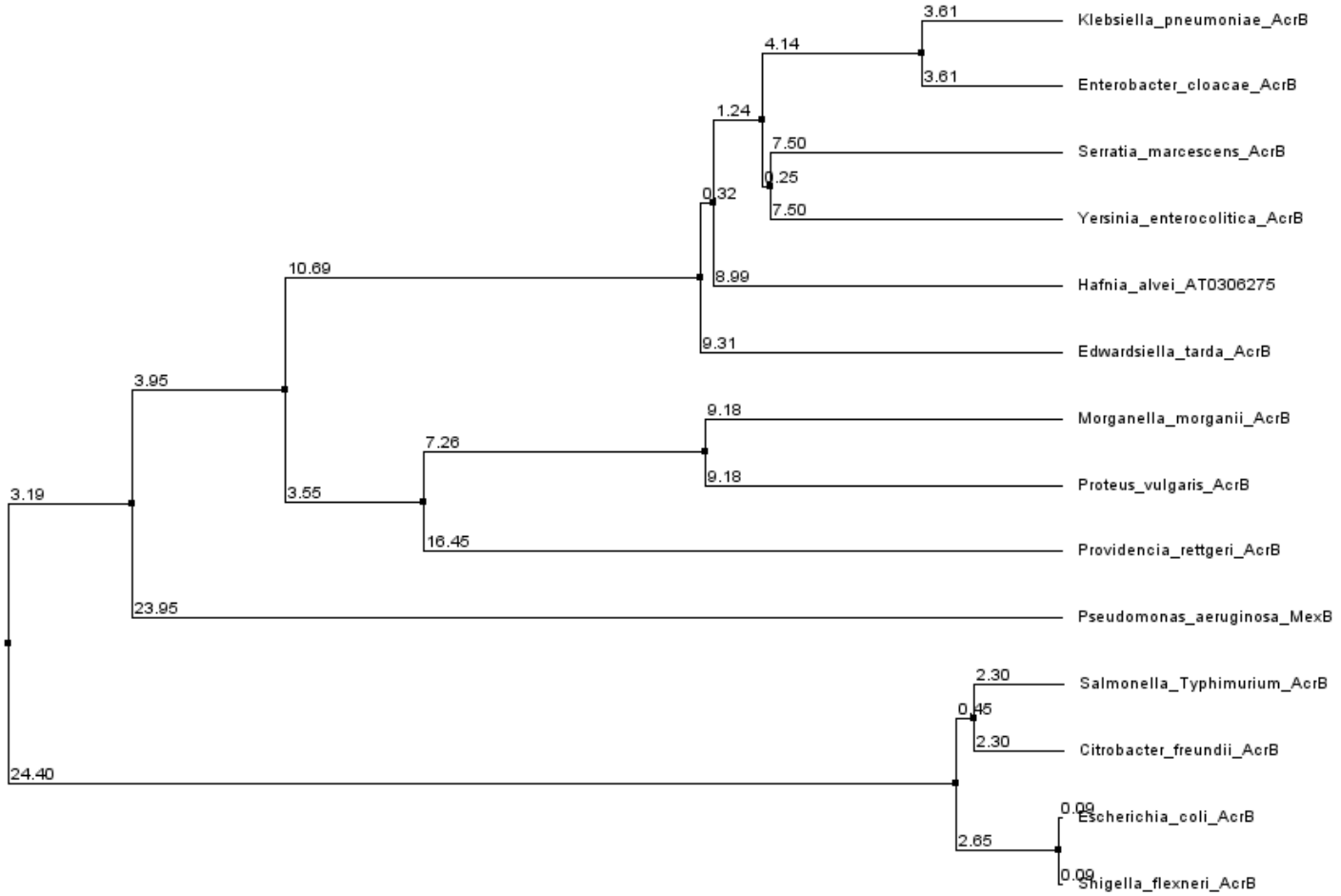

Dendrogram shows the species and protein analysed, the number on each branch shows the percentage of non-identical residues between species or clades. Protein sequences were obtained from Uniprot and sequence similarity was determined by PID (percentage identity). Type of analysis done was average distance. Analyses and dendrogram were constructed with Jalview.

a closed conformation to avoid entrance of undesirable substances into the periplasm. Some evidence suggest that the inner channel of TolC will only open when the OMF comes in contact with the pump (Anes *et al*., 2015). TolC interacts with multiple pumps from different families; therefore, it is considered a 'promiscuous' protein and it is believed to be constantly assembling and disassembling from multiple pumps in order to facilitate efflux. Deletion or inactivation of *tolC* prevents efflux from a variety of pumps and gives rise to a multidrug hypersusceptible phenotype. Surprisingly, only a small proportion of TolC (~5%) is required to maintain full efflux activity in bacteria (Krishnamoorthy *et al*., 2013).

AcrB is a trimeric protein with three domains: docking domain, pore domain and transmembrane domain. Each of the three protomers or subunits of AcrB is formed of 12 transmembrane α-helices (TM1 to TM12) and the protomers are held together by a connecting loop. Drug binding occurs in the pore domain (also known as porter domain) which is subdivided into four subdomains. In this domain, each protomer has a lateral cleft, hypothesised to be the binding site of AcrA (Figure 1.6). Each AcrB protomer has three access channels and two binding pockets, referred to as proximal and distal binding pockets. The accessibility to these sites depends on the conformation of the pump. The binding pockets in each protomer of the AcrB protein can acquire different conformations to facilitate the transport of the drug through the pump, these conformations are known as loose (L), tight (T) and open (O), also referred to as access, extrusion and binding conformations (Murakami *et al*., 2006, Seeger *et al*., 2008, Sun *et al*., 2014) (Figure 1.7). The conformational changes are dependent upon PMF, generated by translocation of protons through the pump (Takatsuka and Nikaido, 2009). TM4, TM10 and TM11 are responsible for proton

Figure 1.6 Structure of AcrB.

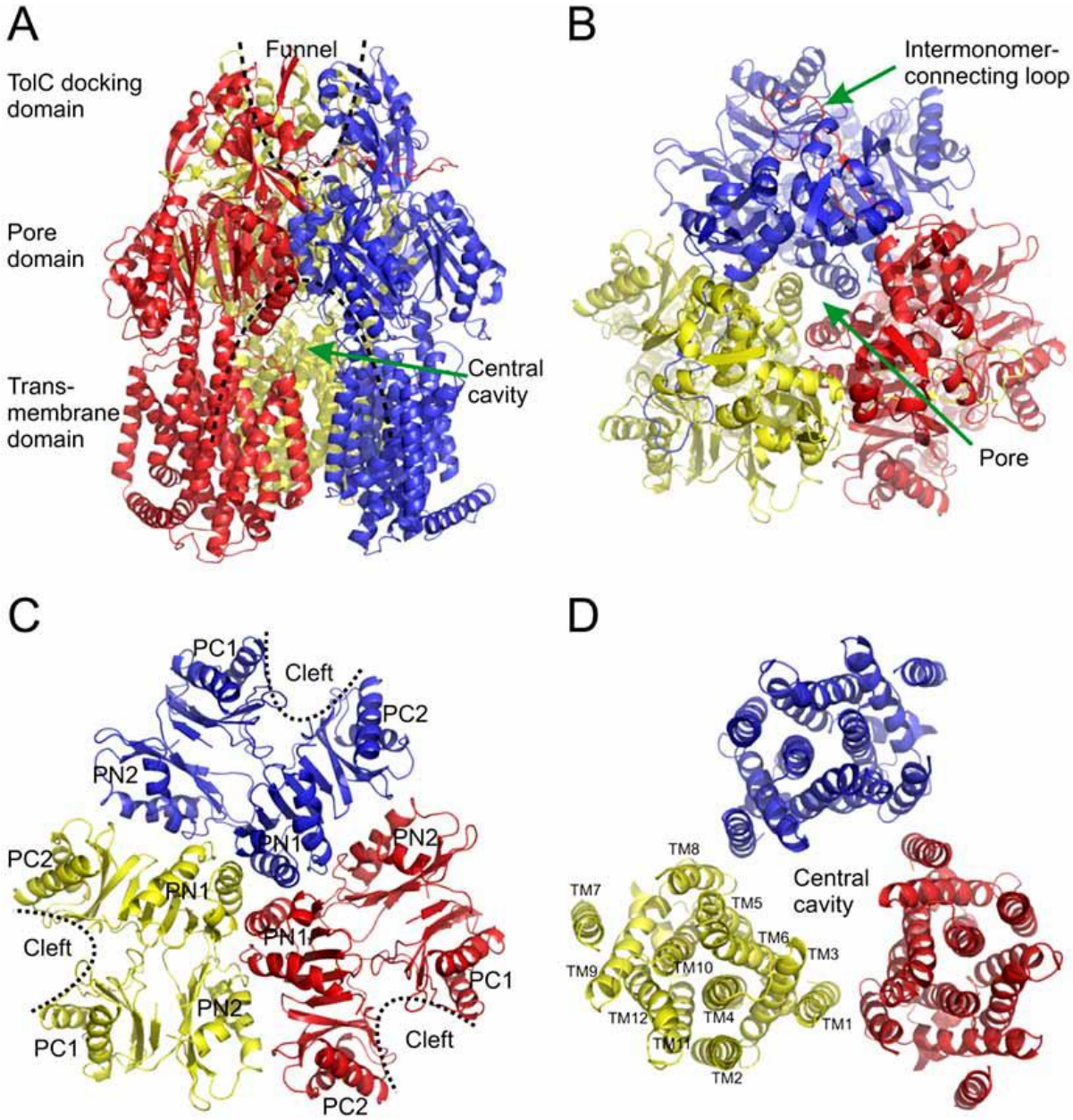

A) Front view of AcrB. Each protomer is shown in a different colour. Top view of the B) docking domain, C) pore domain and D) transmembrane domain. From Seeger *et al*., 2008. Reproduced with permission of the Copyright Clearance Centre (license ID: 4426680321298, confirmation number: 11748015).

Figure 1.7 Depiction of the functional rotation mechanism.

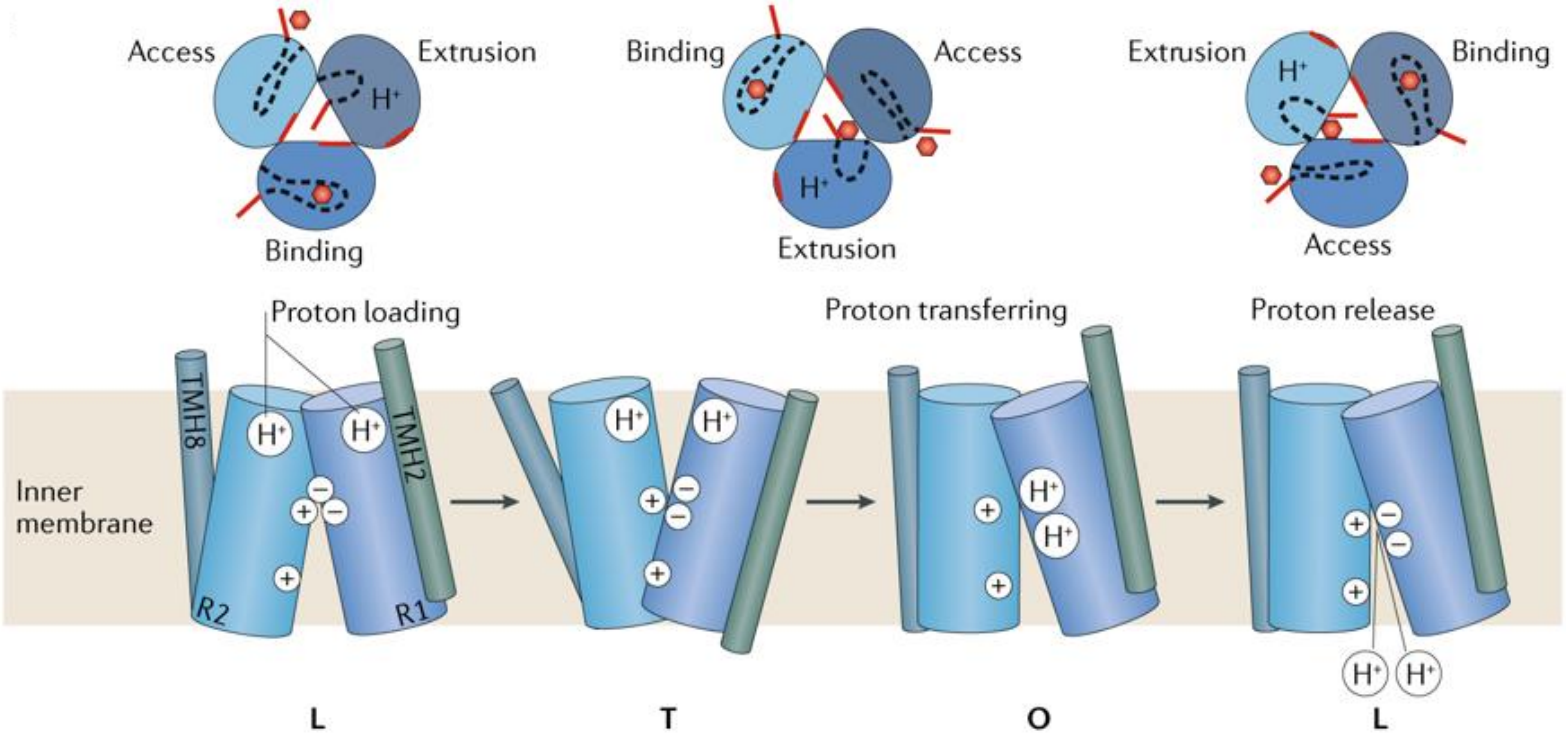

Schematic of the top and front view of AcrB during functional rotation. L, O and T indicate the loose, tight and open conformations of the pump, respectively. From Du *et al*. (2018).

translocation via five residues: D407 (TM4), D408 (TM4), K908 (TM10), T978 (TM11) and R971 (TM11) (Figure 1.6A, B) (Murakami *et al*., 2006, Seeger *et al*., 2008, Su *et al*., 2006, Sun *et al*., 2014, Eicher *et al*., 2014). *In silico* studies have suggested that transport through AcrB is mediated by unidirectional peristaltic movements dependent on conformational changes of the pump, which allow the target drug to be pushed through the pump and into TolC (Seeger *et al*., 2006, Feng *et al*., 2012).

A small accessory protein, AcrZ, has also been shown to interact with AcrB. AcrZ is formed predominantly of α-helices. It is found in the inner membrane, interacting with the transmembrane domain of AcrB (Du *et al*., 2014). The function of AcrZ in the complex is unclear, but may be involved in modulating substrate specificity of the pump (Hobbs *et al*., 2012, Du *et al*., 2015).

The assembly of the pump complex happens spontaneously. However, the stoichiometry of the assembly is still under debate. It is accepted that each complex has one AcrB pump and one TolC OMP, both of which are formed of three protomers each. The number of MFPs remains unclear as some reports indicate that there are three AcrA proteins per complex (3:3:3) (Symmons *et al*., 2009), whereas other studies show six (3:6:3) (Janganan *et al*., 2011, Daury *et al*., 2016). Another debate is the interaction of the OMP with the pump. Initial studies suggested that TolC sits on top of AcrB, in a tip-to-tip interaction (Pos, 2009). The direct interaction of AcrB with TolC triggers conformational changes within the OMF that allows opening of its inner channel and subsequent extrusion of substrates. In this model AcrA is wrapped around TolC and AcrB; therefore, it is named the “Adaptor Wrapping Model” (Anes *et al*., 2015) (Figure 1.8). Recent crystallography studies supports a model where AcrB and TolC do not interact with each other and the whole complex is held together by AcrA, which is found attached to AcrB and interacting tip-to-tip with TolC (Du *et al*., 2014). This

model is referred to as the “Adaptor Bridging Model”, in which the opening of TolC is mediated by AcrA (Anes *et al*., 2015). However, molecular docking simulation studies and thermodynamics analyses support the direct interaction of AcrB with TolC (Touze *et al*., 2004, Schmidt *et al*., 2016). It is important to note that the functional assembly of the complex has not been uncovered. Therefore, these models could represent different stages of the efflux process and are not mutually exclusive.

1.8.1 Regulation of AcrAB expression

The *acrAB* genes are found as part of the same operon, the expression of which is under direct control of the local regulator AcrR, a repressor from the TetR family. *acrR* is found upstream of the *acrAB* operon and is transcribed divergently (Figure 1.9). AcrR binds upstream of the *acrAB* operon and its overexpression results in repression of AcrAB (Ma *et al*., 1996). MDR human and animal isolates with mutations in *acrR* have been identified. These mutations affect the ability of AcrR to repress the *acrAB* operon, causing overexpression of the pump (Webber *et al*., 2005).

The transcription repressor EnvR (also known as AcrS) binds to the same region as AcrR in the promoter region of the *acrAB* operon. The *envR* gene is located upstream of the *acrEF* operon in *E. coli*, which encodes another RND efflux pump and its MFP, respectively. However, EnvR does not affect expression of AcrEF (Hirakawa *et al*., 2008).

Figure 1.8 Models of AcrAB-TolC.

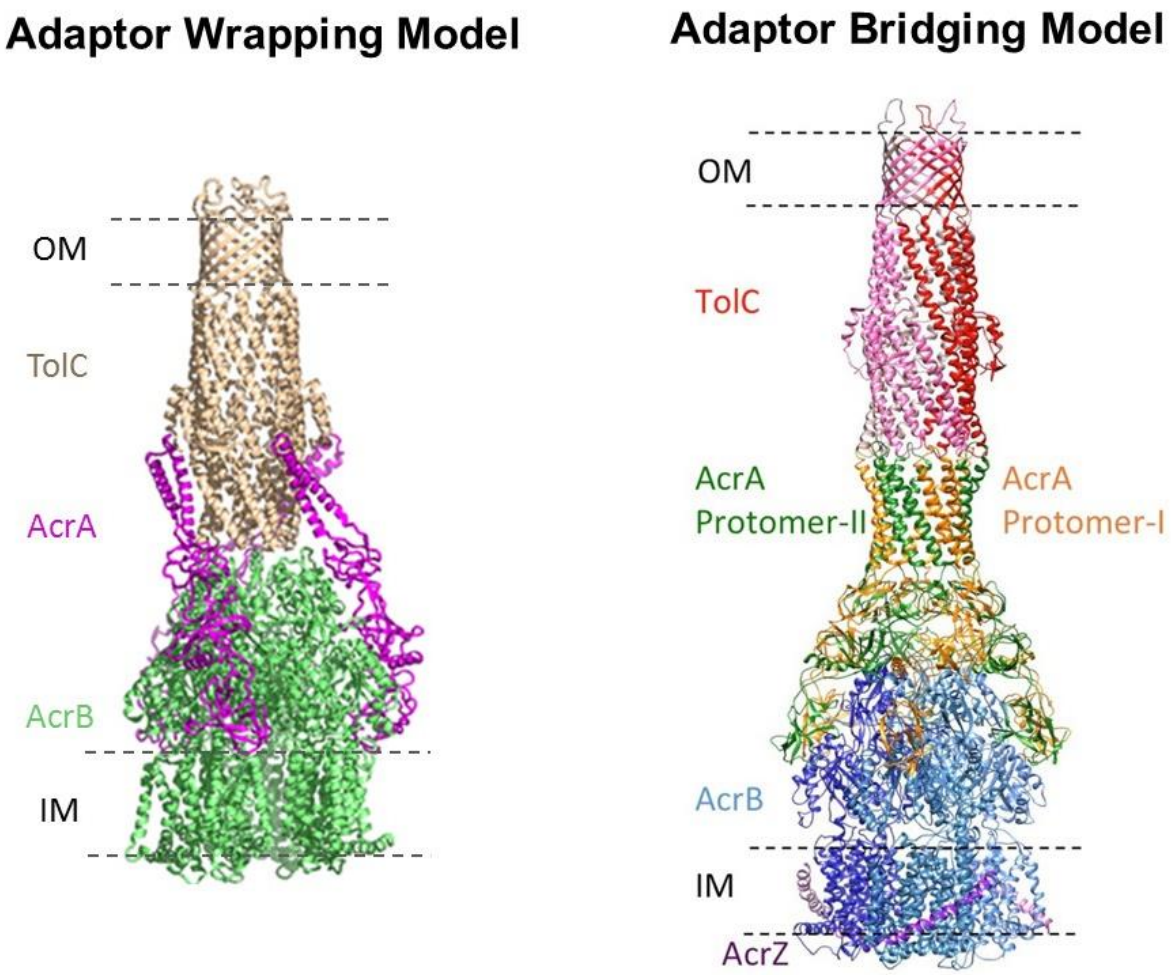

The adaptor wrapping model depicts AcrB and TolC interacting tip-to-tip, with AcrA units wrapped around both transmembrane proteins (from Yamaguchi *et al*., 2015). In the adaptor bridging model there is no interaction between AcrB and TolC. AcrB interacts directly with AcrA and AcrA interacts with TolC tip-to-tip (from Wang *et al*., 2017).

Figure 1.9 Transcription factors that affect the expression of the *acrAB* operon.

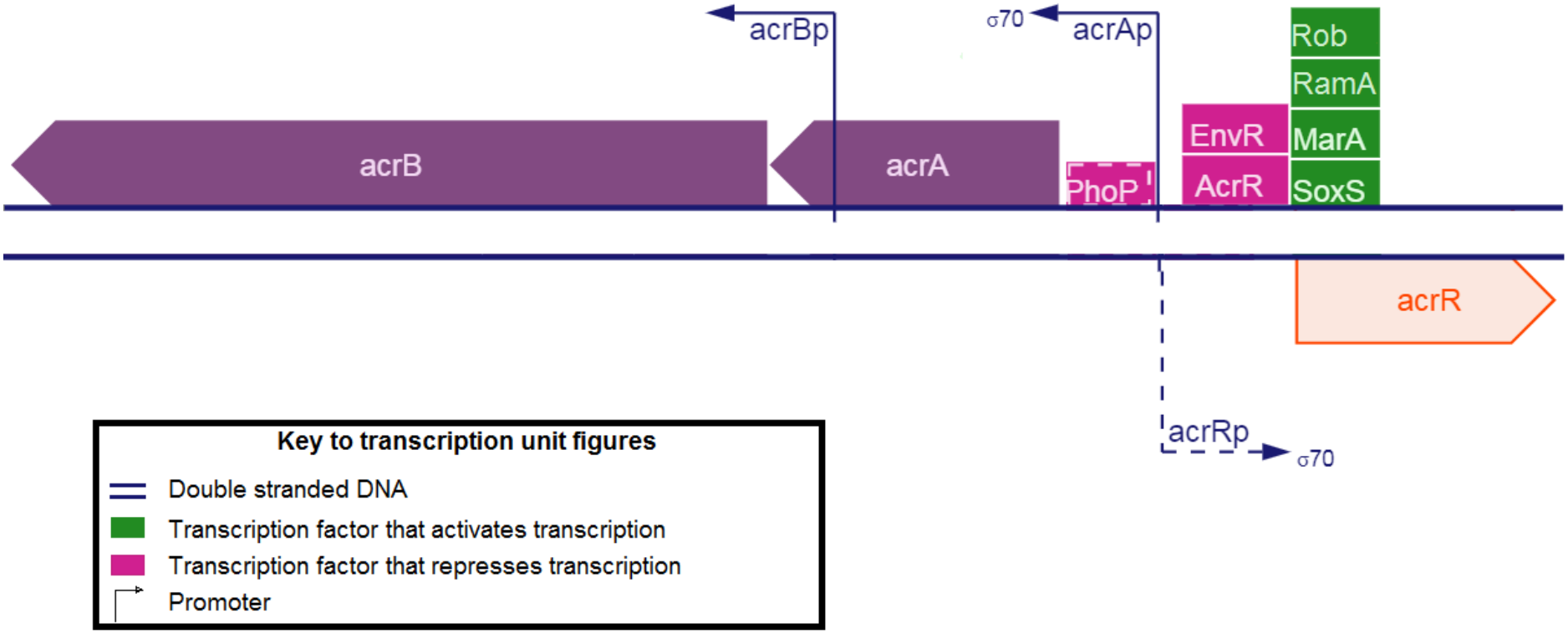

Genes encoding *acrAB* are shown in purple. The local transcription regulator, *acrR*, is shown in orange. Boxes marked with a discontinuous line indicate those promoters/repressors for which more experimental evidence is required. Figure adapted from ecocyc.org

The transcription of *acrAB* is also regulated by global transcription factors. These belong to the AraC/XylS family of transcription activators and they are encoded by *marA, soxS, rob* and *ramA*. These transcription factors are found in all Enterobacteriaceae, except for RamA, which is not in *E. coli* but has been described in *S. enterica*, *Enterobacter cloacae*, and *Klebsiella pneumoniae*. All of these transcription activators are predicted to bind to a sequence upstream of *acrAB* called the marbox, a highly degenerate sequences of approximately 20bp found in multiple sites throughout the genome of Enterobacteriaceae (Weston *et al*., 2017).

Some studies have shown that two-component signalling systems (TCSS) also regulate the expression of AcrAB. TCSS are formed of an inner membrane sensor protein or histidine kinase and a cytoplasmic effector protein. From microarray data, PhoP, the cytoplasmic effector protein from the PhoPQ system, was identified as a possible repressor that binds upstream of the *acrAB* operon in *E. coli* and *S. enterica* (Monsieurs *et al*., 2005). The CpxRA TCSS, involved in sensing membrane stress, indirectly regulates the expression of *acrAB* by controlling transcription of *marA* in *E. coli*. The cytoplasmic effector protein CpxR was shown to bind the promoter of the *mar* operon in *E. coli* and act as a transcription activator (Weatherspoon-Griffin *et al*., 2014). Therefore, activation of the CpxRA TCSS results in overexpression of MarA, leading to upregulation of *acrAB.* Another protein that indirectly regulates expression of *acrAB* is the Lon protease. This is an ATP-dependent protease that degrades a wide range of proteins, including MarA and RamA. Thus, the overexpression of the Lon protease results in decreased transcription of *acrAB*, as the transcription activators are degraded (Weston *et al*., 2017).

Expression of AcrAB is also controlled at a post-transcriptional level. A recent study in *S.* Typhimurium has shown that CsrA, an RNA binding protein involved in carbon

storage regulation, facilitates the translation of the *acrAB* transcript by altering the secondary structure of the mRNA, which in turn helps the binding of ribosomes (Ricci *et al*., 2017).

1.8.2 Physiological role of AcrB

RND efflux pumps receive their name from their role in heavy metal Resistance, Nodulation and cell Division (Dinh *et al*., 1994). In 1994, the RND superfamily was comprised of only six proteins: AcrF (formerly EnvD) involved in cell division in *E. coli*, NolGHI involved in formation of nodules on the roots of legumes by *Rhizobium melitoli* and the CszA and CnrA pumps from *Alcaligenes eutrophus* involved in resistance towards nickel and cobalt (Saier *et al*., 1994). AcrB was later included in the RND superfamily based on its high sequence identity to AcrF.

The *acrB* gene was first identified 40 years ago as the second gene conferring resistance to acriflavine (Nakamura *et al*., 1978), an acridine dye historically used to cure plasmids. Nakamura (1965) showed that *E. coli* had chromosomal determinants that confer resistance to acriflavine; he also showed that strains resistant to acriflavine had cross-resistance to other acidic dyes such as methylene blue and crystal violet. In subsequent studies using the mutants obtained in 1965, he showed that acriflavine resistance was mediated by a gene identified as *acrA* (Nakamura, 1968) and that acriflavine-mediated plasmid curing was more efficient in these mutants (Nakamura, 1974). Mutations downstream of *acrA* were also identified at the time; however, these were not studied until 1978, when they led to the discovery of *acrB*.

The *acrB* gene was re-discovered in 1993 and named *acrE* by Ma *et al*. (1993). The name of the gene was rectified two years later by the same group, when they reported that *acrAB* were responsible for the intrinsic drug resistance of *E. coli* towards novobiocin, erythromycin, bile salts and sodium dodecyl sulphate (SDS, a detergent). They also noticed that fatty acids and bile salts induced expression of *acrAB*. Therefore, they concluded that AcrAB was a "stress-induced efflux system" (Ma *et al*., 1995).

Lacroix *et al*. (1996) described the gene encoding AcrB in *S.* Typhimurium. They confirmed that AcrB is required for resistance to bile salts by testing the susceptibility of an *acrB::*Tn*phoA* mutant, where the gene was inactivated by a transposon insertion. Interestingly, they also observed that the *acrB::*Tn*phoA* mutant was attenuated in a C57BL/6 murine oral infection model. The authors concluded that this was due to the increased susceptibility of the *S.* Typhimurium *acrB* mutant to bile salts. Overall, these results suggested that AcrB played an important role in survival of Enterobacteriaceae in the mammalian gut by conferring innate resistance to bile salts.

Later studies focused on the role of AcrAB and other RND efflux pumps in MDR. Some efforts have been made towards understanding their physiological role. However, this has been complicated as homologous pumps serve different physiological roles in different bacterial species. For example, in *Mycobacterium smegmatis* and *Corynebacterium glutamicum* RND efflux pumps are involved in efflux of precursors of long-chain fatty acids called mycolic and corynomycolic acids, respectively, which are essential cell wall components in these species (Varela *et al*., 2012). In Enterobacteriaceae, the general consensus is that the loss of RND efflux pumps results in loss of virulence (Buckley *et al*., 2006, Bina *et al*., 2008, Padilla *et al*., 2010, Perez *et al*., 2012, Alcalde-Rico *et al*., 2016). This has been shown in multiple species

(Alcalde-Rico *et al*., 2016), including *S. enterica*, where the impact of five RND efflux pumps in virulence was studied. Nishino *et al*. (2006) tested the virulence of insertional inactivation mutants of *acrB*, *acrD*, *acrF*, *mdsB* and *mdtB* of *S.* Typhimurium in a BALB/c murine intragastric infection model. The conclusion of this study was that the *acrB::aph* mutant was the most attenuated mutant when compared to the parental wild-type strain. Other studies showed that the absence of either of the components of the AcrAB-TolC complex results in diminished ability of *S.* Typhimurium to adhere and invade intestinal epithelial cells *in vitro*; again the *acrB* mutant was the most affected (Buckley *et al*., 2006, Blair *et al*., 2015b).

These early studies suggested that the loss of virulence observed in the *acrB* mutant was due to the loss of an intrinsic mechanism of resistance to host-derived antimicrobial compounds, such as bile salts. Apart from bile, AcrAB-TolC also effluxes fatty acids in *E. coli* (Lennen *et al*., 2013), which are in abundance in the human sera and gut (Rodríguez-Carrio *et al*., 2017). Additionally, this RND pump complex is partially involved in resistance to AMPs in *E. coli*. An *acrB::aph* mutant showed increased susceptibility to the cationic AMP LL-37 and human β-defensin HBD-1, but not to α-defensin HNP-2 (Warner and Levy, 2010).

Later studies indicate that loss of virulence may not be due exclusively to the inability of the *acrB* mutant to efflux host-derived compounds. A microarray study showed that inactivation of genes encoding any of the components of AcrAB-TolC in *S.* Typhimurium resulted in significant changes in the transcriptome of the mutant when compared against its parental wild-type strain, without exposure to the host. In the *acrB*::*aph* mutant, genes involved in SPI-1 expression and motility were among the

most downregulated, whereas genes involved in anaerobic metabolism were upregulated (Webber *et al*., 2009).

These changes in transcription indicate that AcrB has an important role in bacterial physiology and virulence. Expression of virulence genes in many bacteria is controlled by quorum sensing (QS). QS is a cell density-dependent mechanism of cell-to-cell communication that relies on the production and accumulation of signalling molecules called autoinducers (AIs) (Whiteley *et al*., 2017). The concentration of extracellular AIs increases proportionally to the number of bacteria in the population. Once the AI threshold is achieved, the AIs are internalised and phosphorylated. This is the first step of a phosphorylation cascade, which results in expression of QS-dependent genes. Analogues of AcrB in *Pseudomonas aeruginosa* export AIs or precursors of AIs (Aendekerk *et al*., 2005, Lamarche and Déziel, 2011, Minagawa *et al*., 2012). It was also proposed that AcrB is involved in efflux of AIs in *E. coli* as an *acrAB*::*aph* mutant reached higher cell density in stationary phase than the parental strain (Yang *et al*., 2006). However, another study could not reproduce these findings (Webber *et al*., 2009) and so to date there is no evidence that AcrB or any of the RND pumps in Enterobacteriaceae export AIs.

There are other studies that support the hypothesis that RND pumps directly export virulence factors. Studies in *E. coli* and *V. cholerae* have shown that RND pumps contribute towards efflux of siderophores (Horiyama and Nishino, 2014, Kunkle *et al*., 2017), small iron-chelating molecules that provide ferrous iron (Fe^{2+}) to bacteria under nutrient-limiting conditions. Strains that overproduce siderophores are often hypervirulent; whereas, strains deficient in siderophore production tend to be attenuated (Holden and Bachman, 2015). This suggests that the virulence attenuation

observed in RND pump-deficient strains could also be caused by decreased export of virulence factors.

Although the contribution of AcrB and its homologous efflux pumps in virulence have been established, the mechanism by which this is mediated remains unclear.

1.9 Project background

Hirakata *et al*. (2002) showed that addition of cell-free culture supernatant from multicystic dysplastic kidney cells (MCDK) infected with *P. aeruginosa* K767 could restore virulence to a Δ*mexAB-oprM* (AcrAB-TolC homologue) triple deletion mutant. While reproducing this experiment in *Salmonella*, Blair (2010) found that adding cell-free culture supernatant from wild-type *S.* Typhimurium SL1344 grown overnight in LB broth (conditioned medium or exometabolome) to a Δ*acrB* mutant restored the ability of the mutant to invade INT-407 embryonic intestinal epithelial cells. Based on these observations, it was hypothesised that AcrB is involved in the efflux of a virulence regulating molecule(s) or a novel virulence factor(s).

To explore this hypothesis, experiments were designed to discover the nature and mechanism of action of the molecule(s). Conditioned medium from *S.* Typhimurium SL1344 was added to Δ*acrB* mutants during infection assays with INT-407 intestinal epithelial cells. This restored the invasive ability of the mutant to almost the same level as the parental wild-type strain when concentrated 3-fold (final concentration of 1.5-fold). To identify the size of the factor(s) and whether it was a protein, conditioned medium was centrifuged using Vivaspin® (GE Healthcare Life Sciences, UK), leaving only molecules smaller than 5 kDa. Surprisingly, this conditioned medium retained its

restorative effect. However, when proteinase K was added, the restorative effect was lost. The virulence-restoring molecule(s) also proved to be stable after heating at 70°C but lost its restorative activity over time (Piddock team, unpublished data) (Appendix VI).

1.10 Hypothesis

AcrB exports bacterially derived molecules important in the virulence of *Salmonella enterica* serovar Typhimurium SL1344.

1.11 Aims and objectives

The aims of this project are:

- To identify the molecule(s) that restore virulence to an AcrB loss-of-function mutant of *Salmonella enterica* serovar Typhimurium SL1344.
- To discover additional physiological roles of AcrB in *S.* Typhimurium.

The objectives are:

- Construct an adequate model that allows differentiation of the effect of loss of AcrB efflux function from the effect of the loss of AcrB protein.
- Determine the phenotypic and transcriptomic differences between a loss of efflux function mutant and the wild-type *S.* Typhimurium mutant.
- Identify candidate molecules that restore virulence to a loss of AcrB function mutant.

CHAPTER 2.

Materials and Methods

2.1 Bacterial strains

All bacterial strains used in this study (Table 2.1) were grown in Lennox lysogeny medium (LB) (Sigma, USA, cat. no. L3022) or MOPS minimal medium (Teknova, USA, cat. no. M2106) at 37°C, unless specified otherwise. All *S.* Typhimurium mutants used in this study are derived from SL1344, an experimental strain derived from a calf isolate (Wray and Sojka, 1978). SL1344 is a laboratory strain commonly used to study virulence of *S.* Typhimurium. It has a histidine autotrophy due to an ablation of the *hisG* gene. Therefore, when grown in minimal medium, histidine is required to a final concentration of 25μM (0.4g/L). All *E. coli* mutants were constructed in a K-12 MG1655 background, a well-characterised strain with "minimal genetic manipulations" when compared against the ancestral K-12 strain (Blattner *et al.*, 1997). This strain has decreased expression of PyrE, which leads to a mild pyrimidine auxotrophy that can be compensated by addition of 1μg/mL of thiamine (*E. coli* Genome Project, 2002-2018).

Strains were routinely checked by Gram-staining and API-20E tests (Biomerieux, France, cat. no. 20100). The API-20E system comprises a variety of biochemical tests that allow identification of Enterobacteriaceae species. To prepare the inoculum for the test, a bacterial suspension (OD_{600}=0.1) was prepared in 5mL of sterile distilled water. The suspension was dispensed into the wells of an API-20E test strip with a sterile Pasteur pipette (Fisher Scientific, UK, cat. no. 12887605). Strips were incubated at the appropriate temperature and results were recorded according to the manufacturer's instructions. Results were introduced into an online system to identify the microorganism.

Table 2.1 Strains used in this study.

Culture collection number	Species	Genotype	Antibiotic resistance	Origin
L354	*S.* Typhimurium	SL1344 Wild-type *hisG*-	None	APHA
L110	*S.* Typhimurium	SL1344 *acrB*::*aph*	Kan^R	Eaves *et al*., 2004
L644	*S.* Typhimurium	SL1344 Δ*acrB*	None	Eaves *et al*., 2004
L1804	*S.* Typhimurium	SL1344 *acrB* G1223C (AcrB D408A substitution)	None	This study
L103	*S.* Typhimurium	SL1344 *ramA*::*aph*	Kan^R	Lawler *et al*., 2013
L1351	*S.* Typhimurium	SL1344 wild-type carrying pSIM18	Hyg^R	Constructed by Dr. Vito Ricci
L1232	*S.* Typhimurium	SL1344 wild-type carrying pMW82+*ramAp-gfp*	Amp^R	Lawler *et al*., 2013
L1353	*S.* Typhimurium	SL1344 Δ*acrB* carrying pMW82+*ramAp-gfp*	Amp^R	Lawler *et al*., 2013
L1812	*S.* Typhimurium	SL1344 AcrB D408A carrying pMW82+*ramAp-gfp*	Amp^R	This study
L1909	*S.* Typhimurium	SL1344 wild-type carrying pMW82+*lexAp-gfp*	Amp^R	This study
L1910	*S.* Typhimurium	SL1344 AcrB D408A carrying pMW82+*lexAp-gfp*	Amp^R	This study
L1407	*S.* Typhimurium	SL1344 wild-type carrying pMW82 empty vector	Amp^R	Lawler *et al*., 2013
L1899	*S.* Typhimurium	SL1344 Δ*acrB* carrying pMW82empty vector	Amp^R	Lawler *et al*., 2013
L1900	*S.* Typhimurium	SL1344 AcrB D408A carrying pMW82 empty vector	Amp^R	This study
L1708	*S.* Typhimurium	SL1344 wild-type carrying pDiGc	Amp^R	This study
L1897	*S.* Typhimurium	SL1344 AcrB D408A carrying pDiGc	Amp^R	This study
L1706	*S.* Typhimurium	SL1344 wild-type carrying pDiGc	Amp^R	This study
L1898	*S.* Typhimurium	SL1344 AcrB D408A carrying pDiGc	Amp^R	This study
L828	*S.* Typhimurium	14028S Wild-type	None	ATCC
L830	*S.* Typhimurium	14028S *acrB*::*aph*	Kan^R	Nishino *et al*., 2006
I364	*E. coli*	K-12 MG1655 Wild-type *ilvG*- *rfb*-50 *rph*-1	None	Blattner *et al*., 1997
I970	*E. coli*	K-12 MG1655 *acrB*::*aph*	Kan^R Amp^R	Constructed by Dr. Vito Ricci
I1144	*E. coli*	K-12 MG1655 Δ*acrB*	None	This study
I1124	*E. coli*	K-12 MG1655 *acrB* A1223C (AcrB D408A substitution)	None	This study
I1122	*E. coli*	K-12 MG1655 carrying pSLTS	Amp^R	This study
I113	*E. coli*	NCTC 10418	None	NCTC

I448	*E. coli*	ATCC 25922	None	ATCC
G191	*Pseudomonas aeruginosa*	PAO1 Wild-type ATCC15692	None	ATCC
F77	*Staphylococcus aureus*	NCTC8532	None	NCTC
V1	*Vibrio harveyi*	TL25 Δ*luxM* Δ*luxPQ* Δ*cqsS*	None	Long *et al*., 2009
V2	*Vibrio harveyi*	TL26 Δ*luxN* Δ*luxS* Δ*cqsS*	None	Long *et al*., 2009
V3	*Vibrio harveyi*	BB170 *luxN::*Tn5	Kan^R	Bassler *et al*., 1993

Kan^R indicates resistance to 50μg/mL of kanamycin, Amp^R indicates resistance to ≥50μg/mL of ampicillin, Hyg^R indicates resistance to 100μg/mL of hygromycin. APHA refers to Animal Health and Plant Agency (UK, formerly Animal Health and Veterinary Laboratories Agency). NCTC refers to the National Collection of Type Cultures (Public Health England, UK). ATCC refers to the American Type Culture Collection (USA).

All strains were stored in Protect™ cryopreservation beads (Technical Service Consultants Ltd., UK, cat. no. Tn/80-GN) at -80°C. Working stocks were stored at -20°C. Stocks were prepared from an agar plate with confluent growth of the respective strain. Bacteria were harvested with a sterile loop and introduced into the cryo-tube. Tubes were vortexed briefly to disrupt bacterial aggregates and excess of cryopreservation media was removed. Tubes were immediately stored at the appropriate temperature.

2.1.1 Growth of bacterial strains

Growth kinetics were carried out in a FLUOstar OPTIMA microplate reader (BMG Labtech, UK). Overnight cultures were diluted 1:1000 when LB broth was used or 1:100 when MOPS minimal medium was used. A 10μL aliquot of the diluted cultures was inoculated into 90μL of fresh broth in a U-bottom 96-well plate (Greiner Bio-One, Germany, cat. no. 655098), to make a starting culture of $1X10^4$ or $1X10^6$ CFU/mL in LB broth or MOPS, respectively. Plates were incubated at 37°C for 18 hours. Absorbance at 600nm was measured every 5 minutes from the bottom of the plate. An orbital adjustment of 2mm to ensure that measurements were taken from the same position of each well. A pathway length correction for 100μL was applied to account for the distortion of light in liquid.

To calculate generation times, OD_{600} values from the start and end of the logarithmic growth phase were multiplied by $1X10^6$ to obtain an estimate of the total number of bacteria per well. The formula used to calculate generation time was:

$$\text{Generation time (minutes)} = \frac{\text{Time interval from start to end of logarithmic phase(minutes)}}{3.3 \times \log\left(\text{No.of bacteria at end of log phase} \Big/ \text{No.bacteria at start of log phase}\right)}$$

Where viable counts were required, an aliquot of 20μL of culture was taken and transferred to 180μL of sterile 1X PBS for serial dilutions. Cultures were diluted from 1:10 to $1:10^{15}$. Dilutions were plated and viable count was carried out by the Miles and Misra method (Miles *et al*., 1938). The formula used to calculate CFU/mL was:

$$\mathrm{CFU/mL} = \mathrm{CFU} \times \frac{1}{\mathrm{Aliquot}} \times \frac{1}{\mathrm{Dilution}}$$

2.1.2 Susceptibility of strains to AcrB substrates

The minimum inhibitory concentration (MIC) of each AcrB substrate was determined as described by the British Society of Antimicrobial Chemotherapy (BSAC) (Andrews, 2001). Doubling dilutions of the antibiotics and dyes were added to 20mL of Iso-Sensitest agar (Oxoid, UK, cat. no. CM0471) (Appendix II). Antibiotic stocks were prepared using the following formula:

The potency of the antibiotic was given by the manufacturer. The volume required was set to 10mL and the final concentration was 10,000μg/mL. Antibiotic powder was weighed on an analytical balance (Denver Instrument, USA, model no. TP214). The powder was transferred into a 10mL volumetric flask and dissolved in the appropriate solvent (Table 2.2).

An aliquot of 10μL of an overnight culture of each test strain grown in Iso-Sensitest broth (Oxoid, UK, cat. no. CM0473) was inoculated on to the agar surface and incubated for 20 to 24 hours at 37°C. *Escherichia coli* ATCC 25922 and *E. coli* NCTC 10418 were used as quality controls. The assay was validated by comparing the MICs of the control strains against the Piddock group internal MIC database and the EUCAST breakpoints (available at: http://www.eucast.org/clinical_breakpoints/).

Table 2.2 Plasmids used in this study.

Plasmid	Description	Temperature sensitive *oriC*	Antibiotic resistance marker	Origin
pUC19	Small plasmid (2.6 Kb) used as positive control for electroporations.	No	Amp^R	New England Biolabs (USA, cat. no. N3041S) (Transformed into culture collection strain I355)
pSLTS	Encodes λ-Red recombinase under the control of an arabinose-inducible promoter (*araBp*) and I-SceI under the control of a tetracycline-inducible promoter (*tetAp*)	Yes	Amp^R	Kim *et al*., 2014
pCP20	Encodes the Flp recombinase under the control of a heat inducible promoter	Yes	Amp^R Chl^R	Datsenko and Wanner, 2000
pWSK30*acrB* A1223C	Encodes AcrB from *S.* Typhimurium SL1344 with the D408A substitution	No	Amp^R	Constructed by Dr. Vito Ricci
pASK*acrAB*	Encodes AcrAB from *E. coli* K-12 MG1655	No	Amp^R	Marshall, 2017
pASK*acrA*+ *acrB*A1223C	Contains the wild-type sequence of *acrA* from *E. coli* K-12 MG1655 plus a mutated *acrB* gene which encodes AcrB with the D408A substitution	No	Amp^R	This study
pT2SK	Template plasmid used for the amplification of the kanamycin selection cassette	No	Amp^R Kan^R	Kim *et al*., 2014

pSIM18	Encodes λ-Red recombinase under the control of a heat-inducible promoter (*pL*)	Yes	Hyg^R	Datta *et al*., 2008
pACBSCE	Encodes I-SceI and λ-Red recombinase under the control of an *araBp*	Yes	Chl^R	Lee *et al*., 2009a
pMW82	Template plasmid used for the construction of promoter-*gfp* reporter strains	No	Amp^R	Lawler *et al*., 2013
pMW82+*ramAp-gfp*	Encodes the promoter region of *ramA* from *S.* Typhimurium SL1344 fused to *gfp*	No	Amp^R	Lawler *et al*., 2013
pMW82+*lexAp-gfp*	Encodes the promoter region of *lexA* from *S.* Typhimurium SL1344 fused to *gfp*	No	Amp^R	Constructed by Dr. Robert Marshall
pDiGc	Encodes a constitutively expressed GFP and DsRed under the control of *araBp*	No	Amp^R	Helaine *et al*., 2010
pDiGi	Encodes a IPTG-inducible GFP and a arabinose-inducible DsRed	No	Amp^R	Helaine *et al*., 2010

Amp^R indicates that the plasmid confers resistance to ≥50μg/mL of ampicillin; Chl^R, to ≥20μg/mL of chloramphenicol; Kan^R, to 50μg/mL of kanamycin and Hyg^R, to 100μg/mL of hygromycin.

2.2 Molecular biology techniques

2.2.1 Isolation of plasmids

All the plasmids used in this study are listed in Table 2.3. Plasmid isolation was carried out with the GeneJET Plasmid Miniprep Kit (Thermo Scientific, UK, cat. no. K0502).

Plasmid-containing strains were sub-cultured onto LB agar plates supplemented with the appropriate antibiotics and incubated overnight at 37°C (or 30°C when plasmids had a temperature-sensitive origin of replication, *oriC*) (Table 2.3). A single colony was used to inoculate 5mL of LB broth with antibiotic as required, followed by overnight incubation with aeration at the appropriate temperature. The culture was centrifuged at 3,600X*g* for 5 minutes in a Hereaus Megafuge 40R (ThermoFisher Scientific, UK) and the pellet was used for plasmid extraction according to the manufacturer's instructions. Plasmids were eluted with 50μL of nuclease-free water (ThermoFisher Scientific, UK, cat. no. 10977035) and stored at -20°C until use.

2.2.2 DNA sequencing of plasmids and PCR amplimers

Before sequencing, PCR amplimers were purified with the QIAquick PCR Purification kit (QIAGEN, Germany, cat. no. 28104) following the manufacturer's instructions. Plasmids extracted as described in section 2.2.1 were used directly for DNA sequencing.

The DNA concentration was quantified using a Nanodrop spectrophotometer (Thermo Scientific, UK). DNA (5-10 ng) was mixed with 0.32 pg/μL of a forward or a reverse primer and made to a final volume of 10μL in nuclease-free water. The

Table 2.3 Generic PCR cycling parameters using MyFi™ or MyTaq™ master mixes.

Step	Temperature	Time	Number of cycles
Initial denaturation	95 °C	5 minutes	1
Denaturation	95°C	30 seconds	30-35
Primer annealing	* °C	30 seconds	30-35
Extension	72 °C	1 minute per kb of amplimer	30-35
Final extension	72 °C	10 minutes	1

(*) annealing temperature varies depending on the melting temperature (Tm) of the primers. Annealing temperatures of 5°C below the Tm of the primer with the lowest Tm were used.

primer-DNA mixture was sequenced at the Functional Genomics Laboratory (The University of Birmingham, UK). Samples were labelled using the BigDye® Cycle Terminator Sequencing kit (Applied Biosystems, USA, cat. no. 4337455) and sequenced in an ABI 3730 Capillary sequencer (Applied Biosystems, USA).

Sequencing results were retrieved from an online repository. Chromatograms were visualised in SeqScanner 2 (Nucleics, Australia). Sequences were transformed to FASTA format and aligned to the reference sequence using the 'Align' tool from MEGA version 6 (Research Center for Genomics and Bioinformatics, Japan).

2.2.3 Preparation of electrocompetent cells

Bacteria were rendered electrocompetent by continuous washing in 15% glycerol. The glycerol solution was prepared by adding 150mL of glycerol (Fisher Reagents, USA, cat. no. BP229-1) to 850mL of distilled water. Concentrated glycerol was prewarmed at 37°C to facilitate pipetting. The solution was filter-sterilised through a 1L, 0.22μm pore, Stericup® Filter Unit (Merck Millipore, UK, cat. no. SCVPU11RE).

A 10mL aliquot of an overnight culture was used to inoculate 100mL of LB broth. Cultures were incubated at 37°C with aeration until an OD_{600} of 0.6-0.8 was reached. Cultures were immediately transferred into two 50mL centrifuge tubes (Greiner Bio-One, Germany, cat. no. 227261) and incubated on ice for 30 minutes. To pellet bacteria, tubes were centrifuged at 4,700X*g* for 15 minutes, at 4°C in a Hereaus Megafuge 40R (ThermoFisher Scientific, UK). The supernatant was discarded and the pellet was carefully resuspended in 20mL of ice-cold 15% glycerol to wash the bacteria. After three consecutive washes in 15% glycerol, pellets were resuspended in 1mL of 15% glycerol and transferred into two 1.5mL microcentrifuge tubes (Greiner

Bio-One, Germany, cat. no. 616201). A final centrifugation step was carried out at 15,000 X*g* in an Eppendorf® refrigerated microcentrifuge (Germany) at 4°C for 3 minutes to concentrate the bacterial cells. Pellets were resuspended in 500μL of glycerol and aliquoted into 100μL portions in ice-cold microcentrifuge tubes. Aliquots were stored at -80°C until use.

2.2.4 Electroporation

A 50μL aliquot of defrosted electrocompetent bacteria was added to an ice-cold electroporation cuvette (Geneflow, UK, cat. no. E6-0060). Plasmid or linear DNA was added to the cuvette, briefly mixed by pipetting and incubated on ice for 5 minutes before electroporation. Two additional cuvettes containing 5μL of nuclease-free water or purified pUC19 plasmid were used as negative and positive controls, respectively.

Electroporation was carried out in a Gene Pulser II electroporator (Bio-Rad, USA). An electric current at 2.5kV for *S.* Typhimurium or 1.8kV for *E. coli* was applied to the cuvette for 5 seconds. Electroporated bacteria were immediately transferred into 1mL of prewarmed LB broth, in a sterile universal tube (Starlabs, UK, cat. no. E1412-3010), and left to recover in an Innova® 44 shaking incubator (Eppendorf, Germany) at the appropriate temperature with aeration. Recovery time varied depending on the plasmid introduced. For transformation with pACBSCE, pMW82, pDiGi and pDiGc, electroporated bacteria were left to recover for 1 to1.5 hours at 37°C. For pSIM18 and pSLTS, transformants were left for 2 to 3 hours at 30°C. Conditions for introducing linear fragments of DNA are detailed in section 2.3.

After the recovery step, an aliquot of 100μL of culture was plated onto LB agar with the appropriate antibiotic to select for transformants (Table 2.3). An additional 100μL was plated onto LB agar without antibiotics to check that the electroporated bacteria were viable. The rest of the culture was concentrated by centrifugation in a Hereaus Megafuge 40R (2,800X*g*, 10 minutes) and plated onto a second LB agar plate with the appropriate antibiotic to maximise recovery of transformants.

2.2.5 Polymerase chain reaction (PCR)

PCRs were carried out using premade master mixes, in a Sensoquest thermocycler (Geneflow, UK). MyFi™ Mix (Bioline, UK, BIO-25049), which contains a high fidelity polymerase, was used for the construction of chromosomal mutants and sequencing reactions. MyTaq™ Red Mix (Bioline, UK, cat. no. BIO-25043) was used for all other PCRs.

A generic reaction mix comprised 12.5μL of master mix, 0.5μL of a 25μM primer stock of each primer and 1μL of template DNA. Reaction mixes were adjusted to a final volume of 25μL with nuclease-free water. Generic PCR cycling parameters are shown in Table 2.4.

Primers were ordered from Invitrogen (Table 2.5). Stock solutions of 100μM were prepared and diluted 1:4 in nuclease-free water to obtain a working concentration of 25μM. Primer stocks were stored at -20°C and thawed on ice when needed.

Table 2.4 Primers used in this study.

Primer number	Primer	Sequence (5' to 3')	Purpose
234	Eco acrB Fwd	CTGATCACCAGTGACGGCAT	Amplification of the *E. coli acrB* gene. Anneal up and downstream of *acrB.*
235	Eco acrB Rev	CGTATGAGATCCTGAGTTGG	
332	STm acrB Fwd	GGATCACACCTTATTGCCAG	Amplification of the *S.* Typhimurium *acrB* gene. Anneal up and downstream of *acrB.*
333	STm acrB Rev	CGGCCTTATCAACAGTGAGC	
2167	Kan pT2SK Fwd	CGTATCACGAGGCCCTT	Amplification of the kanamycin selection cassette for construction of mutation cassettes
2168	Kan pT2SK Rev	CACATGTTCTTTCCTGCG	
2151	STm AcrB D408A Fwd	GTTGTTGGGAACCTTTGCCG	Amplification of the region of *acrB* that has the A1223C mutation in *S.* Typhimurium
2152	STm AcrB D408A Rev	CCATCGCGATACCCACCA AT	
2165	STm HRF SM3*	AAGACATCTCGCCATCGGCTTGCTGGTGGA	Construction of the *S.* Typhimurium AcrB D408A mutation cassette
2166	STm HRF SM5 *	AAAAGGGCCCACGTTCTCGACCACCACGATGG	
2277	Eco A1223C Fwd	CCACAACGATGGCGGCATCCACCAACAGG	Construction of the *E. coli acrB* A1223C plasmid
2278	Eco A1223C Rev	CCTGTTGGTGGATGCCGCCATCGTTGTGG	
2279	Eco AcrB D408A Fwd	CTTCCCGTCGGGTCTGAAAA	Amplification of the region of *acrB* that has the A1223C mutation in *E. coli*
2280	Eco AcrB D408A Rev	AATCGGTTTCAGCATGGTGGC	
2281	Eco HRF SM5*	ACCGCTGCCACTCTTGAGATTTCTTCCGCCATAACACGC	Construction of the *E. coli* AcrB D408A mutation cassette
2282	Eco HRF SM3*	CTAAGCAGGGCGGGGCGTAAGTGCTCGCCATCGGCCTG	
429	ramA check-up Fwd	CCGCTTCCAGTAATGCTTGT	Amplification of the *S.* Typhimurium *ramA*::*aph* cassette. Anneal up and downstream of *ramA.*
430	ramA check-up Rev	GAATCATTGATGACCGCTGC	

(*) SM3 primers were used in combination with AcrB D408A Fwd primers. SM5 primers were used with AcrB D408A reverse primers.

Table 2.5 Antibiotics and dyes used in this study and their solubility.

Antibiotic/dye	Abbreviation	Chemical class	Catalogue number*	Compound purity/ Potency (%)	Solvent
Acriflavine	ACR	Dye	A8126	100	Water
Ampicillin	AMP	β-lactam	A9393	97	0.1M sodium bicarbonate
Carbenicillin	CAR	β-lactam	C1389	89	Water
Ceftazidime	CAZ	Cephalosporin	C3809	95.9	0.1M NaOH
Ceftriaxone	CTX	Cephalosporin	C5793	92	Water
Chloramphenicol	CHL	Chloramphenicol	C0378	98	70% methanol
Ciprofloxacin	CIP	Fluoroquinolone	C17850	98	Water with CH_3COOH
Erythromycin	ERY	Macrolide	E5389	95	70% ethanol
Ethidium bromide	ETBR	Dye	E7637	95	Water
Fusidic acid	FUS	Fusidane	F0881	98	Water
Gentamicin	GEN	Aminoglycoside	G1397	59	Water
Hygromycin B	HYG	Aminoglycoside	H7772	98	70% methanol
Kanamycin	KAN	Aminoglycoside	K1876	65	Water
Minocycline	MIN	Tetracycline	M9511	89-95	Water
Nalidixic acid	NAL	Quinolone	N8878	98	Water
Novobiocin	NOV	Aminocoumarin	N6160	85	Water
Oxacillin	OXA	β-lactam	O1002	81.5	Water
Rhodamine 6G	RHO	Dye	R4127	95	Water
Tetracycline	TET	Tetracycline	T3383	95	Water

(*) all compounds were purchased from Sigma, UK

2.2.6 PCR amplimer visualisation

To visualise PCR amplimers, an agarose (Fisher Bioeagents, Belgium, BP1356-500) gel was prepared in 1X Tris-Borate-EDTA (TBE) buffer (Sigma, USA, cat. no. T445). For amplimers with a size between 200bp to 10kb, a 1% agarose gel and a 1kb Hyperladder™ (Bioline, UK, cat. no. BIO-33053) were used; for amplimers smaller than 200bp, a 2% agarose gel and a 100bp Hyperladder™ (Bioline, UK, cat. no. BIO-33056) were used. To stain double-stranded (ds) DNA, Midori Green Advance (Nippon Genetics, Japan, cat. no. MG04) was added to the gel to a final concentration of 0.05μL/mL. Where needed, PCR amplimers were mixed with a 5X DNA Loading Buffer (Bioline, UK, cat. no. BIO-37045). Loading buffer was diluted 1:5 with amplimer.

Gels were electrophoresed at 100V for approximately 50 minutes in a horizontal gel electrophoresis tank (Cleaver Scientific, UK). Electrophoresed gels were transferred to a G:BOX gel documentation system (Syngene, UK), which uses a blue light transilluminator to visualise stained nucleic acids.

2.3 Construction of an *E. coli* K-12 MG1655 Δ*acrB* mutant

The *acrB*::*aph* cassette was PCR-amplified from a previously constructed *E. coli acrB::aph* mutant that was resistant to kanamycin but also had an additional ampicillin selection marker (Table 2.1). A colony lysate of this strain (1μL) was used as template DNA; the MyFi™ Master Mix and primers 234 and 235 (Table 2.5) were used for this PCR. A DpnI (NEB, USA, cat. no. R0176S) digestion was carried out to remove any template DNA.

To introduce the *acrB::aph* cassette into wild-type *E. coli* MG1655, a λ-Red helper plasmid, pSLTS, was transformed into MG1655 by electroporation. Transformants

were selected by plating onto LB agar with 100μg/mL of ampicillin (AMP100) (Table 2.2) at 30°C. Three colonies were restreaked on to LB AMP100 agar plates. Transformants were confirmed to be *E. coli* by Gram-staining and API-20E test and prepared for cryopreservation.

To induce expression of the λ-Red recombinase, a 5mL culture in LB AMP100 broth was prepared from a single colony of MG1655 carrying pSLTS. The culture was incubated overnight at 30°C with aeration. The overnight culture (1mL) was used to inoculate 100mL of fresh LB AMP100 broth. This culture was incubated in a shaking incubator for 1 hour at 30°C, 200rpm. To induce expression of the recombinase, L-arabinose (Sigma, USA, cat. no. A3256) was added to a final concentration of 2mM (200μL of a 1M arabinose solution). The culture was incubated for another 2 hours until an OD_{600} of 0.7-0.9 was reached. Bacteria were prepared for electroporation as indicated in section 2.2.3.

The *acrB::aph* cassette (50-100ng) was electroporated into the electrocompetent cells. Electroporated bacteria were incubated in a shaking incubator for 3 hours at 30°C, 200rpm, and plated onto LB agar with 50μg/mL of kanamycin (KAN50). Insertion of the *acrB::aph* cassette into the chromosome of MG1655 was confirmed by PCR with primers 234 and 235 (Table 2.4). In the wild-type, an amplimer of 3600bp was expected; whereas a 1500bp amplimer was expected in an *acrB::aph* mutant.

Removal of the selection marker was carried out as described by Datsenko and Wanner (2000). pCP20, an FLP helper plasmid, was transformed into the MG1655 *acrB::aph* mutant by electroporation. Transformants were selected on LB AMP50 agar plates and incubated at 30°C overnight. Ten colonies were restreaked on to LB AMP50

agar to confirm insertion of the plasmid. A single colony from each restreak was used to start an overnight culture in LB AMP50 broth. Overnight cultures were incubated in a shaking incubator at 43°C, 200rpm, to induce the expression of the flippase. A loopful of each culture was streaked onto LB agar plates without antibiotics and the plates incubated at 37°C for 24 hours. Two single colonies from each plate were replica-plated onto LB, LB AMP50 and LB KAN50 agar to confirm loss of pCP20 and excision of the *aph* gene. Colonies that grew on LB agar but not on agar containing antibiotics were screened by PCR (primers 234 and 235). A 600bp amplimer was expected from the Δ*acrB* mutant.

2.4 Construction of an AcrB D408A chromosomal mutant

A modified version of the method described by Kim *et al*. (2014) was used for the construction of the chromosomal mutant. The method consists of two steps: 1) insertion of a mutation cassette into the chromosome of the target organism mediated by a plasmid encoded λ-Red recombinase, followed by 2) the excision of the selection marker from the inserted cassette by a plasmid-encoded I-SceI meganuclease and the repair of the double strand break by the bacterial RecA system.

The mutation cassette comprises a selection cassette and two homologous recombination fragments (HRFs). The selection cassette is formed of an I-SceI restriction site followed by the *aph* kanamycin resistance gene, which served as the selection marker during the first step of the procedure. HRFs are two fragments of the target gene carrying the single nucleotide substitution, located at the 5'-end and 3'-end of the selection cassette, respectively. To facilitate the repair of the double strand

break during the second step of the procedure, the 5'- HRF contained 20 bp of homology to the 3'- HRF and *vice versa*.

2.4.1 Construction of a plasmid encoding AcrB D408A

To obtain the HRFs, a plasmid carrying the mutated *acrB* gene was required. The plasmid encoding the *S.* Typhimurium AcrB D408A substitution was previously constructed by Dr. Vito Ricci using a pWSK30 backbone. The QuikChange® Lightning Site-Directed Mutagenesis kit (Agilent Technologies, USA, cat. no. 210518) was used for its construction.

To construct the plasmid encoding the *E. coli* AcrB D408A, a pASK plasmid carrying wild-type *acrAB* was used (donated by Dr. Robert Marshall). Primers were designed using the QuikChange® Primer Design Program (available at: https://www.genomics.agilent.com/primerDesignProgram.jsp). The sequence of *acrB* from *E. coli* K-12 MG1655 was introduced into the program and the A at position 1223 was chosen to be substituted by C, this mutation translated into the AcrB D408A substitution. As *acrB* is encoded in the reverse strand, the A1223C mutation appears as a T→G substitution in whole genome sequencing.

The kit was used according to the manufacturer's instructions. In brief, 75ng of plasmid was added to a reaction mix containing 125ng of each primer plus the other components in the kit. Nuclease-free water was added to make a final volume of 50μL. A PCR was carried out to introduce the A1223C mutation into the plasmid, followed by DpnI (provided with kit) digestion to remove the template plasmid. Plasmids carrying the mutation were transformed into XL10-Gold Ultracompetent Cells (Agilent Technologies, USA, cat. no. 200315).

Transformants were plated onto LB AMP100 agar. Ten colonies were picked randomly for plasmid extraction and DNA-sequenced to confirm that the A1223C mutation had been introduced. Plasmids carrying the mutated *acrB* sequence were stored at -20 °C until use.

2.4.2 Construction of the mutation cassette

The construction of the mutation cassette was carried out as described previously (Kim *et al.*, 2014). The same procedure was used to construct the *S.* Typhimurium and *E. coli* AcrB D408A mutation cassettes.

The kanamycin-resistance selection cassette was amplified from pT2SK (Addgene, USA, cat. num. 59383). Plasmids expressing AcrB D408A (section 2.4.1) were used as templates for amplification of the region of *acrB* containing the point mutation. Two fragments of ~150bp were amplified and used HRFs. The *acrB* A1223C mutation was located within the 20 bp of homology between the two HRFs to maximise chances of retaining the single nucleotide polymorphism (SNP) after activation of the bacterial RecA system.

Amplimers were cleaned and quantified as described in section 2.2.2. Selection cassette (75fmol) plus 125fmol of each one of the HRFs were made up to 10μL in nuclease-free water. Gibson assembly Master Mix (NEB, UK, cat. num. E5510S) (10μL) was added to the mixture and incubated for 1 hour at 50°C in a Sensoquest thermocycler.

A 4μL aliquot of the assembled product was mixed with 1μL of 5X loading buffer and electrophoresed in a 1% agarose gel to confirm the correct assembly of the mutation

cassette. The selection cassette (5μL) was electrophoresed next to the assembly mix to detect traces of selection cassette that was not assembled. When residual, unassembled, selection cassette was observed, the assembled cassette was gel-purified. In brief, the total volume of the Gibson assembly product (16μL) was electrophosed in a 1% agarose gel for 1 hour at 80V and the mutation cassette band was cut out from the gel using a clean scalpel (Swann-Morton, UK) and an UltraSlim LED transilluminator (Syngene, UK). DNA was recovered from excised gel fragments with the QIAquick Gel Extraction kit (QIAGEN, Germany, cat. no. 28704) and the purified product was eluted in 35μL of nuclease-free water. To confirm its correct assembly, the assembled mutation cassette was sent for sequencing at the Functional Genomics Facility (University of Birmingham, UK) (section 2.2.2). The final assembled mutation cassette was amplified by PCR and stored at -20°C until use.

2.4.3 Insertion of the mutation cassette into the chromosome

2.4.3.1 In *S.* Typhimurium

A previously constructed *S.* Typhimurium SL1344 transformant harbouring pSIM18 was used for this step. pSIM18 is a λ-Red helper plasmid that expresses the λ-phage recombinase under the control of a heat activated promoter.

S. Typhimurium SL1344 + pSIM18 was streaked onto a LB agar plate with 100μg/mL of hygromycin (HYG100) and incubated overnight at 30°C. A single isolated colony was used to inoculate 5mL of LB HYG100 broth, incubated overnight at 30°C, shaking at 200 rpm. The overnight culture was used to inoculate 100mL of LB HYG100 broth, which was incubated under the same conditions as the overnight culture until an OD_{600}

of 0.3 was reached. The culture was transferred into two 50mL centrifuge tubes and incubated in a 42°C water bath for 15 minutes to induce the expression of λ-Red recombinase. Cultures were incubated on ice for 10 minutes and rendered electrocompetent as described in section 2.2.3. Electrocompetent bacteria were resuspended in a final volume of 100μL.

The mutation cassette (50-100ng) was added to 40μL of electrocompetent bacteria in a pre-chilled electroporation cuvette. Additionally, 75-100ng of a *ramA*::*aph* cassette, amplified from a previously constructed SL1344 *acrB::aph,* was added to a second electroporation cuvette and used as positive control for recombination. Electroporated bacteria were immediately recovered in 400μL of SOC (Appendix I) and transferred into a universal tube. Recombinants were incubated at 37°C for 2 hours, with aeration. Bacteria were concentrated by centrifuging at 2,800X*g* for 10 minutes, the supernatant was discarded and the pellet was resuspended in 100μL of LB. The total amount of bacteria was plated on to an LB KAN50 agar plate and incubated at 37°C for 24 hours.

Five colonies were re-streaked onto a LB KAN50 plate and a colony PCR was carried out to determine whether the mutation cassette had inserted correctly.

2.4.3.2 In E. coli

Insertion of the mutation cassette into the chromosome of *E. coli* MG1655 was carried out as described in section 2.3. Recombinants were plated on to LB AMP50 KAN50 plates and incubated for 48 hours at 30°C to maintain pSLTS for the following step.

2.4.4 Deletion of the selection marker

2.4.4.1 In *S.* Typhimurium

Excision of the kanamycin selection cassette from the chromosome of *S.* Typhimuruim SL1344 was carried out with pACBSCE as described by Lee *et al*. (2009a). pACBSCE encodes the I-SceI meganuclease and λ-Red recombinase under the control of an arabinose-inducible promoter. The plasmid also contains the I-SceI restriction site near its origin of replication. Therefore, expression of I-SceI will cure the plasmid from the carrier strain.

The strain containing the mutation cassette was rendered electrocompetent and transformed with pACBSCE as described in sections 2.2.3 and 2.2.4. Transformants were selected by plating onto LB agar supplemented with 20μg/mL of chloramphenicol (CHL20).

The transformed strain was re-streaked onto LB CHL20 agar and a single isolated colony was used to inoculate 5mL of LB CHL20 KAN50 broth. To avoid leaky expression of I-SceI, glucose (Teknova, USA, cat. no. G0521) was added at a final concentration of 0.5%. The culture was incubated overnight at 37°C with aeration and a 10μL aliquot was used to inoculate 1mL of LB CHL20 KAN50 broth. The culture was incubated in a shaking incubator at 37°C, 200 rpm, for 2 hours, followed by centrifugation for 5 minutes at 3,500X*g* to remove antibiotics from the medium. The pellet was resuspended in LB broth without antibiotics and the centrifugation was repeated to ensure removal of antibiotics. Finally, the pellet was resuspended in LB supplemented with 0.5% of arabinose and the culture was incubated for 3 hours at 37°C, with aeration. A 20μL aliquot was used to prepare serial dilutions from 1:10 to $1:10^8$, in 180μL of 1X PBS. One hundred μL of each dilution was plated onto LB agar

plates without antibiotics. The dilution that contained between 50 to 100 colonies was chosen for negative selection.

All colonies were replica-plated on to LB, LB KAN50 and LB CHL20 to select mutants that have lost the selection marker (did not grow on KAN50) and pACBSCE (did not grow on CHL20). Colonies that only grew on LB were screened by PCR for loss of the mutation cassette and PCR amplimers were sequenced at the Functional Genomics Laboratory (University of Birmingham, UK) to confirm correct insertion of the *acrB* A1223C mutation.

To confirm that mutant candidates were not contaminated, an API-20E strip was inoculated with a suspension made from each candidate. The strip was filled according to manufacturer's instructions and interpreted and incubated at 37°C.

2.4.4.2 In E. coli

Five recombinants carrying pSLTS were streaked on to LB AMP50 KAN50 agar plates and incubated overnight at 30°C. One colony from each plate was resuspended in 500μL of sterile 1X PBS in a 1.5mL microcentrifuge tube. The suspension was vortexed briefly and 100μL of each suspension was plated on to LB AMP50 supplemented with 100ng/mL of anhydrotetracycline (aTET100) (Acros Organics, USA, cat. no. 233131000) to induce expression of I-SceI. An additional 100μL was platted onto LB AMP100 agar plates as a culture viability control.

Plates were incubated at 30°C for up to 48 hours. Only a few colonies were expected in the LB AMP100 aTET100 plates as the I-SceI endonuclease induces a lethal double-stranded break with a very low efficiency of recovery (Kim *et al*., 2014).

Four colonies per plate were replica-plated onto LB and LB KAN50 plates to check for loss of kanamycin resistance. Plates were incubated overnight at 37°C to allow plasmid curing. Colonies that only grew on LB agar were screened for loss of the selection marker by amplifying the *acrB* gene. The wild-type *acrB* is 3.6Kb, whereas *acrB* with the selection marker is 5.1Kb. Colonies in which *acrB* was the correct size were streaked onto LB, LB AMP50 and XLD agar plates to check for loss of pSLTS and loss of AcrB efflux function, respectively. Plates were incubated overnight at 37°C. Mutants that did not grow on LB AMP50 and grew poorly on XLD agar were confirmed to be *E. coli* by Gram-staining and API-20E. *acrB* was amplified from the candidate *E. coli* mutants and DNA-sequenced to confirm insertion of the SNP into *acrB.*

2.5 Whole genome sequencing (WGS) and data analysis

The *S.* Typhimurium SL1344 and AcrB D408A chromosomal mutants were sent to Microbes NG (University of Birmingham, UK) for WGS. The *E. coli* K-12 and *acrB* mutants were sent to the Beijing Genomics Institute (BGI) (Hong Kong) for sequencing.

Bioinformatics analyses were carried out on the Galaxy online platform. Raw reads were trimmed using Trimmomatic. Twenty bp was trimmed from the start of the sequence to remove linkers. Quality of the trimmed sequences were assessed by FASTQC. Where required, an additional 10bp was removed from the end of the sequence where the quality of the reads start to decrease. On average, trimmed reads were approximately 100bp. Reference genomes and annotations were download from either EnsemblBacteria or the Genbank. The assemblies used were FQ312003.1 and U00096.3 for *S.* Typhimurium SL1344 and *E. coli* K-12 MG1655, respectively.

For *S.* Typhimurium, reads were aligned and mapped to the reference genome using Bowtie2, which generates a BAM file of the assembled genome. The BAM file was run through BamLeftAlign to align indels in order to detect insertions or deletions. Finally, variant calling was carried out using MPileup, which compares two assemblies and generates a list of all differences and their locations in the genome. The wild-type strain was compared against the reference genome, while the mutant was compared against the assembled wild-type genome and the reference genome, separately.

To validate any SNPs, deletions and insertions, BAM files were viewed on Artemis (Sanger Institute, UK). The location of the variant was identified and the sequence of the mapped reads was verified manually.

For *E. coli*, variant calling was carried out using Snippy on the Cloud Infrastructure for Microbial Bioinformatics (CLIMB) portal. Snippy comprises all the steps up to variant calling in one program and provides the list of variants and BAM files. As with *S.* Typhimurium assemblies, all variants were confirmed manually on Artemis.

acrB is encoded in the reverse strand; therefore, the A1223C mutation appears as a T→G substitution in WGS.

2.6 Western blot of AcrB

Protein samples from *S.* Typhimurium SL1344, *E. coli* MG1655 and their respective Δ*acrB* and chromosomal AcrB D408A mutants were prepared from exponential phase cultures (OD_{600}=0.6). To prepare the cultures, 5mL of LB broth was inoculated with a single colony of the respective strain. The overnight culture was used to inoculate fresh

LB broth. Cultures were incubated in a shaking incubator at 37°C, 200 rpm, until an OD of 0.6 was reached.

Bacteria were harvested by centrifuging at 3,500X*g* for 10 minutes, at 4°C in a Hereaus Megafuge 40R. Pellets were resuspended in 1mL of 10mM Tris-EDTA buffer (Fluka, USA, cat. no. 93283) with 100μg/mL of lysozyme (Sigma, USA, cat. no. L6876). Resuspended pellets were incubated on ice for 30 minutes.

Sonication was carried out using a SoniPrep 150 sonicator (SANYO, Japan). To lyse bacteria, four cycles of 30 seconds sonication plus 30 seconds rest were carried out. Protein preparations were centrifuged at 3,500X*g* for 10 minutes, at 4°C, to remove cellular debris. The supernatant was recovered and stored at -20°C until use.

The protein concentration was quantified using the Qubit™ Protein Assay Kit (Invitrogen, UK, cat. no. Q33221) according to the manufacturer's instructions. This kit provides a fluorescent dye that stains proteins and allows their quantification using a specialised fluorometer. In brief, a working solution was prepared by diluting the dye 1:200 in the provided buffer. The protein preparation (1μL) was added to 199 μL of working solution in a Qubit assay tube (Invitrogen, UK, cat. no. 32856). Standards were prepared by adding 10μL of each standard to 190μL of working solution. All samples were incubated for 30 minutes at room temperature and read in a Qubit 3 Fluorometer (Invitrogen, UK).

Protein samples (10μg) were electrophoresed on a 4-12% NuPAGE® Bis-Tris gel (Life Technologies, USA, cat. no. NP0321BOX) and transferred onto a nitrocellulose membrane using the iBlot® system (Thermo Fisher Scientific, UK) for 7 minutes. The membrane was washed 3 times in 1X TBS pH 7.6 buffer (Appendix I) and blocked by

incubating for 1 hour at room temperature with a 5% skim milk (Sigma-Aldrich, UK, cat. no. 70166) solution in TBS buffer. The blocked membrane was washed three times with TBS 1X and incubated with rabbit anti-AcrB primary antibody (donated by Dr. Helen Zgurskaya, The University of Oklahoma, USA) for 1 hour, followed by a one hour incubation with anti-rabbit IgG secondary antibody linked to horseradish peroxidase (HRP) (Cell Signaling Technology, USA, cat. no. 7074S). The blot developed with the Westar Supernova chemiluminescent substrate kit (Cyanagen, Italy, cat. no. XLS3,0100).

A second blot, prepared at the same time, was incubated with a mouse anti-Enterobacteriaceae RNA polymerase β-subunit primary antibody (BioLegend, USA, cat. no. 664602), followed by an HRP-linked anti-mouse IgG secondary antibody (Cell Signaling Technology, USA, cat. no. 7076S). This blot was used to normalise the amount of AcrB to the amount of total protein per sample, as RNA polymerase is constitutively expressed and its expression levels are not affected by changes in AcrB.

Blots were analysed with the GeneSys program (Syngene, USA); the concentration of AcrB was determined by the intensity of the band given by the number of pixels.

2.7 Accumulation and efflux assays of two AcrB substrates

2.7.1 Hoescht 33342 (bis-benzimide) accumulation assay

Hoescht 33342 (H33342) is a dye that fluoresces when intercalated with DNA. Accumulation of H33342 in bacteria can be measured by monitoring fluorescence over time, which gives an indication of membrane permeability (Blair and Piddock, 2016). The assay was carried out as described by (Coldham *et al*., 2010). A 4% inoculum of an overnight culture was added to 10mL of prewarmed LB broth. Cultures were

incubated at 37°C, under aeration until an OD_{600} of 0.5 was reached. Bacteria were immediately pelleted by centrifugation at 3,500X*g* for 10 minutes and resuspended in sterile Dulbecco's PBS (DPBS) (Sigma, USA, cat. no. D8537). The OD_{600} of the resuspended cultures was measured and all cultures were adjusted to a starting OD_{600} of 0.1 in 1X PBS. Aliquots of 180μL of each adjusted culture were added in triplicate into a black 96-well plate (Corning, USA, cat. no. 3991). Three wells each containing either sterile PBS or heat treated (boiled) bacteria were used as blank and positive control, respectively. The initial fluorescence of the aliquots was measured every minute for three minutes; subsequently, 20μL of a 25μM solution of H33342 (Sigma-Aldrich, UK, cat. no. B2261) was injected into each well to make a final concentration of 2.5μL. Fluorescence was measured every minute for 100 minutes in a FLUOstar Optima microplate reader. An excitation wavelength of 350-10nm with a 460nm emission filter were used. The gain was adjusted to 2315.

2.7.2 Ethidium bromide efflux assay

This method consists of preloading bacteria with ethidium bromide (ETBR), followed by activation of efflux via addition of glucose. Efflux is then monitored by a decrease in fluorescence. Cultures were incubated in the same way as described in section 2.7.1. Bacteria were harvested at an OD_{600} of 0.4, washed in 0.1M PPB (Annex I) by centrifugation (3,500X*g* for 10 minutes) and resuspended in 10mL PPB with 50μg/mL of ethidium bromide ETBR (Sigma, USA, cat. no. E8637) and 100mM of carbonyl cyanide *m*-chlorophenyl hydrazone (CCCP) (Alfa Aesar, UK, cat. no. L06932). Resuspended cultures were incubated for 1 hour at room temperature (~22°C) to allow ETBR to accumulate intracellularly. ETBR and CCCP were removed by centrifugation

(2,500X*g* for 10 minutes at room temperature); cultures were resuspended in 3mL of 0.1M PPB and an aliquot of 180μL was added to a black 96-well plate. Three wells each containing PPB or boiled bacteria were used as blank and positive control, respectively. The initial fluorescence was measured for three minutes, followed by injection of 20μL of a 100mM glucose solution (Sigma, USA, cat. no. G8270) (final concentration of 25mM) to energise the bacteria and activate efflux. Fluorescence was measured every minute for 60 minutes in a FLUOstar Optima microplate reader. An excitation wavelength of 545-10nm with a 600-10nm emission filter were used. The gain was adjusted to 1460.

2.8 Transcriptomic analysis

2.8.1 RNA extraction

A total of six overnight cultures of each test strain were prepared by inoculating 5 mL of MOPS or LB broth with a single colony of the respective strain. Each colony represented a biological replicate. Overnight cultures (4% for MOPS or 0.1% for LB) were used to inoculate 10mL of fresh, prewarmed media. Cultures were incubated at 37 °C, shaking at 200 rpm, in a shaking incubator until an OD_{600} of 0.6 was reached in MOPS, or for 10 hours when RNA was extracted from stationary phase cultures (LB).

Aliquots of 2 mL of each culture were quenched by snap-freezing in liquid nitrogen or by pipetting a 2:5 proportion into a 95% ethanol:5% phenol mixture. For snap-freezing, cultures were aliquoted into a 2mL microcentrifuge tube (Thermo Scientific, UK, cat. no. 69720) and centrifuged for one minute at 13,000X*g* at 4°C. Supernatants were removed and pellets were transferred into liquid nitrogen. Cultures quenched with

phenol:ethanol were incubated on ice for 30 minutes, followed by centrifugation at 3,500X*g* for 10 minutes to pellet bacteria and remove the quenching solution. Quenched cultures were immediately stored at -80°C until use.

For cultures grown in MOPS to an OD_{600} of 0.6, RNA was extracted from samples quenched by snap-freezing. The SV Total RNA kit (PROMEGA, UK, cat. no. Z3100) was used. Bacterial pellets were resuspended in 200μL of Ambion® TE buffer (Invitrogen, UK, AM9849) with 50μg/mL of lysozyme (Sigma, USA, cat. no. L6876). Resuspended pellets were incubated in a heat block at 25°C for 5 minutes to lyse bacteria.

Extraction of good quality RNA from stationary phase cultures grown in LB was carried out using the RNeasy mini kit (QIAGEN, Germany, cat. no. 74104) due to complications obtaining good quality RNA with other kits. RNA was quenched and extracted as described by Kröger *et al*. (2013).

The concentration of RNA and DNA in the samples was assessed using the Qubit™ High Sensitivity RNA and dsDNA kits (Invitrogen, UK, cat. no. Q32852 and Q32854), respectively. Working solutions and standards were prepared as described in section 2.6 for the protein samples. A minimum of two consecutive DNase treatments with the TURBO DNA-free™ kit (Invitrogen, UK, cat. no. AM2238) were carried out to remove residual DNA. Concentration of DNA in samples was monitored after each DNase treatment until the concentration of DNA did not decrease further. To confirm that DNA was successfully removed, a PCR was carried out using primers 938 and 939 (Table 2.6) for *S.* Typhimurium samples or primers 2432 and 2433 for *E. coli* samples.

2.8.2 RNA quality assessment

The quality of the extracted RNA was assessed using a NanoDrop spectrophotometer (Thermo Scientific, UK). This provides an indication of the purity of the RNA by measuring absorbance of RNA at 260 nm, proteins at 280 nm and of any chemical contaminants such as carbohydrates and phenol at 230 nm. The 260/280 ratio indicates contamination by proteins; whereas the 260/230 ratio provides an indication of chemical contamination. A value ≥1.8 for both ratios indicates that the RNA is pure.

A preliminary test to assess the integrity of the extracted RNA, samples were electrophoresed in a 1% agarose gel to visualise the 16S and 23S rRNA bands. Smearing of the bands was used as an indication of RNA degradation. RNA integrity was further assessed using the Agilent 2100 Bioanalyzer (Agilent Genomics, USA), a microfluidics system that provided a chromatogram of the RNA samples. The Agilent RNA 6000 Nano kit (Agilent Genomics, USA, cat. no. 5067-1511) was used. The kit provides a gel and a fluorescent dye that allows to quantify and determine the integrity of the RNA. Gel, dye and marker were prepared and loaded according to the manufacturer's instructions. Twelve samples were loaded on to each RNA Nano chip.

The Bioanalyzer provides a 16S/23S ratio based on the size of the 16S and 23S peaks. A ratio ≥1.0 indicates high RNA integrity. The system also calculates an RNA Integrity Number (RIN) using a built-in algorithm. A RIN ≥7.0 and a flat baseline are indicative of high RNA integrity. In *S.* Typhimurium, the 16S/23S ratio and RIN were disregarded and a flat baseline was used as the only indication of non-degraded RNA. This is due to the system being unable to properly recognise *S.* Typhimurium SL1344 rRNA peaks due to multiple rRNA peaks, thus providing inaccurate 16S/23S ratios and RINs (Bhagwat *et al*., 2013).

2.8.3 RNA-sequencing (RNA-seq) library assembly

Good quality RNA samples were sent to the Beijing Genomics Institute (BGI, Hong Kong) for library construction and quantification of total RNA.

rRNA depletion, RNA fragmentation and cDNA synthesis were carried out by BGI according to their standard operation procedures. An aliquot of 1μg of each RNA sample was used. Library construction was validated by measuring the average length of cDNA in the constructed library in an Agilent 2100 Bioanalyzer, using the Agilent DNA 1000 kit (Agilent Technologies, USA, cat. no. 5067-1504). Quantification of cDNA by real-time quantitative PCR (qPCR) was also carried out with a TaqMan Probe according to BGI standard procedures.

Finally, libraries that passed validation were pair-end sequenced in an Illumina HiSeq 4000 System by BGI.

2.8.4 Bioinformatics to determine differential gene transcription between wild-type and mutants

Analysis of the RNA-seq data for the wild-type strains and their AcrB D408A mutants was carried out in collaboration with Dr. Alasdair Ivens (The University of Edinburgh, UK). Quality of the raw RNA-seq data was analysed by FASTQC. Cutadapt software version 1.9 was used to remove poly-A tails. Bowtie2 was used to map trimmed sequences on to reference genomes. Accession numbers of genomes used were F1312003.1, HE654724, HE654725 and HE654726 for *S.* Typhimurium SL1344 and its three plasmids. For *E. coli* MG1655, the reference genome used was U00096.3. All references were downloaded from the European Nucleotide Archive (ENA) at the European Bioinformatics Institute (EBI). Data normalisation was carried out by scale-

normalising all datasets to the one with the lowest number of mapped reads (counts), counts per gene were converted to log2 and quantile normalised to make datasets comparable. Gene transcription comparisons were carried out using normalised data with the Bioconductor *limma* package. The *limma* package integrates linear modelling and a variety of statistical principles, including the empirical Bayes method, to assess differential gene expression between two RNA-seq datasets (Ritchie *et al*., 2015).

At Birmingham, differentially transcribed genes per species were classified into functional groups using the Clusters of Orthologous Groups (COG) database. COG functional annotations were downloaded from the MicroScope Microbial Genome Annotation and Analysis Platform (http://www.genoscope.cns.fr/agc/microscope/home/index.php).

2.8.5 Validation of RNA-seq data

Significant changes in transcription were validated by quantitative real-time PCR (qRT-PCR) and GFP transcriptional fusion reporters.

2.8.5.1 cDNA synthesis

For experiments carried out with exponential phase cultures (OD_{600} of 0.6), cDNA was synthesised using the SuperScript™ II Reverse Transcriptase. A mixture of 1μg of RNA, 50ng of random hexamers (Thermo Scientific, UK, cat. no. S0142) and 10mM of a dNTP mix (Invitrogen, UK, cat. no. 10297-018) was prepared. The RNA mixture was heated at 65°C for 5 minutes to allow alignment of random hexamers to RNA, followed by 5 minutes incubation on ice. First strand buffer (4μL), 2μL of DTT (dithiothreitol) and 1μL of RiboLock RNase inhibitor (Thermo Scientific, UK, EO0381)

were added to the RNA mix. The reaction mix was incubated for 2 minutes at 23°C before adding 1μL of reverse transcriptase. The final reaction mixture (20μL) was incubated at 42°C for 50 minutes, then 70°C for 15 minutes.

For experiments carried out with stationary phase cultures, cDNA was synthesised with SuperScript™ IV Reverse Transcriptase (Invitrogen, UK, cat. no. 18090010). This enzyme was used instead of SuperScript™ II due to its higher sensitivity. The amount of RNA available in stationary phase cultures was considerably lower than in exponential phase cultures; therefore, a highly sensitive reverse transcriptase was required to obtain cDNA from all transcripts. This was not necessary for RNA-seq as an enrichment step was used.

The RNA mixture was prepared by adding 1μg of RNA to 50μM of random hexamers and 10mM of a dNTP mix. The RNA mixture was heated at 65°C for 5 minutes and incubated on ice for 5 minutes. Next, 4μL of the 5X SSIV buffer was added alongside 1μL of DTT, 1μL of RNase inhibitor and 1μL of reverse transcriptase. The reaction mixture was incubated at 23°C for 10 minutes, followed by 10 minutes at 52.5°C and 10 minutes at 80°C to inactivate the enzyme.

Synthesis of cDNA was confirmed by using 1μL of cDNA as template for a PCR with primers 2406 and 2407 (Table 2.6) for *S.* Typhimurium samples or primers 2432 and 2433 for *E. coli* samples. Aliquots of 5μL of cDNA were prepared and frozen at -20°C until use.

2.8.5.2 Quantitative real-time reverse transcription PCR (qRT-PCR)

The normalised expression ($\Delta\Delta C_T$) method was used to determine transcription levels by qRT-PCR (Pfaffl, 2001). This method calculates transcription levels of a gene of interest by normalising against the number of transcripts of one or more housekeeping genes. To decrease chances of erroneous normalisation, two housekeeping genes were used in all qRT-PCRs. Housekeeping genes were chosen from a list of previously validated genes (Rocha *et al*., 2015), based on the differential gene transcription profile obtained from the RNA-seq data. For cDNA obtained from mid-logarithmic *S.* Typhimurium cultures and stationary phase *E. coli* cultures, *gyrB* and 16S rRNA were used as housekeeping genes. For stationary phase cultures of *S.* Typhimurium, *rpoD* and *rho* were used.

qRT-PCR reactions were prepared with iQ™ SYBR® Green Supermix (BIO-RAD, Singapore, cat. no. 170-8882). cDNA (1μL) was mixed with 12.5μL of supermix, 500nM of each primer and 9.5μL of nuclease-free water to make a 25μL reaction.

Reactions were prepared in a 96-well plate (Starlabs, USA, E1403-0209), covered with a sealing film (Starlabs, USA, cat. no. E2796-9793) to avoid evaporation of the reaction mixture. qRT-PCRs were carried out in a CFX96 Real-Time thermocycler (Bio-rad, USA). The transcription levels of genes of interest were measured using a minimum of three biological replicates with two technical replicates each, per strain. Data was analysed on the CFX manager software (Bio-Rad, USA).

Table 2.6 qRT-PCR primers used in this study.

Primer number	Primer	Sequence (5' to 3')	Target gene	Organism
324	16srRNA Fwd	CCTCAGCACATTGACGTTAC	*16S rRNA*	*S.* Typhimurium and *E. coli*
325	16srRNA Rev	TTCCTCCA ATCTCTACGCA		
1992	gyrB STm RT Fwd	GTATCGGCGTGGAAGTAG	*gyrB*	*S.* Typhimurium
1993	gyrB STm RT Rev	TGCGGAATGTTGTTGGTA		
1057	acrB STm RT Fwd	GTCCTCAAGTAGCTTCCT	*acrB*	*S.* Typhimurium
1058	acrB STm RT Rev	GTAATCCGAAATATCCTCCTG		
1059	acrF STm RT Fwd	GTTCCTGTCGTGTTGCTA	*acrF*	*S.* Typhimurium
1060	acrF STm RT Rev	CAAACATCGTCAGGGTATTG		
1055	acrD STm RT Fwd	CCTTTGTCAAAGCCTCGATTATC	*acrD*	*S.* Typhimurium
1056	acrD STm RT Rev	CAGGAACAGATACATCACCAG		
1053	rob STm RT Fwd	AGTGCTTTATGGGCTTAATGAAA	*rob*	*S.* Typhimurium
1054	rob STm RT Rev	AAGTATTCTATACCACCGCACT		
1672	acrR STm RT Fwd	GTCGGATTTATTCAGTGA	*acrR*	*S.* Typhimurium
1673	acrR RT RT R	CTCTTAATACAGATAGTGGAT		
2058	envR STm RT Fwd	ATAATGGTATGATATCGGAACAG	*envR*	*S.* Typhimurium
2059	envR STm RT Rev	TATGACATCCAGATCAAGACT		
934	marA STm RT Fwd	CAACACTGACGCTATTACTA	*marA*	*S.* Typhimurium
935	marA STm RT Rev	CAGGTGCCATTTGGAA		
938	ramA STm RT Fwd	TGAATCAGCCGTTACG	*ramA*	*S.* Typhimurium
939	ramA STm RT Rev	AGACTCTCCCCTTTGTA		
1792	emrA STm RT Fwd	GCTACTTCTTACCTTGCTCTT	*emrA*	*S.* Typhimurium
1793	emrA STm RT Rev	GCATCATCTGTCTCTTCAATATG		
956	livJ STm RT Fwd	CAACGGCGGCAAAGTATA	*ilvJ*	*S.* Typhimurium
957	livJ STm RT Rev	CGTACTGCTGCTTATCGT		
964	trpA STm RT Fwd	CAGCCATTGTCAAGATTATCG	*trpA*	*S.* Typhimurium
965	trpA STm RT Rev	CTGAGACAAAGGACCTGAG		
752	flgC STm RT Fwd	CCGGAAAAGCTGGTTTATGA	*flgC*	*S.* Typhimurium
753	flgC STm RT Rev	GCTGACATCGTGTTGACCAT		
2295	fliA STm RT Fwd	ATACCAACAACAGCCAACT	*fliA*	*S.* Typhimurium
2296	fliA STm RT Rev	ATCGCATCCATTACCCGC		

924	glnP STm RT Fwd	CCATCCGCCATGTTAT	*glnP*	*S.* Typhimurium
925	glnp STm RT Rev	AACAATAAACAACGAGGT		
956	nirC STm RT Fwd	TAACTGGCTGGTTTGTCT	*nirC*	*S.* Typhimurium
927	nirC STm RT Rev	CACCACCAGATAGCAAGA		
2293	pipC STm RT Fwd	ATTGATGATGGGATACAGGTT	*pipC*	*S.* Typhimurium
2294	pipC STm RT Rev	GCAAAGTCAGGATGTCGT		
1761	rpoD STm RT Fwd	CACTGTTGAACTGTTGAC	*rpoD*	*S.* Typhimurium
1762	rpoD STm RT Rev	CATTGAACCTGGTTGATC		
2450	rho STm RT Fwd	GGTTGAACACAAGAAAGACG	*rho*	*S.* Typhimurium
2451	rho STm RT Rev	TCAATACTTTACCGGAAGCC		
2398	CsrB STm RT Fwd	TTACAAGGAAAGGCTTCAGG	CsrB sRNA	*S.* Typhimurium
2399	CsrB STm RT Rev	CCCGATGTGATAGCTTCTTC		
2400	fliC STm RT Fwd	TGGCACAAGTAATCAACACT	*fliC*	*S.* Typhimurium
2401	fliC STm RT Rev	GATACGCAGACCAGAAGAC		
2402	SL0699 STm RT Fwd	TCACTACAGACATCGCCTTA	SL0699	*S.* Typhimurium
2403	SL0699 STm RT Rev	CCTGACAACAGTAATCCCAG		
2404	pduE STm RT Fwd	TGAAATCTACAACGCCCTTC	*pduE*	*S.* Typhimurium
2405	pduE STm RT Rev	AATCTTTGCCTGATAACGGT		
2406	dnaB STm RT Fwd	CTATCGACCTGATTACGCTC	*dnaB*	*S.* Typhimurium
2407	dnaB STm RT Rev	CTTGGCGTGTTTTTAGACAG		
2408	pabC STm RT Fwd	TTAAAACATCTGAACCGCCT	*pabC*	*S.* Typhimurium
2409	pabC STm RT Rev	GTACGCCAGAACAAATTAGC		
2410	sseE STm RT Fwd	TGGTGCAAGAAATAGAGCAA	*sseE*	*S.* Typhimurium
2411	sseE STm RT Rev	ATAAACTGCTGCCCAAGTAA		
2412	pagC STm RT Fwd	TGTTGAGCCTGAAGGTATTC	*pagC*	*S.* Typhimurium
2413	pagC STm RT Rev	CAGCGCGTATAACGAAAAAT		
2414	siiD STm RT Fwd	TCAGGGCGTTATCACTACTA	*siiD*	*S.* Typhimurium
2415	siiD STm RT Rev	TATCACCCTCGGCTACATAA		
2416	nucD2 STm RT Fwd	ATAAATGTGTGGTACAGCCG	*nucD2*	*S.* Typhimurium
2417	nucD2 STm RT Rev	ACCTTTGACATATACCCAGC		
2418	StyR44 STm RT Fwd	GAAACACAGAACAACGAAAGT	StyR-44 sRNA	*S.* Typhimurium
2419	StyR44 STm RT Rev	TAACCTCACAACCCGAAGAT		
2420	gyrB Eco RT Fwd	ATGGACAAAGAAGGCTACAG	*gyrB*	*E. coli*

2421	gyrB Eco RT Rev	TCACCTCAGAAGAAACCAGT		
2422	ibpB Eco RT Fwd	TCAATGGATCGGTTTTGACA	*ibpB*	*E. coli*
2423	ibpB Eco RT Rev	TAATGCGGTAGTGGTTATCG		
2424	paaA Eco RT Fwd	GGCAGGAGTTTAACGAAGTA	*paaA*	*E. coli*
2425	paaA Eco RT Rev	CTTACGGGCATGTTGTTTTT		
2426	nrdG Eco RT Fwd	GTATCAAACGCCAGGGTATT	*nrdG*	*E. coli*
2427	nrdG Eco RT Rev	AGTTCGTCGAGTTTATAGCC		
2428	hipB Eco RT Fwd	AATTGGTATTAAGCAGGCGA	*hipB*	*E. coli*
2429	hipB Eco RT Rev	GAGAGTTCAAGCGACTGTAA		
2430	patA Eco RT Fwd	AATCGGCTATAACTTTGCCA	*patA*	*E. coli*
2431	patA Eco RT Rev	TTCACACTGTTCAATGGTCA		
2432	dnaJ Eco RT Fwd	GCTTATGAAGTTCTGACCGA	*dnaJ*	*E. coli*
2433	dnaJ Eco RT Rev	CCGAAAACGTCACCAAAAAT		
2434	tisB Eco RT Fwd	TCCTGAACCACAGGAGAC	*tisB*	*E. coli*
2435	tisB Eco RT Rev	TATAAAAGGGGAGCGGTTTC		
2436	norV Eco RT Fwd	GCATGATGACTTACCTGACA	*norV*	*E. coli*
2437	norV Eco RT Rev	GTCTGATCCACTTCATCGTT		
2438	rcnB Eco RT Fwd	TACAACATTAAGCAGTGGCA	*rcnB*	*E. coli*
2439	rcnB Eco RT Rev	AAAAATCTCACCGTCGTAGG		
2440	yjiY Eco RT Fwd	TCACTTCGGTATTCTGTTCG	*yjiY*	*E. coli*
2441	yjiY Eco RT Rev	TTTTTCAGGAACGGGATGAA		
2442	gatD Eco RT Fwd	ACCCTGTTTTACTTGTCCAG	*gatD*	*E. coli*
2443	gatD Eco RT Rev	ATTCAGCAAATCCACCATCA		
2444	plsY Eco RT Fwd	GTTACTGACCGTGCTATTGA	*plsY*	*E. coli*
2445	plsY Eco RT Rev	GGAAGGTGAATTGTGGCTTA		
2446	eutQ Eco RT Fwd	AACTCATCACAGCGAATGAT	*eutQ*	*E. coli*
2447	eutQ Eco RT Rev	GGTAAAACCCAGTAGATCCG		
2448	lldP Eco RT Fwd	TACCGTAACACTGTGGAGTA	*lldP*	*E. coli*
2449	lldP Eco RT Rev	GCAACCAGTTTATCGAGGTA		

2.8.6 GFP reporter assays

To make the reporter plasmid containing an unstable GFP, the promoter of *ramA* or *lexA* was fused with *gfp* in a pMW82 plasmid backbone (Table 2.2). Plasmids were transformed into *S.* Typhimurium SL1344 and its AcrB D408A mutant by electroporation.

ramA reporter assays were carried out as described previously (Lawler *et al*., 2013). In brief, strains carrying the reporter plasmid were grown to an OD_{600} of 0.6 in MOPS. Three technical replicates of 100μL each were aliquoted into a clear-bottom, black, 96-well plate (Greiner Bio-One, Germany, cat. no. 655090). Chlorpromazine (Sigma, USA, cat. no. C8138) at a final concentration of 25μg/mL was used as positive control of *ramA* induction (Lawler *et al*., 2013). Wild-type and mutant strains harbouring a pMW82 empty vector were used as negative controls. The plate was loaded onto a FLUOstar Optima microplate reader (BMG Labtech, UK). Fold-changes in *ramA* induction were calculated at 1.5 hours, where maximum level of *ramA* induction was observed.

lexA induction assays were carried out in the same way as the *ramA* assays. Nalidixic acid at a final concentration of 1.6μg/mL was used as a positive control of *lexA* induction (Dowd *et al*., 2007). Additionally, fluorescence of the *lexA* reporter strains grown to an OD_{600} of 0.6 were measured in an Attune NxT Flow Cytometer (ThermoFisher Scientific, UK). Cultures were diluted 1:100 in filter-sterilised 1X PBS (Sigma, UK, cat. no. D8537). Bacteria were gated using the positive control. GFP fluorescence was measured in channel BL1 (excitation wavelength=448nm, emission filter=530/30nm). The fluorescence of the control samples was measured at 520V, whereas samples without nalidixic acid were measured at 700V (due to low levels of

basal induction of *lexA*). The GFP fluorescence of 20,000 events acquired in the 'bacteria' gate was determined. The median fluorescence intensity per sample was used for statistical analysis.

2.9 Preparation of conditioned media (exometabolome)

To prepare cell-free culture supernatants or conditioned media, 10mL of LB, MOPS or EZ Rich Defined Medium (EZ) (TEKNOVA, USA, cat. no. M2105) was inoculated with three colonies of SL1344 or its AcrB D408A mutant. Overnight cultures were grown at 37°C under aeration and diluted to an OD_{600} of 1.5. The diluted culture (30μL) was used to inoculate 30mL of the respective medium (1:1000 dilution). Cultures were grown for 17.5 hours at 37°C, shaking at 200rpm. Bacteria were pelleted by centrifuging at 3,500X*g* in a Hereaus Megafuge 40R for 25 minutes. Pellets were retained to check the purity of the culture by streaking onto LB and XLD agar plates. PCR of *acrB* and amplimer-sequencing were carried out to confirm the identity of the strains.

Culture supernatant was filter-sterilised using a 0.22μm pore, Stericup® Filter Unit and aliquoted into 50mL centrifuge tubes (21mL per tube maximum) for storing up to a month or into 500mL freeze-drying glass vials for immediate use. Aliquots were frozen at -80°C for a minimum of two hours and freeze-dried in a K4 Modulyo Freeze Dryer (Edwards, UK) for 24 hours or until all the water was removed. Freeze-dried conditioned media was resuspended in 1/3 of its original volume in UltraPure™ Distilled Water (ThermoFisher Scientific, UK, cat. no. 10977035) to make a 3X solution.

2.9.1 Fractionation of conditioned media

Conditioned medium (1X) produced from cultures grown in LB was incubated with Diaion® HP-20 resin (SUPELCO, USA, cat. no. 13606). HP-20 is a polymeric resin formed of styrene chains interlinked with divinylbenzene. It is used to adsorb hydrophobic compounds.

Fractionation with HP-20 was carried out as described by Jauffrais *et al*. (2012). Twenty-five grams of resin was used per litre of conditioned media. The resin was pre-treated by washing three times with 50mL of HPLC-grade methanol (Fisher Scientific, UK, cat. no. A452-1) in a 250mL PVDF membrane, 0.22μm pore, Stericup® Filter Unit (Merck Millipore, UK, cat. no. SCGVU02RE). A final wash with sterile-distilled water was carried out to remove residual methanol. Pre-treated resin was added to the conditioned medium. Medium with resin was subsequently transferred into a 250mL sterile flask and incubated for 24 hours with constant shaking at 200rpm, at 37°C, in a shaking incubator. After incubation, media and resin were transferred into a Büchner funnel covered with filter paper, attached to a Büchner flask. Media was filtered through the funnel under vacuum. Recovered media or hydrophilic fraction (HF) was frozen and freeze-dried as described in section 2.9.

After elution of the hydrophilic fraction, the resin was washed three times with 50mL of acetone (Fisher Scientific, UK, cat. no. 10417440) (Act CM), followed by three washes with 50mL of methanol each (MeOH CM) and another three times with distilled water (H_2O CM). Acetone and methanol fractions were transferred into a round bottom borosilicate flask and dried for 30 minutes in a rotary evaporator (Büchi, Switzerland) at 45°C, with a vacuum pressure of 150mmHg. Dry fractions were dissolved in dimethyl sulfoxide (DMSO) (Sigma, UK, cat. no. D4540) and used in infection assays

(section 2.10.2). The water fraction was freeze-dried and prepared as described in section 2.9.

2.10 Tissue culture

To study the interaction of *S.* Typhimurium with non-polarised and polarised intestinal epithelial cells, the cell lines used were INT-407 embryonic intestinal epithelial cells and Caco-2 colorectal epithelial cells. J774A.1 murine macrophages were used to study the interaction of *S.* Typhimurium with macrophages.

All cell lines were routinely cultured in T75 tissue culture flasks (Falcon, USA, cat. no. 353136). Cells were incubated at 37°C, with 5% CO_2 in a Galaxy® 170S incubator (Eppendorf, Germany). INT-407 cells were grown in Eagle's Minimum Essential Medium (EMEM) (Sigma, USA, cat. no. M2279); whereas, Caco-2 and J774A.1 cells were grown in Dulbecco's Modified Eagle's Medium (Sigma, USA, cat. no. M6546). All media were supplemented with 1% of non-essential amino acids (NEAA) (Sigma, USA, cat. no. M7145), 1% of L-glutamine (Sigma, USA, cat. no. G7513), 10% heat-inactivated foetal bovine serum (Invitrogen, UK, cat. no. 10108-165) and 50µg/mL of gentamicin (Sigma, USA, cat. no. G1397).

2.10.1 Trypan blue exclusion assays

Trypan blue exclusion assays were routinely carried out to assess the viability of the eukaryotic cells. Trypan blue is a viability dye as it cannot traverse the membrane of healthy, intact cells. The dye can only penetrate cells with a damaged membrane.

Therefore, live cells will be colourless and damaged/dying cells will be stained blue (Strober, 2001).

Monolayers were disrupted with trypsin, followed by inactivation of the enzyme by addition of fresh media. Trypsin was removed and cells were concentrated by centrifuging at 1,500X*g* in a Hereaus Megafuge 40R, for 5 minutes at room temperature. When cells were recovered from 24-well plates, the pellet was resuspended in 200μL of fresh, prewarmed media. When T75 flasks were used, the pellet was resuspended in 5 to 8mL of media, depending on the size of the pellet. An aliquot of 10μL of resuspended cells were mixed with 1μL of 0.4% trypan blue (Sigma, USA, cat. no. T8154) and immediately transferred into a Neubauer chamber for cell counting. All cells were counted in the central grid. Number of live and damaged cells per grid were recorded and concentration of live cells was calculated using the following formula:

$$\text{Cells/mL} = \frac{\text{Average number of cells in central grid } \times 10^4 \times 1.1}{\text{Dilution}}$$

2.10.2 Infection assays

The ability of *S.* Typhimurium to colonise, invade and replicate inside the host cell is often studied using cell culture experiments. A common experiment is the gentamicin protection assay. Gentamicin cannot penetrate eukaryotic cells, killing only extracellular bacteria. Therefore, internalised bacteria are not exposed to the antibiotic and can be recovered by viable counting as an indication of the ability of a strain to invade (Lobo and Mandell, 1973, Dandekar *et al*., 2014).

Gentamicin protection assays were carried out as described previously (Buckley *et al*., 2006, Blair *et al*., 2009). Association of *S.* Typhimurium to eukaryotic cells was measured at 2 hours post-infection and invasion was measured at 4 hours post-infection. To prepare eukaryotic cells for the infection assays, two 24-well plates (Costar, USA, cat. no. 3524) per assay were seeded with $1.8X10^5$ cells/mL of Caco-2 or $2X10^5$ cells/mL of INT-407 cells or J774A.1 cells. INT-407 and J774A.1 cells were incubated at 37°C, with 5% CO_2 for 48 hours to allow formation of a confluent monolayer. Caco-2 cells were incubated for two weeks to allow polarisation of the epithelial cells; media was replaced with fresh media every 48 hours.

Confluent monolayers were washed with pre-warmed Hank's Balanced Salt Solution (HBSS) (Gibco, UK, cat. no. 24020-091) three times before proceeding to infect with 1mL of a wild-type or mutant *S.* Typhimurium suspension adjusted to a final concentration of $7.6X10^7$ CFU/mL. Where conditioned media was required, 3X concentrated media was added to the wells in a 1:2 proportion. One plate was used to assess the ability of *S.* Typhimurium to associate to eukaryotic cells, whilst the other one was be used to determine the ability to invade.

To prepare the bacterial suspension, a 10mL overnight culture of *S.* Typhimurium, grown in LB was washed twice in 10mL of sterile DPBS, by centrifuging at 2,800X*g* for 10 minutes in a Hereaus Megafuge 40R. Bacteria were resuspended in 8mL of sterile DPBS and OD_{540} of the washed culture diluted 1:10 in DPBS was recorded. The OD_{540} value was multiplied by a factor of 1.4 to obtain an estimate of the CFU/mL, which was used to adjust the inoculum to $7.6X10^7$ CFU/mL..The formula used was:

$$\mathrm{OD}_{540} \times \frac{1}{\text{dilution}} \times 1.4 = \mathrm{CFU} \times 10^9 \text{ per mL}$$

At 2 hours post-infection, wells were washed three times with pre-warmed HBSS. EMEM or DMEM (2mL) with 100µg/mL of gentamicin was added to the 'invasion' plate and incubated for another 2 hours. The 'association' plate was processed by adding 500µL of 1% Triton X-100 (Sigma, USA, cat. no. T8787) and one magnetic stirrer per well. To release the bacteria from eukaryotic cells, monolayers were mechanically disrupted on a magnetic stirring plate for 10 minutes. Serial dilutions from 1:10 to $1:10^5$ were carried out by adding 20µL of the Triton-treated bacteria suspension to 180µL of sterile 1X PBS. To determine viable counts, a modified version of the Miles and Misra method (Miles *et al*., 1938) was used, in which 20µL of each dilution was plated in triplicate onto LB agar plates.

At 4 hours post-infection, media with gentamicin was removed from the 'invasion' plate. The plate was washed three times with pre-warmed HBSS to remove residual gentamicin and the same procedure as above was carried out to release bacteria from cells and do viable counting.

All agar plates were incubated for 24 hours at 37°C. Colonies were counted and reported as CFU/well. The formula used to calculate CFU/well was:

$$\mathrm{CFU/well} = \mathrm{Number\ of\ colonies} \times \frac{1}{\mathrm{aliquot}} \times \frac{1}{\mathrm{dilution}}$$

Where the aliquot is 0.02mL (20µL) and the dilution is presented as 0.0001 for a $1:10^4$ dilution for example.

2.11 Murine infection assays

Mouse infection assays were carried out by Dr. Barbara Chirullo from the Istituto Superiore di Sanità (Italy). Six groups of 6-8 week old female BALB/c mice with five mice each were used. Three groups were used for oral inoculation and three for intraperitoneal (IP) inoculation. Each group were inoculated with an overnight culture of *S.* Typhimurium SL1344 wild-type or AcrB D408A mutant diluted in sterile PBS. A control group was inoculated with sterile PBS.

Inocula were prepared from overnight cultures incubated at 37°C under aeration. Cultures were washed in sterile PBS by centrifuging at 2,800X*g* for 10 minutes. For oral infection, a 200μL suspension containing $5X10^7$ CFU was administered intragastrically to the mice (Kingsley *et al*., 2003). For intraperitoneal infection, a 200μL suspension containing $3.3X10^7$ CFU was injected into the peritoneum of the mice (Gil-Cruz *et al*., 2009). Mice were constantly monitored for four days and spleen and liver were recovered on the fifth day post-infection to determine the bacterial load by viable counting. Organs were harvested under aseptic conditions, weighed and disrupted to determine the total number of CFU per mg of organ.

The research protocol, approved by the Service for Biotechnology and Animal Welfare of the Istituto Superiore di Sanità and authorized by the Italian Ministry of Health, adhered to the guidelines contained in Italian Legislative Decree 116/92, based on European Directive 86/609/EEC on Laboratory Animal Protection (decree numbers 84/12.B and 255/2012.B).

2.12 Determination of changes in bacterial replication dynamics

Plasmid pDiGi (Table 2.2) was transformed into SL1344 and its AcrB D408A mutant by electroporation. Strains were grown on LB agar with 50μg/mL of carbenicillin to maintain the plasmid.

Bacteria harbouring the plasmid were grown in MgMES minimal medium pH 5 (Appendix I) at 37°C. This medium simulates the conditions that *Salmonella* encounter inside the *Salmonella* containing vacuole and is ideal for expression of DsRed (Helaine *et al*., 2010). Gates for bacteria, GFP and DsRed were set up using an overnight culture of SL1344 grown in MgMES supplemented with the appropriate inducers. In bacteria carrying pDiGi, expression of DsRed and GFP was induced with 0.2% arabinose and 0.5mM of IPTG (Sigma, USA, cat. no. I5502), respectively. Compensation was manually adjusted to avoid false detection of GFP or DsRed due to overlap of the emission spectra of the two fluorescent proteins.

This assay relies on both strains having the same growth rates; therefore, growth kinetics, as described in section 2.1.1, with SL1344 and the AcrB D408A mutant were carried out in MgMES pH 5.0 supplemented with 0.2% glucose or arabinose.

To determine the number of potential persister cells, bacteria carrying pDiGi were grown overnight in MgMES with 0.2% arabinose, under aeration at 37°C, to induce expression of DsRed. A 1% inoculum was added to 10mL of prewarmed MgMES containing 0.2% glucose and 0.5mM IPTG. Cultures were incubated in a shaking incubator at 37°C, at 200rpm. Samples of 10μL were taken every 2 hours and diluted 1:100 in 1X PBS. Diluted samples were vortexed briefly and loaded on to an Attune NxT Flow Cytometer. GFP fluorescence was measured in channel BL1 (excitation wavelength=448nm, emission filter=530/30nm) at 440V; whereas, DsRed

fluorescence was measured in channel YL1 (excitation wavelength=561nm, emission filter= 585/16nm) at 600V. The total number of bacteria expressing DsRed was obtained by counting the number of bacteria in the DsRed gate (+/-) and expressing DsRed and GFP (+/+). The total number of bacteria expressing GFP was measured in the GFP gate (-/+) (Appendix V). A total of 30,000 gated events were acquired due to the sensitivity of the assay.

2.13 Quantification of autoinducer-2 (AI-2)

Cell-free culture supernatants from *S.* Typhimurium SL1344 and its AcrB D408A mutant grown in LB broth, LB supplemented with 0.5% glucose, MOPS and autoinducer bioassay (AB) medium (Appendix I) were used. Supernatants were harvested from cultures grown to an OD_{600} of 0.1, 0.3, 0.6 and 1.0 as described in section 2.9. Culture supernatant from overnight cultures was also harvested. Syringe filters (Starlabs, UK, cat. no. E4780-1226) and 10mL syringes (Becton Dickinson, Spain, cat. no. 302188) were used to filter-sterilise culture supernatants. Supernatants were stored at -20°C until use.

For the AI-2 quantification assay, an overnight culture of *Vibrio harveyi* BB170 AI-2 reporter strain was grown in AB medium at 30°C, shaking at 200rpm (Surette and Bassler, 1998). *V. harveyi* is a bioluminescent marine bacterium that luminesces in presence of autoinducers (Greenberg *et al*., 1979, Bassler *et al*., 1997). Strain BB170 has a transposon insertion that interrupts *luxN*, which encodes the sensor of autoinducer-1; therefore, this strain can only respond to AI-2.

An overnight culture of *V. harveyi* BB170 was diluted 1:5000 in AB medium and aliquoted (90μL) into each well of a clear bottom, black, 96-well plate. Culture

supernatants of *S.* Typhimurium (10μL) were added to the diluted reporter strain. Culture supernatants from *V. harveyi* TL25, TL26 and BB170 were used as positive control, negative control and blank, respectively. The plate was loaded on to a FLUOstar OMEGA plate reader (BMG Labtech, UK). Luminescence and OD_{600} were measured every 10 minutes for 18 hours. Luminescence was divided by OD_{600} to obtain relative luminescence units (RLU).

2.14 Motility assays

The inoculum for motility assays was prepared by diluting an overnight culture of the test strains to an OD_{600} of 0.5 in LB broth or MOPS minimal medium. This culture was used to inoculate LB and MOPS plates containing 0.3% or 0.5% of Difco® Bacto agar (Becton Dickinson, USA, cat. no. 214530) to study swimming or swarming, respectively (Li *et al*., 2014). Plates with 0.3% of agar (swimming plates) were inoculated using a straight loop and stabbing the inoculum into the agar, while plates with 0.5% of agar (swarming plates) were inoculated by spotting 5μL of the inoculum on the surface of the agar (Li *et al*., 2014).

Plates were incubated at 37°C facing up. The best incubation time to obtain an halo of motility that was measurable and did not occupy the whole surface of the agar was determined. In LB, swimming plates were read after 7 hours of incubation, whereas swarming plates were read at 12 hours. In MOPS, swimming plates were read after 24 hours and swarming plates were discarded after 7 days as *S.* Typhimurium did not swarm on MOPS agar. The total area of motility was measured in ImageJ and reported in mm^2.

2.15 Curli production in congo red agar

Expression of curli proteins was visualised on Congo red agar (Baugh, 2014). Congo red dye (Sigma, USA, cat. no. C6277) was added to a final concentration of 40μg/mL in 25mL of LB or MOPS agar. Plates were inoculated with an overnight culture of the respective test strain, grown in the appropriate medium (LB or MOPS depending on the agar used), adjusted to an OD_{600} of 0.1. An aliquot of 5μL was spotted on top of the agar plates.

Plates were incubated for 48 hours at 30 or 37°C and colonies were visualised in a stereoscopic microscope (Nikon, Japan, model no. C-DSS230). Photos were taken with a camera control unit (Nikon, Japan, model no. DS-L2). Strains producing curli gave red, dry and rough colonies; whereas colonies from non-producers had a pink and smooth phenotype (Baugh, 2014).

2.16 Metabolomics

2.16.1 Preparation of exometabolome (ExM or conditioned media)

ExM was prepared in the same way as described in section 2.9. Ten overnight cultures from single colonies were prepared and used to inoculate one universal tube containing 10mL of fresh, prewarmed LB broth each. Cultures were incubated for 17.5 hours at 37°C, shaking at 200rpm. A control sample, which contained sterile LB broth, was also prepared. Cell-free culture supernatants were obtained by filter-sterilising through a 0.22μm pore, PVDF membrane syringe filter (Starlabs, UK, cat. no. E4780-1221), using a 20mL syringe (Becton Dickinson, Spain, cat. no. 300613). Aliquots of 1mL were stored at -80°C, in 1.5mL microcentrifuge tubes (Eppendorf, Germany, cat.

no. 0030125.150). The remaining culture supernatant was freeze-dried and used in infection assays to test for biological activity.

2.16.2 Analysis of the composition of the ExM

Frozen ExM were delivered to Dr. Warwick Dunn (Phenome Centre Birmingham, UK) for analysis by UHPLC-MS (ultra-high performance liquid chromatography-mass spectrometry) as described previously (Winder *et al*., 2008). In brief, ExM samples were diluted in 2/3 of methanol and processed in an UltiMate™ 3000 RSLCnano UHPLC system coupled to a Q Exactive™ Focus Mass Spectrometer (Thermo Scientific, UK). Metabolites in samples were separated via a HILIC column to analyse polar metabolites, or a C_{18} reversed phase column to analyse lipids and other non-polar metabolites. Assays were carried out in positive and negative modes to maximise metabolite detection.

Data was processed on the XCMS platform, using univariate data analysis approaches to identify metabolites that were in a higher concentration in the wild-type ExM when compared against the mutant ExM and the sterile LB broth control. Detected features were given putative identities. Where more than one putative identity was given, literature research was carried out to determine which metabolite was most likely to be synthesised by the strain from which the ExM had been obtained. Pathways and processes in which the identified metabolite participated were identified in the KEGG (http://www.genome.jp/kegg/pathway.html) and Biocyc (http://www.biocyc.org) databases.

2.17 Determination of metabolic constraints in the *S.* Typhimurim SL1344 AcrB D408A mutant using the Metabolic Transformation Algorithm (MTA)

MTA is a mathematical model that identifies genes that are essential for the maintenance of the metabolic state of a wild-type strain compared to a mutant and *vice versa* (Yizhak *et al*., 2013). The aim of using this model was to define metabolic constraints that could account for the loss of virulence in the *S.* Typhimurium SL1344 AcrB D408A mutant. The analysis was done by Dr. Daniel D. Dwyer and Sean Mack (The University of Maryland, USA) using RNA-seq data generated in this project as an input. Differential gene transcription data was run through an integrative metabolic analysis tool (iMAT), which maps genes to reactions or pathways and predicts the rate at which metabolites go through them (flux). Next, pathways or reactions in which fluxes are significantly changed were identified and reactions were classified into 'changed' and 'unchanged' groups. The MTA was applied to identify perturbations that could push the flux of reactions from the changed group to the target state, without affecting the flux of the unchanged reactions. This produced a list of the best "transforming" deletion reactions, which were linked back to genes in specific pathways. The effect of each individual gene-deletion on the metabolic network was modelled. The simulation assigned a transformation score to each gene with which the knockout was ranked. Genes with the highest scores are the most likely to generate a flux change in the right direction (wild-type to mutant metabolic state or mutant to wild-type state) when deleted.

2.18 Statistical analyses

All experiments were repeated at least three times. When curves such as growth kinetic curves were required, the mean of all experiments was plotted. GraphPad Prism version 7 (GraphPad Software, USA) was used for data analyses and construction of plots. A Student's t-test with Welch's correction was used for statistical analysis for all experiments unless specified otherwise. An unpaired Student's t-test was used to compare means of two independent groups, where data is normally distributed and have equal variances. A Welch's correction allowed comparison between datasets with unequal variances and was used to minimise false positives. For mouse infection experiments, a Mann-Whitney U test was used. This test is the equivalent to a Student's t-test for non-parametric datasets. All analyses were performed on raw data even when plots have a logarithmic scale.

For RNA-seq data analysis, Bayesian approaches integrated in the Bioconductor *limma* package were used (Ritchie *et al*., 2015). Bayesian statistics use probabilities to infer the chance of an event being significant or not, it accounts for differences in sampling sizes and provides a more stringent analysis when compared to Student's t-tests and ANOVAs.

In metabolomics studies, a one-way analysis of variances (ANOVA) with Bonferroni correction was used. A one-way ANOVA allows comparison of means between multiple independent groups; it is used to analyse large datasets as doing multiple t-tests increases the chance of Type 1 error that leads to false positives. A Bonferroni correction was applied to further reduce false discovery rates.

A $P<0.05$ was considered statistically significant for all tests.

To validate that values obtained from infection assays were normally distributed and that a Student's t-test was the best statistical test to use, all wild-type and mutant invasion data were tested for normality using the D'Agostino-Pearson omnibus test. This test determines the symmetry and shape of data distribution and compares it against a Gaussian distribution. It produces a *P*-value, where the null hypothesis is that all values belong to a Gaussian distribution; therefore, a $P>0.05$ indicates a normal distribution.

CHAPTER 3.

Construction and characterisation of a loss of AcrB efflux function mutant

3.1 Background

AcrAB-TolC is formed of three proteins: AcrB, the transporter; TolC, the outer membrane protein and AcrA, the periplasmic adapter protein that binds AcrB to TolC (Seeger *et al*., 2008, Symmons *et al*., 2009). Deletion of *Salmonella* Typhimurium *acrB* increases susceptibility of the strain to antibiotics (Eaves *et al*., 2004, Buckley *et al*., 2006) and causes physiological changes such as decreased motility and attenuation of virulence (Buckley *et al*., 2006, Webber *et al*., 2009). Deletion of *acrB* has also been associated with increased transcription of homologous RND pumps *acrD* and *acrF* in *S.* Typhimurium (Blair *et al*., 2015b). However, AcrB is a 114 kDa transmembrane protein, the deletion of which might produce pleiotropic phenotypes unrelated to loss of efflux function. To differentiate between the effects of loss of AcrB protein from loss of efflux function, a mutant that expresses an inactive form of AcrB is required.

AcrB functions as a drug-proton antiporter, where the proton motive force (PMF) is generated by translocation of protons within the protein. The PMF is used by AcrB to undergo the conformational changes required to transport drugs. Five amino acids are essential for proton translocation in *Escherichia coli* AcrB: D407, D408, K940, R971 and T978 (Su *et al*., 2006, Yao *et al*., 2010). Substitution of either of these amino acids with a non-charged amino acid, such as alanine, produced multidrug hyper-susceptibility in *Escherichia coli* (Takatsuka and Nikaido, 2006, Seeger *et al*., 2009). Of these five amino acids, D407 and D408 are the most conserved amongst different bacterial species (Guan and Nakae, 2001, Hou *et al*., 2010).

Due to the high sequence similarity between AcrB in *E. coli* and *S. enterica* and since a mutation in either of the proton translocation residues was predicted to produce the

same phenotype, D408 was chosen to be mutated in AcrB of *S.* Typhimurium SL1344 to generate an AcrB mutant suitable for physiological studies.

The majority of structural studies of AcrB have been carried out using the *E. coli* K-12 protein. For comparative purposes, *E. coli* K-12 MG1655 AcrB D408A and Δ*acrB* mutants were constructed.

3.2 Aims

- To construct a loss-of-efflux-function AcrB chromosomal mutant of *Salmonella* Typhimurium SL1344 and *Escherichia coli* MG1655, by substituting the aspartate (D) at position 408 for an alanine (A).
- To characterise the phenotype of the constructed AcrB D408A mutants.

3.3 Hypothesis

- The D408A substitution in AcrB confers loss of efflux function in *E. coli and S.* Typhimurium.

3.4 Construction of the *S.* Typhimurium SL1344 chromosomal AcrB D408A mutant

The AcrB D408A chromosomal mutant was constructed using the method described by Kim *et al*. (2014). This method relies on pSLTS, a low copy number plasmid which encodes the λ-Red recombinase system and the I-SceI meganuclease under the control of an arabinose-inducible promoter and the *tetA* tetracycline-inducible promoter, respectively. Some modifications were made to the method as pSLTS did

not work and none of the enzymes could be induced, these modifications are explained in the following sections.

3.4.1 Construction of the mutation cassette

Two approaches were tested for constructing the mutation cassette. The first approach was to ligate the selection cassette to the homologous recombination fragments (HRF). The selection cassette and HRF were digested with PciI and EcoO109I. The assembly of the fragments was attempted using a T4 DNA ligase. However, this approach did not work.

The second approach was to construct the mutation cassette using a commercial Gibson assembly master mix as described by Kim *et al.* (2014). The Gibson assembly master mix is a mixture of exonuclease, DNA polymerase and DNA ligase optimised to work at 50 °C in a single reaction. The exonuclease generates 3'-end sticky ends on all the fragments; the polymerase fills in the gaps and the ligase seals the nicks to generate the assembled construct (Gibson *et al*., 2009). The commercial master mix requires between 20 to 50 bp of homology between the fragments to be assembled, so new primers were designed to add 20 bp of homology to the HRF.

The mutation cassette was assembled successfully at the first attempt. However, there was residual selection cassette after the assembly; this required an extra gel-purification step (Figure 3.1).

Figure 3.1 Assembled mutation cassette.

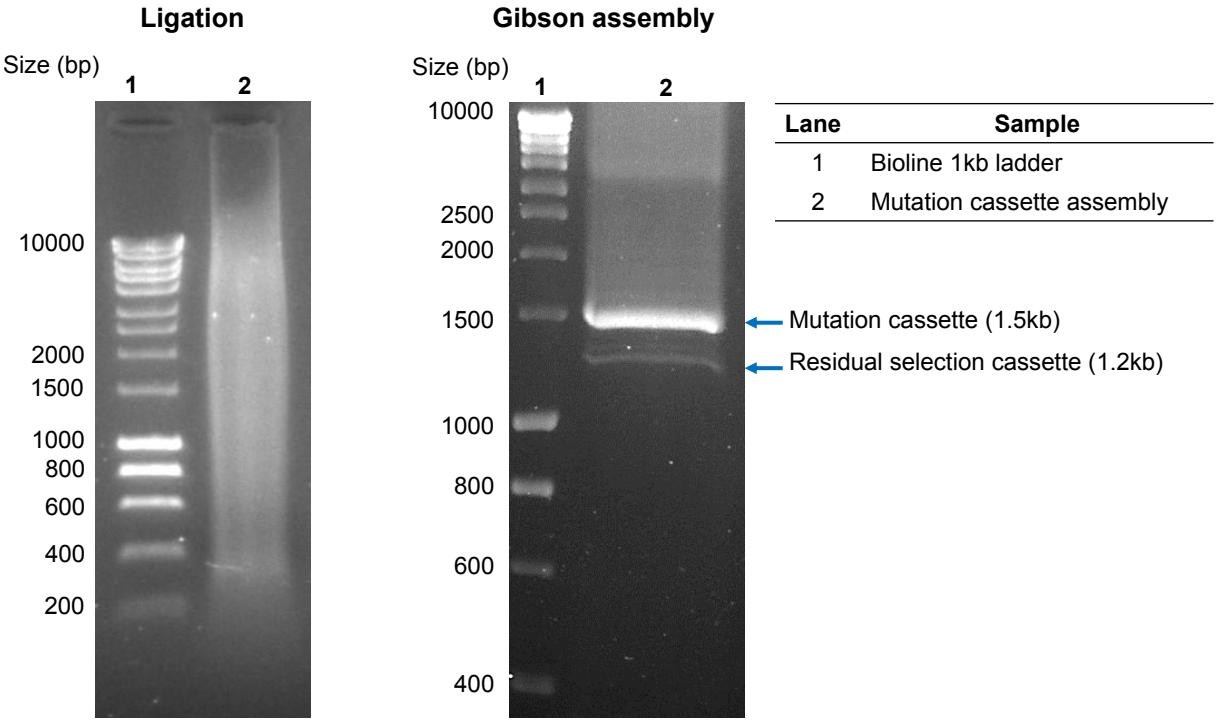

Lane	Sample
1	Bioline 1kb ladder
2	Mutation cassette assembly

Ligation and Gibson assembly products were electrophoresed on a 1% agarose gel. The mutation cassette was assembled with Gibson assembly master mix as ligation did not work; however, there was residual selection cassette.

3.4.2 Insertion of the mutation cassette into the chromosome of *S.* Typhimurium SL1344

For the insertion of the mutation cassette into the chromosome, two approaches were tested. The first approach was to use pSLTS as described by Kim *et al*. (2014) (**Figure 3.2**). However, this approach did not work since the recombinase could not be induced from pSLTS. This was shown by the absence of recombination in the positive control experiment with *ramA*::*aph* carried out in the same way as the insertion of the mutation cassette. The *ramA::aph* gene-disruption is a 1kb fragment that is easily introduced into the chromosome (Bailey *et al*., 2010).

As the recombinase could not be induced from pSLTS in *S.* Typhimurium SL1344, the plasmid was substituted with pSim18 for the recombination process. pSim18 is a low copy number plasmid with a temperature-sensitive origin of replication, which has been used previously as a λ-Red helper plasmid in *S.* Typhimurium SL1344 (Baugh, 2014). This plasmid encodes λ-Red proteins under the control of the *pL* inducer (Lee *et al*., 2009b). *pL* is a transcription factor repressed by CI857; the repressor protein is inactivated at 42°C allowing the expression of the *pL* operon. The temperature-sensitive origin of replication stops the plasmid from being transferred vertically at temperatures higher than 30°C, thus 'curing' the plasmid from the bacterial cell without any further procedures. The plasmid also encodes hygromycin resistance to facilitate monitoring the insertion and loss of the plasmid.

The insertion of the mutation cassette was successful using pSim18, resulting in 72 recombinant colonies at the first attempt. The recombinant strain was also successfully 'cured' from the plasmid after growing at 37°C, as demonstrated by the absence of growth on LB agar plates supplemented with 100μg/mL of hygromicin.

Figure 3.2 Diagram of the method used for genome editing.

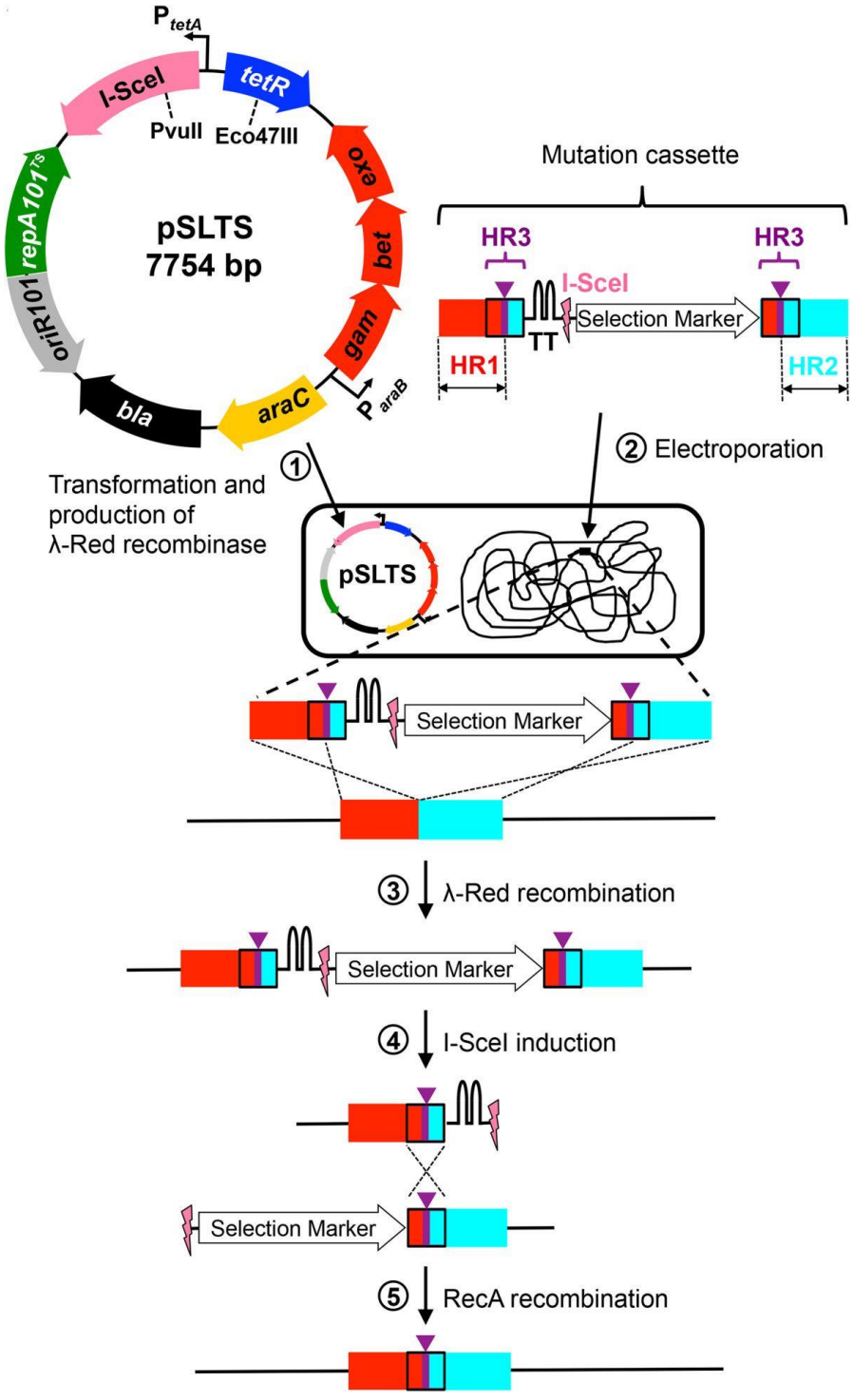

From Kim *et al.,* 2014. To edit the genome of *S.* Typhimurium, pSLTS was replaced with pSim18 for the insertion of the mutation cassette and pACBSCE for the induction of I-SceI. For *E. coli*, the procedure was followed as shown here.

3.4.3 Deletion of selection marker

pSLTS was initially used to delete the selection marker from the genome of the recombinants. However, no mutants were selected in three attempts; therefore, pACBSCE was used instead. pACBSCE was engineered by Lee *et al*. (2009a) to include the I-SceI restriction site and express the I-SceI meganuclease under the control of an arabinose-inducible promoter. This allows the plasmid to be 'cured' once the restriction enzyme is induced, without further procedures. pACBSCE confers chloramphenicol resistance to the transformants to facilitate monitoring the insertion and loss of the plasmid.

I-SceI uses negative selection, thus colonies were replica plated onto LB agar and LB agar supplemented with 50μg/mL of kanamycin; only those colonies that grew in LB alone were selected as candidates. Fifty-two colonies were screened from a $1:10^8$ dilution of bacterial cells, of which four colonies did not grow in LB supplemented with kanamycin. The loss of the selection marker was confirmed in these by PCR (Figure 3.3).

3.5 Construction of the *E. coli* MG1655 chromosomal AcrB D408A mutant

3.5.1 Construction of the mutation cassette

The mutation cassette was constructed using Gibson assembly as described in section 3.4.1. A difficulty encountered with the *E. coli acrB* mutation cassette was that the two HFR fragments assembled to each other. Therefore, a two-step approach was used to facilitate the assembly of the cassette. First, the selection cassette was assembled with either the 5'-HRF or the 3'-HRF. This initial assembly was PCR-amplified and sequenced before proceeding to do a second assembly to attach the

remaining HFR (Figure 3.4). The assembled mutation cassette was gel purified, amplified by PCR and sequenced to confirm its correct assembly.

3.5.2 Insertion of the mutation cassette into the chromosome of *E. coli* MG1655

The initial strategy was to use the same helper plasmids as in the construction of the *S.* Typhimurium SL1344 AcrB D408A mutant. An *acrB::aph* cassette was used as positive control for recombination. Recombination using the pSIM18 λ-Red helper plasmid was tested; however, no recombinants were obtained after multiple attempts. Therefore, an alternative λ-Red helper plasmid was sought after.

Kim *et al*. (2014) reported that pSLTS worked in *E. coli* MG1655. Surprisingly, despite pSLTS failing in *S.* Typhimurium, fourteen recombinant colonies were obtained on the first attempt, all of them had the mutation cassette inserted in the chromosome.

3.5.3 Deletion of selection marker

As pSLTS worked for the recombination step, the plasmid was kept for the expression of I-SceI. Expression of I-SceI was induced by plating 100μL of an emulsion of a single colony in PBS on to agar plates containing 100ng/μL of anhydrotetracycline (aTET100) and AMP50. Of five colonies tested, I-SceI was successfully induced in three, as shown by a significant decrease in the total number of bacteria that grew on aTET100 plates (fifty colonies per plate on average) when compared against the 'lawn' that grew when the emulsion was plated on to LB plates without aTET.

Figure 3.3 Loss of selection marker in AcrB D408A mutant candidate.

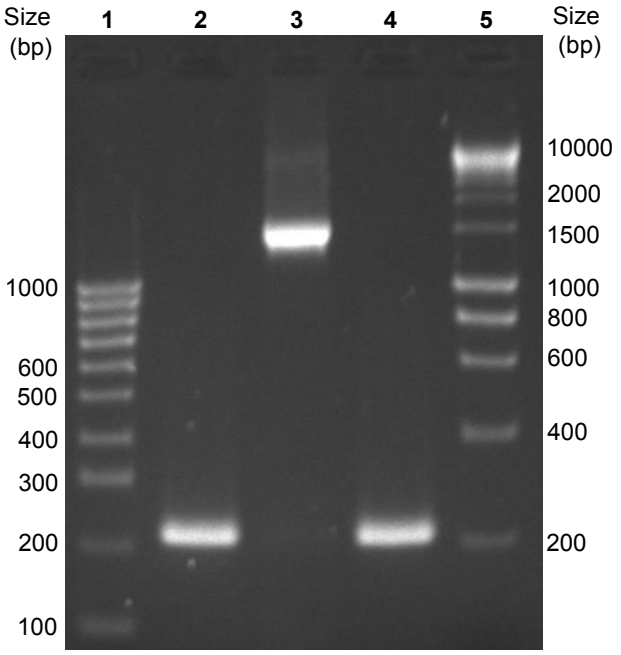

Lane	Sample
1	Bioline 100bp ladder
2	Wild-type *acrB* fragment (~200bp)
3	*acrB* fragment when MC is inserted (~1.5kb)
4	Fragment of *acrB* in the AcrB D408A mutant (~200bp)
5	Bioline 1kb ladder

A fragment of *acrB* was amplified with primers 2151 and 2152. In the wild-type and AcrB D408A strain, a ~200bp amplimer was observed; whereas, in the *acrB* mutant harbouring the mutation cassette, a 1.5kb amplimer was observed. Due to the size of the amplimers, a 2% agarose gel was used.

Figure 3.4 Assembly of the *E. coli* AcrB D408A mutation cassette in two steps.

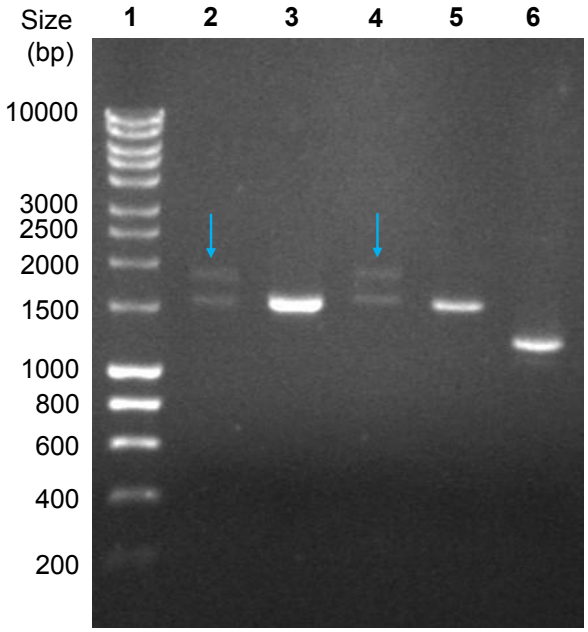

Assembled mutation cassette ~1.8kb

Lane	Sample
1	Bioline 1kb ladder
2	Assembly of 5'-HFR-selection cassette + 3'-HFR
3	5'-HFR-selection cassette assembly (~1.5kb)
4	Assembly of 3'-HFR-selection cassette + 5'-HFR
5	3'-HFR-selection cassette assembly (~1.5kb)
6	Kanamycin selection cassette (~1.2kb)

Assembly products were electrophoresed on a 1% agarose gel. An arrow indicates the assembled mutation cassette (~1.8kb). Each assembly was electrophoresed next to its preceding assembly for size comparison purposes.

Ten colonies from each plate were selected for further characterisation. Of 30 colonies tested, 27 lost the selection cassette as shown by lack of growth on LB KAN50. Ten mutant candidates were restreaked on to LB agar and incubated 37°C to 'cure' the plasmid. Two colonies from each plate were streaked on to LB AMP50 and LB and incubated at 30 and 37°C, respectively. All 20 colonies were 'cured' from pSLTS as shown by lack of growth on AMP50 plates.

3.6 Construction of the *E. coli* MG1655 Δ*acrB* mutant

For the construction of the *E. coli* Δ*acrB* mutant, an aliquot of 100ng of an *E. coli acrB::aph* cassette was electroporated into wild-type MG1655 carrying pSLTS. Fifty mutant candidates were selected on LB KAN50 plates incubated overnight at 37°C to 'cure' pSLTS. Seven colonies were restreaked on to LB KAN50 and LB AMP50 to confirm loss of the helper plasmid.

acrB was PCR-amplified from all seven candidates. The size of the wild-type amplimer was 3.6kb; when *acrB* was replaced with the *aph* gene, a 2kb amplimer was observed, indicating the successful construction of the *acrB::aph* mutant. One of the seven *acrB::aph* mutants was selected for further genome editing.

The *aph* gene was deleted using the pCP20 plasmid, which encodes a flippase. pCP20 was introduced into the *acrB::aph* mutant by electroporation. Twenty μL of plasmid yielded 20 colonies of *acrB::aph* with pCP20 on LB AMP50 plates. Six colonies were inoculated into LB broth and incubated overnight at 43°C to induce expression of the flippase. A loopful of each overnight was streaked on to LB agar and incubated at 37°C. A single colony from each plate was streaked on to LB AMP50 and

KAN50 to select for mutants that had 'cured' pCP20 and lost the *aph* genes, respectively. None of the mutant candidates grew on AMP50 or KAN50 indicating that pCP20 had been 'cured' and that the *aph* gene had been removed from the genome of the mutant. To confirm the later, *acrB* was amplified from each mutant. A 600bp amplimer was observed in each one of the six candidates, confirming the removal of the *acrB* gene from the chromosome of *E. coli* MG1655 (Figure 3.5). Δ*acrB* mutants were confirmed to be *E. coli* by API-20E tests.

3.7 Confirmation of correct insertion of mutation into the chromosome of S. Typhimurium SL1344 and *E. coli* MG1655

3.7.1 Preliminary tests

Several experiments were carried out to determine the correct insertion of the mutation into the chromosome of *S.* Typhimurium SL1344. Initial tests consisted of sequencing *acrB* and growth on xylose-lysine-deoxycholate (XLD) agar. XLD is a highly selective medium designed for isolation of *Salmonella* spp.and *Shigella* spp. from clinical samples (Zajc-Satler and Gragas, 1977), it contains deoxycholate to inhibit growth of Gram-positive bacteria, xylose, sucrose and lactose as carbon sources and phenol red as pH indicator. Other Enterobacteriaceae, such as *Escherichia* spp., also grow in this medium. *E. coli* colonies are easily distinguishable from *Salmonella* and *Shigella* due to fermentation of lactose, which acidifies the medium and changes the colour of the pH indicator. AcrB-mediated efflux confers innate resistance to deoxycholate in Enterobactericeae; as a consequence, strains with an inactivated AcrB or deleted *acrB* gene grow poorly in this medium, making XLD an ideal medium for fast screening for *acrB* mutants.

A *Salmonella* strain with a functional AcrB grew within 24 hours to form translucent colonies with a black centre due to production of sulphydric acid, and a bright pink halo due to decarboxylation of lysine, which results in production of cadaverine that alcalinises the medium. *E. coli* strains with a functional AcrB formed pale yellow colonies with a yellow halo due to fermentation of lactose and production of organic acids that acidify the medium (Appendix III).

Genera and species of mutant candidates were confirmed using the API-20E test system. This system allows the identification of bacterial species from the Enterobacteriaceae family, by using simplified biochemical tests.

3.6.1.1 Selection of AcrB D408A mutant candidates in *S*. Typhimurium SL1344

Four mutant candidates of *S.* Typhimurium were streaked onto XLD agar. Two candidates grew well on XLD agar; thus they were discarded. Sequencing of *acrB* was carried out for the remaining two candidates that did not grow on XLD agar. Sequencing results showed that one of the mutants had the target mutation, whereas the other one did not. Therefore, one *S.* Typhimurium SL1344 mutant candidate was selected. The API-20E test identified the mutant candidate as *Salmonella* spp. confirming the identity of the strain.

Figure 3.5 Screening for Δ*acrB* mutant candidates.

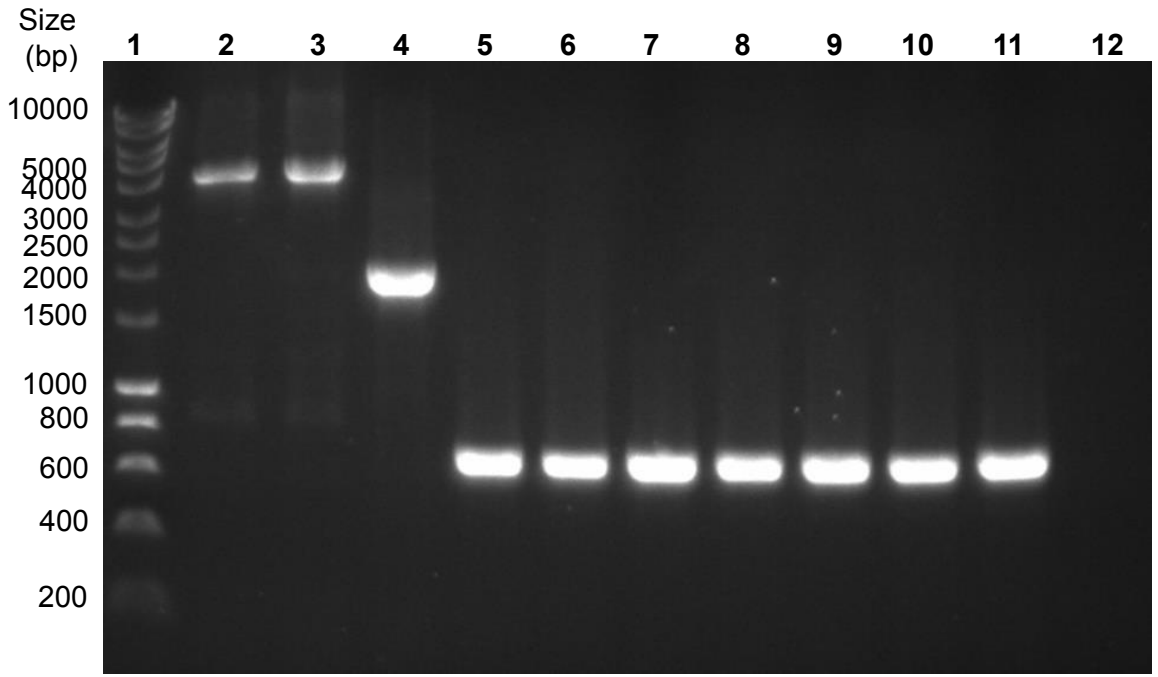

Lane	Sample
1	Bioline 1kb ladder
2	Wild-type MG1655
3	AcrB D408A
4	*acrB::aph*
5	Δ*acrB* candidate 1
6	Δ*acrB* candidate 2
7	Δ*acrB* candidate 3
8	Δ*acrB* candidate 4
9	Δ*acrB* candidate 5
10	Δ*acrB* candidate 6
11	Δ*acrB* candidate 7
12	Contamination control

Seven mutant candidates were screened by colony-PCR. Strains with an intact *acrB* have a ~3.6kb amplimer, when *acrB* is interrupted with the *aph* kanamycin resistance marker a ~2kb amplimer is expected. A ~600bp amplimer is expected in mutants where the *acrB* gene has been deleted.

3.6.1.2 Selection of AcrB D408A mutant candidates in E. coli MG1655

Ten candidates of each *acrB* mutant were replica-plated onto XLD agar. Eight colonies grew on XLD suggesting that the mutation had not been inserted. *acrB* was PCR-amplified and sequence from the two colonies that did not grow on XLD. Both mutant candidates had the GAC→GCC substitution that translates into D408A and were confirmed to be *E. coli* by API-20E test. Therefore, one mutant was selected for further characterisation.

3.7.2 Confirmation of *acrB* mutants by whole genome sequencing (WGS)

WGS was carried out to confirm that mutations did not occur on unintended targets during the genetic modification procedure. When compared against the *S.* Typhimurium SL1344 reference genome FQ312003, WGS of the mutant revealed five SNPs. These SNPs were confirmed by checking the mapped reads on Artemis; only those SNPs consistent in all the reads were considered true. The remainder were disregarded as sequencing errors. Previous data showed that the parental SL1344 in our laboratory contained four of the five SNPs (Ricci *et al*., 2012). The only SNP exclusive to the mutant was located at position 530662 in its chromosome; this mutation corresponds to the T→G substitution in *acrB*, which translates into the AcrB D408A mutation (Figure 3.6). This confirmed that the chromosomal AcrB D408A mutant was correctly constructed and had no additional mutations that could affect its phenotype.

The same procedure was carried out with *E. coli* MG1655 WGS. Reads from wild-type and *acrB* mutants were mapped against the MG1655 reference genome U00096.3.

Figure 3.6 WGS of the *S.* Typhimurium SL1344 AcrB D408A mutant.

SNPs in AcrB D408A mutant

Gene	Position in chromosome	Mutation
caiB	84505	T → C*
acrB	530662	T → G
manX	635606	T → A*
rlpA	699519	A → C*
menC	2411272	T → C*

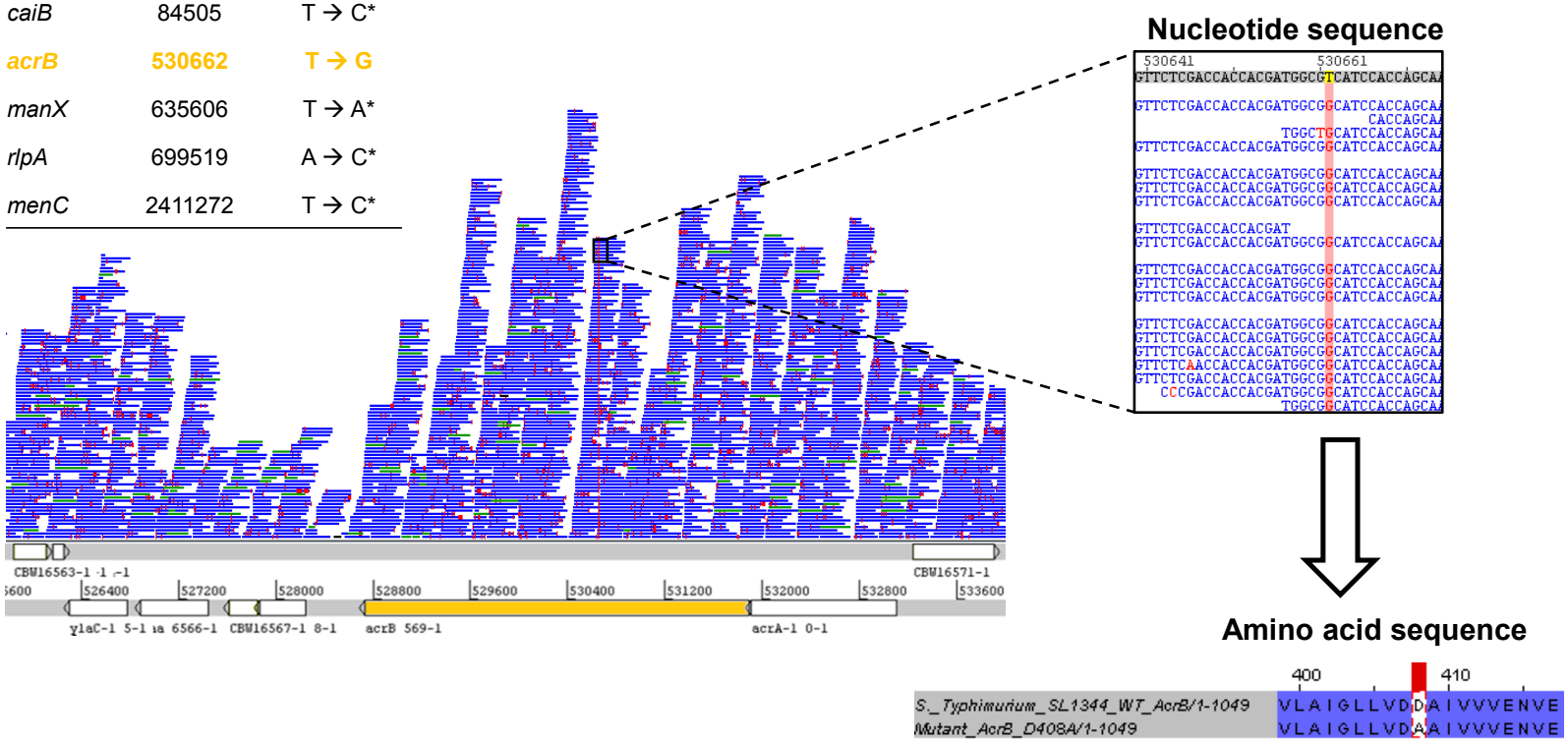

An asterisk at the end of the "Mutation" column denotes the SNPs present in SL1344. Marked in yellow is the *acrB* SNP corresponding to the AcrB D408A mutation. This SNP is shown in the Artemis plot where each one of the blue lines represents a mapped read and the vertical red lines indicates SNPs; only red lines that go across all the reads can be considered true SNPs.

The parental wild-type strain had two SNPs, one insertion and one deletion when compared against the reference genome. These mutations were present in both *acrB* mutants. The AcrB D408A mutant had an additional T→G substitution at position 483181 in the chromosome, which corresponds to the AcrB D408A mutation. The ∆*acrB* mutant had no reads mapped to the *acrB* gene as the gene is not present in the chromosome of the mutant (Figure 3.7).

3.7.3 Quantification of expression of AcrB by Western Blot

Western Blotting of AcrB was carried out to confirm the expression of the protein in the mutants. Protein preparations from the parental strain and its ∆*acrB* mutant were used as positive and negative controls, respectively, for expression of AcrB.

In *S.* Typhimurium AcrB expression of AcrB in the D408A mutant were 100% of the wild-type strain (Figure 3.8). As expected, the ∆*acrB* mutant did not express AcrB. To validate that the results observed were due to changes in amount of AcrB expressed and not to a difference in amount of total protein loaded, the amount of RNA polymerase β-subunit was quantified in parallel. This protein is constitutively expressed and its expression is not affected by *acrB*; therefore, it was used as an indicator of how much total protein was loaded into each well.

Similar results were observed with the *E. coli acrB* mutants. The *E. coli* AcrB D408A mutant expressed on average 97.43% of the wild-type levels of AcrB; the ∆*acrB* mutant did not express AcrB. The small difference in AcrB expression between the wild-type and AcrB D408A was due to a difference in total protein loaded as shown by the RNA polymerase blot (Figure 3.8).

Figure 3.7 WGS of the *E. coli* MG1655 *acrB* mutants.

Mutations in the MG1655 wild-type strain		
Gene	Position in chromosome	Mutation
ybhJ	803662	C→A
mntP	1905761	G→A
b2092 (pseudogene)	2173360	ACCC→AC
b3423 (pseudogene)	3560455	CC→CGC
Intergenic region	4296380	AC→ACGC

AcrB D408A

T→G at position 483181 in the chromosome

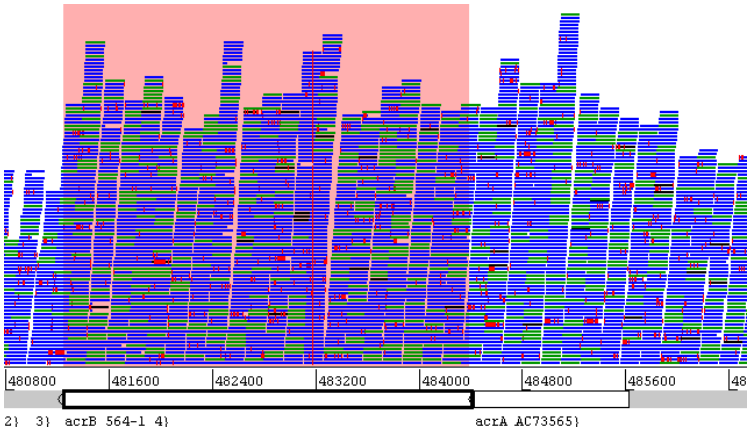

Δ*acrB*

No reads mapped to the *acrB* gene

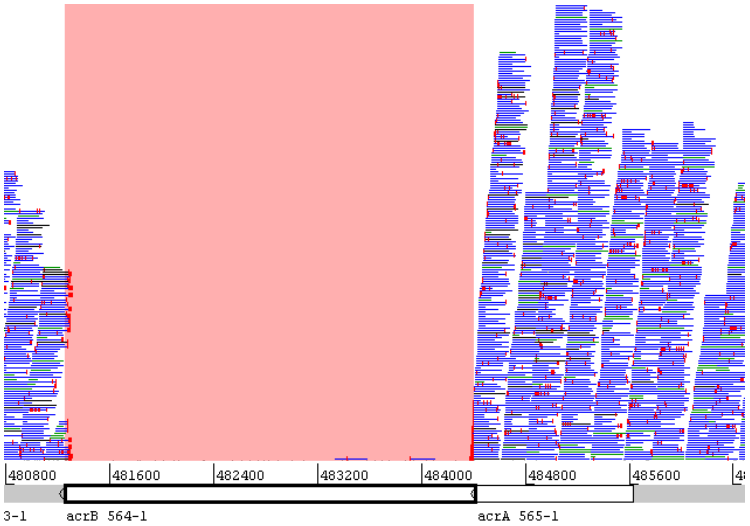

Mutations and their position in the chromosome of the MG1655 wild-type strain used in the laboratory are shown. WGS results are shown in the Artemis plot, where all reads mapped to the *acrB* gene are highlighted in red. Each blue and green horizontal line represents a mapped read. The SNP that translates into the D408A substitution in the AcrB protein is shown as a red vertical line that goes across all mapped reads.

Figure 3.8 Western blot analysis of AcrB from *S.* Typhimurium SL1344, *E. coli* MG1655 and their respective *acrB* mutants.

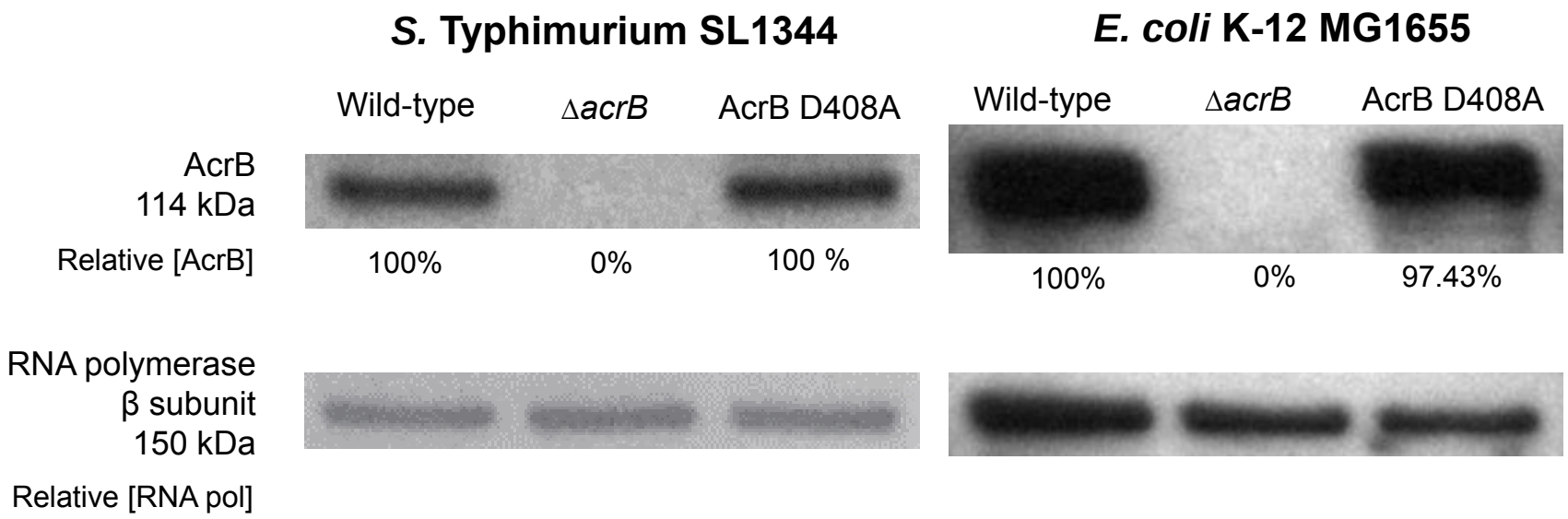

Bands corresponding to AcrB are shown in the figure. Band intensity was determined using GeneSys, this information was used to assign a relative concentration of AcrB to each band, expressed in percentage of wild-type. A Δ*acrB* mutant was used as a negative control.

These results confirmed that AcrB was expressed in the *S.* Typhimurium and *E. coli* chromosomal AcrB D408A mutants.

3.8 Phenotype of *Salmonella* Typhimurium and *E. coli acrB* mutants

3.8.1 Growth kinetics

The growth of the AcrB D408A mutants, Δ*acrB* mutants and their respective parental wild-type strains was monitored by optical density at 600nm (OD_{600}), over time.

The growth curve and generation times of mutants in rich and minimal media were similar to those of the respective wild-type strains, with no statistically significant difference between them (Figure 3.9).

3.8.2 Antimicrobial susceptibility of *acrB* mutants

As the mutation had no effect on growth, the minimum inhibitory concentrations (MIC) of several AcrB substrates were determined in order to assess the activity of the AcrAB-TolC efflux pump. AcrB substrates were selected from the literature. The inclusion criterion for dyes and antibiotics was that MICs of these were decreased following inactivation or deletion of the *acrB* gene (Buckley *et al*., 2006, Seeger *et al*., 2009, Takatsuka *et al*., 2010), or increased when the *acrB* gene was overexpressed (Nishino and Yamaguchi, 2001). The MIC values of all of the compounds tested were at least two two-fold dilutions lower for all *acrB* mutants when compared to those of the parental wild-type strain (Table 3.1).

Figure 3.9 Growth curves and generation times of *S.* Typhimurium SL1344, *E. coli* MG1655 and their respective *acrB* mutants.

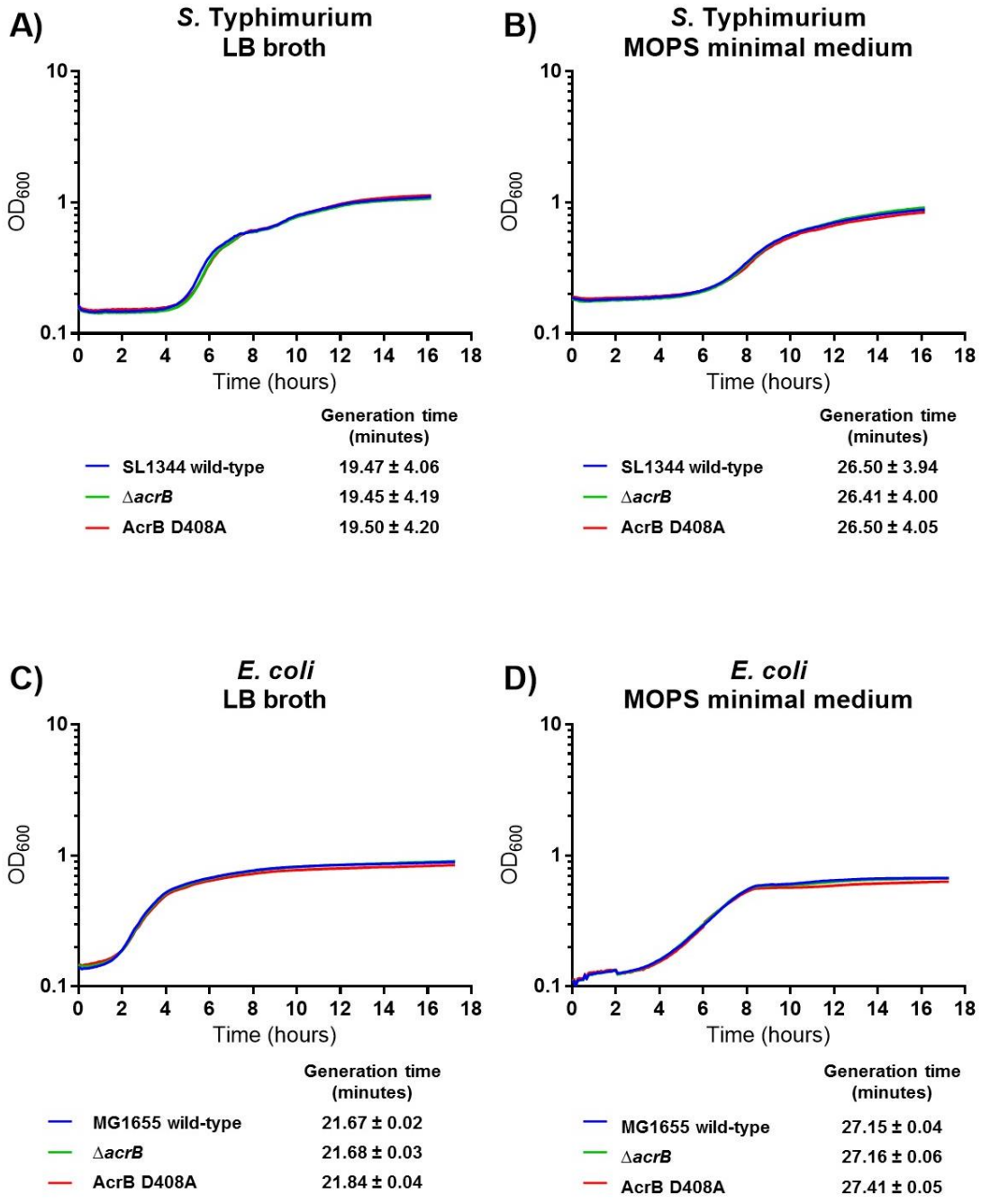

Growth curve and generation times ± standard deviation of A) *S.* Typhimurium and C) *E. coli* strains in LB broth are presented. Growth curve and generation times ± standard deviation of B) *S.* Typhimurium and D) *E. coli* strains in MOPS minimal medium are shown. Growth curves represent the mean of three biological replicates.

Table 3.1 Minimum inhibitory concentrations of AcrB substrates for *S.* Typhimurium SL1344, *E. coli* MG1655 and their respective *acrB* mutants.

Strain	Genotype	MIC (µg/mL)												
		CIP	NAL	NOV	CHL	TET	MIN	FUS	CTX	OX	ERY	ACR	ETBR	RHO
S. Typhimurium SL1344	Wild-type	0.03	4	512	8	2	2	>1024	0.5	512	256	512	>2048	512
	Δ*acrB*	0.008	1	8	2	0.5	0.25	32	<0.008	16	8	64	32	8
	AcrB D408A	0.008	1	8	2	0.5	0.25	16	<0.008	16	8	32	32	8
E. coli MG1655	Wild-type	0.01	8	1024	4	4	4	>1024	0.06	512	256	128	512	512
	Δ*acrB*	<0.008	2	16	1	1	0.5	1024	0.03	4	64	8	32	8
	AcrB D408A	<0.008	2	16	1	1	0.5	1024	0.03	4	64	8	32	8

CIP, ciprofloxacin; NAL, nalidixic acid; NOV, novobiocin; CHL, chloramphenicol; TET, tetracycline; MIN, minocycline; FUS, fusidic acid; CAZ, ceftazidime; CTX, cefoxitin; OX, oxacillin; ERY, erythromycin; ACR, acriflavine; ETBR, ethidium bromide; RHO, rhodamine 6G. Agar dilution MICs were determined 4 times. Mode values are shown. Black font, MIC values for wild-type strains and values that are one dilution lower than wild-type; blue font, MIC values ≥2 dilutions lower than the respective wild-type.

3.8.3 Accumulation and efflux of AcrB substrates by *acrB* mutants

As the MIC data suggested that the efflux activity of the chromosomal AcrB D408A mutants was compromised, efflux activity of all the strains was measured with the Hoescht 33342 (H33342) accumulation and the ethidium bromide (ETBR) efflux assays (Coldham *et al*., 2010, Blair and Piddock, 2016). Both dyes are multi-drug resistance (MDR) efflux pump substrates that fluoresce when bound to double-stranded nucleic acids (Olmsted and Kearns, 1977).

A time-dependent increase in fluorescence was observed when the H33342 dye accumulated inside the bacterial cells; this reached stasis when the amount of dye accumulated reached an equilibrium or steady state. The *acrB* mutants reached an equilibrium concentration faster than their respective parental strains and accumulated a significantly higher amount of dye, observed as a higher level of fluorescence at the end of the assay (Figure 3.10). In *E. coli*, the AcrB D408A mutant accumulated more H33342 than the Δ*acrB* strain, although the difference was not statistically significant. In contrast, there was no difference in H33342 accumulation between the *S.* Typhimurium *acrB* mutants.

To measure efflux, bacteria were preloaded with ETBR by temporarily inhibiting oxidative phosphorylation with carbonyl cyanide m-chlorophenyl hydrazone (CCCP). CCCP acts as a proton (H^+) ionophore, binding irreversibly to H^+. This causes the periplasmic H^+ gradient to dissipate, eventually resulting in loss of protonmotive force (PMF) and decreased ATP synthesis. Preloaded bacteria are subsequently energised with 25mM of glucose, at which point a decrease in ETBR fluorescence over time is observed due to active efflux of the dye (Figure 3.11). In *S.* Typhimurium, the *acrB*

Figure 3.10 Accumulation of Hoescht 33342 in *S.* Typhimurium SL1344, *E. coli* MG1655 and their respective *acrB* mutants.

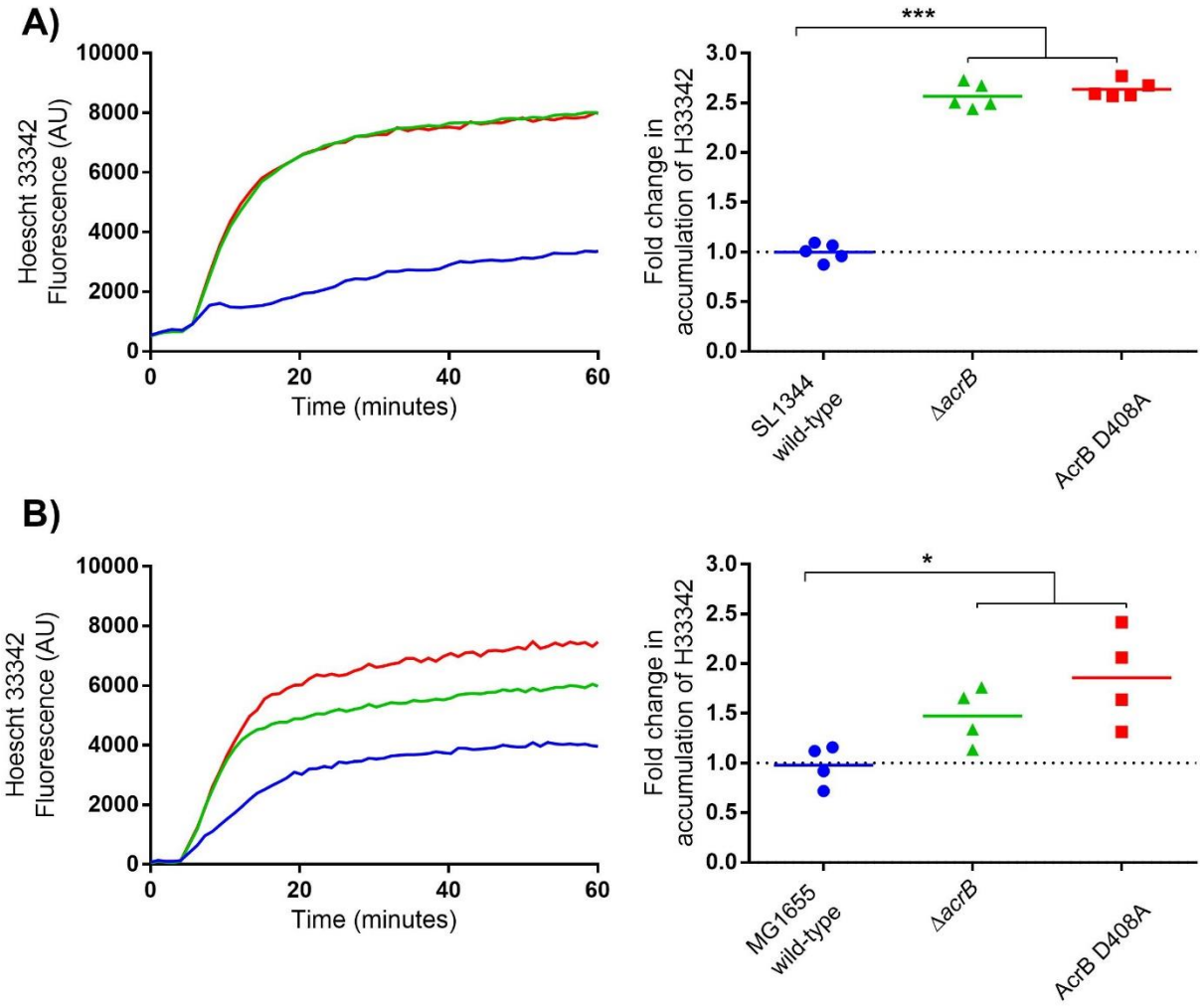

A) shows accumulation kinetics and final fold-change in accumulation of H33342 in *S.* Typhimurium SL1344. B) shows results in *E. coli* MG1655. One and three asterisks denote a significant difference of $P<0.05$ and $P<0.0001$, respectively, between two groups, compared by Student's t-test with Welch's correction.

Figure 3.11 Efflux of ethidium bromide in *S*. Typhimurium SL1344, *E. coli* MG1655 and their respective *acrB* mutants.

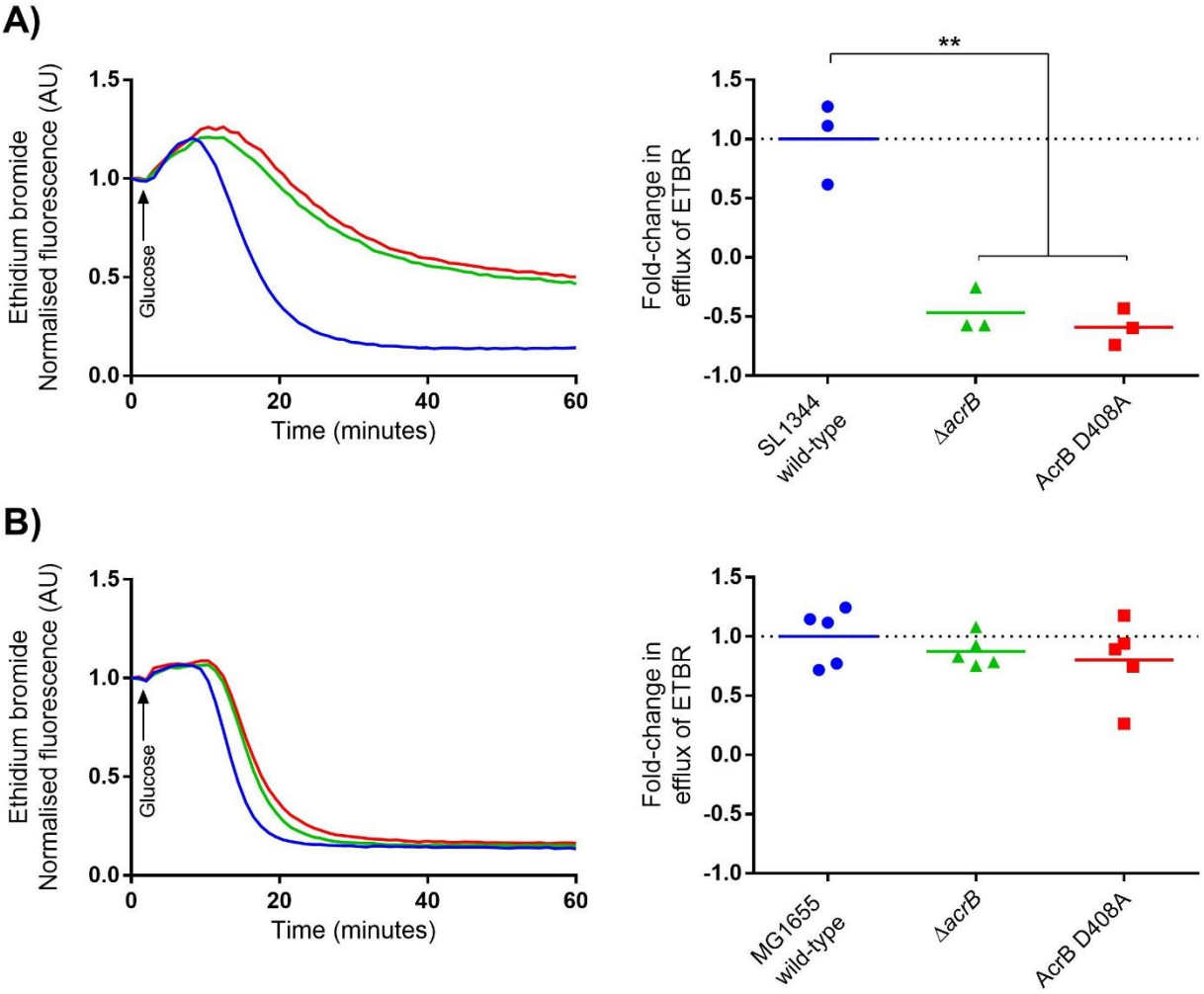

A) shows efflux kinetics and final fold-change in efflux of ethidium bromide in *S.* Typhimurium SL1344. B) shows results in *E. coli* MG1655. Two asterisks denote a significant difference of $P<0.001$ between two groups, compared by Student's t-test with Welch's correction.

mutants reached the steady state concentration faster than SL1344 and effluxed significantly less dye than SL1344. However, surprisingly in *E. coli*, inactivation of AcrB and deletion of the gene had no effect on ETBR efflux (Figure 3.11B).

These data show that the efflux and accumulation kinetics of the chromosomal AcrB D408A mutant are the same as a Δ*acrB* mutant.

3.9 Changes in transcription of RND pumps in *S.* Typhimurium SL1344 AcrB D408A mutant

It was previously reported that the transcription levels of other RND efflux pump genes, *acrD* and *acrF* was significantly increased when the *acrB* gene was deleted in *S.* Typhimurium SL1344 (Blair *et al*., 2015b, Eaves *et al*., 2004). To determine whether increased transcription of these RND pump genes is a consequence of loss of AcrB efflux function or loss of protein, qRT-PCRs were carried out to measure the amount of the *acrD* and *acrF* mRNA in the SL1344 AcrB D408A mutant. Data obtained was compared against published data from the SL1344 Δ*acrB* (Blair *et al*., 2015b). In the AcrB D408A mutant, mRNA levels of *acrB* were the same as in the wild-type parental strain (Table 3.2). Interestingly, inactivation of AcrB did not increase transcription of *acrD* and *acrF*.

Table 3.2 Relative fold-change in transcription of *acrBDF* pumps in *S.* Typhimurium SL1344 and its *acrB* mutants.

Strain	Fold change in gene transcription		
	acrB	*acrD*	*acrF*
Wild-type	1.0	1.0	1.0
Δ*acrB*	- [a]	3.6 [a]*	7.6 [a]
	- [b]	13.4 [b]*	16.0 [b]*
AcrB D408A	1.3	1.2	1.0

[a] Data taken from Eaves *et al*. (2004). [b] Data taken from Blair *et al*. (2015b). An asterisk (*) denotes significantly increased transcription ($P<0.05$) when compared against wild-type.

3.10 Discussion

Several studies have been published showing a role for AcrB in the virulence of *Salmonella* Typhimurium (Buckley *et al*., 2006, Nishino *et al*., 2006, Webber *et al*., 2009) or its homologues in other species (Bina *et al*., 2008, Padilla *et al*., 2010, Perez *et al*., 2012, Spaniol *et al*., 2015, Alcalde-Rico *et al*., 2016). However, all previous research have used gene inactivated or deletion mutants, which has caused some scepticism regarding the phenotype observed. To determine whether the phenotypes observed in *Salmonella* are due to loss of efflux function or loss of a transmembrane protein, an *acrB* mutant incapable of efflux activity was constructed in the present study.

The AcrB efflux pump is a trimer that translocates protons through residues D407, D408, K940, R971 and T978 to generate protonmotive force (PMF). The PMF allows AcrB to change its conformation and efflux a variety of compounds including antibiotics, dyes and detergents. Previous studies have suggested that mutating these residues to non-charged amino acid residues such as alanine, will 'lock' the pump in one conformation rendering it incapable to efflux (Su *et al*., 2006, Takatsuka and Nikaido, 2006). *In silico* studies have shown that substitution of the proton translocation residues with alanine does not significantly alter the structure of the protein (Su *et al*., 2006). Furthermore, *E. coli* Δ*acrB* mutants complemented with a plasmid expressing AcrB with substitutions in any of the proton translocation residues have been demonstrated to be hyper-susceptible to AcrAB-TolC substrates, indicating that AcrB was inactive in these mutants (Takatsuka and Nikaido, 2006, Seeger *et al*., 2009).

Residues essential for substrate binding of AcrB have also been described (Vargiu and Nikaido, 2012). However, modifying the binding pocket residues to inactivate AcrB

is not recommended as mutations in binding pockets occur naturally and can increase as well as decrease efflux of substrates (Blair *et al*., 2015a, Soparkar *et al*., 2015). Unlike the binding pocket, it is thought unlikely that mutations will occur naturally in residues involved in the proton translocation pathway as any changes will partially or totally inactivate the pump. Total inactivation of the pump happens when D407, D408 or K940 are mutated to alanine (Seeger *et al*., 2009). D407 and D408 are the first residues in the proton translocation pathway. As a consequence, mutating D408 to A408 should abolish proton translocation completely making it an ideal target for genetic modification.

The easiest way to introduce a genetically modified protein into a bacterium is by deleting the target gene from the bacterial chromosome and inserting the modified gene in an expression vector, producing a plasmid complementation mutant. However, complementation mutants require constant addition of antibiotics to maintain the plasmid vector and do not always replicate native levels of protein expression. Moreover, addition of antibiotics can interfere with the phenotype of a strain, for example, β-lactams increase elongation in bacteria, which interferes with OD_{600} readings (Catlin, 1975). Chromosomal mutants are better for physiological studies as they do not require addition of selective agents that could interfere with the phenotypes observed. Additionally, having a chromosomal mutant ensures that any changes observed in protein expression are due to changes in the native regulatory network and not due to changes caused by differences in number of complement plasmids. Consequently, in this study an AcrB D408A chromosomal mutant was constructed.

The chromosomal point mutation was carried out in *S.* Typhimurium SL1344 and *E. coli* MG1655, two well-recognised laboratory strains used by many researchers across

the world. Slight variations between genomes of well-established laboratory strains occur frequently due to the multiple passages the strain has undergone since it was first isolated, allowing laboratory strains to divergently evolve (Mikkola and Kurland, 1992, Fux *et al*., 2005, Klockgether *et al*., 2010). To account for possible variations in the phenotype of the *acrB* mutants, the mutants were constructed in an isogenic background and consistently compared against their respective parental wild-type strain. The AcrB D408A mutants constructed in this study contained the same SNPs as their respective parental strains plus the T→G substitution in *acrB*; confirming that the only difference between mutant and parent was a single nucleotide in the genome of the mutant. It is important to note that *acrB* is encoded in the reverse strand of the chromosome; therefore, the mutation inserted in *acrB* is A1223C, the codon was changed from GAC→GCC.

A few difficulties were encountered during the construction of the mutants. The major problem was selecting helper plasmids that worked in each background. Interestingly, pSLTS worked perfectly in *E. coli* MG1655 when it failed in *S.* Typhimurium SL1344. Similarly, pSim18 worked in SL1344 and not in MG1655. In both cases, plasmids were successfully introduced into target bacteria as shown by selection of transformants resistant to the antibiotic the plasmid confers resistance to. However, the recombinase could not be induced from these plasmids as shown by lack of insertion of the positive control DNA. It is unclear why this happened. It is hypothesised that the degree of general DNA supercoiling is different between *E. coli* and *S. enterica* (Cameron *et al*., 2011), which could affect gene expression. This is particularly important for pSim18, which expresses recombinase under the control of *pL* promoter, previously shown to be affected by the degree of DNA supercoiling (Kincade and deHaseth, 1991). Interestingly, pSim18 has been used successfully in *E. coli* K-12 strains DH10B and

BW25113 to introduce linear DNA fragments into their chromosome (Storek *et al*., 2018, Li *et al*., 2013); however, no reports were found where pSim18 was used in MG1655. In one article, the authors used pSim18 to introduce a mutation into DH10B to then transduce the mutation into MG1655 using a P1 phage (Li *et al*., 2013). The rationale behind this procedure was not explained; however, it is plausible that recombinases could not be induced from pSim18 in *E. coli* MG1655. It is important to note that *E. coli* DH10B has a 13.5-fold-higher mutation rate than MG1655 associated with the large number of insertion sequence transpositions in its chromosome (Durfee *et al*., 2008), which could also facilitate insertion of linear DNA into the chromosome.

Regarding I-SceI expression, two plasmids were tested in the different bacterial strains. Both plasmids were highly inefficient as only one colony was obtained with pACBSCE in *S.* Typhimurium and two colonies with pSLTS in *E. coli*. Kim *et al*. (2014) mentioned that the efficiency of I-SceI encoded in pSLTS was very low in highly transcribed genes as the restriction enzyme could not bind to its target site due to constant transcription of the gene where the selection cassette had been introduced. To address this, two terminator sequences were added upstream of the I-SceI restriction site in the selection cassette to facilitate binding of the enzyme to its target. This improved the efficiency of the double-stranded break; however, a minimum of 12 colonies had to be screened (Kim *et al*., 2014). Compared to genes such as *rpoD*, which has 215 transcripts per million (TPM) in mid-logarithmic phase in *S.* Typhimurium, *acrB* is not highly transcribed (123 TPM in mid-logarithmic phase); however, the absolute number of transcripts of *acrB* is still relatively high when compared to metabolic genes such as *trpA*, which only produces eight TPM (Kröger *et al*., 2013). The relatively high transcription levels of *acrB* could account for the low efficiency of I-SceI induced double-stranded break.

Expression of AcrB in the mutants was compared against the parental wild-type strain. In both *E. coli* and *S.* Typhimurium, the inactive AcrB was expressed to the same level as the wild-type strain and there was no expression of AcrB in the Δ*acrB* mutants. In *S.* Typhimurium, this was further confirmed by qRT-PCRs, where the amount of *acrB* mRNA in the AcrB D408A mutant was the same as in the parental strain.

Yang *et al*. (2006) reported that the absence of *acrB* in *E. coli* caused the mutant to reach stationary phase later than the wild-type strain. In this study, none of the *acrB* mutants tested showed any significant changes in growth either in rich or minimal media, in *E. coli* and *S.* Typhimurium. This is in accordance with a previous study in which no differences were observed between the growth kinetics of an *acrB::aph* mutant and the wild-type strain as measured by OD_{600} and viable counts (Webber *et al*., 2009). AcrB is required for contact-dependent inhibition of growth in *E. coli.* However, this is specific to strain EC93, an isolate from rat intestines that is similar to K-12, and has not been shown to occur naturally in any other strain of *E. coli* to date (Ruhe *et al*., 2013a, Ruhe *et al*., 2013b).

MICs of AcrB substrates were significantly lower for the *acrB* mutants when compared to those for the parental strains. Interestingly, the MICs of the AcrB substrates for the AcrB D408A mutant were the same as those for the Δ*acrB* mutant, which suggested that the D408A substitution abolished efflux activity to the same degree a gene-deletion mutant in *S.* Typhimurium and *E. coli*. In accordance with the MICs, in *S.* Typhimurium, assays measuring H33342 accumulation and ETBR efflux indicated that both *acrB* mutants accumulated more H33342 and effluxed less ETBR than the parental SL1344 strain, confirming that the D408A substitution renders the AcrB efflux pump inactive. In contrast, in *E. coli*, the accumulation and efflux kinetics did not reflect the MIC results. Upon initial analysis, the AcrB D408A mutant accumulated more

H33342 than the Δ*acrB* mutant; however, the difference in H33342 accumulation between the two *acrB* mutants was not significant. It is possible that a difference exists between the two mutants but there is not sufficient statistical power to show a difference due to the large standard deviation between each experiment. Regardless of the possible difference in H33342 accumulation between the two *E. coli acrB* mutants, both mutants accumulated significantly more dye than the parental MG1655 strain; however, the fold-change difference in final accumulation between wild-type and mutant *E. coli* strains was smaller (average fold-change of <2) when compared against data obtained for *S.* Typhimurium (average fold-change of 2.5). Furthermore, no significant differences were observed between the *acrB* mutants and the wild-type *E. coli* MG1655 when ETBR efflux was measured. It is possible that in *E. coli* alternative pumps play an important role in active efflux of ETBR in the absence of AcrB function. However, the MIC data indicated that inactivation of AcrB/*acrB* confers multidrug hyper-susceptibility to *E. coli*, suggesting that the alternative pump(s) either do not bind all of the AcrB substrates or are not expressed at a high enough concentration to have a significant effect on drug susceptibility.

A comparison between *E. coli* MG1655 and *S.* Typhimurium SL1344 transporters showed that there are a total of 601 transporters in MG1655 *versus* 631 in SL1344. However, in terms of RND transporters, MG1655 has ten whereas SL1344 has nine (Elbourne *et al*., 2017) (Appendix IV). Of the MDR RND pumps, MG1655 does not express MdsB and SL1344 does not express MdtF. MdsB contributes to virulence in *S.* Typhimurium but does not contribute to the overall drug susceptibility phenotype as shown with a *mdsB::aph* mutant (Nishino *et al*., 2006). MdtF, when deleted, does not affect the drug susceptibility phenotype in *E. coli* (Sulavik *et al*., 2001); however, it slightly increases the MIC of ETBR when it is overexpressed (Nishino and Yamaguchi,

2001). Another RND pump that can slightly increase the MIC of ETBR when overexpressed is AcrF (Nishino and Yamaguchi, 2001), which is expressed in both *E. coli* and *S*. Typhimurium; therefore, AcrF is unlikely to be responsible for the ETBR efflux phenotype. Consequently, it is hypothesised that MdtF rid the cell of non-inhibitory concentrations of ETBR (MIC of ETBR is 512μg/mL, concentration of ETBR used in efflux assay is 50μg/mL) in the absence of AcrB-mediated efflux in *E. coli*, by actively effluxing the dye.

Under the current hypothesis, as *E. coli* MG1655 has more RND efflux pumps that can export ETBR than SL1344, a higher MIC of ETBR would have been expected for MG1655. However, the MIC of ETBR for *E. coli* is lower (512μg/mL) to that for *S.* Typhimurium (2048μg/mL). An alternative hypothesis is that there are major differences in membrane permeability between *E. coli* and *S.* Typhimurium. Differences in membrane permeability accounts for differential influx of antibiotics into the bacterial cell, which would explain the difference in MIC, but could potentially affect efflux assays as it dictates the amount of dye that diffuses in and out of the cell. This hypothesis and the MdtF-mediated efflux are not mutually exclusive.

The AcrB-loss-of-function mutant was constructed to investigate whether deletion of the gene/loss of protein had pleiotropic effects on the physiology of *S.* Typhimurium. A phenotype caused by deletion of *acrB* is the increased transcription of alternative RND pumps *acrD* and *acrF* (Eaves *et al*., 2004, Blair *et al*., 2015b). To determine if this was a general effect of loss of efflux function or loss of protein, qRT-PCRs were carried out. Interestingly, neither *acrD* nor *acrF* were significantly upregulated in the AcrD D408A mutants, suggesting that this is a consequence of loss of AcrB protein. It is hypothesised that *acrDF* are overexpressed in the Δ*acrB* mutant because loss of a

highly expressed large transmembrane protein destabilises the membrane; therefore, to re-stabilise the membrane, the bacterium overexpresses proteins that are similar to AcrB. As AcrB is expressed to the same level as the wild-type in the AcrB D408A mutant, there is no space in the membrane to insert additional RND pump proteins; accordingly, *acrDF* cannot be overexpressed.

3.11 Key findings

- In *S.* Typhimurium SL1344 and *E. coli* MG1655, the AcrB D408A substitution confers a multidrug hyper-susceptible phenotype to the mutant.
- The D408A substitution in AcrB increases accumulation of H33342 in *S.* Typhimurium SL1344 and *E. coli* MG1655.
- Loss of AcrB-mediated efflux reduces efflux of ethidium bromide in *S.* Typhimurium but not in *E. coli* MG1655.
- The substitution does not affect growth of the mutant or expression of the AcrB.
- Increased transcription of *acrDF* is a consequence of loss of AcrB protein and not of loss of efflux function.

3.12 Future work

- More experiments with *E. coli* MG1655 are desirable to determine whether there is a significant difference in H33342 accumulation between the AcrB D408A mutant and the Δ*acrB* mutant.
- Determine if increased MdtF expression occurs in the *E. coli* AcrB D408A mutant and if it is responsible for the phenotype observed in ETBR efflux assays.

- Determine if there are membrane permeability differences between *S.* Typhimurium SL1344 and *E. coli* MG1655 and their AcrB D408A mutants.

CHAPTER 4.

Physiological changes caused by loss of AcrB efflux function in *S.* Typhimurium

4.1 Background

The AcrAB-TolC multidrug resistance efflux complex has been thoroughly studied as a mechanism of innate and acquired resistance to antibiotics. However, few studies have focused on the biological role of the complex. Most efflux pumps such as AcrD and AcrF have low basal expression under laboratory conditions and their expression is only induced after addition of antibiotics. Unlike other pumps, AcrB is constitutively expressed at a high concentration (Nishino *et al*., 2009), suggesting that the pump has a general physiological role. In *S.* Typhimurium, the role of AcrB in virulence is well-established. Nishino *et al*. (2006) analysed the effect of all RND-HAE pumps on virulence of *S.* Typhimurium and found that deletion of *acrB* caused a significant attenuation of virulence in a BALB/c mouse model. This observation has been reproduced in multiple infection models including 1-year old chicks and INT-407 human embryonic intestinal epithelial cells (Buckley *et al*., 2006, Blair *et al*., 2009). Further studies suggested that this was due to decreased transcription of *Salmonella* Pathogenicity Island (SPI) genes (Webber *et al*., 2009); however, the reason behind this significant decrease in transcription remains unknown.

Apart from virulence, AcrB also has a role in motility and biofilm formation of *S.* Typhimurium (Webber *et al*., 2009, Baugh, 2014). An *acrB::aph* mutant produced less biofilm and curli when compared against the isogenic wild-type strain (Baugh, 2014). In *Pseudomonas aeruginosa*, the AcrAB-TolC homologue, MexAB-OprM, is involved in export of quorum sensing (QS) signalling molecules, which regulate the expression of virulence and other genes in a cell-density dependent manner (Evans *et al*., 1998, Minagawa *et al*., 2012).

All previous studies have been carried out using an *acrB*::*aph* or a Δ*acrB* mutant, so it is unclear whether the phenotypes observed are caused by loss of AcrB protein or AcrB-mediated efflux. In this chapter, some of the previously described phenotypes were interrogated using the AcrB D408A mutant and the physiological role of AcrB in *S.* Typhimurium was explored by RNA-sequencing (RNA-seq).

4.2 Aims

- To explore transcriptome changes caused by loss of function of AcrB in *S.* Typhimurium by RNA-seq.
- To identify phenotypes associated with loss of AcrB efflux function.

4.3 Hypotheses

- Loss of AcrB efflux function causes significant changes in the transcriptome of the *S.* Typhimurium AcrB D408A mutant.
- AcrB efflux function is required for virulence and multiple other physiological processes in *S.* Typhimurium.

4.4 Impact of the D408A substitution in AcrB upon the transcriptome of *S.* Typhimurium SL1344

RNA-seq was carried out to study the impact of the D408A substitution in AcrB on the biology of *S.* Typhimurium. Six cultures per strain were grown in parallel in MOPS minimal medium to an OD_{600} of 0.6 under the conditions described in section 2.8.1. Cultures were quenched by snap-freezing before RNA-extraction. Two sets of cultures

were grown in different days and the three RNA samples with the best quality were selected for RNA-sequencing, each sample representing a biological replicate. No pooling of the RNA-samples was carried out.

Significant changes in the transcriptome of the mutant were observed. Of the 5031 genes in the genome of *Salmonella*, 741 were significantly changed in the mutant when compared to wild-type (14.35% of the genome). Of these, 374 and 365 genes had increased and decreased transcription, respectively.

Phage islands, flagellar genes, heat shock proteins A and B (*hslTS*), threonine (*tcd* operon) and nitrogen metabolism genes (*nir* and *nap*) were among the genes with increased transcription. *csgB* involved in curli biosynthesis was the most upregulated gene, followed by *gtgF*, a phage virulence protein (Figure 4.1).

Genes with decreased transcription included SPIs required for host cell invasion; genes encoding ABC transporters, such as the *lsrABCD* operon involved in import of quorum sensing autoinducer-2 (AI-2); genes involved in cysteine biosynthesis (*cys*) and ethanolamine utilisation (*eut*), as well as genes from the *aroPLMQDF* supraoperon for biosynthesis of aromatic amino acids (Figure 4.1). There was also a significant decrease in transcription of several *omp* genes, such as *ompA*, which encodes an outer membrane porin required for pathogenesis. The most underexpressed gene was a methionine charging tRNA ($tRNA^{Met}$).

Figure 4.1 Transcriptional landscape of the SL1344 AcrB D408A mutant.

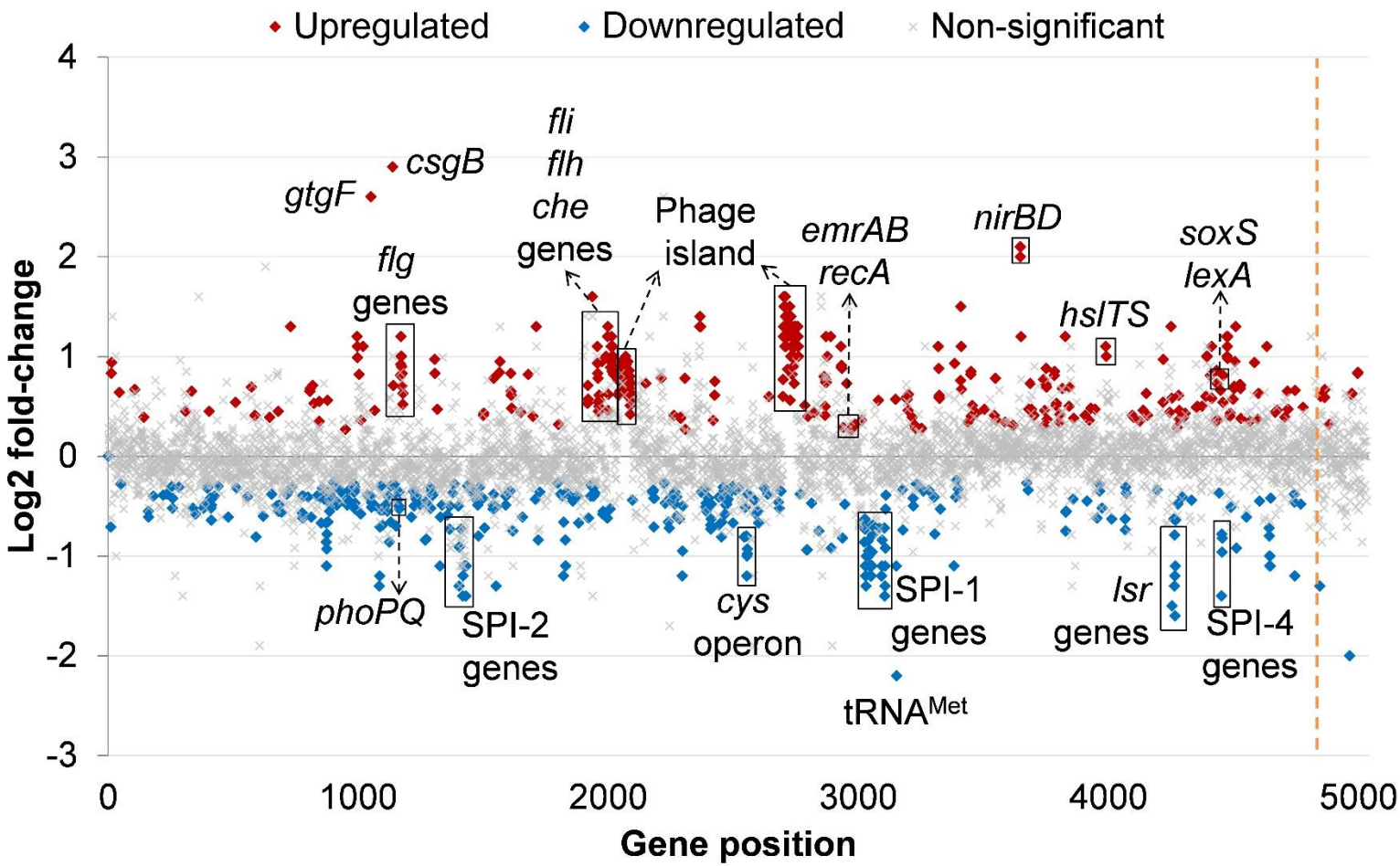

Transcriptome of the mutant was compared to parental SL1344. Significantly upregulated genes in the mutant are marked in red and significantly downregulated genes are marked in blue. Black crosses denote genes with no significant changes between the two strains. The orange dotted line indicates the end of the chromosomal genes and start of the plasmid genes.

4.4.1 RNA-seq data analysis on Clusters of Orthologous Groups (COG)

To facilitate the biological interpretation of data, significantly differentially transcribed genes (hereafter referred to as differentially transcribed genes) were assigned to Clusters of Orthologous Groups (COG) classes (Figure 4.2). The COG database is formed of four process groups; each one of them comprised of several classes of genes that encode proteins that have a similar physiological role. The SL1344 COG database only includes 4615 genes, since sRNA, rRNA, tRNA and plasmid encoded genes are not included in the database.

Most of the differentially transcribed genes were involved in metabolism (33%) and cellular processes and signalling (28%). A large percentage of genes were poorly characterised (24%) (Figure 4.2).

Analysis of COG classes revealed that the transcription of genes involved in cell motility was predominantly increased. Other classes that followed the same trend were “Cell cycle control, cell division, chromosome portioning”; “Replication, recombination and repair”; “Posttranslational modification, protein turnover, chaperones” and “Defence mechanisms” (Figure 4.3). The last COG class encompassed transcriptional activators, hypothetical exported proteins and transporters such as the MDR efflux pump *emrAB*.

COG classes in which gene-transcription was predominantly decreased, belonged to the Metabolism process. These classes included genes involved in amino acid, carbohydrate, lipid and nucleotide transport and metabolism. Additionally, genes in the “Intracellular trafficking, secretion and vesicular transport” class, which includes SPI genes, were also predominantly downregulated. Fifty percent of the genes in the

Figure 4.2 Classification of differentially transcribed genes into COG groups and classes.

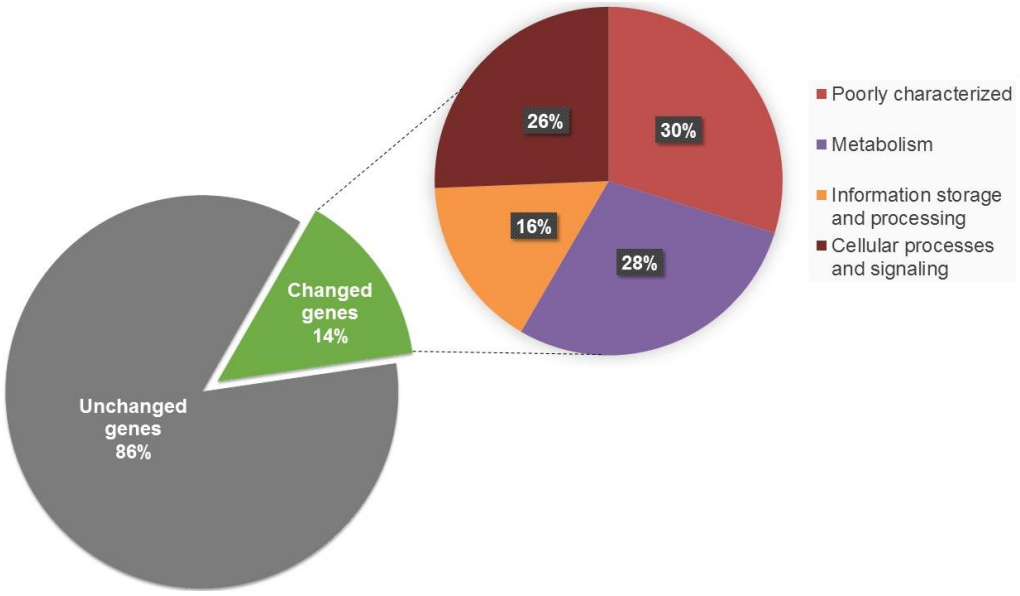

COG process	COG class	% of differentially transcribed genes
Cellular processes and signaling	Signal transduction mechanisms	27.4%
	Posttranslational modification, protein turnover, chaperones	18.2%
	Intracellular trafficking, secretion, and vesicular transport	28.1%
	Extracellular structures	0.0%
	Defense mechanisms	18.0%
	Cell wall/membrane/envelope biogenesis	12.3%
	Cell motility	13.2%
	Cell cycle control, cell division, chromosome partitioning	11.9%
Information storage and processing	Translation, ribosomal structure and biogenesis	15.3%
	Transcription	11.5%
	RNA processing and modification	0.0%
	Replication, recombination and repair	21.5%
Metabolism	Secondary metabolites biosynthesis, transport and catabolism	3.6%
	Nucleotide transport and metabolism	18.0%
	Lipid transport and metabolism	9.4%
	Inorganic ion transport and metabolism	12.3%
	Energy production and conversion	10.3%
	Coenzyme transport and metabolism	9.9%
	Carbohydrate transport and metabolism	9.0%
	Amino acid transport and metabolism	11.1%
Poorly characterized	Function unknown	28.5%
	General function prediction only	18.8%

Each COG group is comprised of different classes. The percentage of differentially expressed genes in each class was calculated by dividing the number genes changed per class by the total number of genes in the class. Therefore, the percentage shown is that of the number of differentially transcribed gene within each class.

Figure 4.3 Percentage of differentially transcribed genes in each COG class.

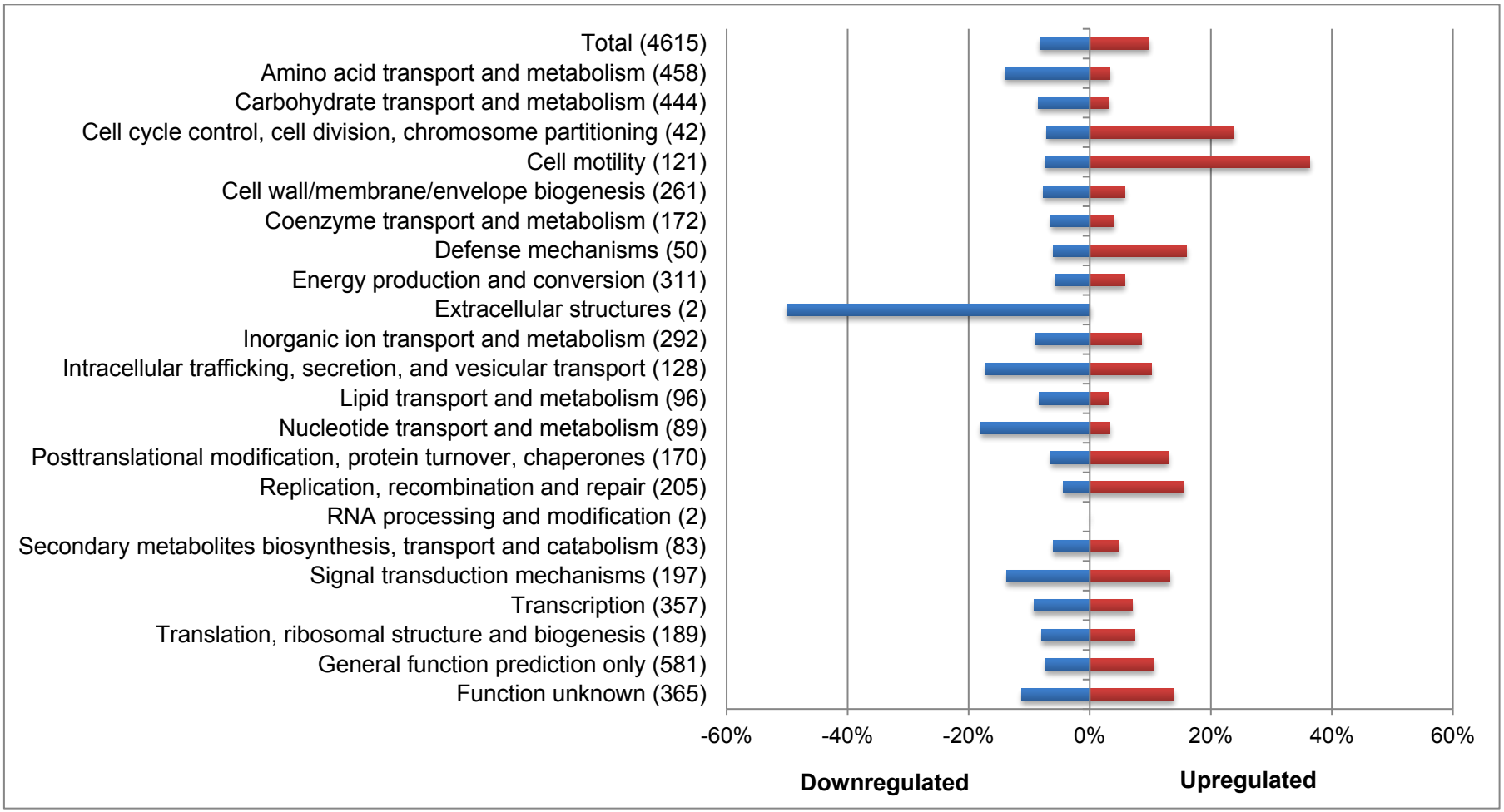

COG classes are shown on the left side of the chart, the total number of genes in this class are indicated in brackets. Percentage of up- and downregulated genes in each class are denoted with red and blue bars, respectively.

"Extracellular structures" COG class had decreased transcription. However, this class only contains two genes: the SPI-1 *sipC* and *sadA*, which encodes an autotransporter. As *sipC* transcription was decreased and *sadA* was not differentially transcribed, a large percentage of the genes in the class was downregulated (Figure 4.3).

4.4.2 Validation of RNA-seq data

To validate the RNA-seq results, significantly up- and downregulated genes, as well as genes that were not differentially transcribed were chosen randomly and their transcription was quantified using quantitative reverse-transcription PCR (qRT-PCR).

16s rRNA and *gyrB* DNA gyrase were used as housekeeping genes as they were not significantly up- or downregulated in the present or previous transcriptomics studies of SL1344 *acrB* mutants (Webber *et al*., 2009).

Transcription values of the target gene in the wild-type and AcrB D408A mutant were normalised against the housekeeping genes. Values were transformed to $\log_2$ fold-change, plotted against the $\log_2$ fold-change in transcription obtained from RNA-seq and fitted by linear regression (Figure 4.4). A positive slope was observed, indicating that genes were changed in the same direction; that is, upregulated genes in RNA-seq had increased transcription as measured by qRT-PCR and genes with decreased transcription in RNA-seq were also transcribed less when measured by qRT-PCR. A R^2 of 0.88 was observed.

Figure 4.4 Validation of RNA-seq results by qRT-PCR.

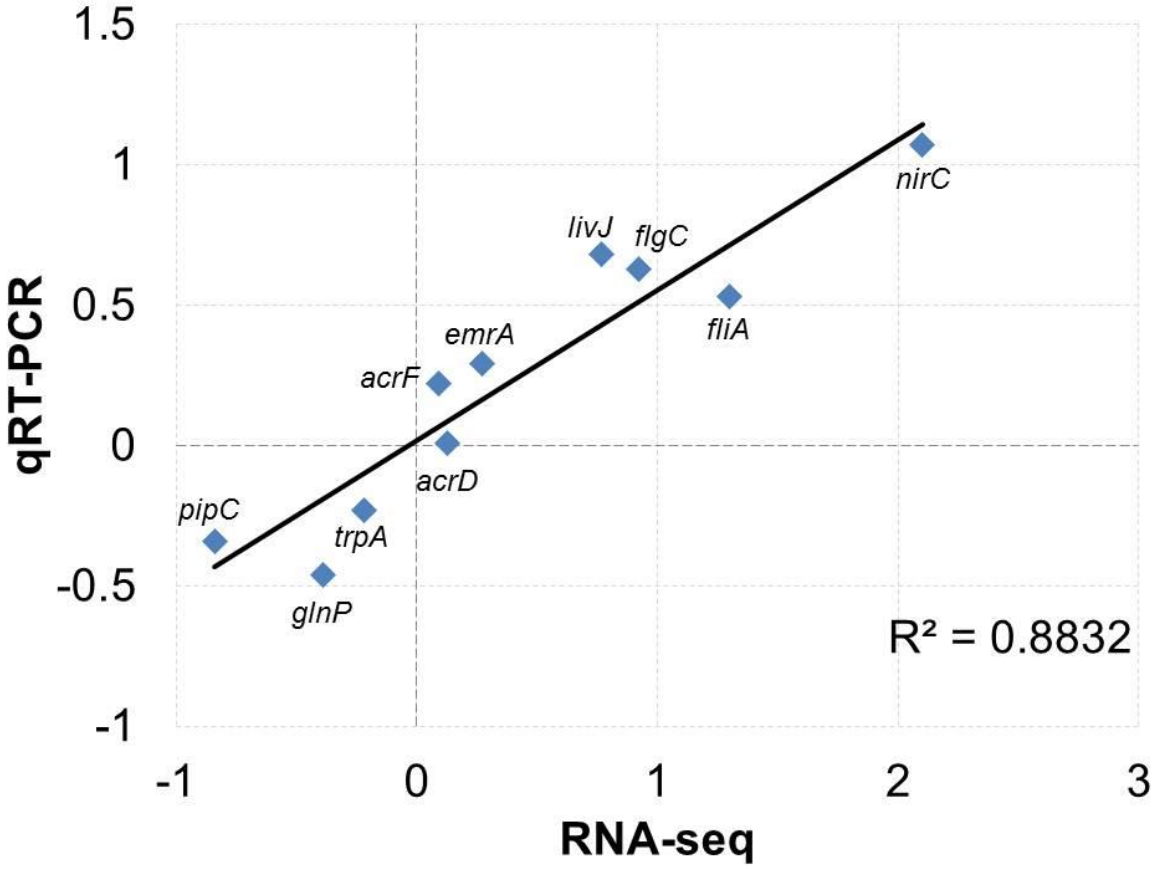

Log_2 fold-change in gene transcription between the AcrB D408A mutant and the wild-type *S.* Typhimurium SL1344 strains are shown. Gene transcription was measured by RNA-seq and qRT-PCR.

4.5 Correlation of differentially transcribed genes in an *acrB::aph* mutant with the AcrB D408A mutant

A *S.* Typhimurium SL1344 *acrB*::*aph* mutant was previously constructed in the Piddock group and its transcriptome was studied by microarray (Webber *et al*., 2009) (ArrayExpress accession number E-MEXP-1981). The microarray study was carried out with cultures grown in MOPS minimal medium to an OD_{600} of 0.6, which were the same conditions used for RNA-seq of the AcrB D408A mutant. Results from the comparison of each mutant transcriptome against its parental wild-type strain (differential gene transcription profiles) were used to determine differences and similarities between the two mutants. The *acrB*::*aph* mutant was reported to have significant changes in the transcription of 569 genes; in the AcrB D408A mutant, 741 genes were significantly changed. When the significantly changed genes in the *acrB*::*aph* mutant were compared against those of the AcrB D408A mutant, only 190 genes matched. Of these, 85 genes were changed in the same direction; that is, 44.7% of differentially transcribed genes were equally up- or downregulated. The rest of the genes (55.3%) were changed in opposite directions. In accordance with this, when $\log_2$ fold-change values obtained from RNA-seq of the AcrB D408A mutant were plotted against those from microarray data of the *acrB*::*aph* mutant, a slightly negative slope was observed (Figure 4.5). R^2 was used to find the correlation between the two datasets, the correlation between the two datasets was very weak and did not follow any trendline as shown by a R^2 of 0.06 (Figure 4.5).

Figure 4.5 Correlation between the transcriptome of a *S.* Typhimurium SL1344 *acrB*::*aph* mutant and the AcrB D408A mutant.

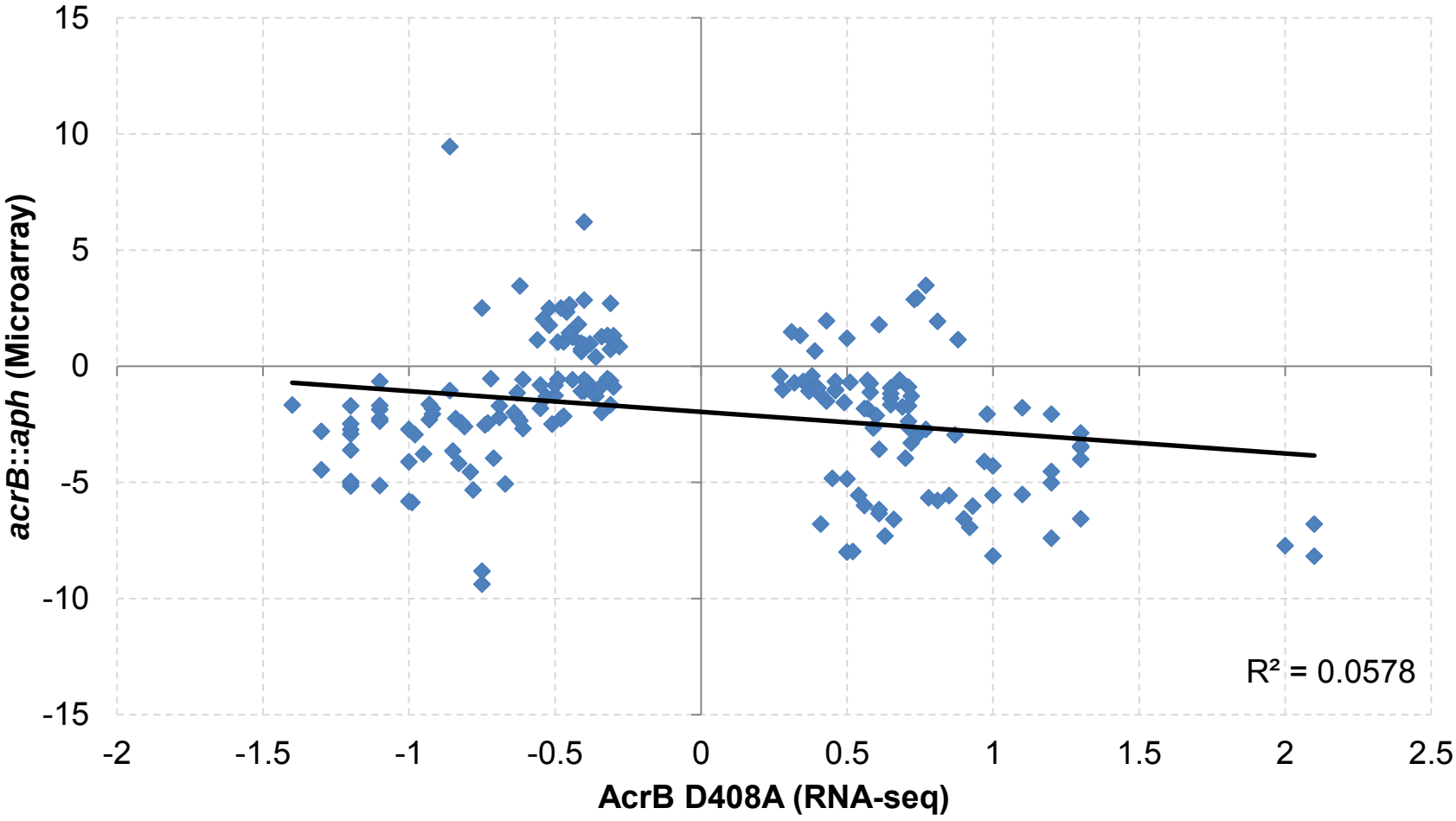

Log_2 fold-change between mutant and wild-type is plotted. Only genes that were differentially transcribed with a $P<0.05$ are shown.

Comparison of COGs revealed that genes involved in cell motility were primarily upregulated in the AcrB D408A mutant, whereas they were downregulated in the *acrB*::*aph* mutant. Similar patterns were observed in three other COG classes: nucleotide transport and metabolism; post-translational modification, protein turn over and chaperones; and replication, recombination and repair. Only three COG classes had a similar percentage of down and upregulated genes in both mutant strains, these were: cell wall/membrane/envelope biogenesis; secondary metabolites biosynthesis, transport and catabolism; and transcription (Figure 4.6).

4.6 Comparison of motility phenotypes between an *acrB*::*aph*, Δ*acrB* and AcrB D408A mutants

The "Cell motility" COG class was one of the COG classes with the most differentially transcribed genes in the *acrB*::*aph* and AcrB D408A mutants. Genes were also transcribed in opposite directions between the two mutants. To explore changes in the motility phenotype, motility assays in semisolid agar were carried out. A Δ*acrB* mutant was included as it was expected to have the same phenotype as either the *acrB*::*aph* mutant or the AcrB D408A mutant.

To measure swimming, *S.* Typhimurium SL1344 and its *acrB* mutants were stabbed into MOPS minimal medium with 0.3% of agar to allow movement of bacteria through the pores of the agar. Consistent with the transcriptome analysis, the *acrB*::*aph* mutant was significantly less motile than the wild-type strain, whereas the Δ*acrB* and the AcrB D408A mutants were significantly more motile (Figure 4.7).

Figure 4.6 Comparison of COGs between an SL1344 *acrB*::*aph* mutant and the AcrB D408A mutant.

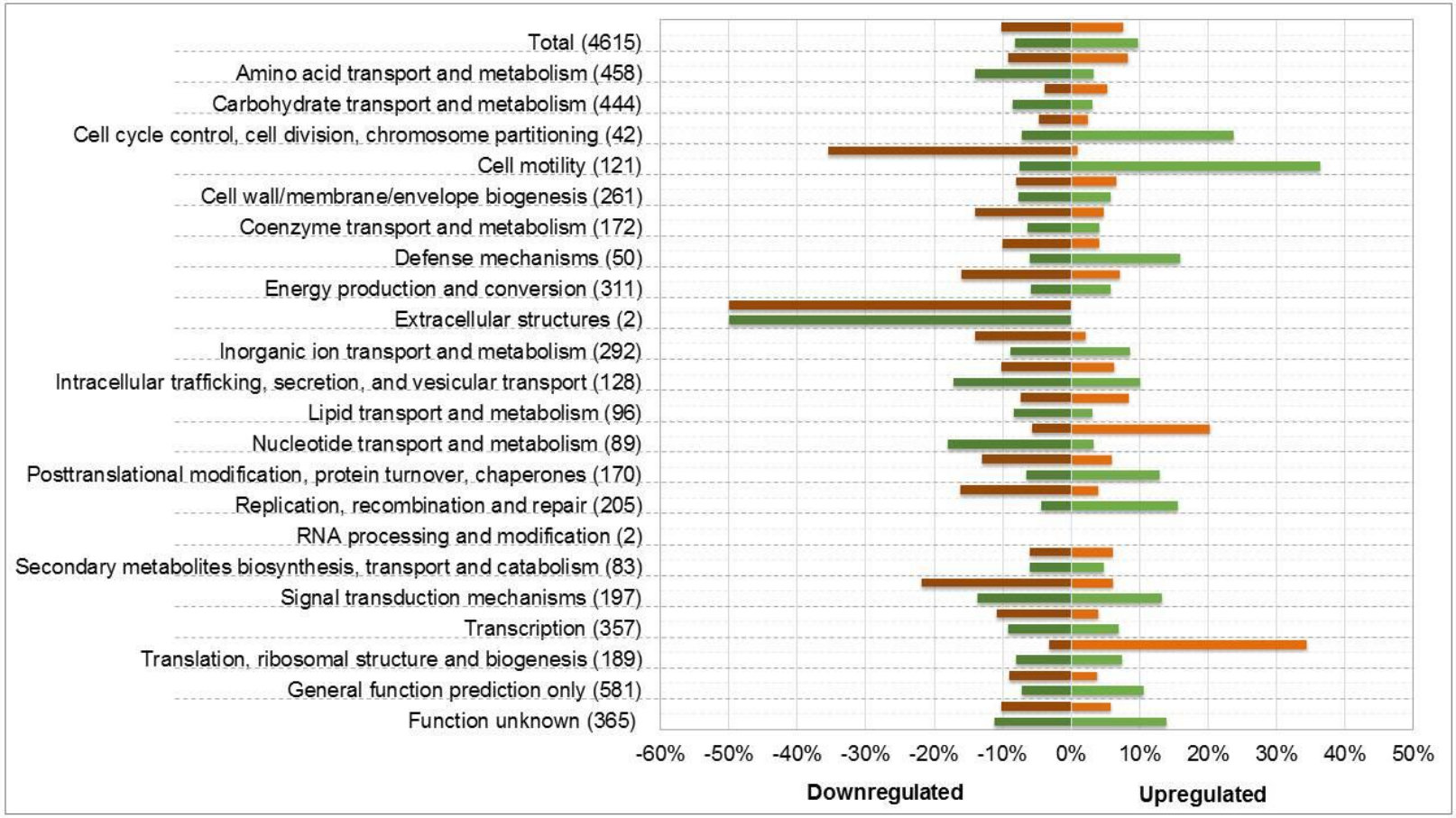

COG classes are shown on the left side of the chart, the total number of genes in this class are indicated in brackets. Orange bars show results for the *acrB*::*aph* mutant, orange bars indicate results for the AcrB D408A mutant. Percentage of downregulated genes in each class are denoted with dark-coloured bars, whereas percentage of upregulated genes are shown with light-coloured bars.

Figure 4.7 Swimming of *S.* Typhimurium SL1344 and its *acrB* mutants in MOPs minimal medium with 0.3% agar.

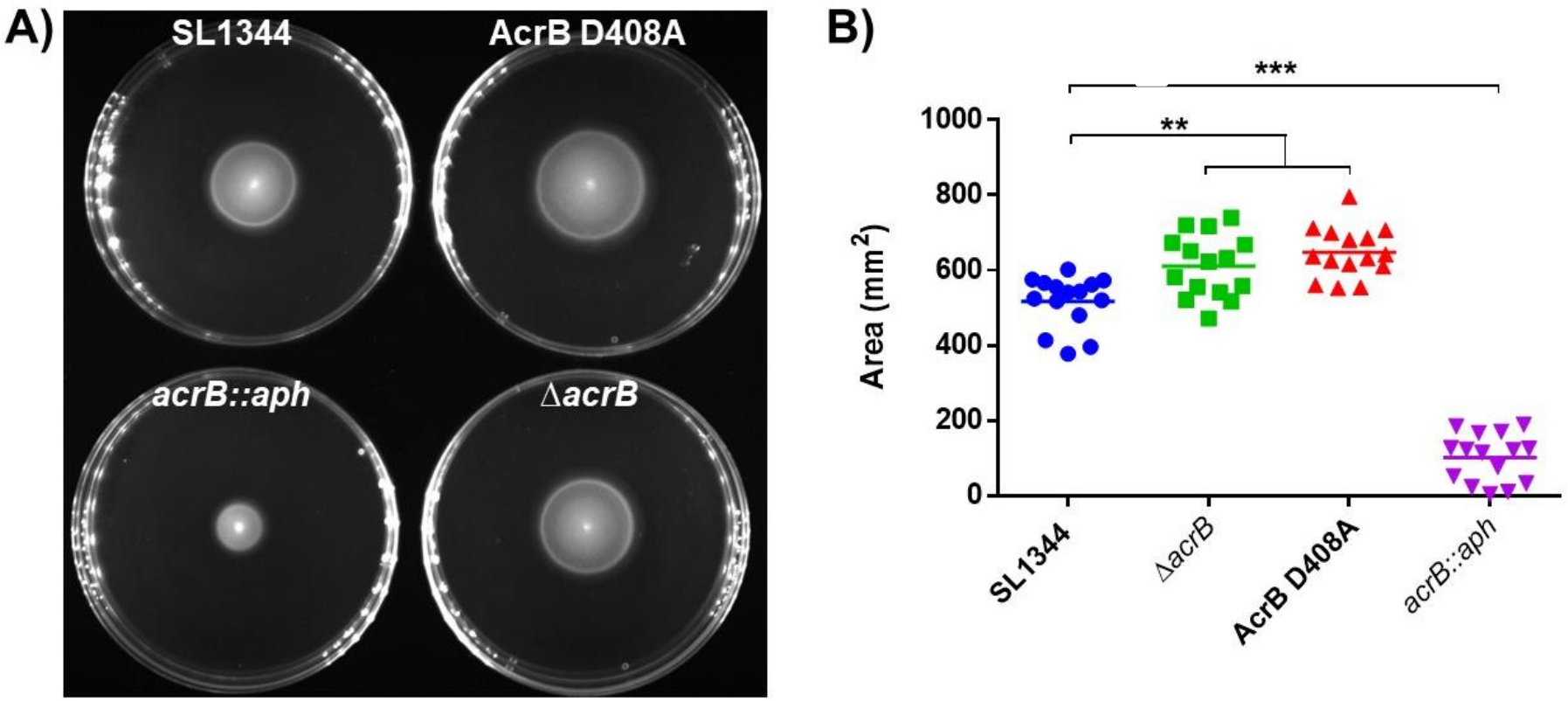

A) shows motility halos formed by swimming *S.* Typhimurium. The inoculum was stabbed into the middle of the plate and *S.* Typhimurium swam to form concentric circles around the inoculum. B) shows area of the motility halos as measured in mm^2 in ImageJ. Each dot represents a biological replicate and the line in the middle represents the mean of each dataset. A Student's t-test with Welch's correction was carried out between the wild-type strain and each mutant to determine statistical significance. Two asterisks (**) indicate a significant difference with a $P<0.01$, three asterisks (***) denote a significant difference with a $P<0.001$.

Swarming motility was also measured. Swarming consists of the movement of bacteria across the surface of semisolid agar (0.6% agar in this case). Assays were attempted using MOPS minimal agar; however, no swarming was observed after five days of incubation. Therefore, LB semisolid agar supplemented with 4g/L of glucose was used (Harshey and Matsuyama, 1994). Similar to what was observed with swimming, the *acrB*::*aph* mutant swarmed significantly less than the other *acrB* mutants. Interestingly, no significant increase in motility was observed in the AcrB D408A and the Δ*acrB* mutants (Figure 4.8).

To test whether the loss of the hyper-motility phenotype in the AcrB D408A and the Δ*acrB* mutants were due to changes in media composition, swimming assays were carried out in LB semisolid agar. As LB medium is richer in nutrients than MOPS, *S.* Typhimurium grew faster and, consequently, swam faster through the agar. Therefore, incubation times were reduced to seven hours to obtain a good measurement of the halo of motility. In LB medium, no significant differences in swimming were observed between the wild-type and its *acrB* mutants (Figure 4.9), suggesting that the motility phenotype is specific to minimal media.

4.7 Changes in the transcription of the *acrAB* transcription regulator *ramA* and the SOS response regulator *lexA* in the AcrB D408A mutant

4.7.1 Differential transcription of *ramA*

The global transcription regulator *ramA* is known to control the expression of AcrAB in *S.* Typhimurium. Previous studies have shown that the transcription of this gene is significantly increased in an *acrB*::*aph* mutant and a Δ*acrB* mutant, and also when efflux inhibitors, such as phenyl-alanine β-naphtylamide (PAβN) and chlorpromazine

Figure 4.8 Swarming motility of *S.* Typhimurium SL1344 and its *acrB* mutants in LB medium supplemented with glucose with 0.5% agar.

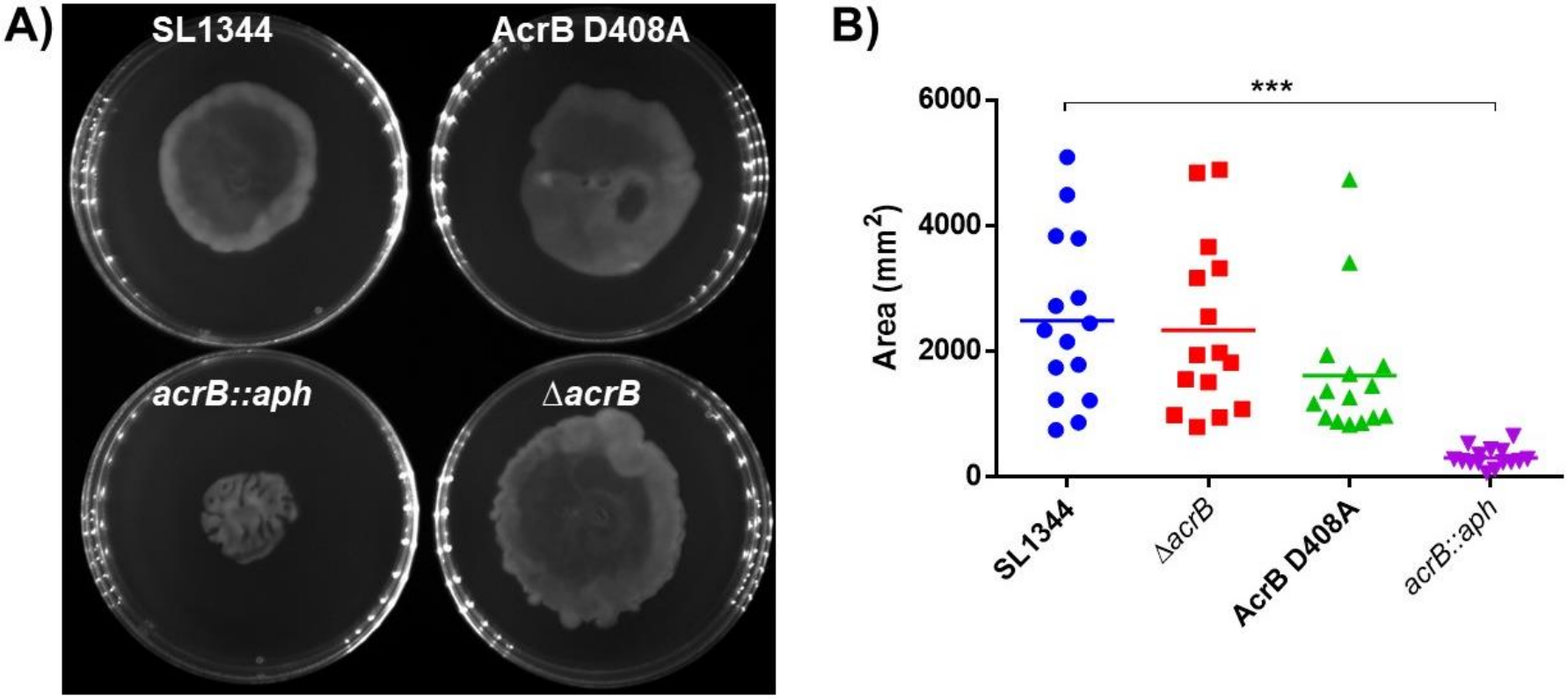

A) shows motility patterns formed by swarming of *S.* Typhimurium. The inoculum was spotted onto the agar, in the middle of the plate. B) shows area of motility as measured in mm^2 in ImageJ. Each dot represents a biological replicate and the line in the middle represents the mean of each dataset. A Mann-Whitney U test was carried out between the wild-type strain and each mutant to determine statistical significance. This test was used as data did not pass the normality test. Three asterisks (***) denote a significant difference with a $P<0.001$.

Figure 4.9 Swimming motility of *S.* Typhimurium SL1344 and its *acrB* mutants in LB medium with 0.3% agar.

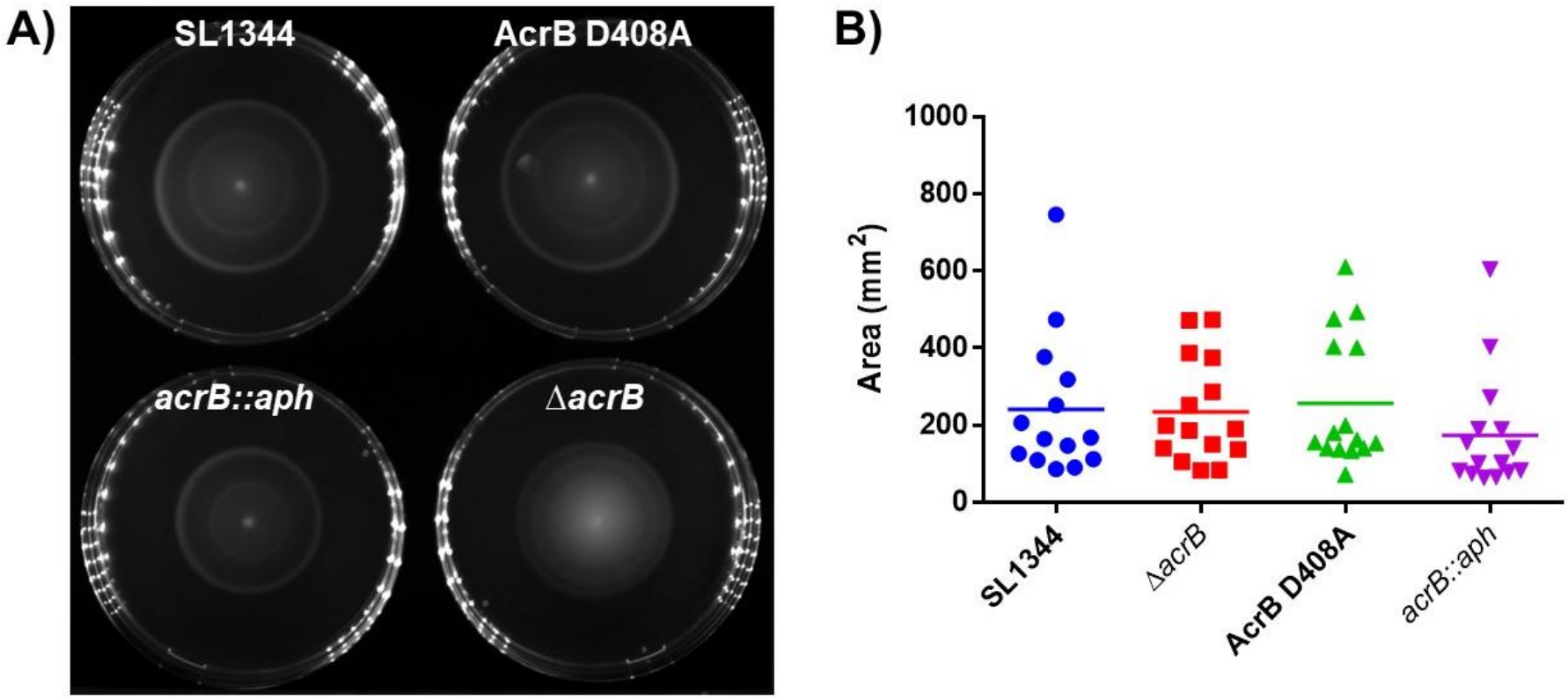

A) shows motility halos formed by swimming *S.* Typhimurium. The inoculum was stabbed into the middle of the plate. *S.* Typhimurium swam in concentric circles around the inoculum. B) shows area of the motility halos as measured in mm^2 in ImageJ. Each dot represents a biological replicate and the line in the middle represents the mean of each dataset. A Mann-Whitney U test was carried out between the wild-type strain and each mutant to determine statistical significance. This test was used as data did not pass the normality test.

(CPZ), were added *S.* Typhimurium. Therefore, it was expected that *ramA* would be upregulated in the AcrB D408A mutant. However, RNA-seq revealed that this gene was not differentially transcribed in the mutant. To validate this result, a *ramA* induction assay was carried out using a *ramA*-GFP reporter plasmid. The plasmid was constructed by fusing the *ramA* promoter region to a gene encoding a green fluorescent protein (GFP) in a pMW82 background (Lawler *et al*., 2013). Induction of the transcription of *ramA* resulted in expression of GFP, the fluorescence intensity of which was measured and normalised against the OD_{600} of the culture to assess the induction of *ramA* transcription relative to number of bacteria. CPZ was used as positive control for *ramA* induction and a promoterless pMW82-*gfp* was used to detect leaky expression of GFP. In accordance with previous studies, *ramA* was overinduced in an Δ*acrB* mutant (fold-change of 5.75±1.61); however, no significant changes in *ramA* induction were observed in the AcrB D408A mutant (fold-change of 1.68±0.82) (Figure 4.10).

4.7.2 Differential transcription of *lexA*

The *lexA* gene, involved in regulation of the SOS DNA repair response, was significantly upregulated in the AcrB D408A mutant as shown by the RNA-seq results. To validate this finding, induction of transcription of *lexA* was assessed using a *lexA*-GFP reporter construct (p*lexA*). The construct was tested using varying concentrations of nalidixic acid (NAL) as this antibiotic is known to induce expression of the SOS response by inhibiting bacterial DNA gyrase. This in turn causes DNA damage and activation of the SOS response, characterised by increased transcription of *recA* and

Figure 4.10 Induction of *ramA* in *S.* Typhimurium SL1344 and its *acrB* mutants.

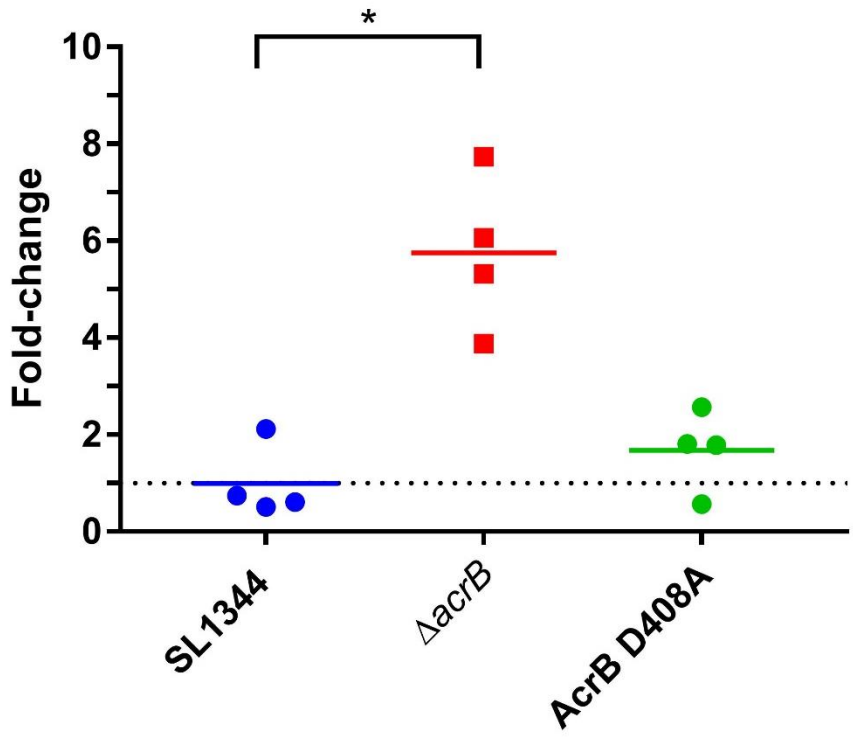

Fold-change in gene induction was calculated by dividing the relative fluorescence of the *acrB* mutant by the relative fluorescence of the wild-type. Each dot represents an independent experiment. The line in the middle represents the mean of each dataset. A Student's t-test with Welch's correction was carried out between the parental strain and the *acrB* mutants to determine statistical significance. An asterisk indicates a significant difference ($P<0.05$).

lexA response regulators and response effectors. A concentration of NAL of ≥1.6μg/mL was required to cause a significant induction of *lexA* when compared against the control (0μg/mL of NAL). Maximum induction of *lexA* was observed at 10μg/mL, after which, the relative fluorescence started to decrease; although induction of *lexA* was still significant up to 80μg/mL of NAL (Figure 4.11A). As a positive control for the *lexA* induction assay, 1.6μg/mL was chosen since it did not affect growth of the AcrB D408A mutant and simultaneously induced transcription of *lexA*. Unfortunately, the reporter strain was not suitable for assessing native levels of *lexA* induction as SL1344+p*lexA* emitted the same amount of fluorescence as the SL1344+pMW82 empty vector (fold-change of 0.91±0.46) (Figure 4.11B). Since the aim of this experiment was to validate the RNA-seq results, which showed an increase in the native levels of *lexA* transcription in the AcrB D408A mutant; the measurements obtained from the fluorescence reader could not be used as it could not differentiate between the empty vector and reporter strain. Therefore, a more sensitive instrument was required. The experiment was repeated in a flow cytometer. A voltage of 520V was used to differentiate fluorescent from non-fluorescent bacteria in the positive control; that is, SL1344+p*lexA* and AcrB D408A+p*lexA* exposed to 1.6μg/mL of NAL. The positive control sample separated into two peaks, one of relative GFP intensity (GFP-expressing) and the other with lower relative intensity (non-fluorescent). However, when *S.* Typhimurium without exposure to NAL was analysed, no high fluorescence peaks were observed, but a shift in fluorescence between the strains carrying p*lexA* to those carrying the empty vector was seen (Appendix V). The voltage was increased to 700V in order to try to separate the fluorescent from the non-fluorescent subpopulation, yet fluorescence intensity patterns remained the same.

Figure 4.11 Induction of *lexA* in *S.* Typhimurium SL1344 exposed to nalidixic acid.

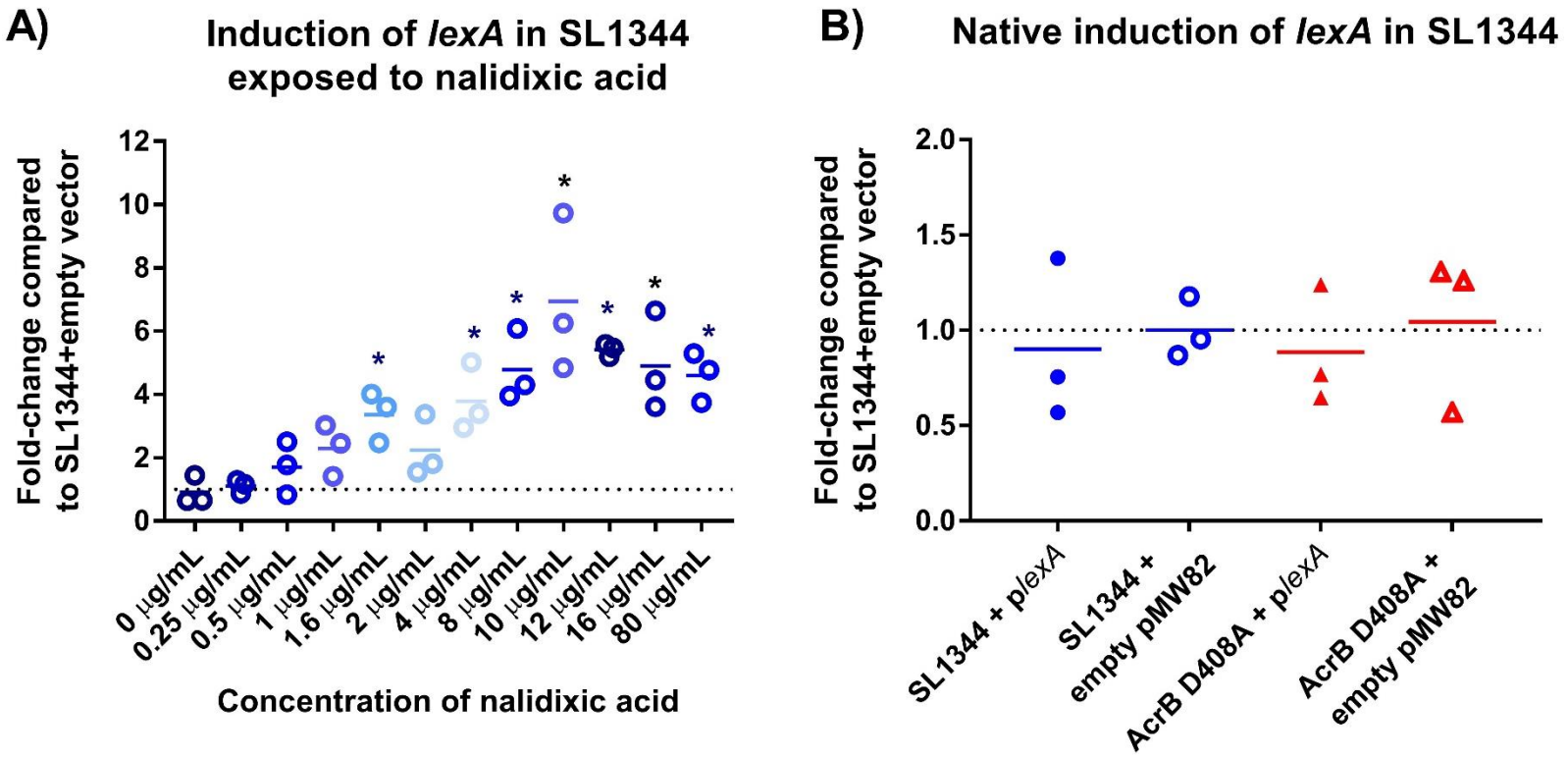

A) shows the induction of *lexA* in *S.* Typhimurium SL1344 during exposure to varying concentrations of NAL. B) shows the native induction of *lexA* in the wild-type SL1344 and its AcrB D408A mutant in the absence of inducers. Fold-changes in induction were calculated by dividing the relative fluorescence of the *S.* Typhimurium in the presence of NAL by the relative fluorescence of *S.* Typhimurium grown without NAL. Each dot represents an independent experiment. The line in the middle represents the mean of each dataset. A Student's t-test with Welch's correction was carried out between the control without NAL and each concentration of NAL to determine statistical significance. An asterisk indicates a significant difference ($P<0.05$) at the given concentration of NAL when compared against the control without NAL.

Nonetheless, there was a slight difference in fluorescence intensity between SL1344+p*lexA* and AcrB D408A+p*lexA* (Figure 4.12).

Median fluorescence intensity was used to determine whether *lexA* was significantly induced in the AcrB D408A mutant when compared against the parental SL1344 strain. The median was used as the fluorescence intensity histograms did not follow a normal distribution (Figure 4.12). In the AcrB D408A mutant, *lexA* was induced 0.314-fold (31.4%) more than in the wild-type strain (Figure 4.13). The difference was statistically significant with $P<0.05$.

4.8 Attenuation of virulence of *S.* Typhimurium as a consequence of loss of AcrB efflux function

4.8.1 Infection of human intestinal epithelial cells and murine macrophages by the AcrB D408A mutant

The transcriptomics results indicated that many SPI genes were significantly downregulated in the *acrB* mutant compared to its parental SL1344 strain. SPI genes are essential for invasion and survival of *Salmonella* spp. in host cells. The decreased transcription of these genes suggested that the ability of the AcrB D408A mutant to invade intestinal cells and macrophages was compromised. To test this hypothesis, association and invasion of the mutant into intestinal epithelial cells and macrophages was measured in gentamicin protection assays and compared against the parental SL1344 and a previously constructed Δ*acrB* mutant.

INT-407 and Caco2 are human intestinal epithelial cell lines. INT-407 cells are derived from human embryonic intestinal tissue, whereas Caco2 cells derived from a human

Figure 4.12 Induction of *lexA* in *S.* Typhimurium SL1344 as measured in an Attune Nxt flow cytometer.

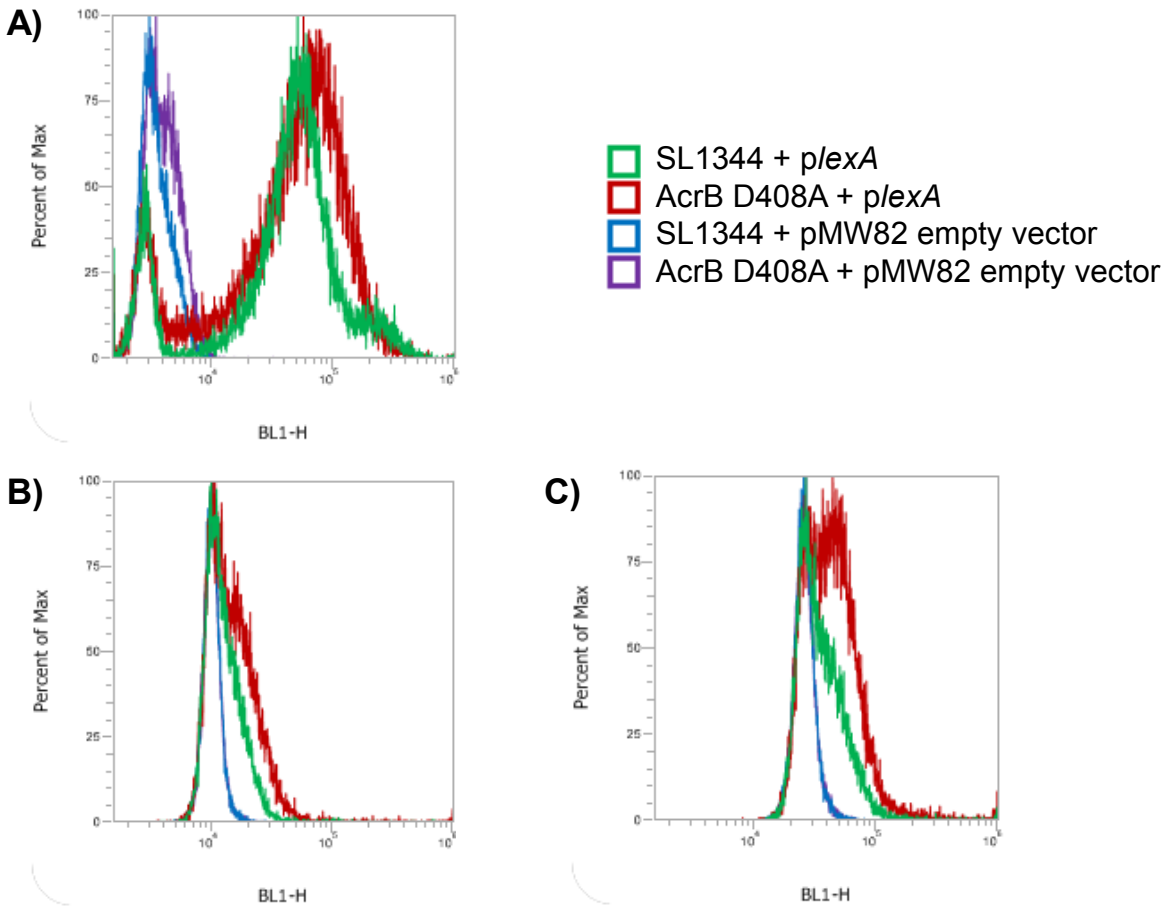

Induction of transcription was *lexA*, as given by GFP fluorescence intensity, was measured in a flow cytometer. GFP fluorescence intensity, measured in the BL1 channel (X axis), was plotted against the number of bacteria detected and normalised to percentage (Y axis) to allow comparison between strains. A) shows the fluorescence intensity of SL1344 and its AcrB D408A mutant carrying the reporter plasmid (p*lexA*) or the empty vector, after exposure to 1.6μg/mL of nalidixic acid (NAL). B) shows the fluorescence intensity of test strains and negative controls without exposure to NAL, measured at 540V. C) shows the fluorescence intensity of test strains and negative controls without exposure to NAL, measured at 700V.

Figure 4.13 Induction of *lexA* in *S.* Typhimurium SL1344 and its AcrB D408A mutant.

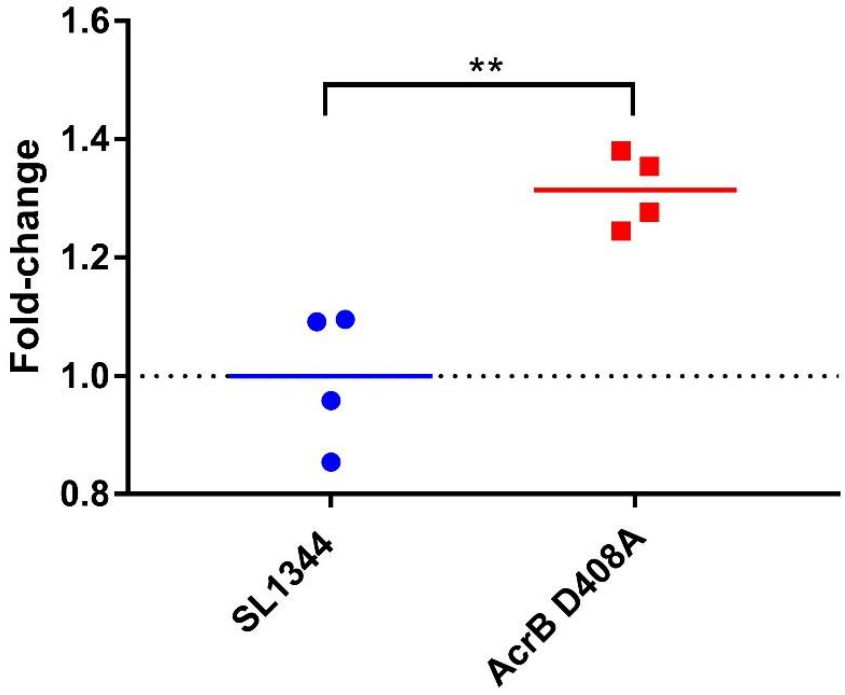

The fold-change induction of *lexA* in the AcrB D408A mutant when compared against its parental wild-type strain is shown. Each dot represents an independent experiment. The line in the middle represents the mean of each dataset. Two asterisks (**) indicate a statistically significant difference with a $P<0.01$ as calculated with a Student's t-test with Welch's correction.

colorectal adenocarcinoma. The main difference between these two cell lines is that Caco2 cells form polarised monolayers with well-differentiated apices and bottoms, whereas INT-407 cells can only form plain, undifferentiated, monolayers. In INT-407 cells, the *acrB* mutants associated and invaded epithelial cells less than 2% of that seen with SL1344. In Caco2 cells, invasion was decreased to 12-17%. The loss of virulence phenotype was stronger during invasion than association (Figure 4.14).

The J774A.1 cell line derives from blood macrophages of BALB/c mice. Infection assays with this macrophage lineage showed similar results to those observed with epithelial cells. None of the *acrB* mutants were able to associate or invade the macrophages resulting in invasion levels as low as 1% of those seen with the parental strains SL1344 (Figure 4.15).

4.8.2 Infection of BALB/c mice by the AcrB D408A mutant

To validate that the decreased invasion of intestinal epithelial cells and macrophages happened *in vivo*, groups of five BALB/c mice were inoculated orally or intraperitoneally with the wild-type and the AcrB D408A mutant. Mice were sacrificed at five days post-infection and liver and spleen were recovered to assess the degree of systemic infection. In general, mice infected with the AcrB D408A mutant had less CFU/mg of organ than when infected with the parental SL1344 strain. The difference was significant, except in the liver of mice inoculated orally, where the *P*-value equalled 0.05 (Figure 4.16).

Figure 4.14 Infection assays with SL1344 and its *acrB* mutants in A) INT-407 and B) Caco2 intestinal epithelial cells.

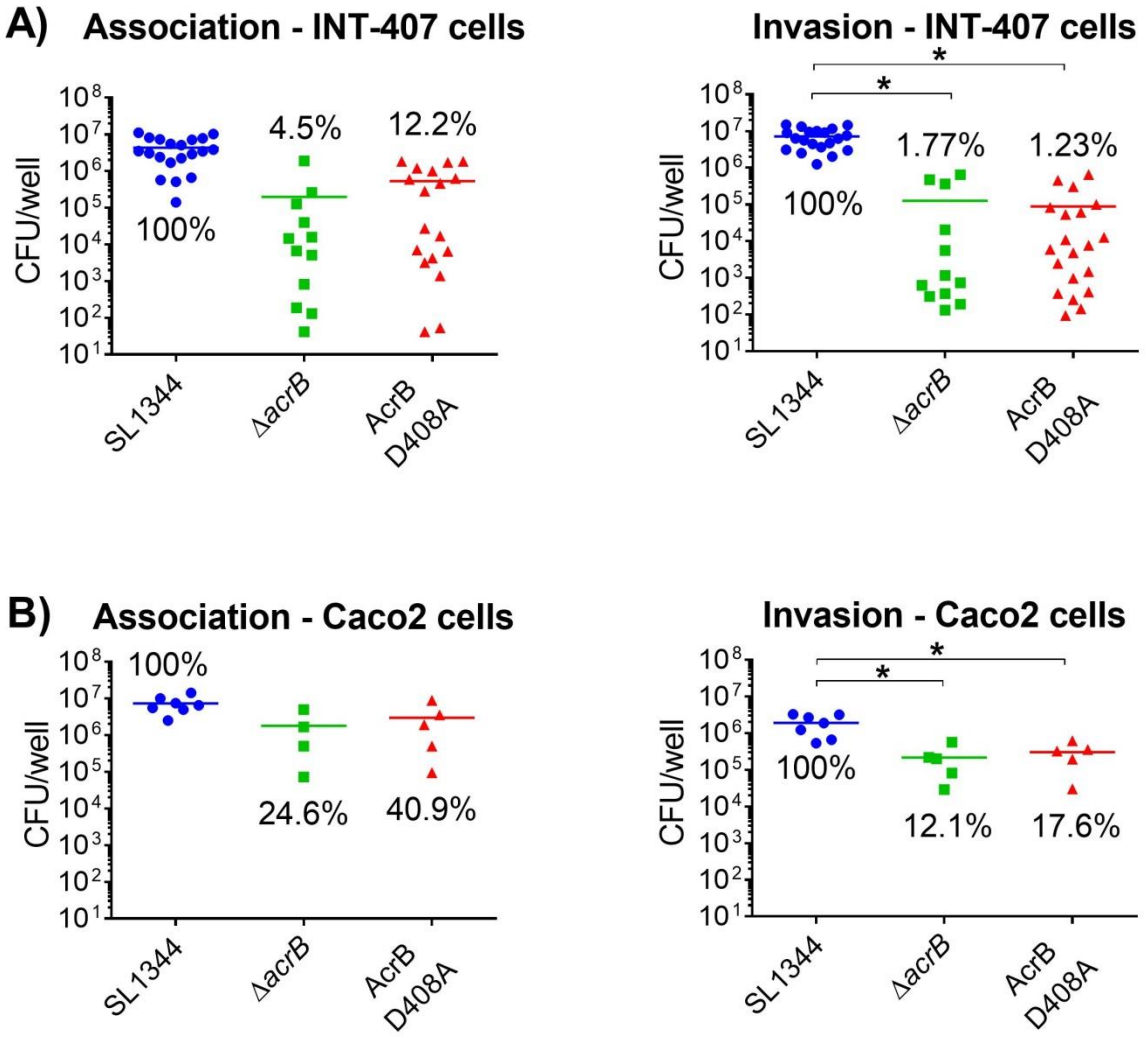

Association and invasion of a *S.* Typhimurium SL1344 Δ*acrB* and AcrB D408A mutant in A) INT-407 and B) Caco2 cells is shown. Each dot represents an independent experiment. The line in the middle represents the mean of each dataset. An asterisk denotes a significant difference of $P<0.05$ between two groups, compared by Student's t-test with Welch's correction.

Figure 4.15 Infection assays with SL1344 and its *acrB* mutants in J774A.1 murine macrophages.

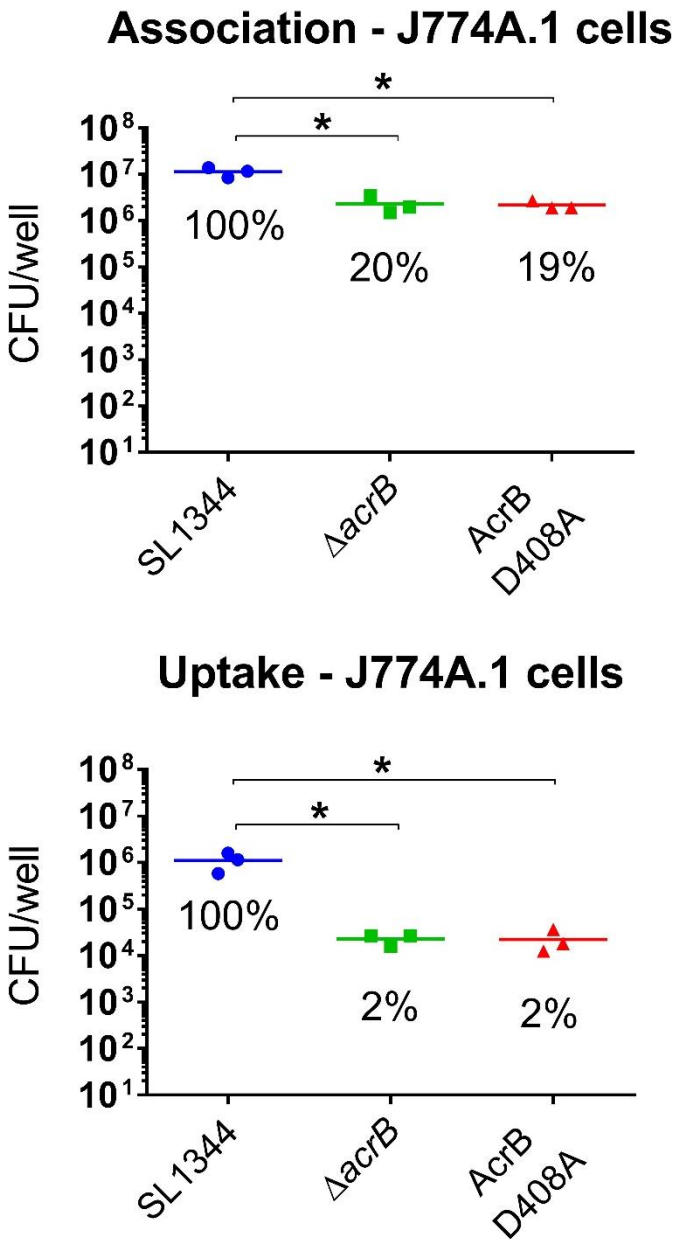

Association and uptake of a *S.* Typhimurium SL1344 Δ*acrB* and AcrB D408A mutant in J774A.1 murine macrophage cell-line is shown. Each dot represents an independent experiment. The line in the middle represents the mean of each dataset. An asterisk denotes a significant difference of $P<0.05$ between two groups, compared by Student's t-test with Welch's correction.

Figure 4.16 Assessment of systemic infection of BALB/c mice inoculated with SL1344 and its AcrB D408A mutant.

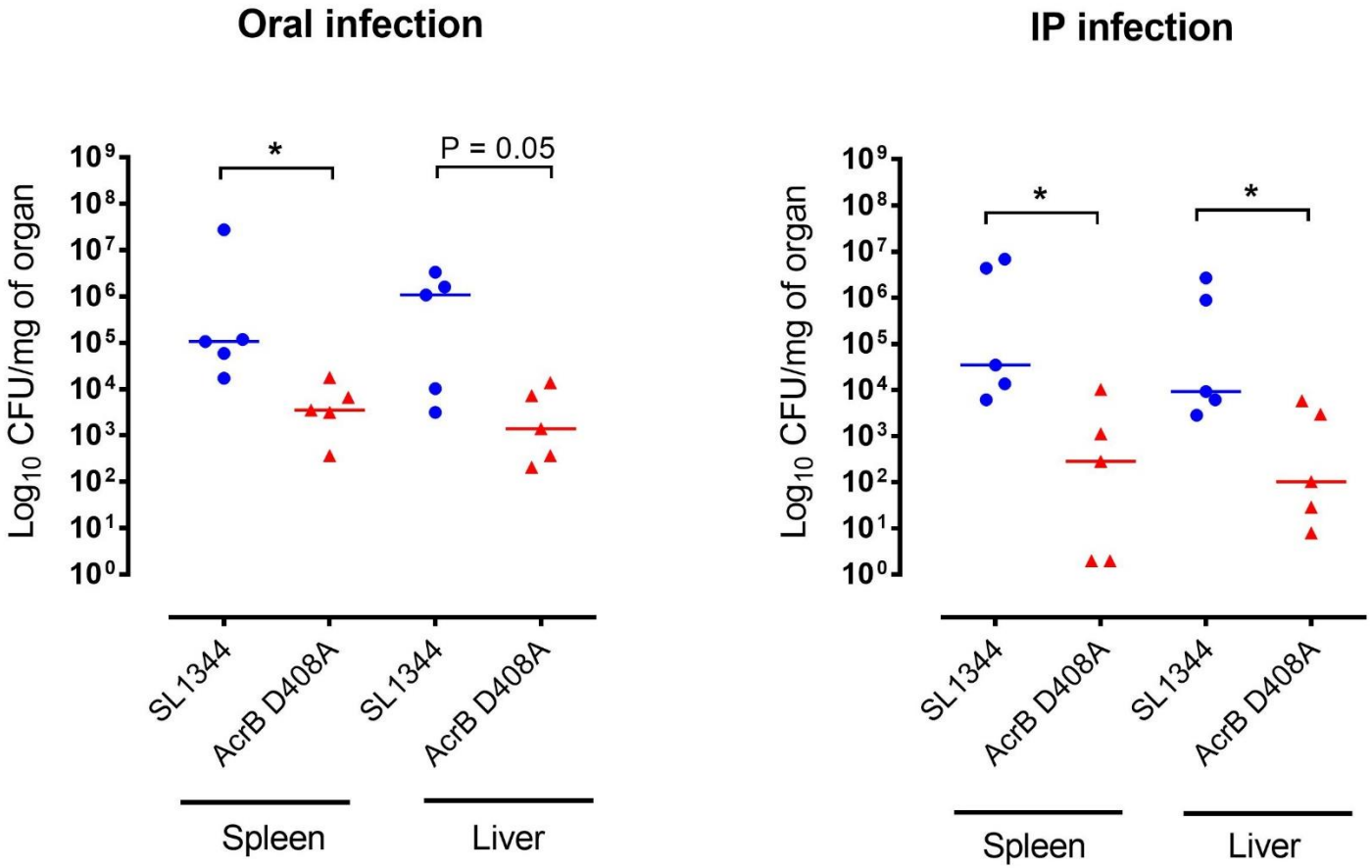

Groups of five 6-8-week old female BALB/c mice were infected A) orally with $5X10^7$ CFU/mL or B) intraperitoneally (IP) with $3X10^3$ CFU/mLof wild-type or mutant *S.* Typhimurium. Bacterial burden in spleen and liver was assessed by viable counting. Each dot represents a mouse. The line in the middle represents the mean of each dataset. A Mann-Whitney-U test was used to determine significant differences between the wild-type and mutant. A significant difference ($P<0.05$) is represented by an asterisk.

4.9 Loss of AcrB efflux function and its effect on the replication dynamics of *S.* Typhimurium SL1344

RNA-seq of the AcrB D408A mutant showed that expression of $tRNA^{Met}$ was significantly decreased. Literature research revealed that $tRNA^{fMet}$ in *Salmonella enterica* is cleaved by the *vapC* toxin, which led to formation of persisters, a subpopulation of slow-growing or transiently non-replicating bacteria (Winther and Gerdes, 2011).

Toxin-antitoxin modules (TA) are not correctly annotated in FQ312003, the reference genome used in the analysis of RNA-seq data. Therefore, a list of all toxin-antitoxin modules was obtained from a recently published study and modules were identified manually (Lobato-Marquez *et al*., 2015). The *vapBC* TA was significantly upregulated in the AcrB D408A mutant when compared against its parental SL1344 strain; whereas, the T4-A4 module was significantly downregulated. Interestingly, the *sehA* toxin, from the *sehAB* TA, was significantly upregulated, but the *sehA* antitoxin was not (Table 4.1).

Changes in TA and $tRNA^{Met}$ suggested that the AcrB D408A mutant was more susceptible to entering a persister state than the parental wild-type strain. To explore this hypothesis, replication dynamics of SL1344 and its isogenic AcrB D408A mutant were measured using the pDiGi plasmid. This plasmid encodes an IPTG-inducible GFP and an arabinose-inducible DsRed. The fluorescent proteins are best expressed in MgMES minimal medium, which simulates the conditions *S. enterica* encounters within a macrophage (Helaine *et al*., 2010). Therefore, experiments were carried out in this medium.

Table 4.1 Differential transcription of toxin-antitoxin modules identified in *S.* Typhimurium SL1344, between the AcrB D408A mutant and its parental strain.

Protein code	Start of gene	End of gene	Gene	Log_2 fold-change	*P*-value
SL1344_1479	1583418	1583702	-	0.15	0.46
SL1344_1480	1583692	1583940	-	0.1	0.7
SL1344_2379	2527069	2527431	*yfeC*	0.059	0.75
SL1344_2380	2527433	2527825	*yfeD*	-0.058	0.75
SL1344_2658	2836766	2837056	*rnfH*	-0.011	0.95
SL1344_2659	2837046	2837501	*yfjG*	0.18	0.17
SL1344_2935	3123641	3123898	-	-0.16	0.45
SL1344_2936	3123903	3124178	-	-0.2	0.22
SL1344_3011	3215876	3216274	*vapC*#	0.46	0.019*
SL1344_3012	3216274	3216501	*vapB*#	0.62	0.0082*
SL1344_3437	3641837	3642439	*fic*	0.16	0.57
SL1344_3438	3642429	3642596	*yhfG*	0.58	0.19
SL1344_3483	3701215	3701490	-	0.27	0.2
SL1344_3484	3701493	3701753	-	0.43	0.13
SL1344_3524	3749258	3749626	*kil*	-0.68	0.28
SL1344_3525	3749623	3749850	*phd*	-0.73	0.43
SL1344_3617	3859051	3859536	T4#	-0.56	0.011*
SL1344_3618	3859524	3859811	A4#	-0.55	0.023*
SL1344_3743	4000107	4000466	-	-0.062	0.76
SL1344_3744	4000450	4000773	-	-0.064	0.63
SL1344_3866	4137213	4137530	-	0.19	0.46
SL1344_3867	4137527	4137868	-	0.062	0.81
SL1344_3976	4261087	4261515	*sehB*#	0.14	0.39
SL1344_3977	4261530	4261841	*sehA*#	0.54	0.022*
SL1344_3979	4263074	4263385	-	0.21	0.45
SL1344_3980	4263386	4263676	-	0.018	0.95
SL1344_4253	4583140	4583433	-	0.18	0.28
SL1344_4254	4583430	4583921	-	0.1	0.54
SL1344_4379	4712031	4712273	*relB*	-0.063	0.79
SL1344_4380	4712263	4712547	*relE*	-0.14	0.6
SL1344_4459	4806232	4806519	-	0.13	0.56
SL1344_4460	4806506	4806808	-	0.0082	0.97

Toxin-antitoxin (TA) modules are shown in pairs. The location of the gene in the chromosome of SL1344, in sequence FQ312003, is indicated in the start and end of the gene columns. Gene annotations are shown, an (#) at the end of the gene name indicates that the gene name was introduced manually. Log_2 fold-change in transcription between the mutant and the wild-type is presented as well as the *P*-value, which was calculated using Bayesian approaches. An (*) at the end of each *P*-value indicates statistical significance ($P<0.05$). Significantly upregulated and downregulated genes are highlighted in red and blue, respectively.

An overnight culture of *S.* Typhimurium SL1344 and its AcrB D408A mutant carrying the plasmid was prepared in MgMES with arabinose to produce an inoculum that only expressed DsRed. This culture was diluted in MgMES supplemented with glucose, to 'wake up' potential persisters from the inoculum, and IPTG to induce the expression of GFP (Appendix V, Figure A). Growth of *S.* Typhimurium was monitored by viable counting and OD_{600} measurements every 2 hours for the first 10 hours, then every 24 hours until 72 hours. Bacterial replication at a single-cell level was measured by flow cytometry (gating strategy is shown in Appendix V, Figure B) and changes in replication dynamics were assessed by quantifying the number of bacteria that retained DsRed and the number of bacteria that only expressed GFP. No significant differences were observed between growth of the wild-type and mutant at a population level (Figure 4.17A, B). Viable counting showed that both strains grew equally during exponential growth phase and that the death phase started after 24 hours post-inoculation. Interestingly, the AcrB D408A mutant maintained consistently higher viable counts than the wild-type after 24 hours post-inoculation. At a single-cell level, a larger subpopulation of DsRed-retaining bacteria was observed in the AcrB D408A mutant when compared against the wild-type and the proportion of GFP-expressing AcrB D408A mutant was significantly lower than in the wild-type (Figure 4.17C, D). However, results were unclear and no conclusions can be drawn from this experiment.

4.10 Effect of loss of AcrB-mediated efflux on quorum sensing (QS)

QS is mechanism of cell-to-cell communication used by bacteria to regulate the expression of genes in a population density-dependent manner. In *S*. Typhimurium, the QS signalling molecule, autoinducer-2 (AI-2), is imported into the bacterium via an

Figure 4.17 Replication dynamics of *S.* Typhimurium SL1344 and its AcrB D408A mutant carrying pDiGi.

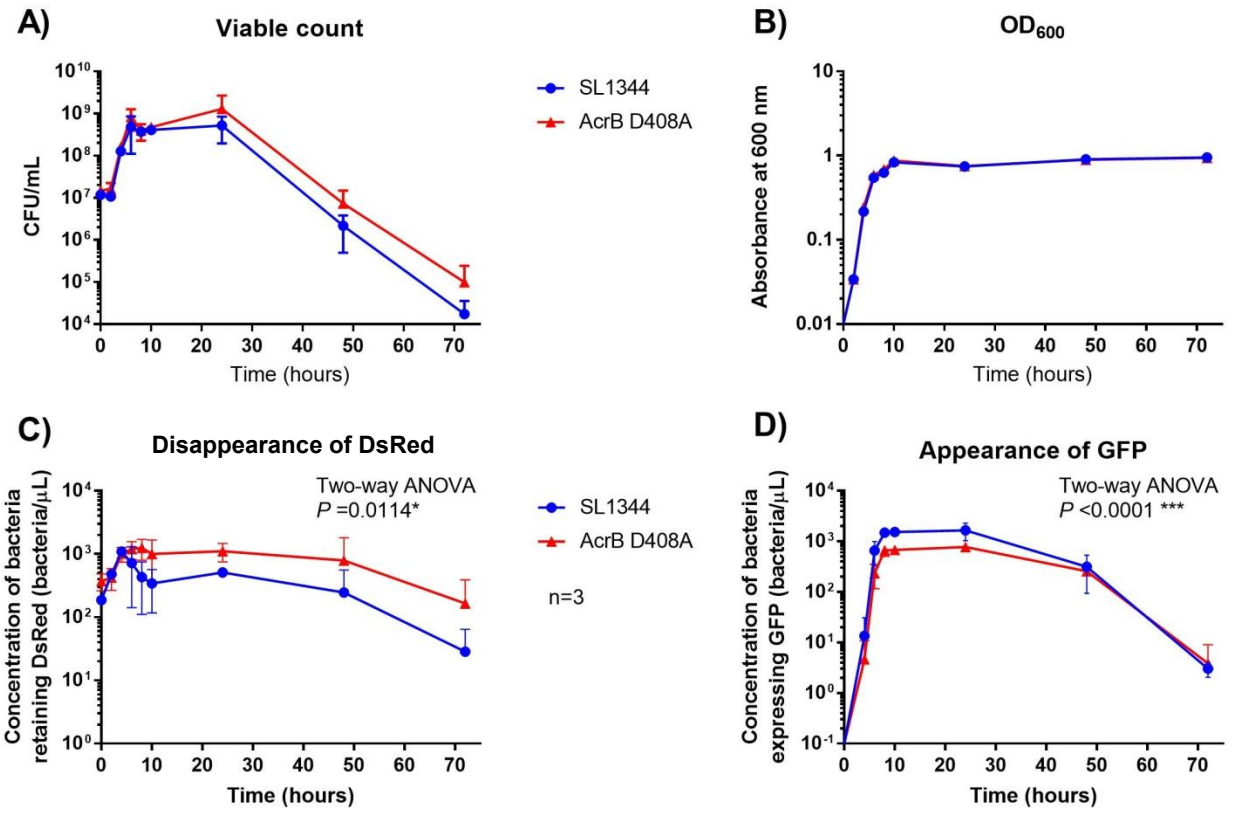

Replication dynamics at a population level were measured by A) viable counting using the Miles-Misra method and B) OD_{600} measurements. At a single-cell level, fluorescence dilution was measured in a flow cytometer. C) shows the proportion of bacteria that retain DsRed and D) shows the proportion of bacteria that have diluted DsRed and only express GFP as measured in a flow cytometer. The number of bacteria/µL was determined using the number of events counted in the 'Bacteria' gate, divided by the number of µL that were processed. The average of three experiments ± standard deviation is shown. A two-way ANOVA was used to determine statistical significance between replication dynamics of the wild-type and the mutant, a $P<0.05$ was considered statistically significant.

ABC-type transporter, encoded by *lsrABCD*. AI-2 is then phosphorylated by LsrK, encoded in the *lsrKR* operon adjacent to the *lsrABCD*. Differential gene transcription analysis of the AcrB D408A mutant revealed a significant downregulation of the *lsr* operon, including the accessory genes *lsrKR*. As the *lsr* operon does not export nor synthesise AI-2, it was hypothesised that import of AI-2 is decreased in the AcrB D408A mutant; therefore, more AI-2 would be present in the culture supernatant.

To test this hypothesis, the bioluminescent *Vibrio harveyi* strain BB170 was used. This strain is considered a bio-reporter of AI-2 as it contains a Tn5 transposon insertion in the *luxN* gene, making it unable to respond to other types of autoinducers (Bassler *et al*., 1997). The reporter strain was exposed to cell-free culture supernatants from SL1344 and its AcrB D408A mutant collected from various growth phases in different media. Luminescence and OD_{600} readings were taken every 10 minutes to determine the point of maximum luminescence. For three of the four media tested (MOPS, AB and LB), maximum luminescence was detected at 10 hours, for LB supplemented with glucose, maximum luminescence was detected at 10.5 hours. Therefore, these timepoints were used for data analysis.

No significant differences were observed between the effect of the wild-type and the mutant supernatant in MOPS, AB and LB medium. However, in LB supplemented with glucose, the supernatant from the AcrB D408A mutant caused a significant increase in relative luminescence of the reporter strain when compared to the parental strain (Figure 4.18). This suggested that in LB with glucose, the loss of AcrB-mediated efflux impeded internalisation of AI-2 but did not affect export.

Figure 4.18 Relative luminescence of *Vibrio harveyi* BB170 exposed to cell-free culture supernatants from *S.* Typhimurium SL1344 and its AcrB D408A mutant.

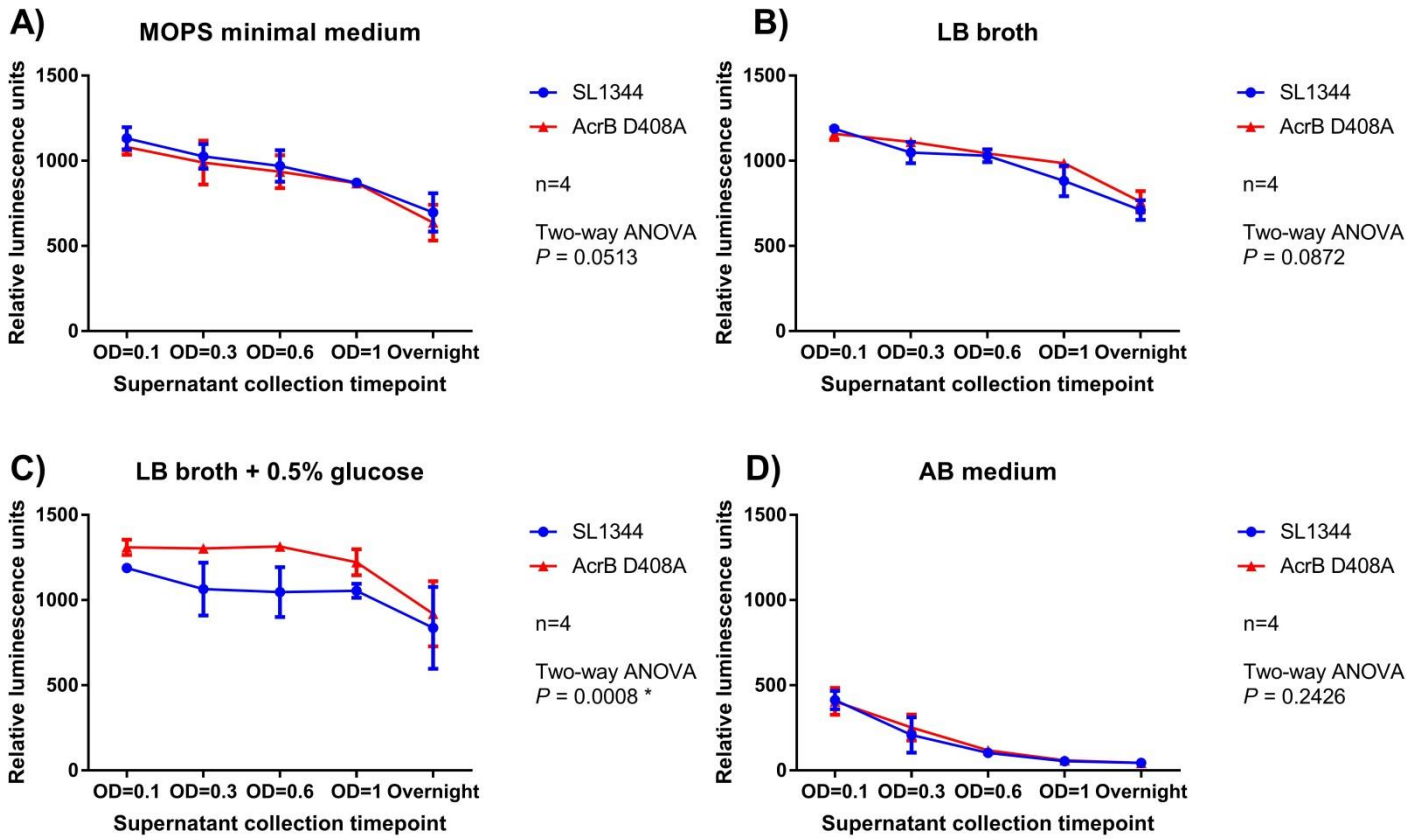

V. harveyi BB170 was exposed to cell-free culture supernatant of *S.* Typhimurium SL1344 and its AcrB D408A mutant collected from multiple timepoints in different media. Relative luminescence units were obtained at 10 hours for MOPS, AB and LB medium; whereas 10.5 hours was used for LB with glucose. An average of four experiments ± standard deviation is shown. A two-way ANOVA was used to determine statistical significance between replication dynamics of the wild-type and the mutant, a $P<0.05$ was considered statistically significant.

4.11 Changes in curli production in the AcrB D408A mutant

Curli is an amyloid fibre produced by multiple bacteria that has been associated with biofilm formation. A gene essential for curli production is *csgB*, which was significantly upregulated in the AcrB D408A mutant when compared against the parental wild-type strain. This was surprising as a previous study showed that curli was significantly downregulated in an *acrB*::*aph* mutant with a corresponding phenotypic effect (Baugh, 2014).

To determine if curli production was affected by loss of AcrB efflux function, *S.* Typhimurium SL1344 and its *acrB* mutants were grown on Congo red agar. Bacteria that produce curli form red colonies with a rough and dry appearance due to the staining of curli proteins on the outer membrane of Gram-negative bacteria. Bacteria that do not produce curli form pink or white colonies with a smooth appearance.

Previous studies were carried out with *S.* Typhimurium 14028S wild-type and its *acrB*::*aph* mutant (Baugh, 2014). These strains were used as controls for the assay. In accordance with the previous report, the 14028S *acrB*::*aph* mutant formed smooth, pink colonies on LB agar at 37°C; whereas, the wild-type 14028S strain formed rough, red colonies, suggesting a lack of curli production in the mutant. However, in SL1344, there were no visible changes in phenotype between the wild-type and the *acrB* mutants (Figure 4.19).

The experiment was repeated on MOPS minimal agar with Congo red to simulate the conditions under which RNA-seq was carried out. Curli-producing phenotypes were not observed on this agar in any of the strains used (Figure 4.20).

Figure 4.19 Production of curli by *S.* Typhimurium SL1344 and 14028S and their respective *acrB* mutants on LB agar at 37°C.

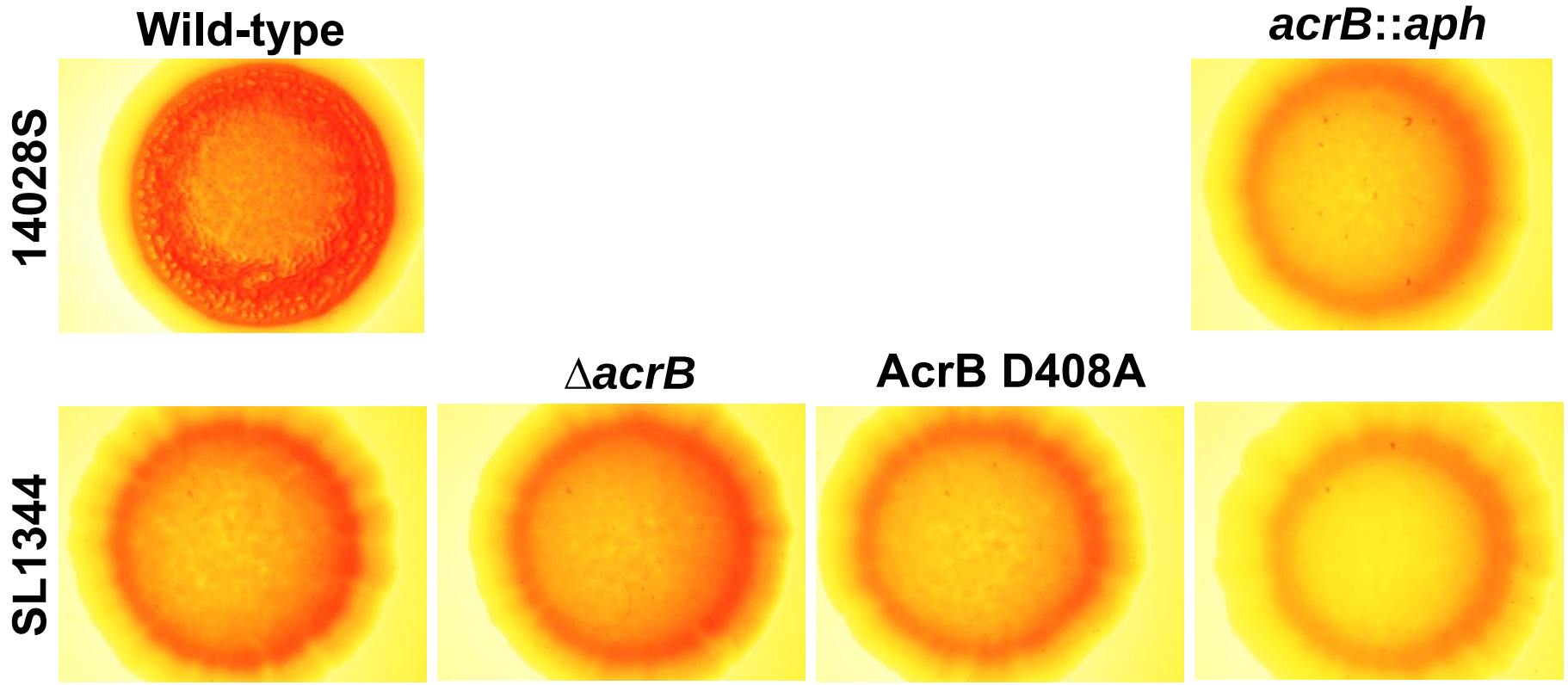

Curli-producing bacteria form red colonies with a rough appearance. Non-curli producing bacteria form colonies with a pale pink colour and a smooth appearance. A representative figure from four assays is shown.

Figure 4.20 Production of curli by *S.* Typhimurium SL1344 and 14028S and their respective *acrB* mutants on MOPS agar at 37°C.

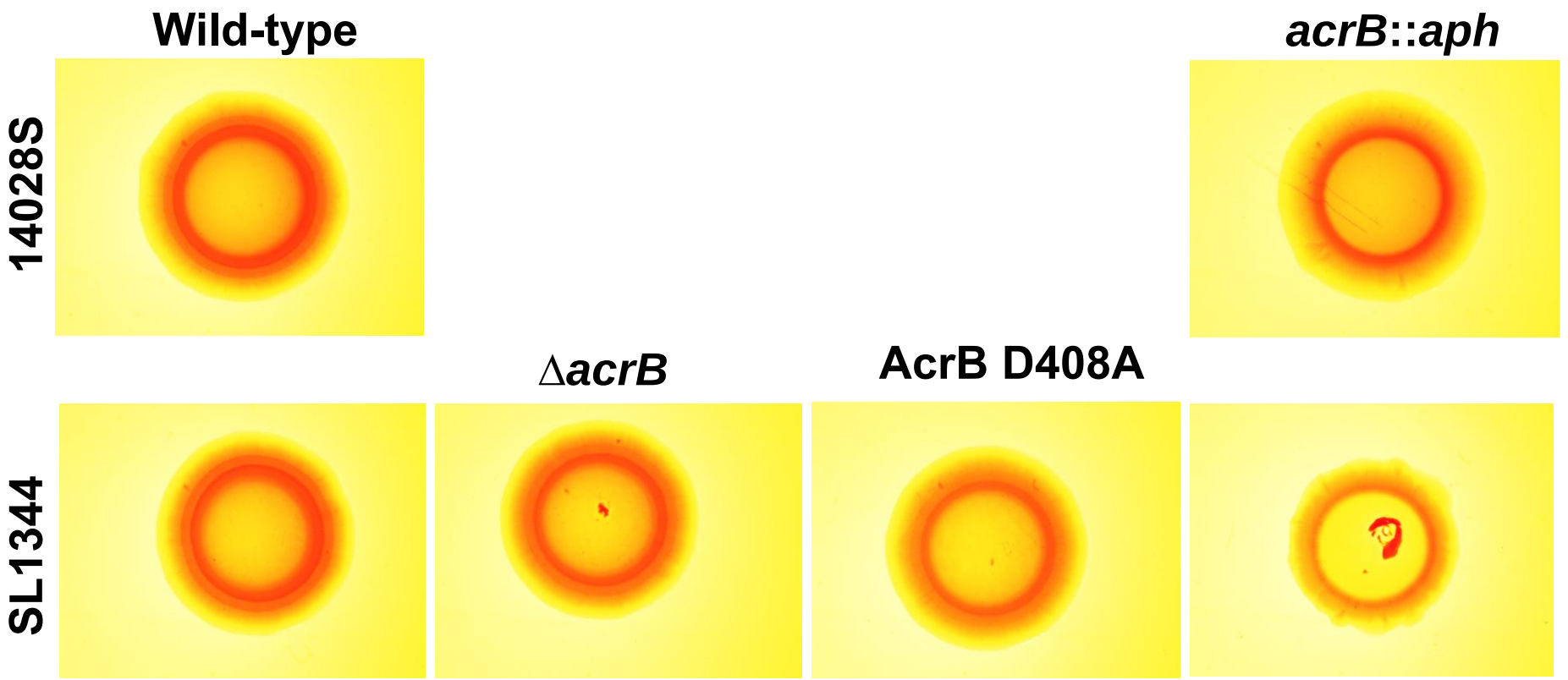

Curli-producing bacteria form red colonies with a rough appearance. Non-curli producing bacteria form colonies with a pale pink colour and a smooth appearance. A representative figure from four assays is shown.

Baugh (2014) previously reported that curli production was better observed when *S.* Typhimurium was incubated at 30°C. Therefore, experiments in LB and MOPS agar were repeated at 30°C. Similar to what was observed at 37°C, the curli production phenotype was only observed on LB agar when 14028S wild-type strain was used, with its *acrB*::*aph* mutant forming a pink, smooth colony. Interestingly, at 30°C, the wild-type SL1344 colony had a slightly rougher appearance than the colonies formed by *acrB* mutants. However, the phenotype was not clear (Figure 4.21). On MOPS agar, in accordance with the results obtained at 37°C, the curli-producing phenotype was not observed in any of the strains used (Figure 4.22).

4.12 Metabolic implications of loss of AcrB efflux function

The transcription of multiple genes involved in metabolism was significantly changed in the AcrB D408A mutant, suggesting a general change in metabolism. To determine which genes were responsible for the metabolic shift in the AcrB D408A mutant, Metabolic Transformation Algorithm (MTA) was applied (Yizhak *et al*., 2013). The algorithm uses differential gene transcription data to model the metabolism of *S.* Typhimurium. In this case, the same differential gene transcription data shown in section 4.4 was used as input for the analysis. Differential gene transcription data was run through an integrative metabolic analysis tool (iMAT), which maps genes to reactions or pathways and predicts the rate at which metabolites go through them (flux), generating a reconstructed metabolic network. MTA uses the iMAT networks to identify perturbations that could push the flux of reactions from the changed group to the target state, without affecting the flux of the unchanged reactions. This generates

Figure 4.21 Production of curli by *S.* Typhimurium SL1344 and 14028S and their respective *acrB* mutants on LB agar at 30°C.

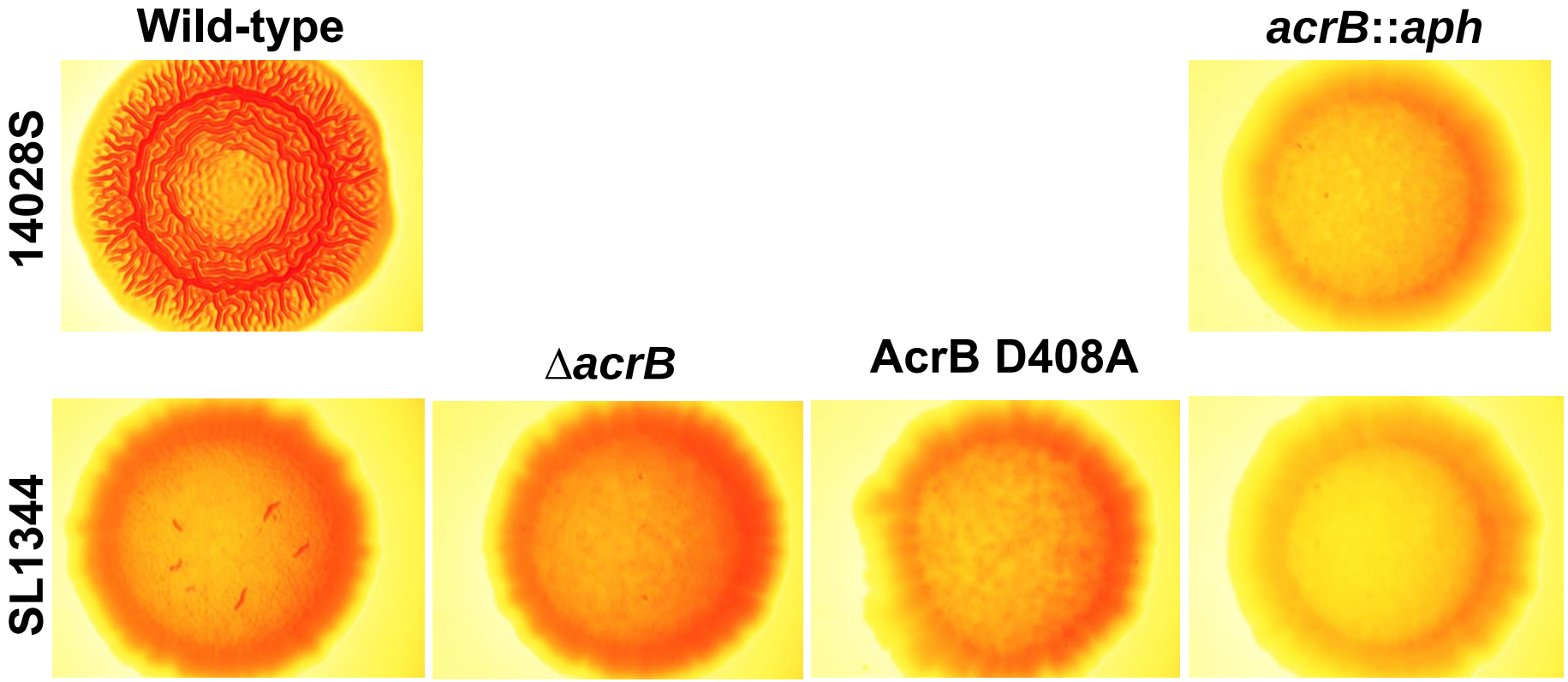

Curli-producing bacteria form red colonies with a rough appearance. Non-curli producing bacteria form colonies with a pale pink colour and a smooth appearance. A representative figure from four assays is shown.

Figure 4.22 Production of curli by *S.* Typhimurium SL1344 and 14028S and their respective *acrB* mutants on LB agar at 30°C.

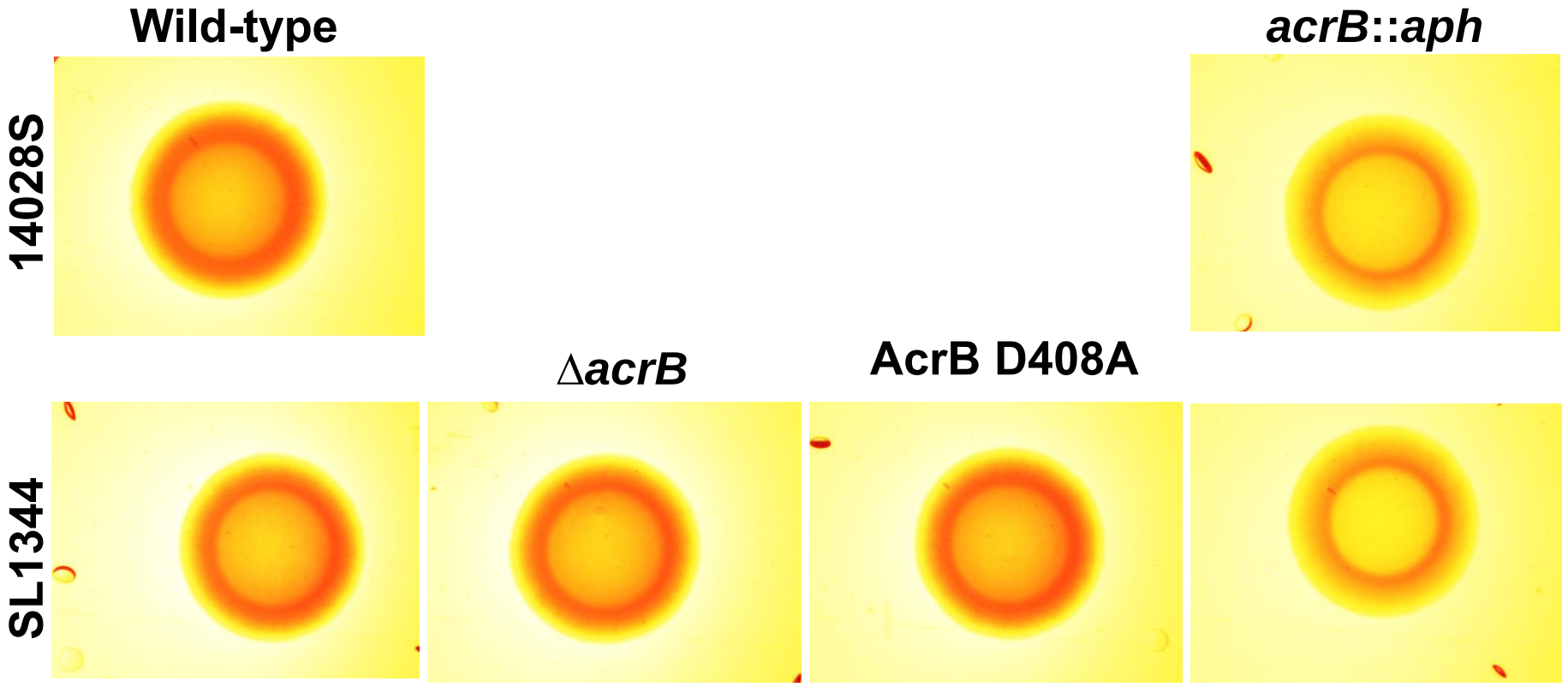

Curli-producing bacteria form red colonies with a rough appearance. Non-curli producing bacteria form colonies with a pale pink colour and a smooth appearance. A representative figure from four assays is shown.

a list of reactions/genes that, when deleted, are likely to cause a metabolic shift in the 'right direction'. These genes can also be interpreted as those that are essential in the maintenance of the metabolic state of the source state (Figure 4.23). In this study, the two directions of interest were 1) AcrB D408A mutant to the wild-type metabolic state (hereafter referred to as Direction 1) and 2) wild-type to the AcrB D408A metabolic state (referred to as Direction 2).

For each direction, the algorithm produced a list with genes scored in order of relevance. MTA uses a cut-off value of 1, where the higher the score, the most likely the gene deletion was to cause a metabolic shift in the right direction. The gene with the highest score in the Direction 1 list was *fadB* (score=7.15), which encodes a protein essential for β-oxidation of fatty acids (Table 4.2). For Direction 2, the top two genes had similar scores, differing only by 0.12 (Table 4.3). These genes were *glpK* (score=1.48) and *lamB* (score=1.36), which encode a glycerol kinase and a maltoporin, respectively.

4.13 Discussion

AcrB and its homologues have different physiological roles in different bacteria. In *S.* Typhimurium, the most frequently described phenotype is the attenuation of virulence (Buckley *et al*., 2006, Nishino *et al*., 2006, Webber *et al*., 2009), but it is not the only phenotype associated to absence of AcrB. In a previous study, it was shown that genetic inactivation of either of the components of the AcrAB-TolC complex in *S.* Typhimurium SL1344 led to significant changes in the transcriptome of the respective mutant as measured by microarray. Interestingly, of all three mutants, the *acrB*::*aph* mutant was the most affected. In the present study, the transcriptome of a SL1344

Figure 4.23 Schematic representation of the workflow used to find genes implicated in maintenance of the metabolic state of the SL1344 AcrB D408A mutant using MTA.

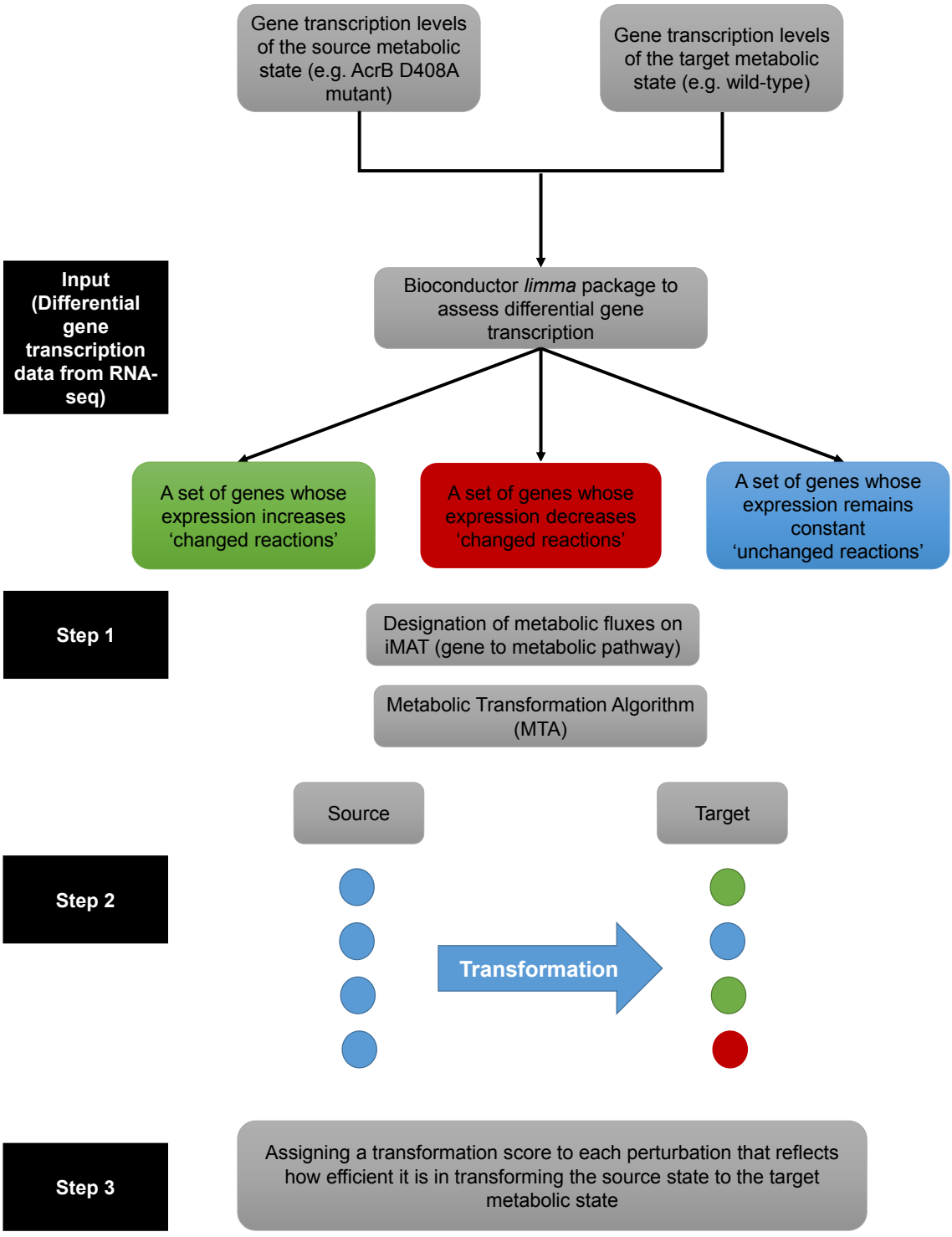

Figure adapted from Yizhak *et al*. (2013).

Table 4.2 List of genes that are predicted to shift the AcrB D408A mutant metabolic state to the same as the wild-type SL1344.

Protein code*	Gene	Description	Score
STM3983	*fadB*	Fatty acid oxidation complex subunit alpha	7.1500
STM3010	*aas*	Bifunctional protein Aas	3.6417
STM3330	*gltB*	Glutamate synthase, large subunit	3.4432
STM3331	*gltD*	Glutamate synthase, small subunit	3.4432
STM1238	*icdA*	Isocitrate dehydrogenase [NADP]	3.0434
STM0066	*carA*	Carbamoyl-phosphate synthase small chain	2.9543
STM0067	*carB*	Carbamoyl-phosphate synthase large chain	2.9543
STM4081	*tpiA*	Triosephosphate isomerase	2.4659
STM2051	*pduP*	Propanediol utilization CoA-dependent propionaldehyde dehydrogenase	2.4403
STM3243	*tdcC*	Threonine/serine transporter TdcC	2.3940
STM0620	*citX*	Putative cytoplasmic protein	2.3122
STM1076	*mgsA*	Methylglyoxal synthase	2.2486
STM4119	*ppc*	Phosphoenolpyruvate carboxylase	2.2374
STM2952	Enolase (*eno*)	Enolase	2.2164
STM3614	*dctA*	Aerobic C4-dicarboxylate transport protein	2.1898
STM3225	*sstT*	Serine/threonine transporter SstT	2.0860
STM0158	*acnB*	Aconitate hydratase B	1.9963
STM0368	*prpB*	2-methylisocitrate lyase	1.9963
STM0369	*prpC*	2-methylcitrate synthase	1.9963
STM0370	*prpD*	2-methylcitrate dehydratase	1.9963
STM1756	*purU*	Formyltetrahydrofolate deformylase	1.9547
STM0970	*pflA*	Pyruvate formate-lyase-activating enzyme	1.9229
STM0730	*gltA*	Citrate synthase	1.6573
STM3939	*cyaA*	Adenylate cyclase	1.6222
STM3968	*udp*	Uridine phosphorylase	1.6196
STM2555	*glyA*	Serine hydroxymethyltransferase	1.6171
STM0542	*folD*	Bifunctional protein FolD	1.5923
STM3334	NA	Putative cytosine deaminase	1.4961
STM1349	*pps*	Phosphoenolpyruvate synthase	1.4561
STM0732	*sdhC*	Succinate dehydrogenase cytochrome b556 subunit	1.4517
STM0733	*sdhD*	Succinate dehydrogenase hydrophobic membrane anchor subunit	1.4517
STM0734	*sdhA*	Succinate dehydrogenase flavoprotein subunit	1.4517

STM0735	*sdhB*	Succinate dehydrogenase iron-sulfur subunit	1.4517
STM3979	*fre*	NAD(P)H-flavin reductase	1.3696
STM1883	*purT*	Formate-dependent phosphoribosylglycinamide formyltransferase	1.2784
STM0977	*serC*	Phosphoserine aminotransferase	1.2319
STM3062	*serA*	D-3-phosphoglycerate dehydrogenase	1.2319
STM4578	*serB*	3-phosphoserine phosphatase	1.2319
STM1098	*hpaC*	4-hydroxyphenylacetate 3-monooxygenase reductase component	1.2234
STM3359	*mdh*	Malate dehydrogenase	1.2169
STM2472	*maeB*	NADP-dependent malic enzyme	1.1987
STM4569	Phosphopentomutase	Phosphopentomutase	1.1876
STM1299	*gdhA*	NADP-specific glutamate dehydrogenase	1.1292
STM2200	*lysP*	APC family lysine-specific permease	1.0783
STM1627	NA	S-(hydroxymethyl)glutathione dehydrogenase	1.0178
STM3877	*asnA*	Aspartate--ammonia ligase	1.0079

(*) Protein code was obtained from *S.* Typhimurium LT2. The genome annotation of this strain was used for the genome-wide reconstruction of the metabolic network of *S.* Typhimurium. NA indicates that the gene is not annotated. Genes with a score>1 are shown. The higher the score, the more likely the deletion of the gene is to cause a metabolic shift in the mutant towards de wild-type state.

Table 4.3 List of genes that are predicted to shift the wild-type SL1344 metabolic state to the same as the AcrB D408A mutant.

Protein code*	Gene	Description	Score
STM4086	*glpK*	Glycerol kinase	1.4841
STM4231	Maltoporin (*lamB*)	Maltoporin	1.3621
STM2927	*surE*	5'/3'-nucleotidase SurE	1.0724
STM1883	*purT*	Formate-dependent phosphoribosylglycinamide formyltransferase	1.0533
STM2500	*purN*	Phosphoribosylglycinamide formyltransferase	1.0282
STM2947	*cysI*	Sulfite reductase [NADPH] hemoprotein beta-component	1.0090
STM2948	*cysJ*	Sulfite reductase [NADPH] flavoprotein alpha-component	1.0090
STM1193	*fabH*	3-oxoacyl-[acyl-carrier-protein] synthase 3	1.0073
STM4087	*glpF*	Glycerol diffusion MIP channel	1.0060
STM3078	Agmatinase (*speB*)	Agmatinase	1.0056
STM0066	*carA*	Carbamoyl-phosphate synthase small chain	1.0039
STM0067	*carB*	Carbamoyl-phosphate synthase large chain	1.0039
STM2548	*asrA*	Anaerobic sulfite reductase subunit A	1.0035
STM2549	*asrB*	Anaerobic sulfite reductase subunit B	1.0035
STM2550	*asrC*	Anaerobic sulfite reductase subunit C	1.0035
STM2081	*gnd*	6-phosphogluconate dehydrogenase, decarboxylating	1.0018
STM3186	*tolC*	Outer membrane channel	1.0008
STM0589	*fepE*	Ferric enterobactin (Enterochelin) transporter	1.0006
STM0051	*rihC*	Non-specific ribonucleoside hydrolase RihC	1.0006
STM0321	*proB*	Glutamate 5-kinase	1.0004
STM0322	*proA*	Gamma-glutamyl phosphate reductase	1.0004

(*) Protein code was obtained from *S.* Typhimurium LT2. The genome annotation of this strain was used for the genome-wide reconstruction of the metabolic network of *S.* Typhimurium. Genes with a score>1 are shown. The higher the score, the more likely the deletion of the gene is to cause a metabolic shift in the wild-type towards the mutant state.

AcrB D408A mutant was studied by RNA-seq and the differential gene transcription profile was compared against the previously reported *acrB*::*aph* microarray profile. Culture growth conditions and RNA extraction was carried out in the same way in both studies. A brief summary of the discussion is shown in Figure 4.24.

More genes were differentially transcribed in the AcrB D408A than in the *acrB*::*aph* mutant. This difference is likely caused by the sensitivity of the techniques used, as the transcriptome of the AcrB D408A mutant was studied by RNA-seq, which is more sensitive than the microarray used to study the transcriptome of the *acrB*::*aph* mutant. Interestingly, little correlation was observed between the transcriptomes of the two mutants. Comparison of COG classes revealed that genes involved in motility, such as flagella synthesis and chemotaxis, were upregulated in the AcrB D408A mutant and downregulated in the *acrB*::*aph* mutant. Other classes, such as posttranslational modifications and replication followed the same trend.

To further explore the discrepancy in transcription of motility genes, swimming and swarming on semisolid agar was measured. To determine if the motility phenotype was caused by loss of AcrB efflux function or loss of protein or was an artefact of the *aph* insertion, *acrB* mutants (AcrB D408A, Δ*acrB* and *acrB*::*aph*) derived from the same parental SL1344 strain were used. No antibiotics were used in these experiments as all mutants carried stable mutations on the chromosome. In accordance with the transcriptomic analyses, the AcrB D408A mutant swam more than the parental SL1344 strain, the same hyper-motile phenotype was observed in the Δ*acrB* mutant. This observation is supported by a study in *E. coli* BW25113, in which

Figure 4.24 Summary of phenotypes affected by loss of AcrB efflux function and possible causes of these in *S.* Typhimurium.

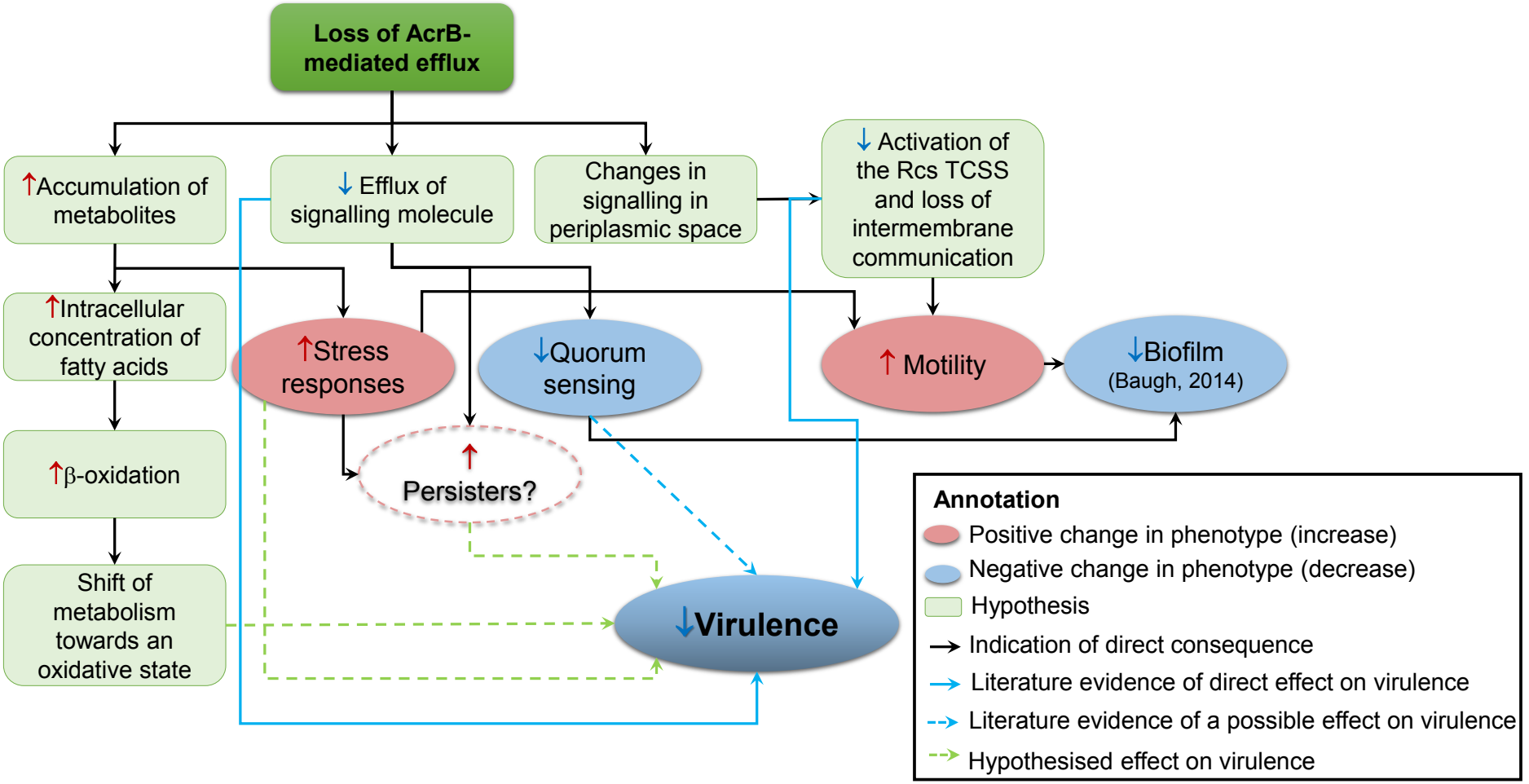

A schematic of the points discussed in Chapter 4 is shown. Red and blue arrows next to a physiological activity/phenotype, indicate an increase or decrease in these, respectively. A dotted box indicates an unconfirmed phenotype.

an Δ*acrB* mutant swam significantly more than the wild-type strain (Ruiz and Levy, 2014). In contrast, the *acrB*::*aph* mutant was significantly less motile than the wild-type in MOPS minimal agar, suggesting that the decreased motility phenotype is an artefact of the *aph* insertion. To confirm this, swimming and swarming assays in LB agar were carried out. Interestingly, no significant differences were observed between the *acrB* mutants and the parental wild-type strain when swimming was measured in LB. This observation will be discussed later.

Swarming could not be measured using MOPS minimal agar as the medium does not have the adequate nutrients to induce swarming in *S.* Typhimurium. Swarming of *S.* Typhimurium is stimulated in rich media, such as LB or nutrient broth, supplemented with glucose (Harshey and Matsuyama, 1994, Kim and Surette, 2005); therefore, swarming was only measured in LB with glucose. No significant differences were found between the Δ*acrB*, the AcrB D408A and the parental wild-type strain when swarming was measured. However, the *acrB*::*aph* mutant swarmed significantly less than the other three strains, confirming that the changes in the motility phenotype of the *acrB*::*aph* mutant are an artefact of the *aph* gene. The lack of changes in swarming motility in the AcrB D408A and the Δ*acrB* mutant is not surprising, as only mutants with alterations in flagella and LPS synthesis have altered swarming phenotypes (Toguchi *et al*., 2000, Kim and Surette, 2005). The decreased swarming in the *acrB*::*aph* mutant is likely to be related to the significant decrease in transcription of flagella genes. In order to swarm, *S.* Typhimurium requires entering a hyper-flagellated state (Harshey and Matsuyama, 1994, Toguchi *et al*., 2000) and a significant downregulation of genes encoding flagella assembly is likely to stop *Salmonella* from becoming hyper-flagellated. The significant downregulation of genes involved in flagella synthesis may be accountable for the decreased overall motility of the

acrB::*aph* mutant. It may also be possible that the decreased motility in the *acrB*::*aph* mutant is related to the decreased transcription of genes in the “Posttranslational modification, protein turnover, chaperones” COG class. The significant decrease of genes in this COG class suggests that general protein synthesis is likely to be affected in the *acrB*::*aph* mutant. A recent study showed that reduced fidelity in general protein synthesis decrease motility of *E. coli* (Fan *et al*., 2016); thus, it may be that a decrease in posttranslational modifications leads to a decrease in motility. Another hypothesis involves the interaction of *aph* with “*Salmonella* factors”. A recent study showed that the *aphA1* gene in combination with an “unknown *Salmonella* factor” enhanced swarming of MDR clinical isolates of *S.* Typhimurium (Brunelle *et al*., 2017). However, the motility phenotype was only observed in specific isolates and the phenotype was the contrary to what was reported in this study. Therefore, this hypothesis is deemed unlikely.

No differences in swimming between the mutants and the wild-type were observed in LB medium, indicating that changes in the swimming phenotype of the *acrB* mutants depend on nutrient availability. Analysis of the RNA-seq of the AcrB D408A mutant shows that genes involved in amino acid, carbohydrate and nucleotide transport and metabolism were significantly downregulated in the mutant when compared against the parental wild-type strain. As a significant decrease in transport and metabolism of these essential nutrients is observed in the AcrB D408A mutant, it is likely that the mutant starves in MOPS minimal medium; therefore, it increases motility in order to move to a more favourable environment and gain more nutrients. As nutrients are readily available in LB medium, the hyper-motility phenotype is lost.

S. Typhimurium exhibits positive chemotaxis towards most L-amino acids, expect for tryptophan and valine; it is also attracted towards multiple carbohydrates such as L-

fumarate, L-malate, D-glucose, methyl-α,D-glucopyranoside, D-fructose, among others (Melton *et al*., 1978). All these chemoattractants are found in LB medium and are likely to influence swimming motility. It is hypothesised that the *acrB*::*aph* mutant is more sensitive to these chemoattractants than the other strains, resulting in a 'normal' swimming phenotype in LB semisolid agar. It is unlikely that components of LB compensated any side effects caused by the *aph* gene as this would have also reflected in the swarming assays.

Whether the effect of the *aph* gene on motility is *S.* Typhimurium-specific and/or *acrB*-specific is unknown. The *E. coli* MG1655 *acrB*::*aph,* ∆*acrB* and AcrB D408A mutants mentioned in the previous chapter could be used to address these questions.

The decrease in transcription of metabolic genes and increase in motility can also be associated with the general upregulation of stress responses, such as *recA*, *lexA*, *hslTS* and *cpxP*, observed in the AcrB D408A mutant. Bacteria increase motility to escape from unfavourable environments; therefore, if the AcrB D408A mutant senses stress, it will increase flagella transcription in order to escape from the stress.

Increased transcription of genes involved in general stress responses is hypothesised to be a consequence of accumulation of toxic by-products from metabolic pathways. The AcrB efflux pump is best known for its role in export of xenobiotics (for example, antibiotics); however, multiple authors have proposed that AcrB effluxes toxic metabolic by-products generated during normal bacterial growth (Helling *et al*., 2002, Piddock, 2006, Rosner and Martin, 2009, Ruiz and Levy, 2014). Interestingly, the proposed substrates of AcrB include products of cysteine and purine biosynthesis, products of gluconeogenesis and enterobactin or derivatives of enterobactin (Ruiz and Levy, 2014). These substrates can be classified as products of amino acid, nucleotide

or carbohydrate metabolism, which were COG classes dominated by significantly downregulated genes in the AcrB D408A mutant. Metabolic pathways have a feedback loop, where the end product of a pathway can repress its own biosynthesis to avoid accumulation of toxic metabolites or metabolic by-products (Sauro, 2017). If the end product of a metabolic pathway is a substrate of AcrB, then inactivation of AcrB may result in intracellular accumulation of said product, which may consequently cause feedback repression of the pathway and could potentially lead to decreased transcription of metabolic genes. At the same time, accumulation of metabolic products could cause activation of general stress responses and, possibly, overexpression of other efflux pumps that have similar substrate specificity to AcrB. In line with this hypothesis, increased transcription of the *emrAB* multidrug efflux pump in the AcrB D408A mutant was observed. EmrAB shares some substrates with AcrB, such as Rhodamine 6G and deoxycholate (Nishino and Yamaguchi, 2001), and can efflux fatty acids from *E. coli* when *acrAB* is deleted (Lennen *et al*., 2013).

Accumulation of metabolites also induces activation of the SOS response, involved in repairing damaged DNA, as shown recently in *E. coli* O157:H7 exposed to D-serine (Connolly *et al*., 2015). RecA and LexA are the main regulators of the SOS response system, which repairs damaged DNA. To confirm whether general DNA damage responses were significantly upregulated in the AcrB D408A mutant, induction of transcription of *lexA* was measured using a reporter plasmid, which encoded GFP under the control of the *S.* Typhimurium *lexA* promoter. The constructs were validated by testing induction of *lexA* in presence of varying concentrations nalidixic acid (NAL). A minimum of 1.6µg/mL of NAL is required to observe a significant increase in *lexA* induction, this result is in accordance with a previous study in which a significant

increase in transcription of *lexA* and *recA* was observed in a microarray of *S.* Typhimurium 14028S exposed to the same concentration of NAL (Dowd *et al*., 2007).

Measuring induction of *lexA* in strains without exposure to NAL proved challenging. When measured in a fluorescence reader, the basal level of *lexA* induction was so low that the reporter strains were indistinguishable from the negative control strains, which carried the empty vector. Hence, a more sensitive method, such as flow cytometry was used. In the flow cytometer, a small induction of *lexA* in the absence of NAL was observed, the GFP signal was weak but it allowed differentiation of the test from the negative control strains. Activation of the SOS response is tightly controlled at multiple levels as it results in a high number of mutations and deletions that can be detrimental to bacteria (Kim *et al*., 1997, Simmons *et al*., 2008). Therefore, it was expected that the induction of the transcription of *lexA*, as a regulator of the SOS response, would be very low. Interestingly, a significant increase of 31.4% in induction of *lexA* was observed in the AcrB D408A mutant when compared against the wild-type strain, indicating that loss of AcrB-mediated efflux induced transcription of *lexA* in *S.* Typhimurium. However, further experiments measuring induction of *recA* are desirable to complement this experiment, as well as Western blotting LexA and RecA.

An interesting difference between the *acrB*::*aph*, the ∆*acrB* and the AcrB D408A mutant was the degree of transcription of *ramA*. *ramA* is a global transcription regulator, which induces transcription of *acrAB* by binding upstream of the promoter region of the operon (Weston *et al*., 2017). Transcription of this gene is induced in a *S.* Typhimurium SL1344 ∆*acrB* mutant and when wild-type SL1344 is exposed to efflux inhibitors, such as PaβN, and the antipsychotic drug chlorpromazine (CPZ) (Lawler *et al*., 2013). These observations led to the conclusion that induction of *ramA* occurs as a response to efflux inhibition; therefore, it was hypothesised that *ramA* would be

induced in the AcrB D408A mutant. However, *ramA* was not upregulated in the AcrB D408A mutant when compared against the parental SL1344 strain. To validate this observation, induction of the transcription of *ramA* was measured using a GFP-reporter plasmid and compared against the Δ*acrB* mutant and the parental strain. In accordance with data reported by Lawler *et al*. (2013), a significant increase in *ramA* induction (average fold-change of 5.75) was observed in the Δ*acrB* mutant. However, no significant increase in *ramA* induction was observed in the AcrB D408A mutant, suggesting that the increased transcription of *ramA* is not a consequence of loss of AcrB-mediated efflux. It may be that the loss of the AcrB protein in the Δ*acrB* mutant triggers other physiological responses that result in increased transcription of *ramA*. For example, in the previous chapter it was discussed that loss of the AcrB protein results in overexpression of additional RND efflux pumps to fill in the empty spaces in the membrane where AcrB should be. It is possible that the loss of AcrB leads to membrane instability and the increased transcription of *ramA* is a response to membrane damage rather than loss of efflux function. In line with this hypothesis, PAβN and CPZ have been reported to cause extensive membrane damage at high concentrations (Lamers *et al*., 2013, De Filippi *et al*., 2007).

An interesting observation in the AcrB D408A mutant was the decreased transcription of multiple genes encoding outer membrane porin from the *omp* family. Similar observations were previously reported in a *S.* Typhimurium *acrB*::*aph* mutant (Webber *et al*., 2009). The downregulation of *omp* genes suggested that loss of efflux causes decreased membrane permeability. In line with the hypothesis that loss of AcrB-mediated efflux leads to accumulation of toxic metabolites, the decreased production of OMPs or decreased transcription of *omp* genes would serve to stop the influx of potential toxic compounds from the environment. However, as expression of OMPs is

regulated post-transcriptionally (Masi and Pagès, 2013), further experiments are required to determine if expression of OMP proteins is affected.

The increased transcription of *cpxP*, which encodes the effector protein of the CpxRA two-component signalling system (TCSS) involved in the sensing of membrane stress, suggests that CpxRA was activated in the AcrB D408A mutant. This has been previously observed in a *Vibrio cholerae* mutant that lack all RND efflux pumps (Kunkle *et al*., 2017). Kunkle *et al*. (2017) hypothesised that the activation of CpxRA in the RND pump gene-deletion mutant was a response to intracellular accumulation of the siderophore vibriobactin, proposed to be exported by the VexGH RND pump in *V. cholerae*. Accumulation of vibriobactin would consequently decrease intracellular availability of iron and cause malfunction of cytochromes, making *V. cholerae* more susceptible to reactive oxygen species (ROS). ROS target disulphide bonds and causes denaturation of proteins. The denaturation of membrane proteins is detected by CpxA, which activates the TCSS in response. This hypothesis not only provides an explanation for the activation of the CpxRA TCSS, but also proposes that RND pumps in Enterobacteriaceae are involved in the export of siderophores, which are classified as virulence factors. The two main siderophores synthesised by *S. enterica* are enterobactin and salmochelin (Achard *et al*., 2013). Enterobactin was previously suggested to be exported by AcrB in *E. coli* (Ruiz and Levy, 2014). However, experimental evidence suggests that the majority of enterobactin is exported by the EntS MFS pump in *E. coli* and that only a small proportion of the siderophore is exported by AcrB and other RND efflux pumps (Horiyama and Nishino, 2014). The export of salmochelin in *S.* Typhimurium remains unstudied. Therefore, it is hypothesised that salmochelin is exported by AcrB and that its intracellular accumulation is responsible for the increased transcription of *cpxP* in the AcrB D408A

mutant. It is also possible that loss of export of salmochelin will impact the virulence of *S.* Typhimurium.

A phenotype that is consistent throughout all *S.* Typhimurium *acrB* mutants is the attenuation of virulence. To determine if the virulence phenotype was an effect of loss of AcrB-mediated efflux or loss of AcrB protein, gentamicin protection assays were carried out using the AcrB D408A and Δ*acrB* mutants. Association and invasion of the mutants into polarised and non-polarised human intestinal epithelial cells (INT-407 and Caco2, respectively) and murine macrophages (J774A.1) was compared against the parental wild-type strain. In general, more bacteria were recovered at the association stage of the assay than at the invasion stage. At the 2 hours association time point, infected monolayers were washed to remove unattached bacteria, monolayers were then disrupted to recover attached *Salmonella*. A limitation of this assay is that *S.* Typhimurium invades the host cell as soon as 15 minutes post-infection (Lorkowski *et al.*, 2014); therefore, bacteria recovered from the association time point was a mixture of non-internalised as well as internalised *Salmonella*. At the 4 hours invasion time point, infected monolayers were treated with gentamicin to kill non-internalised *Salmonella*, as gentamicin cannot penetrate eukaryotic cells, so only bacteria that have been internalised are recovered. These two time points provide a rough indication as to whether the *acrB* mutants fail to colonise the host cells or if there is a deficiency in invasion. Both *acrB* mutants tested showed a significant decrease in invasion into host cells when compared against the parental SL1344 strain, indicating that the mutants can colonise and but cannot invade host cells proficiently. Loss of AcrB-mediated efflux attenuated *S.* Typhimurium to the same extent as the Δ*acrB* mutant, indicating that is the efflux activity and not the AcrB protein that is required for virulence.

The attenuation of virulence was further studied in a BALB/c murine infection model, where the bacterial burden in liver and spleen was measured as an indication of systemic infection at five days post-inoculation. Two methods of inoculation were used: oral and intraperitoneal (IP). In the oral model, *S.* Typhimurium traverse the enteric barrier to be engulfed by macrophages and disseminated systemically via the lymphatic system. Additionally, ingested *S.* Typhimurium can be engulfed by $CD18^{+}$ phagocytic cells in the gut and disseminated via blood (Vazquez-Torres *et al*., 1999). In the IP model, the lack of direct contact of the microorganism with the host gut reduces variability caused by differences in the pH of the stomach acid of each mouse, as the acidic pH can decrease the amount of *Salmonella* in the initial inoculum. In both models, the AcrB D408A mutant disseminated systemically, but to a lesser extent than the parental strain as significantly less mutant bacteria were recovered from spleen and considerably less were recovered from liver when compared against wild-type bacterial burdens. These results correlate with a decrease in the ability of the mutant to invade intestinal epithelial cells and macrophages; the first may reflect on its ability to traverse the enteric barrier. However, with the current results it is difficult to determine whether AcrB plays a role in invasion or survival of *Salmonella* in the host. Further experiments are required to assess the ability of the mutant to survive in mammalian cells.

A previous study attributes the loss of virulence in an *acrB*::*aph* mutant to a decrease in transcription of genes essential for host invasion, encoded in the *Salmonella* Pathogenicity Island (SPI) 1 and 2 (Webber *et al*., 2009). In accordance with this, a significant decrease in transcription of SPI-1, 2 and 4 genes was observed in the AcrB D408A mutant when compared against the parental wild-type strain. SPI-1 genes are essential for invasion of non-polarised epithelial cells; whereas SPI-4, in combination

with SPI-1 are required for invasion of polarised epithelial cells (Lorkowski *et al*., 2014). In contrast, SPI-2 is required for maintenance of the intracellular lifestyle of *Salmonella* and survival in phagocytic cells such as macrophages (Jennings *et al*., 2017). Therefore, it is hypothesised that the decreased transcription of SPI genes is, at least, partially responsible for the attenuation of virulence in *acrB* mutants, as virulence regulation in *S.* Typhimurium is complex and is affected by multiple factors, which will be discussed later.

It remains unclear why SPI genes have decreased transcription in *acrB* mutants. Interestingly, the decreased transcription of SPIs was accompanied by downregulation of the PhoPQ TCSS, which senses environmental changes and induces or represses transcription of SPIs in response. A hypothesis is that AcrB exports signalling molecules that are detected by TCSS; therefore, when efflux activity of AcrB is abolished, the signalling molecules accumulate in the periplasm causing overactivation of TCSS. To avoid overexcitation of PhoPQ, the transcription of the TCSS is reduced. Apart from PhoPQ, the transcription of *rcsF*, which encodes a lipoprotein essential for the function of the Rcs TCSS, was also decreased. The Rcs system senses changes in the periplasm and induces cytoskeleton rearrangements that are required for motility and expression of SPI genes (Bulmer *et al*., 2012a). The decreased transcription of *rcsF* suggests that the Rcs TCSS is only partially activated, which could account for the decreased expression of SPI genes.

An alternative hypothesis to explain the decreased transcription of SPIs is that energy used in synthesis of SPI proteins is translocated to other essential functions such as replication and general maintenance of the bacterium, to survive the stress imposed by accumulation of toxic metabolites. This hypothesis is based on the observation that

the majority of genes in COG classes involving cell division and replication are significantly downregulated in the AcrB D408A mutant.

A phenotype that would support the general stress response hypothesis is a change in the replication dynamics of the loss-of-efflux-function mutant, at a single-cell level. At a population level, no significant differences were observed between the growth of the AcrB D408A mutant and the wild-type; however, it is possible that the growth of the mutant is affected at a single cell level. Results obtained from studying the replication dynamics of the AcrB D408A mutant at a single-cell level were not conclusive. However, transcriptional signatures of persister formation, such as a decrease in expression of $tRNA^{Met}$ and changes in transcription of TAs were observed in the AcrB D408A mutant. Persisters are a subpopulation of growth-arrested bacteria, with minimal metabolic activity, that are associated with antibiotic tolerance and recurring infections (Fisher *et al*., 2017). *S.* Typhimurium persisters form naturally during infection of murine and human macrophages (Helaine *et al*., 2014, Rycroft *et al*., 2018) and can be studied *in vitro* using minimal media, such as MOPS or MgMES, which simulate the conditions *Salmonella* encounters inside a macrophage (Beuzon *et al*., 1999, Blair *et al*., 2013). It is worth noting that the poor annotation of the *S.* Typhimurium SL1344 reference genome made it difficult to identify which TAs were differentially transcribed in the *acrB* mutant. A recently published article identified all TAs in SL1344 (Lobato-Marquez *et al*., 2015); this information was used to identify the differentially transcribed modules. The transcription of three TAs was significantly affected by the loss of AcrB-mediated efflux: *vapBC* and the *sehA* toxin from the *sehAB* TA were significantly upregulated and the T4/A4 module was significantly downregulated. The *vapBC* module encodes the VapB antitoxin and VapC toxin; the latter is involved in induction of growth-arrest in *S.* Typhimurium LT2 via selective

cleavage of $tRNA^{fMet}$ (Winther and Gerdes, 2011). It is unlikely that increased transcription of *vapBC* on its own causes growth-arrest, since the effect of VapC is neutralised by VapB, the transcription of which was higher than *vapC* suggesting that most VapC activity was quenched. However, it is likely that the residual VapC activity is responsible for the significant underexpression of $tRNA^{Met}$. Although $tRNA^{Met}$ and $tRNA^{fMet}$ are different and VapC is highly specific to $tRNA^{fMet}$ (Winther and Gerdes, 2011), a detailed analysis of the current annotation of the reference SL1344 genome revealed six $tRNA^{Met}$ and no $tRNA^{fMet}$. Three of the six $tRNA^{Met}$ were significantly underexpressed by at least 1.1 $\log_2$ fold-change (2.14 fold-change) in the AcrB D408A mutant, the other three were also underexpressed, but the difference was not statistically significant. Since the annotation of the reference SL1344 genome has its flaws, it is possible that at least one of these tRNAs corresponds to $tRNA^{fMet}$.

If formation of persisters is increased by the loss of AcrB-mediated efflux, this is likely to be caused by the SehA toxin. Expression of SehA on a plasmid caused growth-arrest in *S.* Typhimurium LT2 (De la Cruz *et al*., 2013), this observation was also reported in SL1344 (Lobato-Marquez *et al*., 2015). Furthermore, transcription of the antitoxin *sehB* was not significantly affected in the AcrB D408A mutant; therefore, no antitoxin is available to counteract the effects of the SehA toxin.

Regarding the significantly downregulation of T4-A4 module, overexpression of T4 induced growth-arrest in *S*. Typhimurium SL1344 (Lobato-Marquez *et al*., 2015). However, not much information is available as it is a recently discovered TA. Hence, the biological significance of the decreased transcription of T4-A4 cannot be elucidated.

TAs have a significant role in the virulence of *S.* Typhimurium. Previous studies have reported that activation of TAs is essential for survival of *Salmonella* inside the host (De la Cruz *et al*., 2013, Lobato-Marquez *et al*., 2015). It is hypothesised that this is due to the presence of 'backup bacteria' to ensure the survival of the population. I hypothesise that TAs help *S.* Typhimurium evade the immune system. TAs have multiple modes of action, including degradation of mRNA (Coussens and Daines, 2016). The host immune system differentiates between live and dead bacteria by sensing bacterial mRNA (Sander *et al*., 2011), TAs reduce the number of mRNA copies, which would 'trick' the immune system into believing that *Salmonella* are dead. In the case of the AcrB D408A mutant, activation of TAs is likely to be a direct consequence of the stress induced by accumulation of toxic metabolites. IT is also hypothesised that the activation of TAs may increase the persister subpopulation, which might help the *Salmonella* mutant survive in the hostile environment of the host given that its ability to colonise and invade is impaired.

Another physiological process that could have an effect on virulence is quorum sensing (QS), a population density-dependent mechanism of cell-to-cell communication that controls the expression of genes involved in biofilm formation and virulence at a population level in multiple bacterial species. Multiple types of QS signalling molecules exist; in *S.* Typhimurium, one has been studied thoroughly: autoinducer-2 (AI-2). This molecule is introduced into the bacterial cell via the LsrABCD ABC-type transporter, where it is immediately phosphorylated by LsrK to stop AI-2 from being exported again (Taga *et al*., 2003). In the AcrB D408A mutant, *lsrABCDKR* were significantly downregulated when compared against the parental strain; this suggested that AI-2 was not internalised into the mutant. Consistent with this, significantly more AI-2 was detected in the cell-free culture supernatant of the

mutant. However, this was only observed when the strains were grown in LB supplemented with 0.5% glucose. No difference was observed between strains grown in LB without glucose and minimal media, such as MOPS and autoinducer bioassay (AB) media. Surette and Bassler (1998) reported that production of AI-2 by *S.* Typhimurium was induced in LB supplemented with glucose; in the absence of glucose, AI-2 was barely detected. Maximum production of AI-2 is detected between mid-logarithmic and early stationary growth phase, after which AI-2 disappears from the culture supernatant as it is internalised into the bacterial cell (Surette and Bassler, 1998, Wattanavanitchakorn *et al*., 2014). Consistent with this, culture supernatant harvested from early growth phases induced bioluminescence better than those obtained from overnight cultures. The increase in AI-2 in the cell-free culture supernatant of the AcrB D408A mutant grown in LB with glucose was consistent throughout the growth curve (from OD_{600}=0.1 to 1.0), suggesting a deficient internalisation or increased production of AI-2. Increased production of AI-2 is an unlikely event in the AcrB D408A mutant as no significant changes were observed in transcription of *luxS*, essential for the synthesis of AI-2 in *S. enterica* and *E. coli* (Taga *et al*., 2003). This suggests that the increase in extracellular AI-2 is due to a decrease in internalisation of AI-2 caused by decreased expression of LsrABCD and/or LsrKR.

In some bacteria such as *Pseudomonas aeruginosa*, autoinducers play an important role in virulence as they facilitate the expression of virulence factors (Whiteley *et al*., 2017). In *S.* Typhimurium, the effect of AI-2 on virulence is debatable (Perrett *et al*., 2009, Choi *et al*., 2012). However, QS has a role in sensing of metabolites (Goo *et al*., 2015). AI-2 is a by-product of metabolism of S-adenosyl-methionine (SAM) (Schauder *et al*., 2001), which regulates biosynthesis of cysteine and methionine through the SAM riboswitch (Batey, 2011). Cysteine biosynthesis products are hypothetical

substrates of AcrB (Ruiz and Levy, 2014); so the decreased intake of AI-2 might be related to accumulation of metabolic by-products regulated by the SAM-riboswitch.

It is important to note that although internalisation of AI-2 is reduced in the AcrB D408A mutant, it is unclear whether QS activation and QS-mediated phenotypes are affected in the mutant. As a direct way to measure QS activation in *S.* Typhimurium, future experiments can be performed with the pBB1 reporter cosmid (Miller *et al*., 2002). This cosmid encodes the *V. harveyi* enzymatic machinery to bioluminesce when QS is activated and allows direct measurements of QS activity when introduced into the target Enterobacteriaceae. Regarding QS-regulated phenotypes, a well-studied phenotype regulated by QS is the formation of biofilms (Eberl and Riedel, 2011, Wolska *et al*., 2016). However, SL1344 is not an adequate strain to study biofilm formation as it forms biofilms poorly (Baugh, 2014). The reference strain for biofilm studies in *S.* Typhimurium is 14028S. In order to determine if biofilm formation is altered by decreased import of AI-2 in a *S.* Typhimurium AcrB D408A mutant, a 14028S mutant must be constructed.

A previous study showed that biofilm and curli production were significantly decreased in a 14028S *acrB*::*aph* mutant (Baugh, 2014). Curli is a proteinaceous fiber that is essential for the formation of biofilms and colonisation of the host. The curli protein is synthesised by CsgA and polymerised by CsgB (Barnhart and Chapman, 2006). Interestingly, *csgB* was significantly upregulated in the AcrB D408A mutant, but no other genes from the *csg* operons were differentially transcribed. To test if this had a phenotypic effect, overnight cultures of SL1344 and its *acrB* mutants were spotted onto agar containing Congo red to allow qualitative identification of curli production. For comparative purposes, 14028S and its *acrB*::*aph* mutant were used. In accordance with the previous report (Baugh, 2014), the 14028S *acrB*::*aph* mutant did

not produce curli. However, it is unclear if this is caused by the *aph* gene. In SL1344, a weak curli production phenotype was observed, the colony morphology was slightly drier than that of the *acrB* mutants, but no conclusions can be drawn from this experiment. Therefore, the experiment needs repeating with a 14028S AcrB D408A mutant and curli production needs to be measure qualitatively.

Metabolic changes in the AcrB D408A mutant have been mentioned throughout this chapter. To identify the genes responsible for the metabolic change, a Metabolic Transformation Algorithm (MTA) was applied. The modelling results suggested that deletion of *glpK* and *lamB* in SL1344 would replicate the metabolic state of the AcrB D408A mutant in the wild-type strain; in contrast, deletion of *fadB* in the mutant would revert the metabolism of *S.* Typhimurium back to the wild-type state. These three genes encode a glycerol phosphatase, a maltoporin and the α-subunit of the fatty acid oxidation complex, respectively (Uniprot Consortium, 2014). Deletion of *fadB* would cause the AcrB D408A mutant to lose its ability to use fatty acids as a carbon/energy source, forcing *Salmonella* to use other carbon sources. In contrast, deletion of *glpK* and *lamB* in the wild-type strain would cause *S.* Typhimurium to become unable to utilise glycerol and maltose as carbon/energy sources, forcing the strain to use alternative sources of energy such as fatty acids. These results suggest that fatty acids play an important role in the maintenance of the metabolism of the AcrB D408A mutant. Supporting this observation is a study that shows that AcrB is the main exporter of free fatty acids in *E. coli* (Lennen *et al*., 2013); therefore, loss of AcrB-mediated efflux is likely to cause intracellular accumulation of fatty acids. Under this assumption, it would be expected that β-oxidation would be increased in the mutant as a mechanism to cope with the excess of fatty acids. A long-term increase in β-oxidation would cause a shift in metabolism towards an oxidative state in the AcrB

D408A mutant. Supporting this hypothesis, Zampieri *et al*. (2017) showed that antibiotic-induced overexpression of AcrB in *E. coli* caused carbon metabolism to shift towards a fermentative state when compared against a isogenic strain that expressed basal levels of AcrB. Changes in metabolism lead to loss of virulence in *S.* Typhimurium, as this microorganism requires a robust metabolism in order to survive in the host (Steeb *et al*., 2013, Herrero-Fresno and Olsen, 2018).

4.14 Key findings

- The transcription of 14.35% of the genome of *S.* Typhimurium SL1344 is significantly affected by the loss of AcrB-mediated efflux.
- The decrease in motility in the *acrB*::*aph* mutant is an artefact of the *aph* insertion, unrelated to loss of *acrB* function.
- The transcription of the global transcriptional regulator *ramA* is not significantly induced in the AcrB D408A mutant.
- Genes encoding outer membrane porins from the *omp* family are significantly downregulated in the AcrB D408A mutant when compared against the parental SL1344 strain.
- AcrB-mediated efflux is essential for virulence and maintenance of the metabolic state of *S.* Typhimurium.
- AcrB-induced loss of virulence may be influenced by many factors including activation of stress responses, decreased transcription of TCSS, persister formation and changes to metabolism.

4.15 Future work

- Determine whether the *aph* effect on motility is *S.* Typhimurium-specific, additional motility assays using *E. coli* MG1655 *acrB* mutants will be carried out. To determine if the effect is *acrB*-specific, insertional inactivation and gene deletion mutants will be used in motility assays.
- Assess if expression of OMPs is affected in the *S.* Typhimurium SL1344 AcrB D408A mutant.
- Determine if replication dynamics at a single-cell level is affected by the loss of AcrB efflux function.
- To study the effect of loss-of-efflux function on biofilm formation and curli production, construct a *S.* Typhimurium 14028S AcrB D408A mutant.
- Determine if loss of AcrB efflux function causes accumulation of fatty acids and shifts metabolism of *S.* Typhimurium towards an oxidative state.
- Determine the mechanism of AcrB-induced loss of virulence.

CHAPTER 5.

Does AcrB efflux virulence factors?

5.1 Background

Deletion of AcrB or loss of AcrB-mediated efflux is associated with a drug hypersusceptible phenotype in Enterobacteriaceae. In *S.* Typhimurium, deletion or inactivation of AcrB/*acrB* is also associated with attenuation of virulence (Lacroix *et al*., 1996, Buckley *et al*., 2006, Nishino *et al*., 2006, Blair *et al*., 2015b). AcrB is involved in export of bile; therefore, an early hypothesis was that attenuation of virulence *in vivo* was due to the hypersusceptibility of the strain to bile (Lacroix *et al*., 1996). However, later studies showed that *S.* Typhimurium *acrB* mutants were also attenuated in cultured cell lines, where they were not exposed to bile (Buckley *et al*., 2006). Similarly, a *Pseudomonas* aeruginosa Δ*mexAB-oprM* mutant, homologue of *acrAB-tolC*, was significantly attenuated in Madin-Darby canine kidney (MDCK) cells and in a murine infection model (Hirakata *et al*., 2002). An increase in the virulence of the Δ*mexAB-oprM* mutant on MDCK cells was observed when cell-free culture supernatants from cells infected with wild-type *P. aeruginosa* was added to the mutant. Supernatant from cells infected with the mutant also increased virulence of the Δ*mexAB-oprM* mutant, but the increase was 10-fold lower than what was observed with the wild-type supernatant. The conclusion of this study was that MexAB-OprM was involved in the export of a virulence factor in *P. aeruginosa* (Hirakata *et al*., 2002).

Following the observations made by Hirakata *et al*. (2002), the hypothesis that AcrAB-TolC was involved in the export of a virulence factor was explored by Blair (2010). Cell-free culture supernatant of *S.* Typhimurium SL1344 grown overnight in LB at 37°C (SL1344 ExM) was harvested and added to the isogenic Δ*acrB* mutant in gentamicin protection assays on INT-407 intestinal epithelial cells. Surprisingly, addition of the SL1344 ExM significantly increased virulence of the Δ*acrB* mutant without affecting the viability of the cells (Appendix VI, Figure A). Further experiments carried out in the

Piddock group (unpublished data) revealed that the restorative effect of SL1344 ExM was best observed at 4 hours post-infection (two hours after addition of gentamicin), when ExM was triple-concentrated (3X) and added in a 1:2 proportion to inoculation medium (final concentration of ExM of 1.5X) (Appendix VI, Figures B and C). To determine the chemical nature of the virulence-restoring molecule(s), SL1344 ExM treated with proteinase K was used. Interestingly, the virulence-restoration effect was partially lost, suggesting that a protein or peptide might be involved in restoration of virulence (Appendix, Figure D). However, SL1344 ExM heated for 10 minutes at 95°C or 1 hour at 70°C remained fully active (Blair, 2010), as did ExM recovered after filtering through a 5kDa filter. Therefore, it is unlikely that the virulence-restoring factor(s) is a protein, but it is likely to have peptide bonds. Further efforts into identifying the virulence-restoring molecule(s) and other natural substrates of AcrB in *S.* Typhimurium and *E. coli* are described in this chapter.

5.2 Aims

- To discover a native AcrB substrate involved in the virulence of *S.* Typhimurium.
- To identify native molecules exported by AcrB in *S.* Typhimurium and *E. coli* that are derived from bacterial metabolism.

5.3 Hypotheses

- One or more molecules exported by AcrB are involved in the virulence of *S.* Typhimurium.
- Apart from xenobiotics, AcrB is used by *E. coli* and *S.* Typhimurium to export products of their own metabolism.

5.4 The effect of media composition on production of the virulence-restoring factor(s) in SL1344 ExM

In previous experiments, it was observed that the virulence-restoring effect of SL1344 ExM was highly variable as some batches of ExM would restore virulence of a Δ*acrB* mutant better than others. This was likely a consequence of variation in the composition of LB medium; therefore, to reduce the variation in the biological effect of the SL1344 ExM, a chemically defined medium that favoured the synthesis of the virulence-restoring factor(s) was required.

Initial experiments were carried out with MOPS minimal medium (MOPS). However, three-times concentrated SL1344 ExM (hereafter referred to as SL1344 ExM) produced from MOPS did not restore virulence to a ∆*acrB* mutant when compared against the ExM produced in LB. Therefore, this medium could not be used (Figure 5.1).

It was hypothesised that the lack of virulence-restoration observed with SL1344 ExM produced from MOPS was due to the low nutritional availability in the medium. Therefore, a chemically defined rich medium was tested. EZ Rich Defined Medium (EZ) is a MOPS-based medium, supplemented with a defined combination of amino acids, vitamins, nucleotides and other nutrients (Appendix I, section G). Similar to the results with MOPS, SL1344 EZ ExM restored virulence significantly less than the SL1344 LB ExM (Figure 5.2). As a strong virulence-restoration effect was required for the experiments, MOPS and EZ ExM were discarded and LB was used for the rest of the experiments.

Figure 5.1 Virulence restoration effect of SL1344 ExM produced in MOPS minimal medium, on a Δ*acrB* mutant.

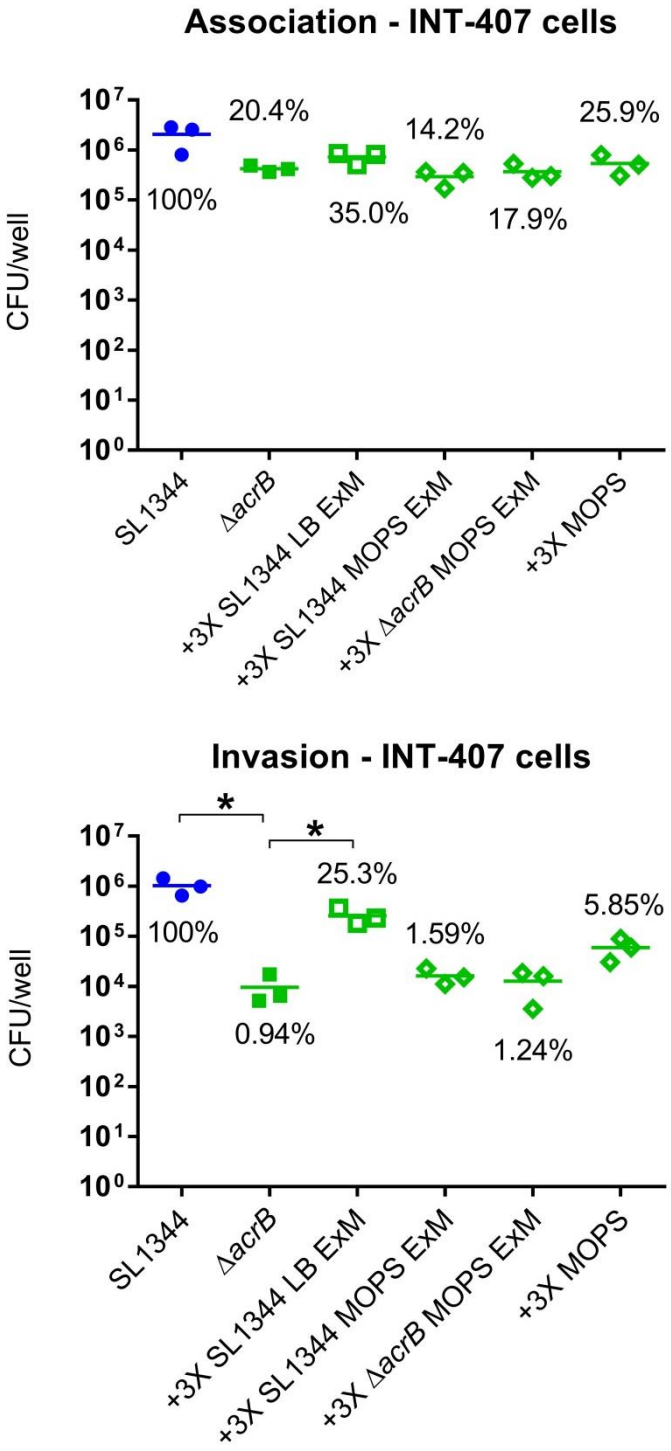

Association and invasion were measured at 2 and 4 hours post-infection, respectively. An SL1344 Δ*acrB* mutant was exposed to 3X-concentrated SL1344 ExM. Each point represents a biological replicate, a line represents the mean of each dataset. An asterisk denotes a significant difference of $P<0.05$ between two groups, compared by Student's t-test with Welch's correction.

Figure 5.2 Virulence restoration effect of SL1344 ExM produced in EZ rich defined medium, on a Δ*acrB* mutant.

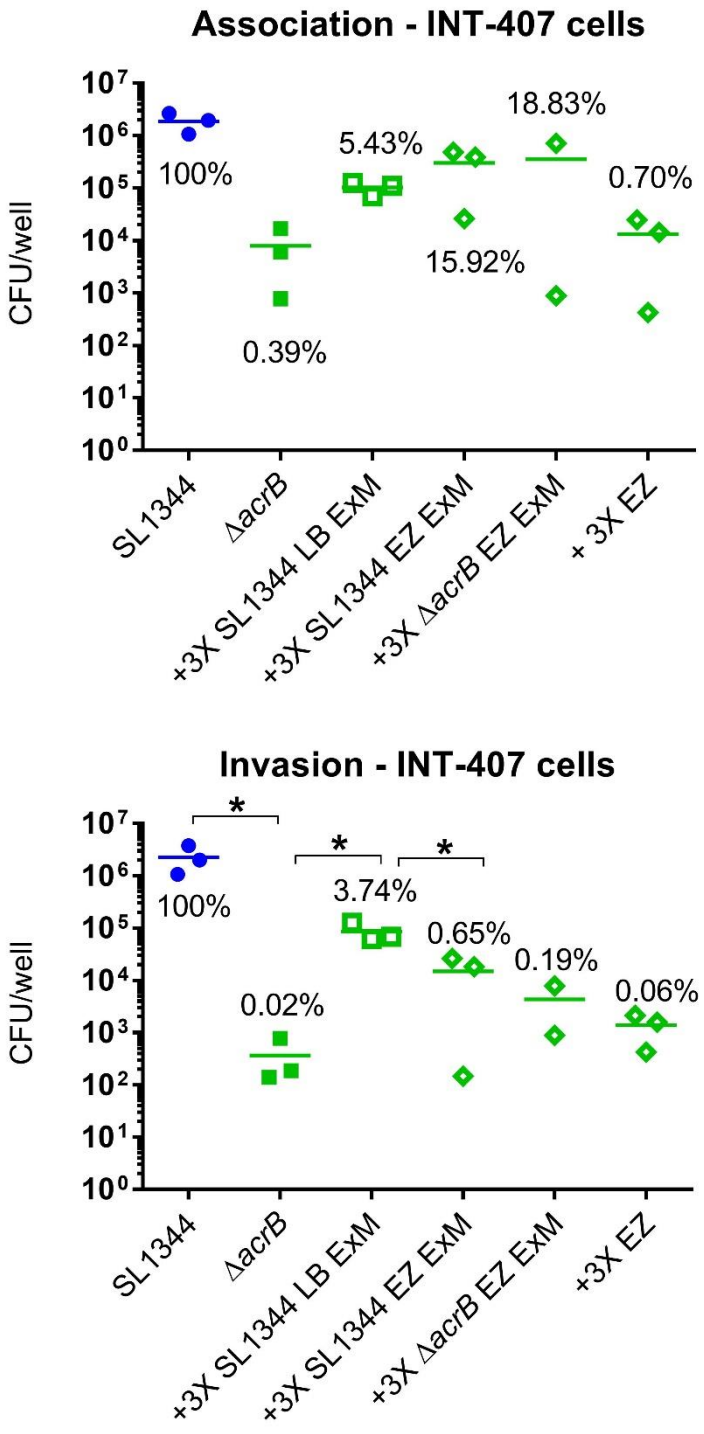

Association and invasion were measured at 2 and 4 hours post-infection, respectively. An SL1344 Δ*acrB* mutant was exposed to 3X-concentrated SL1344 ExM. Each point represents a biological replicate, a line represents the mean of each dataset. An asterisk denotes a significant difference of $P<0.05$ between two groups, compared by Student's t-test with Welch's correction.

5.5 Chemical fractionation of SL1344 ExM

As LB could not be replaced with a chemically defined medium, fractionation of SL1344 ExM was attempted to isolate the virulence-restoring molecule(s). Fractionation was carried out using the Diaion® HP-20 resin. This resin captures hydrophobic compounds by adsorption. Adsorbed compounds can then be recovered by washing the resin with the appropriate solvent.

SL1344 ExM was exposed to HP-20 resin overnight to separate ExM into a hydrophobic (adsorbed to resin) and a hydrophilic fraction (non-adsorbed media). The resin was recovered and washed with acetone (Act ExM), methanol (MeOH ExM) and water (H_2O ExM) to recover adsorbed compounds. These fractions were concentrated to test for biological activity. The residual media after resin exposure, or residual hydrophilic fraction (HF ExM), was also tested.

The Act and HF fractions had the best restorative activities on the Δ*acrB* mutant, where they restored invasion to 1.72% and 1.24% of wild-type, respectively. The H_2O ExM had the least restorative activity (0.11% of wild-type). However, none of the fractions significantly increased virulence of the Δ*acrB* mutant when compared against the mutant without exposure to ExM. Only the unfractioned ExM significantly increased virulence of the Δ*acrB* mutant (Figure 5.3). Therefore, unfractioned ExM was used for the rest of the experiments.

Figure 5.3 Virulence restoration effect of SL1344 LB ExM fractions on a Δ*acrB* mutant.

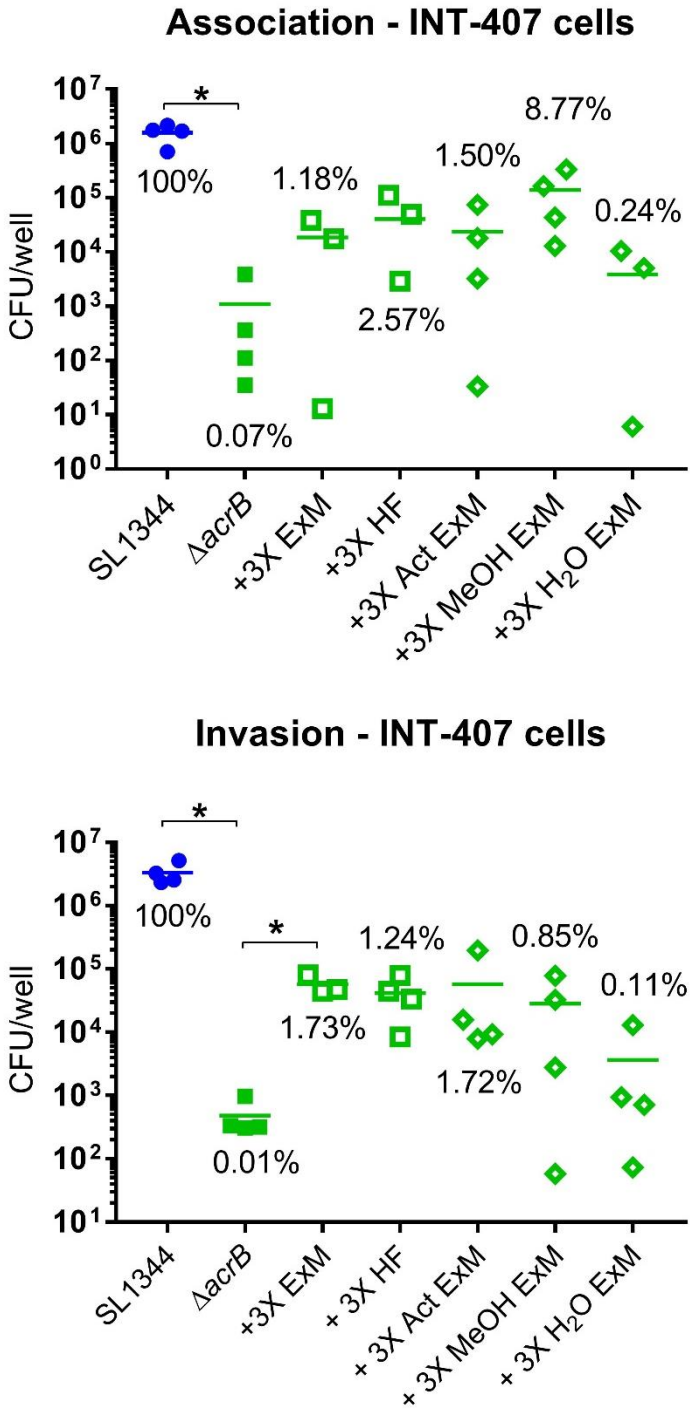

Association and invasion were measured at 2 and 4 hours post-infection, respectively. An SL1344 Δ*acrB* mutant was exposed to 3X-concentrated SL1344 ExM or its fractions. Each point represents a biological replicate, a line represents the mean of each dataset. An asterisk denotes a significant difference of $P<0.05$ between two groups, compared by Student's t-test with Welch's correction.

5.6 Restoration of virulence on a *S.* Typhimurium AcrB D408A mutant

All previous experiments were carried out with a SL1344 Δ*acrB* mutant, which, as mentioned in Chapter 3, overexpresses additional RND efflux pumps as a consequence of loss of the AcrB protein. The additional pumps might give rise to confounding phenotypes in the Δ*acrB* mutant; hence, restoration of virulence was validated with a SL1344 AcrB D408A mutant.

The virulence-restoration effect of ExM on intestinal epithelial cells was tested with a SL1344 AcrB D408A mutant. Non-polarised INT-407 and polarised Caco2 intestinal epithelial cells were used. The Δ*acrB* mutant was used for comparative purposes.

As shown previously, the Δ*acrB* and the AcrB D408A mutant were significantly attenuated when compared against the parental wild-type strain. The AcrB D408A mutant had the same phenotype as the Δ*acrB* mutant under all conditions tested. Addition of SL1344 ExM increased invasion of both mutants to ~10% in INT-407 cells (Figure 5.4A) and ~50% of the wild-type invasion levels in Caco2 cells (Figure 5.4B). Addition of 3X Δ*acrB* ExM slightly increased invasion of the mutants into epithelial cells; however, this increase was not significant when compared against the respective mutant without exposure the ExM. The same increase in invasion was observed when 3X AcrB D408A ExM and 3X LB were added to the AcrB D408A mutant, suggesting that this non-significant increase in virulence is a response to components of the media and not *Salmonella*-derived molecules. As only SL1344 ExM significantly restored virulence to the *acrB* mutants, it was concluded that export or synthesis of a *Salmonella*-virulence factor was dependent on AcrB.

Figure 5.4 Restoration of virulence in *S.* Typhimurium *acrB* mutants on intestinal epithelial cells.

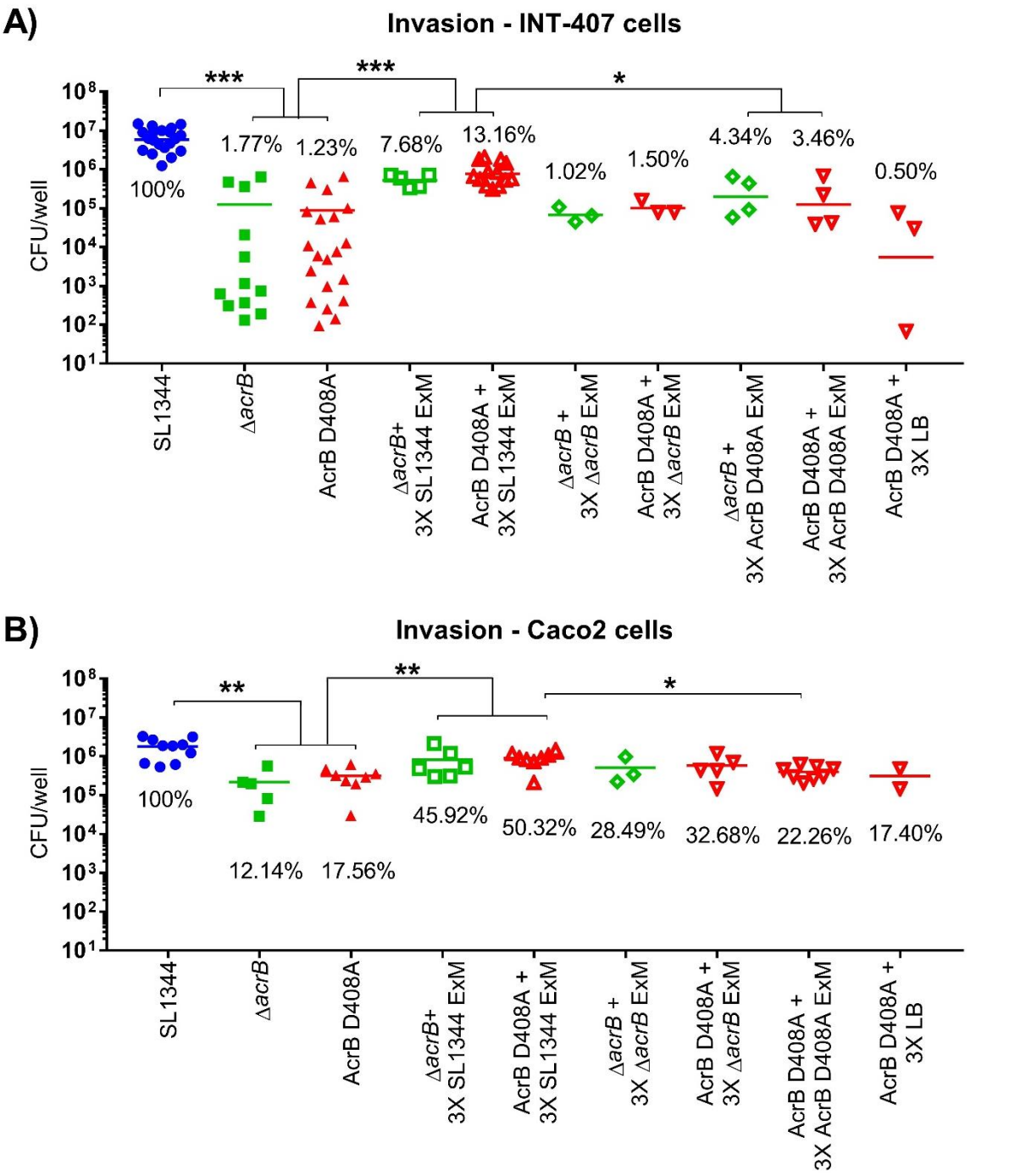

Invasion of *S.* Typhimurium into A) non-polarised INT-407 and B) polarised Caco2 intestinal epithelial cells was measured at 4 hours post-infection, when the maximum restorative effect of ExM was observed. Δ*acrB* and AcrB D408A mutants of *S.* Typhimurium SL1344 were exposed to 3X-concentrated LB and ExM from SL1344 and *acrB* mutants. Each point represents a biological replicate, a line represents the mean of each dataset. An asterisk denotes a significant difference of $P<0.05$ between two groups, compared by Student's t-test with Welch's correction; two and three asterisks denote a difference of $P<0.01$ and $P<0.001$, respectively.

5.7 Production of the virulence-restoring factor(s) is dependent on the *S.* Typhimurium growth phase

To determine in which growth phase was the virulence-restoring molecule produced, ExM from SL1344 was harvested from different growth phases. To assess which time points correspond to which growth phase, growth kinetics of SL1344 was measured by viable count. Samples of SL1344 growing in LB were taken every hour for the first ten hours and at 18 and 24 hours to determine CFU/mL. Under the conditions tested, SL1344 had a short lag phase of approximately 2 hours, after which, it entered exponential growth phase (log phase) and continued to grow at the same rate until 6 hours post-inoculation. Late log phase occurred between 6 to 8 hours as the growth rate was slower when compared to early time points. An early stationary phase was observed between 8 to 10 hours. Stationary phase continued until 18 hours, followed by a decrease in CFU/mL between 18 to 24 hours (Figure 5.5A).

To make results comparable, the same number of bacteria were required for each time point. This was to ensure that if a significant change in virulence-restoration was observed, the effect would be a consequence of decreased export/synthesis of the factor(s) and not because of a difference in number of bacteria producing the molecule(s). To equalise the total CFU at each time point, cultures were scaled up. However, this could only be done with late logarithmic phase (7 hours), early stationary phase (8, 9 and 10 hours) and late stationary phase cultures (18 hours) as the number of bacteria in earlier growth phases was too low and a considerable amount of culture would be required to equalise the amount of bacteria to later growth phases.

Harvested ExM was concentrated and added to the SL1344 AcrB D408A mutant to assess their virulence-restoration activity. ExM from all time points, except for 7 hours, significantly increased virulence of the AcrB D408A mutant (Figure 5.5B). Interestingly,

the later the ExM was harvested, the higher was its virulence-restoration effect on the AcrB D408A mutant. This observation was validated by linear regression, where a correlation between CFU/mL of AcrB D408A mutant recovered from infected cells and time of harvest of ExM was observed (Figure 5.5C).

It is worth noting that the high CFU/mL obtained from the viable counts may be attributed to the method used. The Miles-Misra method was used for viable counting, in which an aliquot of 20µL of each dilution is spotted on to the agar. This aliquot is not spread and is left to be absorbed by the agar. In order to count the colonies accurately, two to 20 colonies per spot are required. As the spots are not spread, a higher dilution is required to accurately count well separated colonies, which may result in higher CFU/mL reads than when the spread plate technique is used.

5.8 Effect of ExM on J774A.1 murine macrophages

Previous experiments from the Piddock group showed that SL1344 ExM could not restore virulence in murine macrophages (Appendix VI, Figure E). To test this, J774A.1 murine macrophages were infected with SL1344 and its *acrB* mutants with and without exposure to ExM. Gentamicin protection assays were carried out in the same way as with intestinal epithelial cells; however, a disruption of the monolayer and a considerable loss of cells was observed in wells that contained ExM at 2 hours post-infection (Figure 5.6). The experiment was stopped at this point as a decrease in the total number of host cells would produce unreliable results.

The disruption of the monolayer was not caused by *S.* Typhimurium invasion or addition of LB, as only the monolayers exposed to ExM from either wild-type SL1344 or the AcrB D408A mutant were disrupted (Figure 5.6). This suggests that a

Figure 5.5 Effect of SL1344 ExM harvested from different time points on restoration of virulence of a SL1344 AcrB D408A mutant.

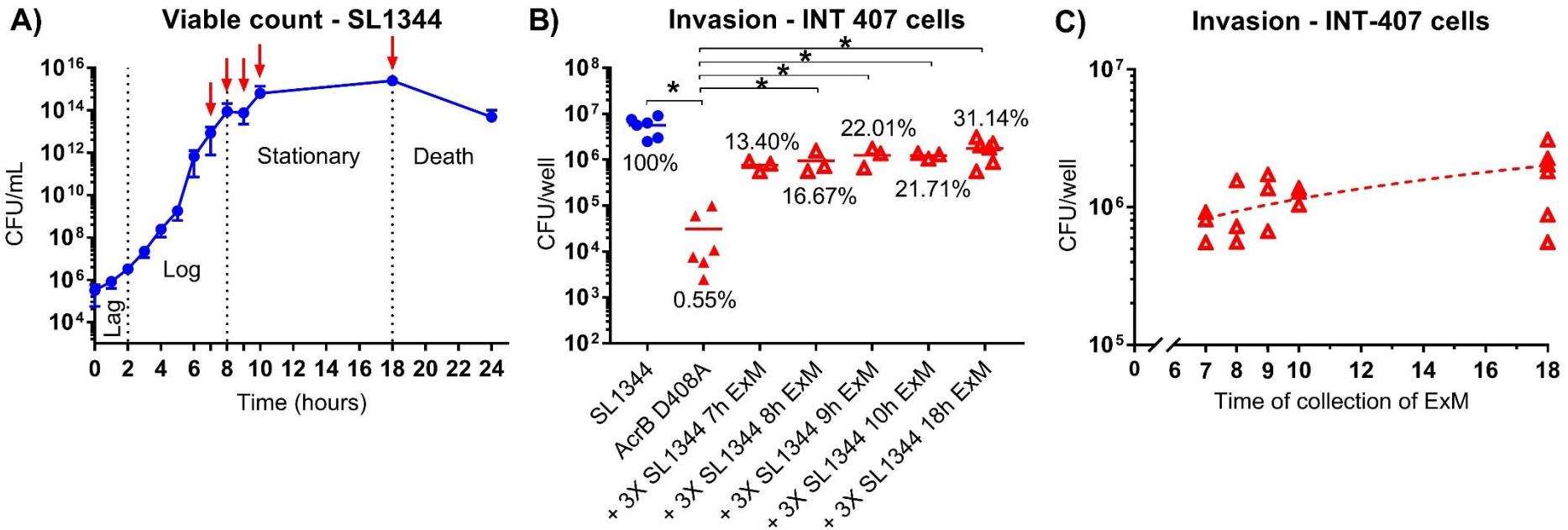

A) CFU/mL of wild-type SL1344 was measured every hour. Mean and standard deviation of three experiments is shown. The start and end of each growth phase is indicated with dotted lines, with the name of each phase shown underneath the curve. Time points at which ExM was harvested are indicated with red arrows. B) The virulence-restorative effect of the harvested SL1344 ExM on the AcrB D408A mutant was measured at 4 hours post-infection, when the maximum restorative effect of ExM was observed. Each point represents a biological replicate, a line represents the mean of each dataset. An asterisk denotes a significant difference of $P<0.05$ between two groups, compared by Student's t-test with Welch's correction; two and three asterisks denote a difference of $P<0.01$ and $P<0.001$, respectively. C) The time of collection of ExM and the number of bacteria recovered at 4 hours post-infection was plotted, lineal regression, shown as a dotted line, was used to determine the correlation between the virulence-restoration effect of ExM and growth phase of SL1344.

Figure 5.6 Monolayers of J774A.1 murine macrophages infected with *S.* Typhimurium SL1344 or its *acrB* mutants, in presence and absence of ExM and LB.

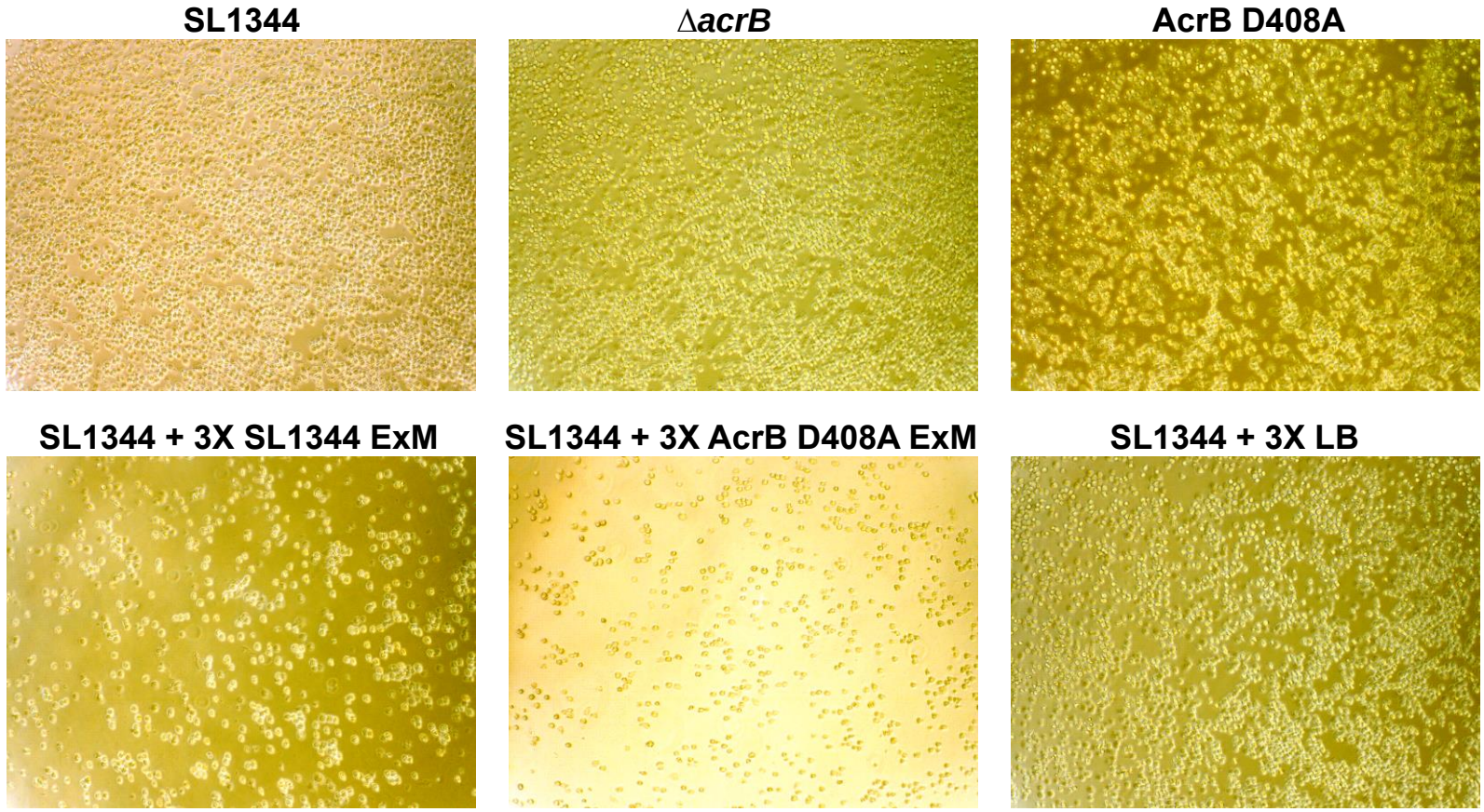

J774A.1 monolayers were examined in an inverted microscope at 2 hours post-infection, following addition of 100μg/mL of gentamicin. Photos were taken with at 10X amplification. The *S.* Typhimurium strain infecting the monolayer as well as the condition tested is shown on top of each photo.

macrophage-killing factor is being produced by *S.* Typhimurium independent of AcrB efflux activity. To determine the extent of the damage caused by addition of ExM, confluent monolayers of J774A.1 were exposed to sterile LB broth and ExM from SL1344 and its *acrB* mutants. Monolayers were washed at the 2 hours time point and macrophages were recovered for viable counting by trypan blue exclusion. A significant decrease in the number of viable cells was observed in monolayers exposed to ExM, where only ~50% of the macrophages survived the treatment (Figure 5.7). However, no significant changes in cell viability were observed in monolayers exposed to LB, indicating that the decreased viability of J774A.1 cells is caused by *Salmonella*-derived molecules, the synthesis and export of which is independent of AcrB.

5.9 Identification of bacterial metabolites effluxed by AcrB

5.9.1 Untargeted metabolomics

To identify molecules exported by AcrB in *S.* Typhimurium (including those that restored virulence), untargeted metabolomics by high-resolution liquid chromatography mass spectrometry (HPLC-MS) was carried out. To eliminate interference from components of the growth medium, peaks obtained from sterile LB medium were subtracted from the spectra of the *S.* Typhimurium samples. The relative abundance of each metabolite feature (hereafter referred to as feature), given by the area under the curve, was used to calculate fold-change in concentrations of each feature between the wild-type and mutant strains.

Thousands of features were identified in each HPLC-MS run. To facilitate identification of AcrB substrates, the ExM of *S.* Typhimurium AcrB D408A and the Δ*acrB* mutant

Figure 5.7 The effect of 3X SL1344 ExM on viability of J774A.1 murine macrophages.

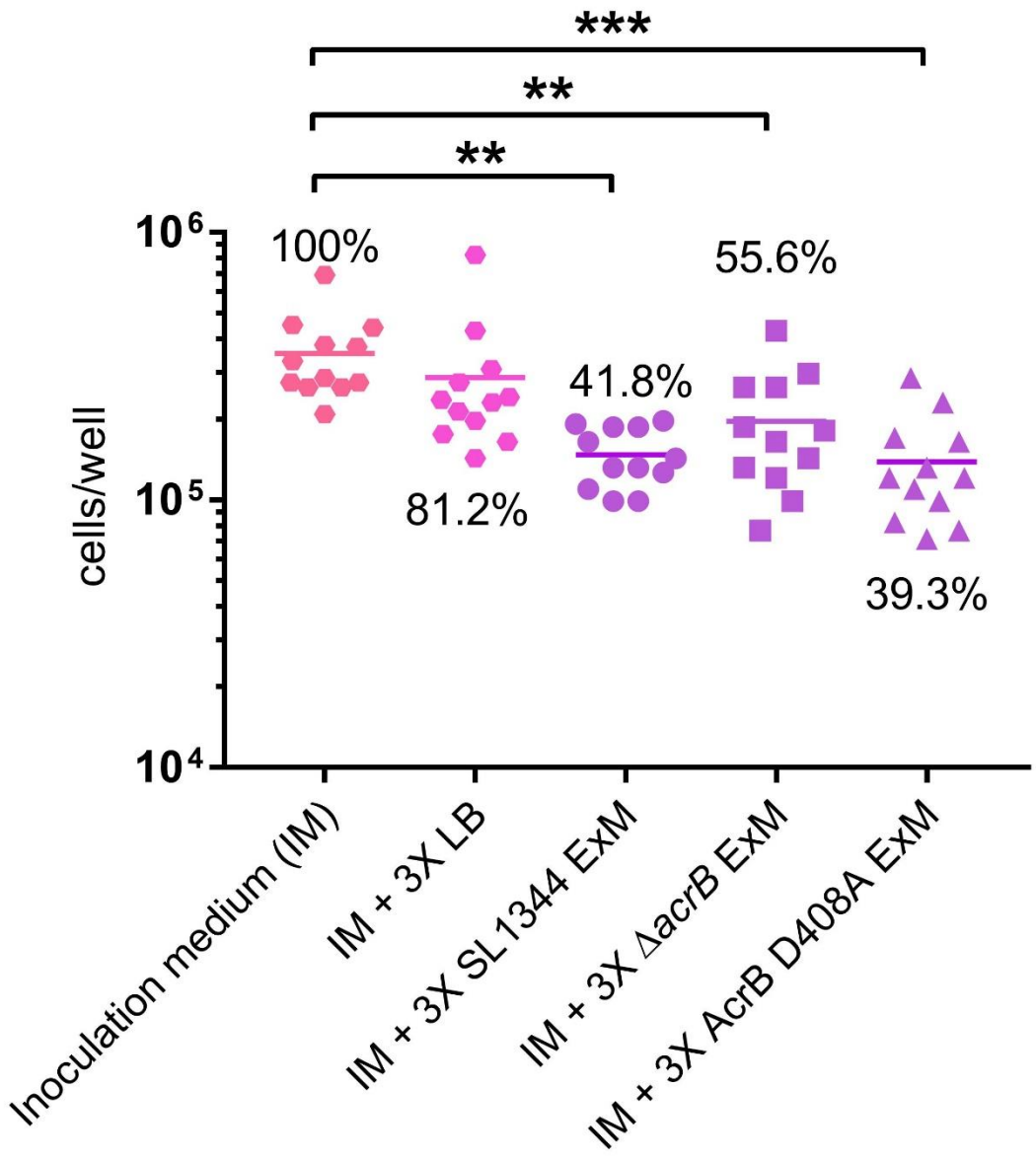

Confluent monolayers of J774A.1 macrophages were exposed to 3X LB or 3X SL1344 ExM. ExM was prepared in LB with and without NaCl. Each point represents a biological replicate, a line represents the mean of each dataset. A Student's t-test with Welch's correction was performed to compare each group against the inoculation medium. Two (**) and three asterisks (***) denote a significant difference of $P<0.01$ and $P<0.001$, respectively. Statistical analyses were performed on raw, non-log transformed data.

were analysed. Following statistical analyses, 54 features were found in a significantly higher concentration in the wild-type SL1344 ExM when compared against the ExM of both *acrB* mutants and the sterile LB broth. A putative metabolite identity (ID) was assigned to each feature based on their masses and retention times. Multiple databases including the Human Metabolome Database, KEGG and Biocyc were screened for metabolites that would fit the mass and retention time obtained for each feature. Where more than one putative ID was assigned to a feature, literature research was conducted to find the most likely ID of the feature. Features were assigned to metabolite classes based on putative IDs. The full list of features is shown in Appendix VII (Table A). Most of the identified features were tryptophan degradation products (20%), followed by fatty acid and alcohols (15%), acylcarnitines and their degradation products (13%) and peptides (13%) (Figure 5.8). The top 20 metabolites with the highest fold-changes between wild-type and *acrB* mutants included fatty acids and alcohols, acyl-carnitines and tryptophan degradation products (Table 5.1). The feature with the highest fold-change was annotated as pyridoxamine (vitamin B_6) or octadienol, a fatty alcohol. Two features, identified as homocysteine and arginyl-asparagine, respectively, were not found in the sterile LB medium.

To explore other native substrates of AcrB exported by Enterobacteriaceae, the ExM of *E. coli* MG1655 and its AcrB D408A mutant were also studied. Initial analyses revealed that 19 features were likely to be in a considerably higher concentration in the wild-type ExM when compared against the mutant. These features were annotated; however, annotation of the *E. coli* ExM proved more challenging than that of *S.* Typhimurium. Multiple features identified in the *E. coli* metabolomics were annotated as terpenes, aromatic phytochemicals and human metabolites (Appendix VII, Table B). In general, multiple fatty acids and fatty alcohols, aromatic compounds

Figure 5.8 Classification of metabolites identified in abundance in the ExM of *S.* Typhimurium SL1344 relative to its *acrB* mutants.

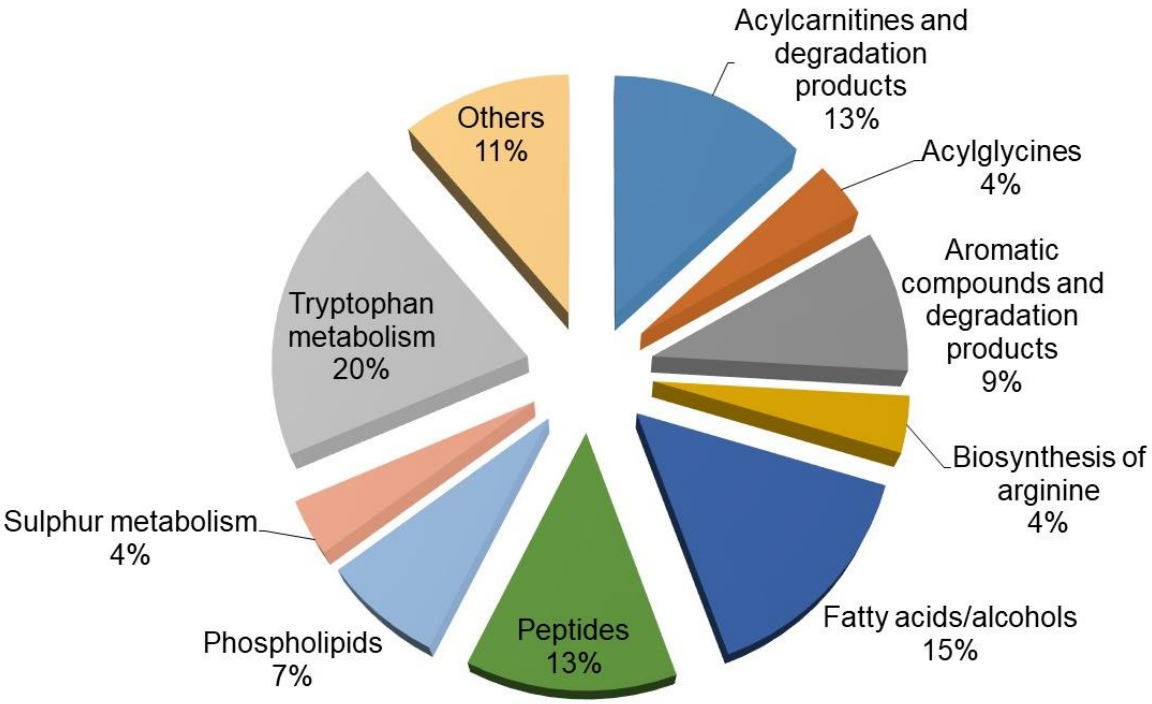

Figure shows a graphic representation of the proportion of each metabolite group. A total of 54 features were found in a significantly higher concentration in the ExM of SL1344 when compared against its *acrB* mutants and sterile LB broth. Features were assigned into groups according to putative metabolite IDs.

Table 5.1 List of top 20 metabolites identified in abundance in the ExM of *S.* Typhimurium SL1344 relative to its *acrB* mutants and LB broth.

Metabolite putative ID	Classification of metabolite	Fold- change		
		SL1344/ Δ*acrB*	SL1344/ AcrB D408A	SL1344/ LB
Pyridoxamine; octadienol	Others (vitamin B_6); fatty acids/alcohols	37.54	23.26	4.45
Tridecatrienediynol; methyl-oxooctanoic acid	Fatty acids/alcohols	23.78	15.83	3.96
Quinaldic acid	Tryptophan metabolism	9.57	7.42	3.38
Octenoylcarnitine	Acylcarnitine	7.81	5.29	2.74
Homocystine	Sulphur metabolism	4.60	4.96	NDM
Benzylsuccinate;D-4-O-methyl-myo-inositol	Aromatic compounds and degradation products; others (inositol phosphate metabolism)	5.77	4.86	3.09
Methionyl-methionine	Peptides	3.95	4.71	19.14
Pantetheine 4'-phosphate	Others (pantothenate –vitamin B_5– and CoA biosynthesis)	3.57	4.67	1.35
N-(2-hydroxyisobutyl)-2,4,8,10,12-tetradecapentaenamide	Others (acylamine)	3.65	4.25	2.51
Kynurenic acid	Tryptophan metabolism	4.65	4.21	2.83
Arginyl-asparagine	Others (polyamine derivative); peptide	3.38	3.75	NDM
Hexenoylcarnitine; serinyl-lysine	Acylcarnitine; peptide	3.38	3.45	1.70
5-Hydroxyindoleacetaldehyde	Tryptophan metabolism	3.80	3.39	2.15
Glycyl-valine; *N*-acetylornithine	Peptide; others (arginine biosynthesis)	3.28	3.35	2.05
Heptanoylglycine	Acylglycine	3.60	3.30	3.23
Hydroxybutyrylcarnitine	Acylcarnitine	2.97	3.29	2.82
3-Methylglutarylcarnitine	Acylcarnitine	3.85	3.28	2.94
Pyridoxolactone; formylanthranilic acid	Tryptophan metabolism	3.88	3.25	1.90
Argininic acid; citrulline	Biosynthesis of arginine	3.91	3.19	0.50
Aspartyl-tryptophan	Peptides	4.07	3.17	2.34

NDM indicates that the metabolite was not identified in LB.

and some tryptophan metabolism products were identified. Further statistical analyses revealed that only five features were significantly changed between the MG1655 wild-type and AcrB D408A mutant (P<0.05), two of which were unidentified (Table 5.2). The feature that had the greatest change between the wild- type and the AcrB D408A mutant had multiple putative identities, but was most likely to be a fatty acid/alcohol or an aromatic compound.

5.9.2 RNA-seq

Metabolomics studies are often complemented with RNA-seq, as changes in transcription of metabolic genes often lead to changes in the metabolome. To complement the metabolomics study, differential gene transcription analysis was carried out with RNA extracted from stationary phase cultures of *S.* Typhimurium and *E. coli* wild-type and AcrB D408A mutant in LB. Unfortunately, good quality RNA could not be extracted from 18-hour cultures (late stationary phase); therefore, 10-hour cultures were used (early stationary phase).

Very few significant differential changes were observed in both species. In *S.* Typhimurium, most changes occurred in regulatory small or non-coding RNAs, such as the carbon storage regulator CsrB, the flavin mononucleotide (FMN) riboswitch and the SsrA tmRNA, which were significantly overexpressed in the AcrB D408A mutant. *Salmonella* Pathogenicity Islands (SPI) 1, 2, 4 and 11, StyR-44 sRNAs, as well as multiple rRNAs and repeat regions of unknown function were significantly downregulated in the mutant (Figure 5.9).

In accordance with the metabolomics results, where fewer significantly changed features were found for *E. coli* than for *S.* Typhimurium, fewer differentially transcribed genes were observed in the *E. coli* AcrB D408A mutant when compared against

Table 5.2 List of metabolites identified in abundance in the ExM of *E. coli* MG1655 relative to the AcrB D408A mutant.

Metabolite putative ID	Classification of metabolite	Fold-change AcrB D408A/MG1655	*P*-value
1,3-Diphenyl-1-propanone; 1,3-Diphenyl-2-propanone; p-methoxystilbene; ethyl -Decatrienoate	Fatty acids/alcohols; aromatic compounds	0.0029686	0.036145
Ginsenoyne A linoleate	Unknown (not a bacterial metabolite, eukaryotic membrane fatty acid)	0.083557	0.025242
L-alpha-glutamyl-L-hydroxyproline; Lauric acid(d3); n-decanohydroxamic acid	Others (glutamine metabolism); fatty acids/alcohols	0.10652	0.012811
Unidentified	Unknown	0.10876	0.021636
Arginyl-Isoleucine;Arginyl-Leucine;Isoleucyl-Arginine;Leucyl-Arginine; N5-Hexanoylspermidine	Peptide; others (polyamine derivative)	0.19288	0.0086543

Figure 5.9 Transcriptional landscape of a *S.* Typhimurium SL1344 AcrB D408A mutant in early stationary phase in LB.

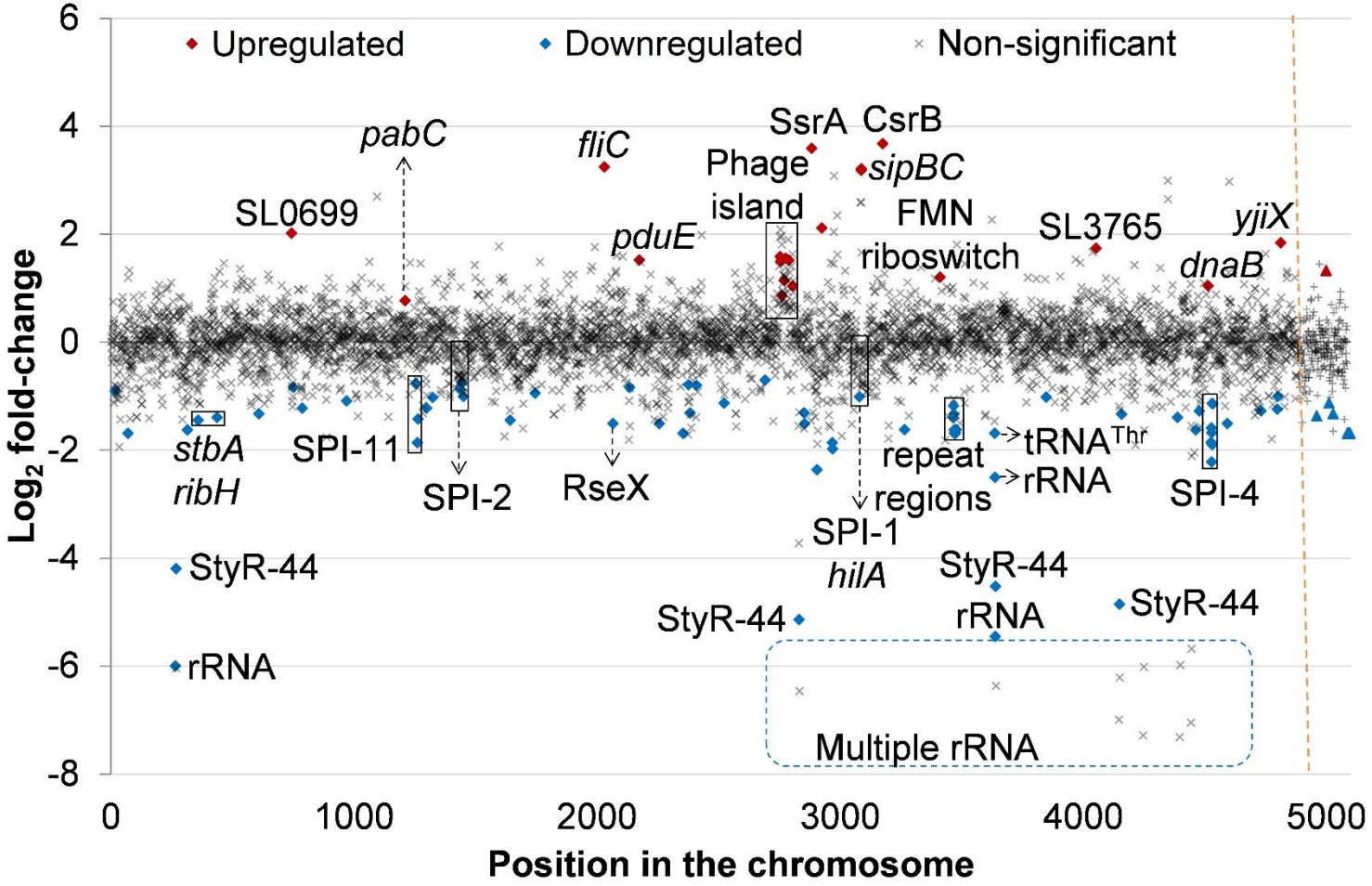

Transcriptome of the mutant was compared to parental SL1344. Significantly upregulated genes in the mutant are marked in red and significantly downregulated genes are marked in blue. Black crosses denote genes with no significant changes between the two strains. The orange dotted line indicates the end of the chromosomal genes and start of the plasmid genes.

S. Typhimurium (32 and 109 genes, respectively). Among the upregulated genes in the *E. coli* AcrB D408A mutant were *tisB* and *hipB* from toxin-antitoxin modules; *ibpAB*, *dnaK* and *grpE*, which encode heat shock proteins, and the regulatory sRNA DsrA. Interestingly, all the downregulated genes were involved in metabolic processes, except for a repeat region of unknown function (Figure 5.10).

RNA-seq data was validated by qRT-PCR. Up and downregulated genes were randomly selected and their number of transcripts was determined by qRT-PCR. For data normalisation, *gyrB* and 16S were used as housekeeping genes for *E. coli*. However, 16S could not be used for *S.* Typhimurium due to the general decrease in expression of rRNAs as shown in the transcriptome of the AcrB D408A mutant (Figure 5.9). Therefore, *rho* and *gyrB* were used as housekeeping genes for *S.* Typhimurium as these housekeeping genes had been validated by others in previous studies (Rocha *et al*., 2015) and non-significant transcription changes were observed for these genes in RNA-seq. A positive correlation between RNA-seq and qRT-PCR datasets, with a R^2>0.9, was observed for both species (Figure 5.11A,B).

Differentially transcribed genes in *S.* Typhimurium and *E. coli* were assigned to their respective COG groups. COGs of the two species were compared against each other to find a common signature of loss of AcrB-mediated efflux. Only two COG classes had the same pattern in both microorganisms: “Energy production and conversion”, and “Carbohydrate transport and metabolism” (Figure 5.12).

Figure 5.10 Transcriptional landscape of a *E. coli* MG1655 AcrB D408A mutant in early stationary phase in LB.

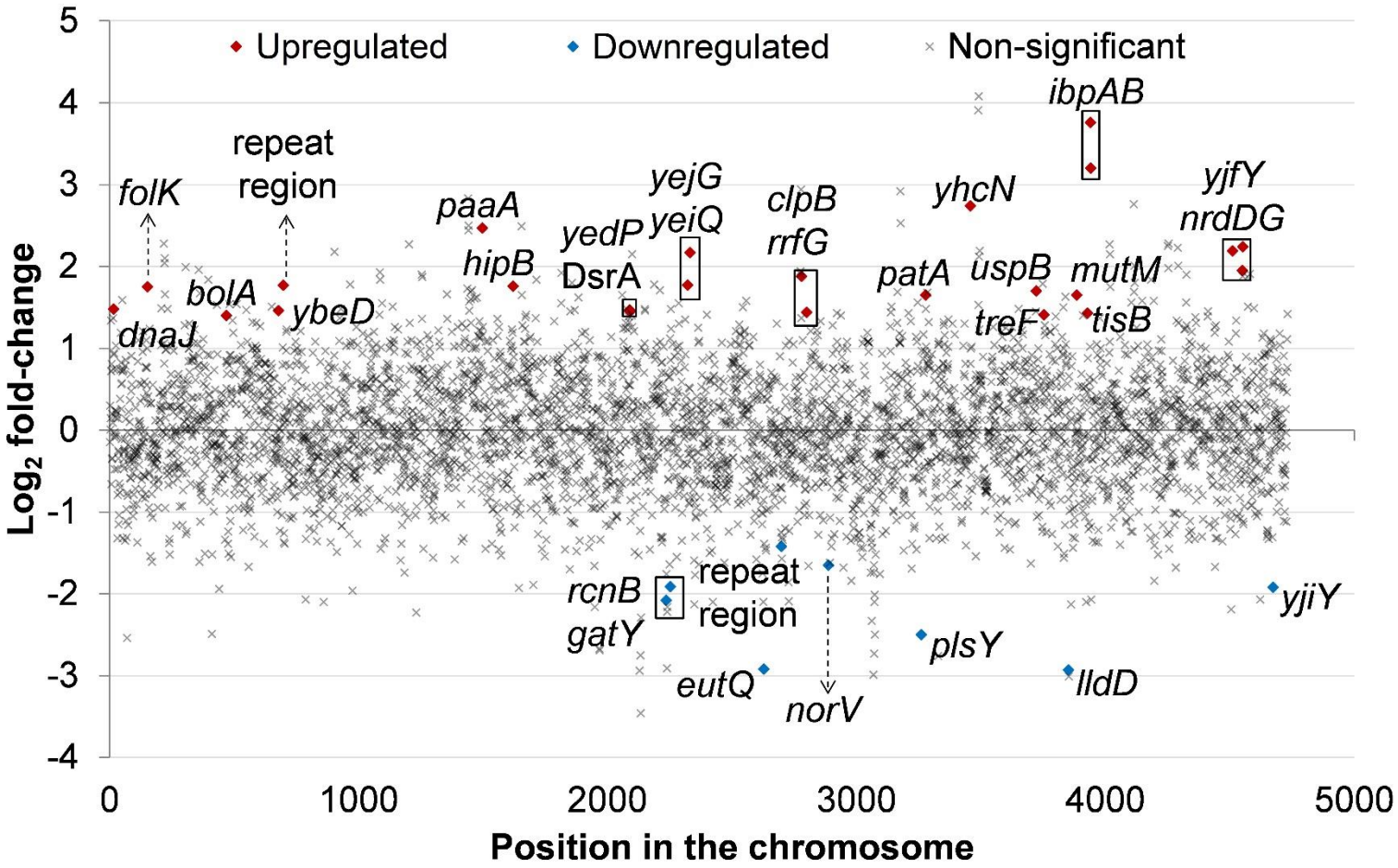

Transcriptome of the mutant was compared to parental SL1344. Significantly upregulated genes in the mutant are marked in red and significantly downregulated genes are marked in blue. Black crosses denote genes with no significant changes between the two strains.

Figure 5.11 Validation of RNA-seq results by qRT-PCR in *S.* Typhimurium SL1344 and *E. coli* MG1655.

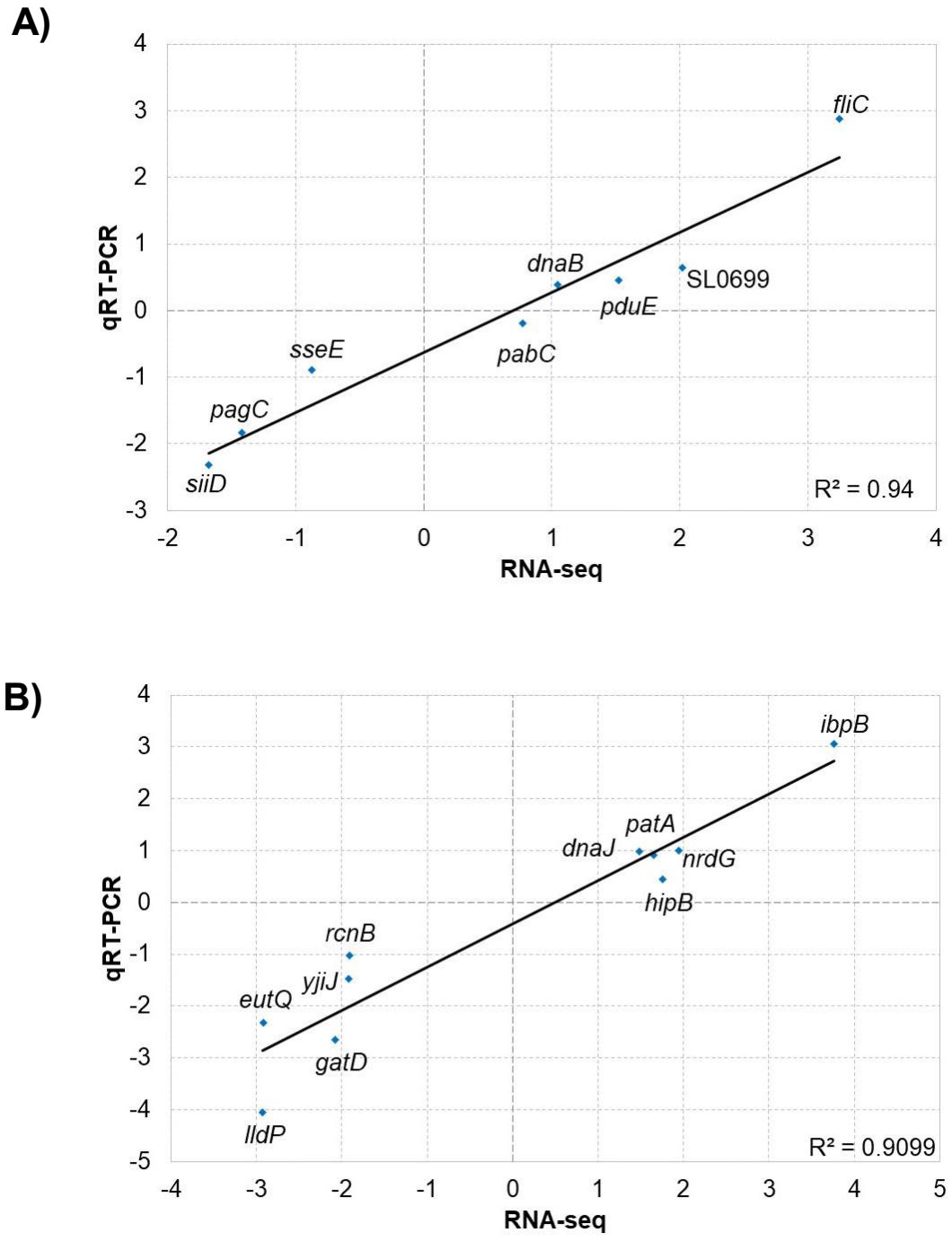

Log_2 fold-change in gene transcription between the AcrB D408A mutant and the wild-type A) *S.* Typhimurium SL1344 and B) *E. coli* MG1655 are shown. Gene transcription was measured by RNA-seq and qRT-PCR and correlation between the two datasets was determined by lineal regression, shown as a black line.

Figure 5.12 Comparison of COGs between an *S.* Typhimurium SL1344 and an *E. coli* MG1655 AcrB D408A mutant.

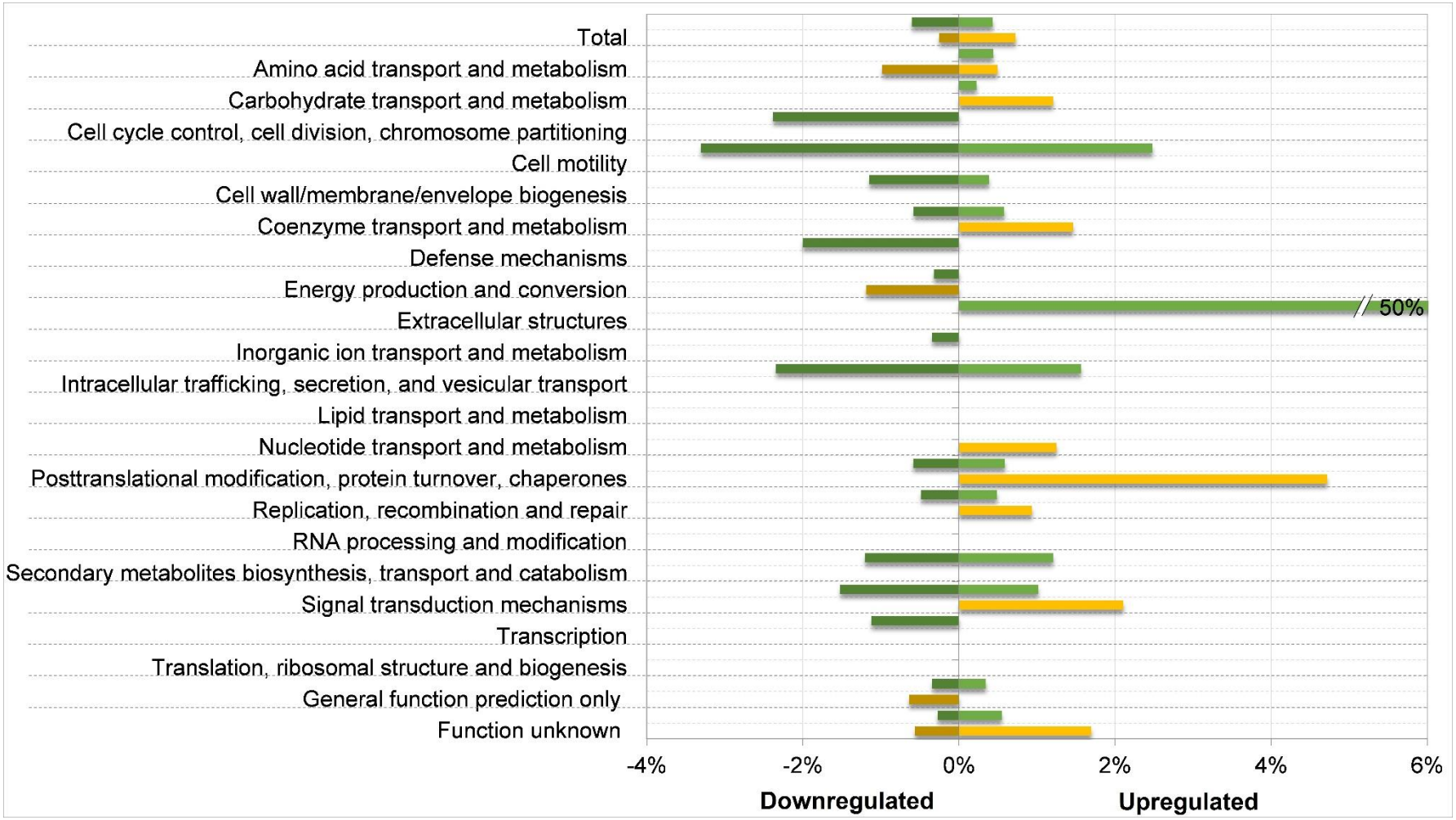

COG classes are shown on the left side of the chart, the total number of genes in this class are indicated in brackets. Green bars show results for *S.* Typhimurium SL1344, yellow bars indicate results for *E. coli* MG1655. Percentage of downregulated genes in each class are shown in dark-coloured bars, whereas percentage of upregulated genes are shown in light-coloured bars.

5.10 Discussion

The AcrAB-TolC MDR efflux system is well-known for its role in export of antibiotics and other xenobiotics, such as detergents, dyes and bile (Ma *et al*., 1993, Ma *et al*., 1995, Lacroix *et al*., 1996, Nishino and Yamaguchi, 2001, Nikaido, 2009). This system is constitutively expressed and its expression is increased when bacteria are exposed to substrates of the pump; however, the constitutive expression of AcrB is very high in comparison to other RND pumps (Nishino *et al*., 2009). A hypothesis for the high basal expression of AcrB is that the pump has a general physiological role, such as exporting toxic metabolic by-products (Ruiz and Levy, 2014). Additionally, in *S.* Typhimurium and multiple other microorganisms, deletion of *acrB* or chemical inhibition of AcrB efflux causes attenuation of virulence (Lacroix *et al*., 1996, Hirakata *et al*., 2002, Buckley *et al*., 2006, Bina *et al*., 2008, Padilla *et al*., 2010, Perez *et al*., 2012, Spaniol *et al*., 2015, Alcalde-Rico *et al*., 2016). In the previous chapter, it was discussed that the loss of virulence could be a consequence of a general metabolic shift caused by intracellular accumulation of toxic metabolites. An alternative hypothesis was that AcrB exported a virulence factor or a signalling molecule required for virulence.

To determine if AcrB exported molecules involved in the virulence of *S.* Typhimurium, Blair (2010) added cell-free culture supernatant (exometabolome or ExM) from overnight cultures of wild-type SL1344 in LB to a Δ*acrB* mutant. Addition of the ExM significantly increased virulence of the Δ*acrB* mutant. In accordance with the hypothesis that AcrB effluxes a virulence factor/regulator, addition of ExM from the Δ*acrB* mutant grown under the same conditions as SL1344 did not restore virulence to the mutant, indicating that a molecule(s) effluxed by AcrB was required for virulence. Further experiments showed that the maximum virulence-restoration effect was observed when SL1344 ExM was concentrated three times (Appendix VI, Figure A).

It is worth noting that the virulence-restoration activity of ExM was highly variable, with some batches of ExM having higher virulence-restoration activity than others. This was attributed to changes in the composition of the LB medium, used in the production of ExM. LB is composed of tryptone, NaCl and yeast extract (Bertani, 1951). The exact composition of tryptone and yeast extract has not been fully defined and there is variation in the concentration of the known compounds in between batches (Grant and Pramer, 1962, Rayner *et al*., 1990, Merck, 2018, Solabia Group Biotech, 2018). This variation between batches of LB medium could account for variations in biological activity of the ExM. To reduce variation, a chemically defined medium was required. As the exact composition of LB is unknown, the medium cannot be reproduced synthetically. Therefore, commercially available synthetic media, MOPS and EZ, were tested. MOPS minimal medium could not be used as ExM produced from this medium did not restore virulence of a Δ*acrB* mutant. This was attributed to the low availability of nutrients in the medium; thus, a synthetic rich medium, EZ, was then tested. This medium contains a mixture of amino acids, nucleotides, salts and vitamins B_5 (panthotenate) and B_1 (thiamine) (Appendix I, section G). SL1344 ExM produced from EZ did not restore virulence of the Δ*acrB* mutant to the same extent as ExM produced from LB, suggesting that one or more components of LB is essential for the synthesis of the virulence-restoring molecule(s). An early study showed that LB medium is rich in amino acids and cyclic nucleotides, but also contains phospholipids, polyphosphate and sugar monophosphate esters (Rayner *et al*., 1990); which are not present in chemically defined media. Furthermore, the chemically defined media tested also lack aluminium, barium, cadmium and other trace elements found in yeast extract (Grant and Pramer, 1962), as well as multiple vitamins (Solabia Group Biotech, 2018). It is likely that synthesis of the AcrB-exported virulence molecule(s) is dependent on a

vitamin or a trace element that is absent in synthetic media, as these nutrients are essential cofactors of multiple enzymes involved in a variety of metabolic pathways (Garcia-Angulo, 2017, Fitzpatrick *et al*., 2007).

During experiments with ExM, it was observed that liquid ExM stored at 4°C lost its restorative effect within 2 hours and freeze-dried ExM lost its biological effect within a month, suggesting that the molecule(s) is unstable. However, ExM boiled for 10 minutes at 95°C or heated at 70°C for one hour did not lose its biological effect, indicating that the molecule(s) is heat resistant (Blair, 2010, Appendix VI, Figure D). Additionally, ExM filtered through a 5kDa filter retained its activity, indicating that the molecule(s) is unlikely to be a protein (Appendix VI, Figure D). However, treatment of ExM with proteinase K caused partial loss of activity, suggesting that 1) a molecule with peptide bonds is involved in virulence-restoration and 2) the biological effect of ExM may be produced by a mixture of molecules. To further aid the identification of the virulence-restoring molecules, SL1344 was chemically fractioned using the HP-20 resin, which adsorbs hydrophobic compounds. After incubation in SL1344 ExM, the resin was washed with acetone, methanol and water to recover compounds that were adsorbed. Acetone has a lower polarity index than methanol and water (Reichardt and Welton, 2010); therefore, it was used to recover predominantly non-polar compounds, but some semi-polar compounds might be recovered as well. Methanol was used to recover predominantly semi-polar compounds and water was used to extract polar compounds adsorbed by the resin. Each of the individual fractions restored virulence of the Δ*acrB* mutant, but none of the fractions restored virulence to the same extent as the unfractioned ExM; further supporting the hypothesis that a mixture of compounds exported by AcrB is responsible for the restoration of virulence in the Δ*acrB* mutant. Fractionation of SL1344 ExM was previously attempted; hexane,

chloroform, methanol and a residual hydrophilic fraction were tested for virulence restoration activity (Appendix VI, Figure F). The hexane and chloroform fractions did not show any biological activity, whereas the methanol fraction partially restored virulence of a Δ*acrB* mutant and the residual hydrophilic fraction restored virulence of the mutant to the same extent as the unfractioned ExM. This experiment indicates that the virulence-restoring factors are predominantly polar and semi-polar compounds. In the present study, the acetone and the residual hydrophilic fractions had the highest restoration activity. Although acetone was used to extract non-polar compounds, the solvent is highly polar when compared to hexane and chloroform (Reichardt and Welton, 2010); thus, it is likely that semi-polar compounds were present in the acetone fraction, which could include some of the virulence-restoring compounds.

All previous experiments were carried out in a SL1344 Δ*acrB* mutant, which overexpresses other RND pumps to compensate for the loss of the AcrB protein (Eaves *et al*., 2004, Blair *et al*., 2015b). In the Δ*acrB* model, it was unclear whether the virulence-restoration effect was related to overexpression of additional RND pumps; therefore, experiments were carried out with an isogenic AcrB D408A mutant and compared against the Δ*acrB* mutant. Both *acrB* mutants had the same phenotype in infection of INT-407 and Caco2 intestinal epithelial cells in the presence and absence of ExM. The virulence-restoring effect of the SL1344 ExM was better observed in Caco2 polarised epithelial cells than in INT-407 cells (~50% vs. 8-13%, respectively). However, as discussed in the previous chapter, basal invasion levels of the *acrB* mutants was higher in polarised than in non-polarised cells, which could account for the difference in restoration of virulence of the SL1344 ExM. This experiment indicates that the restoration of virulence in the Δ*acrB* mutant is independent of the overexpression of *acrD* and *acrF*, which correlates with previous

work indicating that these pumps are not involved in virulence in *S.* Typhimurium (Nishino *et al*., 2006, Buckner *et al*., 2016).

When compared against the mutants without exposure to ExM, ExM obtained from the *acrB* mutants slightly increased invasion of the mutants, but the difference was not statistically significant. This experiment provides evidence that a virulence factor or a virulence-signalling molecule is exported by AcrB in *S.* Typhimurium.

The virulence-restoration effect was best observed in ExM harvested from an overnight culture of SL1344, which corresponds to late stationary phase in the growth curve of SL1344. ExM harvested from late logarithmic phase did not significantly restore virulence of the AcrB D408A mutant, suggesting that the virulence-restoring molecules are not produced at a high enough concentration in the logarithmic phase to induce a significant increase in invasion. Additionally, when the virulence-restoration activity of ExM was plotted against its time of collection, a positive correlation was observed, indicating that the virulence-restoring effect of ExM increased as the culture became ‘older’. This observation led to two hypotheses: 1) virulence-restoring factors derive from primary metabolism (generated as part of normal bacterial growth (Kumar, 2018)) and are accumulated in ExM over time or 2) a second virulence-restoring molecule is produced at later time points, which enhance the effect of the first one. Secondary metabolites, such as antibiotics, are produced by microorganisms in late stationary phase, when nutrients are scarce and cell density is high (Mehta *et al*., 2018). They are hypothesised to confer an ecological advantage by killing other microorganisms to reduce competition and generate more nutrients. Secondary metabolites also serve as signalling molecules and virulence regulators. For example, the aromatic alcohols farnesol and tyrosol control multiple biological processes in *Candida albicans*; farnesol was also associated with pathogenesis as it increases

resistance of *Candida albicans* towards reactive oxygen species (Dufour and Rao, 2011). Similarly, aureusimines and phevalins, peptides derived from secondary metabolism, are used by *Staphylococcus aureus* to regulate expression of virulence factors and modulate survival in host cells (Wyatt *et al*., 2010, Blättner *et al*., 2016). The two hypotheses are not mutually exclusive and the virulence-restoration effect observed with 18 hours SL1344 ExM could be a combination of a primary metabolite that accumulated over time and a secondary metabolite.

Previous experiments showed that SL1344 ExM could not restore virulence to a Δ*acrB* mutant in murine macrophages (Appendix VI, Figure E). While reproducing this experiment in J774A.1 murine macrophages, a considerable disruption of the monolayer was observed at 2 hours post-infection. The disruption was only observed on monolayers exposed to ExM either from SL1344 or the AcrB D408A mutant, it was not observed in macrophages exposed to LB broth. Therefore, it was concluded that the disruption of the monolayer was not caused by uptake and replication of *S*. Typhimurium in the macrophages, but by a factor in ExM that was produced independently of AcrB efflux activity. The identity and chemical nature of the macrophage-killing molecule is unknown. It has been speculated that *S.* Typhimurium might synthesise a toxin similar to the *S.* Typhi typhoidal toxin, which kills leukocytes at high concentrations (Song *et al*., 2013, Chong *et al*., 2017). Therefore, the virulence-restoring effect of SL1344 ExM could not be studied in macrophages due to the presence of an AcrB-independent macrophage-killing secreted factor in *S.* Typhimurium.

To identify the virulence-restoring molecules exported by AcrB, untargeted metabolomics by LC-MS was carried out. Fifty-four metabolites were found in abundance in the SL1344 ExM when compared against its *acrB* mutants. Most of

these metabolites were tryptophan degradation products, fatty acids and fatty alcohols, acylcarnitines and peptides. A large number of biological signalling molecules derive from tryptophan metabolism; for example, indole attenuates virulence of *S.* Typhimurium, although *S. enterica* cannot synthesise it (Nikaido *et al*., 2012, Kohli *et al*., 2018). Other examples are quinolones, such as the *Pseudomonas* spp. PQS signal, which regulates virulence in *P. aeruginosa* and a precursor of which is exported by an RND efflux pump (Lamarche and Déziel, 2011). Interestingly, *S.* Typhimurium has a natural tropism towards tumours (Pawelek *et al*., 1997), which overproduce kynurenine, a tryptophan degradation product that attenuates the immune system (Brandacher *et al*., 2006, Kuan and Lee, 2016). It is suggested that *S.* Typhimurium is attracted towards tumours because it finds a favourable, nutrient-rich environment in which to proliferate hidden from the immune system (Leschner *et al*., 2009). It is possible that *S.* Typhimurium is attracted towards tumours by the abundance of kynurenine, which was also found in excess in the SL1344 ExM. Therefore, it is hypothesised that kynurenine and other metabolites derived from tryptophan metabolism are involved in virulence-restoration of the AcrB D408A mutant. It is further hypothesised that any tryptophan degradation product is more likely to act as a signalling molecule than a virulence factor as no evidence was found in the literature of tryptophan degradation products acting as virulence factors (Figure 5.13).

Fatty acids/alcohols and acylcarnitines may also be involved in virulence restoration. A previous study demonstrated that fatty acids are exported by AcrB in *E. coli*

Figure 5.13 Summary of metabolites in the SL1344 ExM that could contribute towards virulence-restoration in an AcrB D408A mutant.

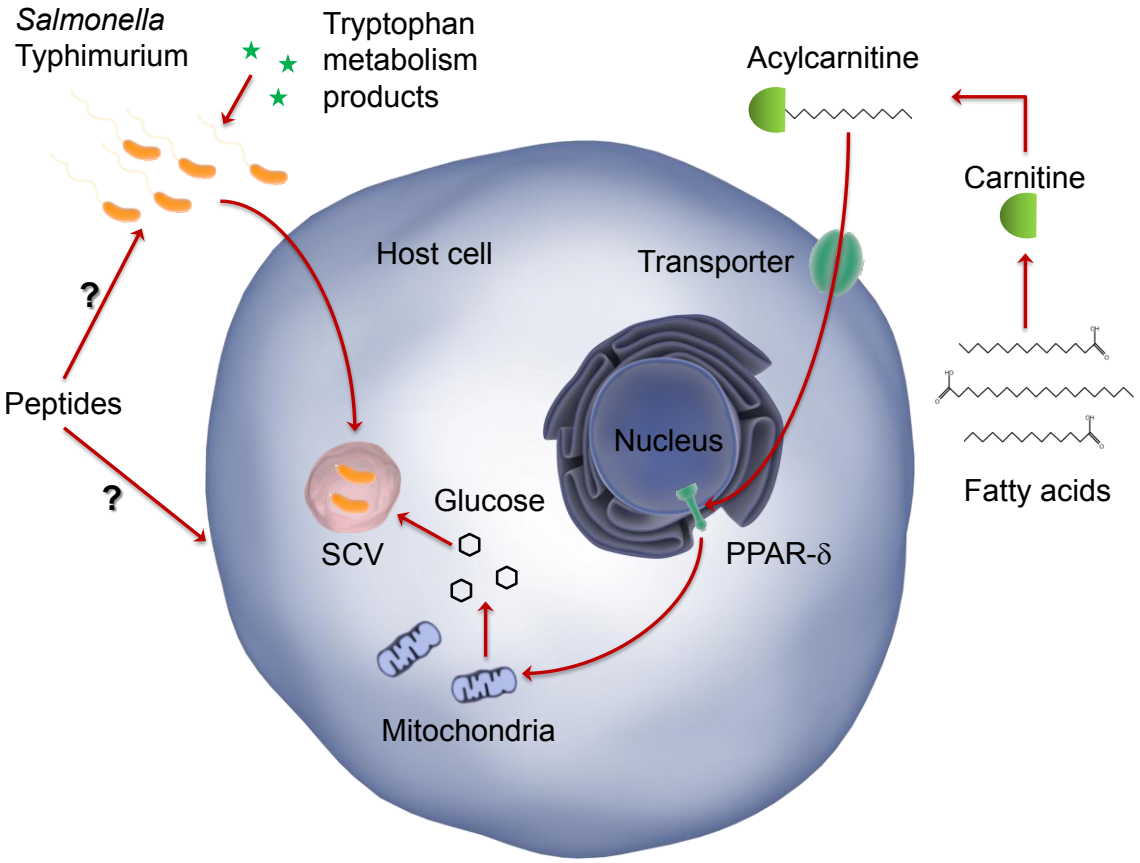

S. Typhimurium (orange) infects the host cell (blue) and survives inside SCVs (red). It is hypothesised that intracellular survival of *S.* Typhimurium is favoured by addition of exogenous fatty acids. Fatty acids interact with carnitines to form acylcarnitines, which are transported inside the host cell and detected by PPAR-δ. Activation of PPAR-δ increases mitochondrial activity, which results in fatty acid oxidation and an increased production of glucose. The increased intracellular glucose availability favours replication of *S.* Typhimurium in the SCV. It is also hypothesised that a signalling molecule derived from tryptophan metabolism increases invasion of *S.* Typhimurium into the host cell. Vitamins and peptides are likely to be involved in virulence, but their contribution is unclear. Figure was constructed with elements from the Library of Science and Medical Illustrations.

(Lennen *et al*., 2013). A direct correlation between *Salmonella*-derived fatty acids and virulence has not been established. However, there is evidence that the host fatty acid regulator PPAR-δ (peroxisome proliferator-activated receptor δ) is required for the intracellular maintenance of *S.* Typhimurium (Eisele *et al*., 2013). PPAR-δ is a receptor found in the nucleus of mammalian cells, this receptor responds to intracellular availability of fatty acids and increases fatty acid oxidation in mitochondria, accordingly (Ravnskjaer *et al*., 2010). Activation of PPAR-δ also increases intracellular availability of glucose, which favours replication and survival of *S.* Typhimurium in the *Salmonella*-containing vacuole (SCV) in macrophages (Eisele *et al*., 2013). This has not been shown in intestinal epithelial cells; however, PPAR-δ is present in all cells and *S.* Typhimurium can only replicate once inside a SCV. Thus, it is hypothesised that fatty acids present in the ExM of SL1344 interact with PPAR-δ, favouring intracellular survival of AcrB mutants. However, fatty acids cannot easily traverse the membrane; hence, they are attached to a carnitine and delivered into the host cell to increase the intracellular concentration of fatty acids that will consequently activate PPAR-δ (Figure 5.13). To test this hypothesis in gentamicin protection assays, a Δ*Pparδ* intestinal epithelial cell line is needed; however, no cell lines with the required characteristics were found. A murine infection model could be used to indirectly test the hypothesis, as previous experiments were carried out in *Pparδ* $^{-/-}$ 129/SvImJ mice (Eisele *et al*., 2013). If the hypothesis is correct and fatty acids and acylcarnitines exported by AcrB are required for virulence, the AcrB D408A mutant would not be attenuated in a *Pparδ* $^{-/-}$ mouse. The hypothesis could also be tested in bone marrow derived macrophages obtained from *Pparδ* $^{-/-}$ mouse, where the same results would be expected.

Accumulation of fatty acids/alcohols seems to be a common characteristic of inactivation of AcrB. When compared against their respective wild-type strains, there were fewer fatty acids/alcohols in the ExM *S.* Typhimurium and *E. coli* AcrB D408A mutants. This observation is supported by RNA-seq data. For example, the CsrB ncRNA was overexpressed in *S.* Typhimurium. This ncRNA inhibits CsrA (Suzuki *et al*., 2002), which is involved in activation of glycolysis and inactivation of gluconeogenesis (Romeo, 1998). Overexpression of CsrB in the *S.* Typhimurium AcrB D408A mutant suggested that CsrA was less active in the mutant. Hence, glycolysis was likely to be decreased and usage of alternative carbon sources, such as fatty acids, would be required. In accordance with this observation, *pduE*, which encodes a protein essential for propanediol degradation (Uniprot Consortium, 2014), was upregulated, suggesting that fatty alcohols were being used. This supports the hypothesis of fatty acids accumulating intracellularly in the absence of AcrB-mediated efflux. In *E.* coli, genes involved in utilisation of carbon sources like tagatose (*rcnB*) and lactate (*lldP*) (Uniprot Consortium, 2014) and phospholipid biosynthesis (*plsY*) (Yoshimura *et al*., 2007) were significantly downregulated, which may also be linked to accumulation of fatty acids in the AcrB D408A mutant. If fatty acids were used as carbon sources and to make membrane lipids, then utilisation of alternative carbon sources and phospholipid biosynthesis would not be required.

Previous experiments showed that SL1344 ExM treated with proteinase K partially lost its virulence-restoration activity, indicating that a molecule with peptide bonds may be involved in restoration of virulence. Multiple dipeptides were found in relative abundance in the SL1344 ExM. Peptides are likely to be substrates of AcrB as the peptidomimetic compound PAβN binds tightly to AcrB (Yu *et al*., 2005, Sjuts *et al*., 2016); however, the role of peptides in virulence of *S*. Typhimurium is unknown. The

biological function of peptides has been described for other species. For example, in Gram-positive bacteria, peptides are quorum sensing signalling molecules (Whiteley *et al*., 2017), in *S. aureus*, dipeptides contribute towards survival of the bacterium in host cells and regulate expression of virulence factors (Wyatt *et al*., 2010, Blättner *et al*., 2016); additionally, cyclic dipeptides produced by *P.* aeruginosa have a cytotoxic effect (Vázquez-Rivera *et al*., 2015). Therefore, it is hypothesised that dipeptides exported by AcrB have a role in pathogenesis of *S.* Typhimurium. Further studies are required to explore this hypothesis and determine their role (if any) in virulence-restoration of the AcrB D408A mutant.

The role of AcrB in export of native bacterial metabolites was further studied in *E. coli* by analysing the composition of the ExM of the wild-type MG1655 and its isogenic AcrB D408A mutant. Initial screening of raw data revealed 19 features; however, annotation of the features proved challenging and multiple features were misannotated. Although the annotation was incorrect, the structure of the compounds resembled that of xenobiotics exported by AcrB; for example, some metabolites were annotated as cucujolides, these are macrolide lactones derived from fatty acids and are used as pheromones by beetles and frogs (Hotling *et al*., 2014). Macrolide antibiotics, such as erythromycin and azithromycin, are substrates of AcrB (Chollet *et al*., 2004) and hence, cucujolides could be substrates of AcrB.

Surprisingly, only five metabolites were found in a significantly lower concentration in the *E. coli* AcrB D408A mutant relative to its parental strain; this is approximately 10% of what was observed in *S.* Typhimurium. Similarly, fewer genes were differentially transcribed in the *E. coli* AcrB D408A mutant when compared against the *S.* Typhimurium mutant. These data either suggest that many of the metabolites were involved in virulence (or other *Salmonella*-specific traits) or that AcrB might not be as

essential in export of metabolites in *E. coli* as it is in *S.* Typhimurium. It is noted that *E. coli* has more RND and ABC transporters than *S.* Typhimurium (Elbourne *et al*., 2017), which could export some of the substrates exported by AcrB in *Salmonella*.

The metabolites found in *E. coli* were predominantly fatty acids, aromatic compounds, a peptide and an unidentified molecule. This correlates with upregulation of *paaA*, which is involved in degradation of aromatic compounds (Uniprot Consortium, 2014). In contrast to *S.* Typhimurium, acylcarnitines and tryptophan metabolism products were not significantly changed between the wild-type and the mutant *E. coli*. This could be due to differences in metabolism between *E. coli* and *S.* Typhimurium as the latter might synthesise more of these metabolites. Although *S.* Typhimurium and *E. coli* are phylogenetically related, their metabolism is very different, including the production of indole, which *E. coli* synthesises but *S.* Typhimurium does not (Sargo *et al*., 2015). Even metabolic pathways that have conserved genes in both microorganisms seem to act in different ways and depend on the species. For example, the toxic metabolite 2-aminoacrylate is processed by *E. coli* via RidA pathway, which is conserved between *E. coli* and *Salmonella*. However, exogenous addition of 2-aminoacrylate to a *ridA* mutant had different effects, suggesting that the compound is detoxified in different ways depending on the species (Borchert and Downs, 2017)

It is also likely that acylcarnitines and tryptophan metabolism products are important for virulence of *S.* Typhimurium. *E. coli* K-12 MG1655 is a non-virulent laboratory strain; therefore, it may be expected that its ExM would not contain virulence-restoring factors. To test this hypothesis, ExM from *E. coli* should be added to the *S.* Typhimurium SL1344 AcrB D408A mutant in a gentamicin protection assay.

To corroborate the metabolomics findings, RNA-seq was carried out. Due to the late growth phase at which RNA was harvested, not many significant differences in gene transcription was observed between the *E. coli* and *S.* Typhimurium wild-type and mutant strains (Hazen *et al*., 2015). Multiple genes involved in stress responses were upregulated in both *S.* Typhimurium and *E. coli* AcrB D408A mutants. In *E. coli*, *ibpA*, *ibpB*, *dnaJ* and *grpE* encoding heat shock proteins; *tisB* toxin and *hipB* antitoxin, the *bolA* general stress response transcriptional regulator (Uniprot Consortium, 2014) and the DsrA stress regulator (Seo *et al*., 2017) were upregulated. In *S.* Typhimurium, increased transcription of *dnaB* involved in DNA replication, and *yjiX* involved in DNA damage response (Uniprot Consortium, 2014), suggest a degree of DNA damage in the AcrB D408A mutant.

Interestingly, in *S.* Typhimurium, rRNAs were significantly underexpressed in the AcrB D408A mutant, suggesting that protein synthesis might be reduced. This was accompanied by underexpression of multiple StyR-44 ncRNAs. StyR-44 is found in all rRNA operons, upstream of the 23S rRNA in *S.* Typhi (Chinni *et al*., 2010). No biological activity has been attributed to StyR-44 and it is suggested to be an "RNA intermediate formed during maturation of rRNA" (Chinni *et al*., 2010). It is hypothesised that this may be a mechanism of stress response as decreased expression of proteins may lead to slower growth rates and dormancy, which may help *S.* Typhimurium reduce any potential damage caused by accumulation of toxic metabolites in the AcrB D408A mutant.

Differential gene transcription also hints towards changes in the synthesis of vitamins. For example, in *S.* Typhimurium increased transcription of *pabC* may suggest changes in synthesis of folic acid (vitamin B_9). Folic acid is transformed into tetrahydropholate and used as a cofactor in multiple biosynthetic pathways. Interestingly, *folK*, a gene

involved in biosynthesis of tetrahydropholate was upregulated in the *E. coli* AcrB D408A mutant, suggesting that the mutant might overproduce tetrahydropholate. These observations suggest that loss of AcrB-mediated efflux may cause an increase in the synthesis of folic acid or a derivative. It is hypothesised that this is related to an increase in transcription of genes involved in general stress responses, as tetrahydropholate is used in the synthesis of nucleic acids and amino acids that are required to fix damaged DNA and synthesise new proteins.

Synthesis of riboflavin or vitamin B_2 is likely to be decreased in the *S.* Typhimurium AcrB D408A mutant as *ribH*, involved biosynthesis of riboflavin (Uniprot Consortium, 2014), is downregulated. This observation is in accordance with the overexpression of the FMN riboswitch, which inhibits synthesis of riboflavin in abundance of intracellular flavin mononucleotide (FMN) (Pedrolli *et al*., 2015).

Vitamins have their specialised transporters in bacteria; however, it is possible that AcrB exports precursors or vitamins under certain circumstances. For example, a recent study showed that the AcrAB-TolC complex in *Bacteroides vulgatus* is involved in export of retinol (vitamin A_1) (Hibberd *et al*., 2017). However, changes in export and synthesis of vitamins are also likely to be a consequence of the metabolic changes induced by loss of AcrB efflux function. Thus no conclusions can be drawn until more evidence is obtained.

Precursors of vitamin B_5 and B_6, but not B_2 and B_9, were found in abundance in the SL1344 ExM. It is important to note that RNA-seq was carried out with early stationary phase cultures; whereas ExM was obtained from late stationary phase cultures, which might account for some of the differences between the exometabolome and the transcriptome of the AcrB D408A mutant. Additionally, changes in the transcription of

genes do not always translate into altered protein expression, since post-transcriptional regulation that impacts the expression of proteins is not accounted for in RNA-seq.

For future experiments involving late stationary phase cultures, proteomics is recommended instead of transcriptomics as proteins are more stable than RNA and may better reflect the metabolomic data.

Comparison of differentially transcribed genes grouped into COG classes revealed that only carbohydrate transport and metabolism and energy production and conversion were equally affected by loss of AcrB efflux in both *E. coli* and *S.* Typhimurium. These changes are likely associated with the intracellular accumulation of fatty acids in the mutants. Fatty acids are used as carbon source by β-oxidation; therefore, they are likely to affect carbon metabolism and energy production, consequently.

5.11 Key findings

- An AcrB-independent macrophage-killing molecule is excreted by *S.* Typhimurium.
- Multiple metabolites may be involved in restoration of virulence of a *S.* Typhimurium AcrB D408A mutant. Tryptophan metabolism products, fatty acids, acylcarnitines and peptides are the most likely metabolites involved in virulence-restoration.
- Loss of AcrB efflux function causes increased transcription of general stress responses in *S.* Typhimurium and *E. coli*.
- Loss of AcrB-mediated efflux function has a greater metabolic burden in *S.* Typhimurium than in *E. coli*.

- Fatty acids and alcohols are native substrates of AcrB in *E. coli* and *S.* Typhimurium. Inactivation of AcrB may cause intracellular accumulation of these, which may result in changes in carbohydrate utilisation and energy production.
- Function of AcrB is likely to affect synthesis of vitamin B_9 in *E. coli* and *S.* Typhimurium, and B_2 in *S.* Typhimurium.

5.12 Future work

This study has provided a list of putative metabolites that could be exported by AcrB. The identity of these metabolites needs to be confirmed using untargeted metabolomics with purchased or synthesised standards. This method will also provide an indication of the concentration of each metabolite. Once identified, the metabolites (alone and in combination) should be tested in gentamicin protection assays for virulence-restoration activity on a SL1344 AcrB D408A mutant. To confirm that metabolites are substrates of AcrB, *in silico* simulations should be used. Where possible, simulation results should be confirmed experimentally using a proteoliposome system such as the one described by Verchere *et al*. (2015), where AcrAB is inserted into a liposome and TolC is carried by a biotinilated liposome. Metabolites should be added to the proteoliposome system and the TolC liposome should be recovered and analysed by mass spectrometry for the tested metabolite.

Other experiments include:

- Determine if ExM acts on host cells alone and/or on *S.* Typhimurium alone.
- Assess if ExM harvested from wild-type *E. coli* MG1655 restores the virulence of the *S.* Typhimurium SL1344 AcrB D408A mutant.
- Determine the link between vitamin biosynthesis and AcrB-mediated efflux, as this could be exploited for industrial purposes.

CHAPTER 6.

Overall Discussion and Conclusions

6.1 Overall Discussion and Conclusions

Multidrug resistance (MDR) efflux pumps confer innate and acquired resistance to antibiotics and other chemicals. The main MDR efflux pump in Enterobacteriaceae is AcrB. Inactivation or deletion of *acrB* or its homologues in other Gram-negative bacteria not only increases susceptibility of the bacterium to antibiotics but also attenuates virulence in *S. enterica*, *Neisseria gonorrhoeae*, *Vibrio cholerae*, *Klebsiella pneumoniae*, *Enterobacter cloacae*, *Campylobacter jejuni*, and *Moraxella catharralis* among other Gram-negative bacteria (Lacroix *et al.*, 1996, Jerse *et al.*, 2003, Buckley *et al.*, 2006, Bina *et al.*, 2008, Padilla *et al.*, 2010, Perez *et al.*, 2012, Spaniol *et al.*, 2015, Alcalde-Rico *et al.*, 2016). This suggests that AcrB has a physiological role in virulence. However, the mechanism by which this occurs is unknown. Additionally, whether AcrB has additional biological functions in Gram-negative bacteria is unexplored.

Previous virulence studies have been carried out in gene-deletion and/or gene-inactivation mutants. A major conundrum was whether the observed phenotypes were an effect of loss of AcrB efflux function or an effect of loss of the AcrB protein. To address this question, an AcrB D408A mutant, which expressed the same amount of protein as the wild-type strain but showed no AcrB efflux activity, was constructed in *S.* Typhimurium SL1344 and *E. coli* K-12 MG1655. The AcrB D408A mutants had the same phenotype as an isogenic Δ*acrB* mutant and allowed differentiation of loss of AcrB protein from that of loss of efflux via this protein. Both mutants were hypersusceptible to AcrB substrates and accumulated more H33342 indicating that the D408A substitution in AcrB abolishes AcrB-mediated efflux in *S.* Typhimurium and *E. coli*. Thus, these mutants provide more suitable models to study the biological

effects of inhibition of AcrB efflux function than gene-deletion (or gene-inactivation) mutants, where loss of protein confounds the phenotype.

To understand how AcrB contributed to virulence and which other biological processes are affected by AcrB function in *S.* Typhimurium, the transcriptome of the AcrB D408A mutant was determined. In accordance with the attenuation of virulence observed in the AcrB D408A mutant, SPI genes essential for invasion and survival of *Salmonella* in host cells were transcribed significantly less than in the parental wild-type strain. An interesting observation was that loss of efflux in the AcrB D408A mutant increased transcription of genes involved in nitrate and nitrite respiration from the *nir* and *nap* operons, essential for the survival of *Salmonella* in the inflamed host intestine (Sparacino-Watkins *et al*., 2014, Lopez *et al*., 2015). Increased transcription of these genes had been previously observed in an *acrD*::*aph S.* Typhimurium SL1344 mutant (Buckner *et al*., 2016). In contrast, transcription of these operons was significantly decreased in an *acrB*::*aph* mutant (Webber *et al*., 2009). This discrepancy may be due to the presence of the *aph* gene as discussed in Chapter 4.

Increased nitrate and nitrite respiration and decreased expression of SPI genes suggest that the D408A mutant is more likely to adopt an intestinal lifestyle than an intracellular one. This hypothesis was prompted by a recent study in which a *S.* Typhimurium mutant lacking the *ydi* operon (butyrate utilisation) and carrying a truncated *fepE* gene (Fe^{3+} transport) and the *viaB* locus from *S.* Typhi (capsule) could not cause intestinal inflammation and adopted an intracellular lifestyle (because the mutant was at a disadvantage in the host intestine) (Bronner *et al.*, 2018). Based on this report, it was hypothesised that the increased transcription of genes encoding proteins involved in nitrate and nitrite respiration in the *S.* Typhimurium AcrB D408A mutant favoured survival of the strain in the host intestine. It was further speculated

that this was related to the decrease in transcription of SPI genes as SPI effectors are essential for invasion and intracellular survival, the lack of which could force *Salmonella* to remain and survive in the host intestine.

To explain the decrease in transcription of SPI genes, it was hypothesised that when AcrB was inactivated in *S.* Typhimurium, to ensure the survival of the bacterium, energy from non-essential functions, such as virulence, was translocated to essential functions, such as replication. Additional hypotheses to explain the loss of virulence in the *S.* Typhimurium AcrB D408A mutant were 1) lack of virulence-regulating factors exported by AcrB and 2) a general change in *Salmonella* metabolism caused by intracellular accumulation of metabolites.

To determine if a virulence-regulating factor is exported by AcrB, the exometabolome (ExM) of *S.* Typhimurium *acrB* mutants was compared against that of the parental wild-type strain. From the analysis of the ExM, it was hypothesised that two types of molecules were most likely to be exported by AcrB and affect the virulence of the bacterium. These were 1) signalling molecules to increase virulence of *S.* Typhimurium; most likely a tryptophan degradation product, and 2) metabolites that help intracellular survival of the bacterium, such as acylcarnitines.

To find common substrates of AcrB in Enterobacteriaceae, the AcrB effluxome of the *S.* Typhimurium mutant was compared against that of *E. coli*. Surprisingly, the effluxome of AcrB was different between *E. coli* and *S.* Typhimurium, which suggests that the role of AcrB varies depending on the bacterial species. It is possible that AcrB and its homologues have different natural substrates depending on the species as different bacteria have different metabolism and ecological niches. AcrB has a wide substrate-specificity and is highly conserved between species (Figure 1.5 from

Chapter 1), suggesting that the small differences in protein sequence between species may be a consequence of adaptation to the specific metabolites synthesised by each species.

Interestingly, fatty acids/alcohols were found to be a common group of compounds exported by AcrB in both *S.* Typhimurium and *E. coli*. Fatty acids were previously reported to be substrates of AcrB in *E. coli* (Lennen *et al*., 2013), thus it was hypothesised that inactivation of AcrB caused intracellular accumulation of fatty acids in the AcrB D408A mutants. The hypothesis was further supported by the Metabolic Transformation Algorithm (MTA) analysis, which showed that *fadB*, a gene required for utilisation of fatty acids by β-oxidation, was essential in the maintenance of the metabolic state of the *S.* Typhimurium AcrB D408A mutant. Intracellular accumulation of fatty acids may cause a shift in the metabolism of the bacterium, but loss of translocation of long-chain fatty acids could also impact the composition of the outer membrane. An early study showed that the "envelope" of *S.* Gallinarum is formed of approximately 60% long-chain saturated fatty acids (Cho and Salton, 1966). Recently, it was shown that the overall lipid composition of *Acinetobacter baumannii* is significantly affected upon deletion of genes encoding RND efflux systems and that deletion of the three major RND efflux systems in this species alters the relative proportion of glycerophospholipids found in its membrane (Leus *et al.*, 2018). Another study on *Mycobacterium smegmatis* and *Corynebacterium glutamicum* showed that RND efflux pumps are required for exporting mycolic acid precursors, an important component of the membrane of these bacteria (Varela *et al.*, 2012). Therefore, it is proposed that AcrB may be involved in export of membrane lipids in *S.* Typhimurium and *E. coli* and that loss of export of these lipids changes the proportion of membrane lipids, which may affect the permeability and elasticity of the outer membrane.

Consequently, the drug hyper-susceptibility phenotype observed in *acrB* mutants could be partially caused by the changes in the composition of the outer membrane rather than being completely attributed to retention of higher concentrations of drug within the cell. Similarly, the increased transcription of general stress responses observed in different growth phases in *S.* Typhimurium and in stationary phase in *E. coli* may be caused by the partial loss of outer membrane stability as well as the intracellular accumulation of toxic metabolites.

COG analysis of RNA-seq from stationary phase cultures revealed that energy production was compromised in both *S.* Typhimurium and *E. coli* when AcrB efflux function was abolished. Decreased energy production is associated with slower bacterial growth, which decreases damage caused by antibiotics and other toxic substances (Eng *et al.*, 1991). In accordance with the previous hypothesis, energy production is decreased in the AcrB D408A mutants to minimise further damage caused by accumulation of toxic metabolites.

Decreased energy production and increased transcription of toxin-antitoxin modules in the AcrB D408A mutants also suggested that a larger subpopulation of persister cells is formed when compared to the parental strains. This hypothesis was confirmed in *S.* Typhimurium and is supported by a recent study in which the *acrB* gene was identified to be essential for antibiotic-induced persister formation in *E. coli*, alongside multiple DNA repair genes involved in general stress response (Cui *et al.*, 2018). Persisters allow survival of bacteria under adverse conditions. In the AcrB D408A mutant, it is possible that persisters are formed as a response to the general stress caused by accumulation of metabolites and membrane instability.

There are possible limitations in the data arising from the D408A mutant. The AcrAB-TolC efflux complex assembles spontaneously. However, energy derived from the proton-motive force (PMF) is required for the disassembly of the complex (Bavro *et al.*, 2008, Ntsogo Enguene *et al.*, 2015). Therefore, in the AcrB D408A mutant, where the PMF is abolished, the complex cannot disassemble due to lack of energy. This may limit the availability of TolC, which interacts with other efflux pumps from diverse families. However, this is unlikely to be significant as only ~5% of the total amount of synthesised TolC is required to keep full efflux function in *E. coli* (Krishnamoorthy *et al.*, 2013). Therefore, the limited availability of TolC should not cause pleiotropic phenotypes. Another concern with using the AcrB D408A mutant is that the assembled efflux complex may cause stretching of the inter-membrane distance, which could interfere with signalling in the periplasmic space (Asmar *et al.*, 2017). The width of the periplasmic space in *S.* Typhimurium and *E. coli* ranges from 17 to 32nm (Matias *et al.*, 2003, Cohen *et al.*, 2017, Asmar *et al.*, 2017), but the current model of the AcrAB-TolC efflux complex measures 317.4Å (equivalent to 31.74nm) (Du *et al.*, 2014), which is at the upper limit of the inter-membrane distance. In a wild-type strain, the efflux complex is constantly assembled and disassembled, which transiently changes the distance between the inner and the outer membrane. In the AcrB D408A mutant, the complex cannot disassemble. Consequently, the distance between the bacterial membranes may be increased in the mutant. Increasing the inter-membrane distance inhibited activation of the Rcs two-component signalling system in *E. coli* (Asmar *et al.*, 2017). The activation of the Rcs system is closely related to cytoskeleton rearrangements necessary for expression of SPI-encoded T3SS and flagella genes in *S.* Typhimurium (Bulmer *et al.*, 2012b). Further studies are required to determine if

there are any changes to the size of the periplasmic space in the AcrB D408A mutant and that could contribute to its phenotype.

Although a potential increase in the width of the periplasmic space may be a limitation towards the study of the physiological role of AcrB, addition of efflux inhibitors is likely to have the same effect on the AcrAB-TolC complex as the D408A substitution. AcrB exposed to inhibitors becomes 'locked' in one conformation (Wang *et al.*, 2017), which suggests that proton translocation through the pump is abolished. Therefore, no PMF would be available for the disassembly of the complex in the presence of chemical inhibitors. The D408A substitution in AcrB simulates this effect as it abolishes proton translocation through the pump (Takatsuka and Nikaido, 2009, Seeger *et al*., 2009). This makes the AcrB D408A mutant an excellent model to study the consequences of exposure to efflux inhibitors, particularly those developed to target only AcrB.

Inhibition of efflux pumps has been proposed as an alternative to restore effectiveness to antibiotics, reduce virulence and reduce biofilm formation (Li *et al.*, 2015, Reens *et al.*, 2018, Du *et al.*, 2018). Understanding the physiological role of the pumps allows the assessment of the risks of using efflux inhibitors as it determines any adverse effect their use might have on treatment of infections. The research described in this thesis suggests that AcrB, apart from being a MDR efflux pump, may function as a general 'detoxification' system in *E. coli* and *S.* Typhimurium, by freeing the bacterial cell from toxic metabolic by-products. It was also hypothesised that AcrB may contribute to outer membrane stability by exporting long-chain fatty acids. Inhibition of AcrB alters the cellular homeostasis of *E. coli* and *S.* Typhimurium, which results in a variety of phenotypic alterations, including increased motility and decreased AI-2 import, which is likely to affect quorum sensing, and virulence in *S.* Typhimurium. Of the observed phenotypes, the only possible adverse consequence of inhibiting AcrB

may be an increase in the subpopulation of persisters. However, further studies are required to confirm this phenotype and the clinical and environmental importance of persisters is yet to be confirmed.

6.2 Future work in addition to that proposed in sections 3.12, 4.15 and 5.12

Two additional hypotheses have been generated:

- Inhibition of AcrB in *S.* Typhimurium and *E. coli* may cause a change in the proportion of lipids in the outer membrane due to lack of export of long-chain fatty acids. This could impact the stability of the outer membrane. The proportion and composition of lipids in the bacterial membranes can be easily measured by extracting the lipids with organic solvents, followed by lipidomics analysis by LC-MS with a reverse phase column. Testing the impact of any changes in membrane lipid composition on stability of the membrane is very challenging, as any compound that damages the membrane and most basic dyes are likely to be substrates of AcrB. Therefore, it may not be possible to differentiate lack of efflux activity from outer membrane instability using whole cells. Specific efflux assays for substrates that do not confer membrane instability will need to be developed to explore this hypothesis.
- Inhibition of AcrB may increase the width of the periplasmic space with adverse effects on signalling via the Rcs two-component signalling system. Cryo-electron microscopy can be carried out to measure the width of the periplasm in the AcrB D408A mutant and in the wild-type strain post-exposure to efflux inhibitors. To determine if changes in the intermembrane distance are caused by AcrB, the protein could be tagged with an fluorescent antibody before electron microscopy, as described by Zhang *et al.* (2007).

Publications resulting from this study

Wang-Kan X, Blair JMA, Chirullo B, Betts J, La Ragione RM, Ivens A, Ricci V, Opperman TJ, Piddock LJV. 2017. Lack of AcrB efflux function confers loss of virulence on *Salmonella enterica* serovar Typhimurium. mBio 8:e00968-17.

Conference presentations resulting from this study

"The D408A substitution in the AcrB multi-drug efflux protein of Salmonella Typhimurium SL1344 confers loss of function". **Xuan Wang-Kan**, Vito Ricci, Jessica M.A. Blair, Laura J.V. Piddock. Poster no. S1/P2 at the Microbiology Society Annual Conference, 2016. Liverpool, UK.

"Lack of AcrB function confers loss of virulence to *Salmonella* Typhimurium". **Xuan Wang-Kan**, Vito Ricci, Alasdair Ivens, Jessica M.A. Blair, Laura J.V. Poster no. 61 at the Gordon Research Conference on Multi-Drug Efflux Systems, 2017. Galveston, USA.

References

- ACHARD, M. E., CHEN, K. W., SWEET, M. J., WATTS, R. E., SCHRODER, K., SCHEMBRI, M. A. & MCEWAN, A. G. 2013. An antioxidant role for catecholate siderophores in *Salmonella*. *Biochem J,* 454**,** 543-9.
- AENDEKERK, S., DIGGLE, S. P., SONG, Z., HOIBY, N., CORNELIS, P., WILLIAMS, P. & CAMARA, M. 2005. The MexGHI-OpmD multidrug efflux pump controls growth, antibiotic susceptibility and virulence in *Pseudomonas aeruginosa* via 4-quinolone-dependent cell-to-cell communication. *Microbiology,* 151**,** 1113-25.
- AGBAJE, M., BEGUM, R. H., OYEKUNLE, M. A., OJO, O. E. & ADENUBI, O. T. 2011. Evolution of *Salmonella* nomenclature: a critical note. *Folia Microbiol (Praha),* 56**,** 497-503.
- ALCALDE-RICO, M., HERNANDO-AMADO, S., BLANCO, P. & MARTINEZ, J. L. 2016. Multidrug Efflux Pumps at the Crossroad between Antibiotic Resistance and Bacterial Virulence. *Front Microbiol,* 7**,** 1483.
- ANDINO, A. & HANNING, I. 2015. *Salmonella enterica*: survival, colonization, and virulence differences among serovars. *ScientificWorldJournal,* 2015**,** 520179.
- ANDREWS, J. M. 2001. Determination of minimum inhibitory concentrations. *J Antimicrob Chemother,* 48**,** 5-16.
- ANES, J., MCCUSKER, M. P., FANNING, S. & MARTINS, M. 2015. The ins and outs of RND efflux pumps in *Escherichia coli*. *Front Microbiol,* 6**,** 587.
- ARNOLDINI, M., VIZCARRA, I. A., PENA-MILLER, R., STOCKER, N., DIARD, M., VOGEL, V., BEARDMORE, R. E., HARDT, W. D. & ACKERMANN, M. 2014. Bistable expression of virulence genes in *Salmonella* leads to the formation of an antibiotic-tolerant subpopulation. *PLoS Biol,* 12**,** e1001928.
- ASMAR, A. T., FERREIRA, J. L., COHEN, E. J., CHO, S.-H., BEEBY, M., HUGHES, K. T. & COLLET, J.-F. 2017. Communication across the bacterial cell envelope depends on the size of the periplasm. *PLoS Biol,* 15**,** e2004303.
- BAILEY, A. M., IVENS, A., KINGSLEY, R., COTTELL, J. L., WAIN, J. & PIDDOCK, L. J. 2010. RamA, a member of the AraC/XylS family, influences both virulence and efflux in *Salmonella enterica* serovar Typhimurium. *J Bacteriol,* 192**,** 1607-16.
- BARNHART, M. M. & CHAPMAN, M. R. 2006. Curli biogenesis and function. *Annu Rev Microbiol,* 60**,** 131-47.
- BARRETT, J. & FHOGARTAIGH, C. N. 2017. Bacterial gastroenteritis. *Medicine,* 45**,** 683-689.
- BASSLER, B. L., GREENBERG, E. P. & STEVENS, A. M. 1997. Cross-species induction of luminescence in the quorum-sensing bacterium *Vibrio harveyi*. *J Bacteriol,* 179**,** 4043-5.
- BASSLER, B. L., WRIGHT, M., SHOWALTER, R. E. & SILVERMAN, M. R. 1993. Intercellular signalling in Vibrio harveyi: sequence and function of genes regulating expression of luminescence. *Mol Microbiol,* 9**,** 773-86.
- BATEY, R. T. 2011. Recognition of S-adenosylmethionine by riboswitches. *Wiley Interdiscip Rev RNA,* 2**,** 299-311.
- BAUGH, S. 2014. *The Role of Multidru Efflux Pumps in Biofilm Formation of Salmonella enterica serovar Typhimurium.* Doctor of Philosophy, University Of Birmingham
- BAVRO, V. N., PIETRAS, Z., FURNHAM, N., PEREZ-CANO, L., FERNANDEZ-RECIO, J., PEI, X. Y., MISRA, R. & LUISI, B. 2008. Assembly and channel opening in a bacterial drug efflux machine. *Mol Cell,* 30**,** 114-21.
- BERTANI, G. 1951. STUDIES ON LYSOGENESIS I. : The Mode of Phage Liberation by Lysogenic *Escherichia coli*. *J Bacteriol,* 62**,** 293-300.
- BEUZON, C. R., BANKS, G., DEIWICK, J., HENSEL, M. & HOLDEN, D. W. 1999. pH-dependent secretion of SseB, a product of the SPI-2 type III secretion system of *Salmonella typhimurium*. *Mol Microbiol,* 33**,** 806-16.

- BHAGWAT, A. A., YING, Z. I., KARNS, J. & SMITH, A. 2013. Determining RNA quality for NextGen sequencing: some exceptions to the gold standard rule of 23S to 16S rRNA ratio. *Microbiol Discov,* 1.
- BINA, X. R., PROVENZANO, D., NGUYEN, N. & BINA, J. E. 2008. *Vibrio cholerae* RND family efflux systems are required for antimicrobial resistance, optimal virulence factor production, and colonization of the infant mouse small intestine. *Infect Immun,* 76**,** 3595-3605.
- BLAIR, J. M. 2010. *The Role of AcrA in Antibiotic Resistance and Virulence of Salmonella enterica serovar Typhimurium* Doctor of Philosophy, University Of Birmingham
- BLAIR, J. M., BAVRO, V. N., RICCI, V., MODI, N., CACCIOTTO, P., KLEINEKATHFER, U., RUGGERONE, P., VARGIU, A. V., BAYLAY, A. J., SMITH, H. E., BRANDON, Y., GALLOWAY, D. & PIDDOCK, L. J. 2015a. AcrB drug-binding pocket substitution confers clinically relevant resistance and altered substrate specificity. *Proc Natl Acad Sci U S A,* 112**,** 3511-6.
- BLAIR, J. M., LA RAGIONE, R. M., WOODWARD, M. J. & PIDDOCK, L. J. 2009. Periplasmic adaptor protein AcrA has a distinct role in the antibiotic resistance and virulence of *Salmonella enterica* serovar Typhimurium. *J Antimicrob Chemother,* 64**,** 965-72.
- BLAIR, J. M. & PIDDOCK, L. J. 2016. How to Measure Export via Bacterial Multidrug Resistance Efflux Pumps. *MBio,* 7.
- BLAIR, J. M., RICHMOND, G. E., BAILEY, A. M., IVENS, A. & PIDDOCK, L. J. 2013. Choice of Bacterial Growth Medium Alters the Transcriptome and Phenotype of *Salmonella enterica* Serovar Typhimurium. *PloS One,* 8**,** e63912.
- BLAIR, J. M., SMITH, H. E., RICCI, V., LAWLER, A. J., THOMPSON, L. J. & PIDDOCK, L. J. 2015b. Expression of homologous RND efflux pump genes is dependent upon AcrB expression: implications for efflux and virulence inhibitor design. *J Antimicrob Chemother,* 70**,** 424-31.
- BLAIR, J. M., WEBBER, M. A., BAYLAY, A. J., OGBOLU, D. O. & PIDDOCK, L. J. 2015c. Molecular mechanisms of antibiotic resistance. *Nat Rev Microbiol,* 13**,** 42-51.
- BLATTNER, F. R., PLUNKETT, G., 3RD, BLOCH, C. A., PERNA, N. T., BURLAND, V., RILEY, M., COLLADO-VIDES, J., GLASNER, J. D., RODE, C. K., MAYHEW, G. F., GREGOR, J., DAVIS, N. W., KIRKPATRICK, H. A., GOEDEN, M. A., ROSE, D. J., MAU, B. & SHAO, Y. 1997. The complete genome sequence of *Escherichia coli* K-12. *Science,* 277**,** 1453-62.
- BLÄTTNER, S., DAS, S., PAPROTKA, K., EILERS, U., KRISCHKE, M., KRETSCHMER, D., REMMELE, C. W., DITTRICH, M., MÜLLER, T., SCHUELEIN-VOELK, C., HERTLEIN, T., MUELLER, M. J., HUETTEL, B., REINHARDT, R., OHLSEN, K., RUDEL, T. & FRAUNHOLZ, M. J. 2016. *Staphylococcus aureus* Exploits a Non-ribosomal Cyclic Dipeptide to Modulate Survival within Epithelial Cells and Phagocytes. *PLoS Pathog,* 12**,** e1005857.
- BORCHERT, A. J. & DOWNS, D. M. 2017. The Response to 2-Aminoacrylate Differs in *Escherichia coli* and *Salmonella enterica*, despite Shared Metabolic Components. *J Bacteriol,* 199.
- BOUMART, Z., VELGE, P. & WIEDEMANN, A. 2014. Multiple invasion mechanisms and different intracellular Behaviors: a new vision of *Salmonella*-host cell interaction. *FEMS Microbiol Lett*.
- BRANDACHER, G., PERATHONER, A., LADURNER, R., SCHNEEBERGER, S., OBRIST, P., WINKLER, C., WERNER, E. R., WERNER-FELMAYER, G., WEISS, H. G., GOBEL, G., MARGREITER, R., KONIGSRAINER, A., FUCHS, D. & AMBERGER, A. 2006. Prognostic value of indoleamine 2,3-dioxygenase expression in colorectal cancer: effect on tumor-infiltrating T cells. *Clin Cancer Res,* 12**,** 1144-51.
- BRONNER, D. N., FABER, F., OLSAN, E. E., BYNDLOSS, M. X., SAYED, N. A., XU, G., YOO, W., KIM, D., RYU, S., LEBRILLA, C. B. & BAUMLER, A. J. 2018. Genetic Ablation

of Butyrate Utilization Attenuates Gastrointestinal *Salmonella* Disease. *Cell Host Microbe,* 23**,** 266-273.e4.
- BRUNELLE, B. W., BEARSON, B. L., BEARSON, S. M. D. & CASEY, T. A. 2017. Multidrug-Resistant *Salmonella enterica* Serovar Typhimurium Isolates Are Resistant to Antibiotics That Influence Their Swimming and Swarming Motility. *mSphere,* 2.
- BUCKLEY, A. M., WEBBER, M. A., COOLES, S., RANDALL, L. P., LA RAGIONE, R. M., WOODWARD, M. J. & PIDDOCK, L. J. 2006. The AcrAB-TolC efflux system of *Salmonella enterica* serovar Typhimurium plays a role in pathogenesis. *Cell Microbiol,* 8**,** 847-56.
- BUCKNER, M. M. C., BLAIR, J. M. A., LA RAGIONE, R. M., NEWCOMBE, J., DWYER, D. J., IVENS, A. & PIDDOCK, L. J. V. 2016. Beyond Antimicrobial Resistance: Evidence for a Distinct Role of the AcrD Efflux Pump in *Salmonella* Biology. *mBio,* 7.
- BULMER, D. M., KHARRAZ, L., GRANT, A. J., DEAN, P., MORGAN, F. J., KARAVOLOS, M. H., DOBLE, A. C., MCGHIE, E. J., KORONAKIS, V., DANIEL, R. A., MASTROENI, P. & KHAN, C. M. 2012a. The bacterial cytoskeleton modulates motility, type 3 secretion, and colonization in *Salmonella*. *PLoS Pathog,* 8**,** e1002500.
- BULMER, D. M., KHARRAZ, L., GRANT, A. J., DEAN, P., MORGAN, F. J. E., KARAVOLOS, M. H., DOBLE, A. C., MCGHIE, E. J., KORONAKIS, V., DANIEL, R. A., MASTROENI, P. & ANJAM KHAN, C. M. 2012b. The Bacterial Cytoskeleton Modulates Motility, Type 3 Secretion, and Colonization in *Salmonella*. *PLoS Pathog,* 8**,** e1002500.
- CAMERON, A. D., STOEBEL, D. M. & DORMAN, C. J. 2011. DNA supercoiling is differentially regulated by environmental factors and FIS in *Escherichia coli* and *Salmonella enterica*. *Mol Microbiol,* 80**,** 85-101.
- CATLIN, B. W. 1975. Cellular elongation under the influence of antibacterial agents: way to differentiate coccobacilli from cocci. *J Clin Microbiol,* 1**,** 102-5.
- CETINKAYA, Y., FALK, P. & MAYHALL, C. G. 2000. Vancomycin-Resistant Enterococci. *Clin Microbiol Rev,* 13**,** 686-707.
- CHERAYIL, B. J., MCCORMICK, B. A. & BOSLEY, J. 2000. *Salmonella enterica* serovar typhimurium-dependent regulation of inducible nitric oxide synthase expression in macrophages by invasins SipB, SipC, and SipD and effector SopE2. *Infect Immun,* 68**,** 5567-74.
- CHINNI, S. V., RAABE, C. A., ZAKARIA, R., RANDAU, G., HOE, C. H., ZEMANN, A., BROSIUS, J., TANG, T. H. & ROZHDESTVENSKY, T. S. 2010. Experimental identification and characterization of 97 novel npcRNA candidates in *Salmonella enterica* serovar Typhi. *Nucleic Acids Res,* 38**,** 5893-908.
- CHITSAZ, M. & BROWN, M. H. 2017. The role played by drug efflux pumps in bacterial multidrug resistance. *Essays Biochem,* 61**,** 127-139.
- CHO, K. Y. & SALTON, M. R. 1966. Fatty acid composition of bacterial membrane and wall lipids. *Biochim Biophys Acta,* 116**,** 73-9.
- CHOI, J., SHIN, D., KIM, M., PARK, J., LIM, S. & RYU, S. 2012. LsrR-mediated quorum sensing controls invasiveness of *Salmonella typhimurium* by regulating SPI-1 and flagella genes. *PLoS One,* 7**,** e37059.
- CHOLLET, R., CHEVALIER, J., BRYSKIER, A. & PAGES, J. M. 2004. The AcrAB-TolC pump is involved in macrolide resistance but not in telithromycin efflux in *Enterobacter aerogenes* and *Escherichia coli*. *Antimicrob Agents Chemother,* 48**,** 3621-4.
- CHONG, A., LEE, S., YANG, Y. A. & SONG, J. 2017. The Role of Typhoid Toxin in *Salmonella* Typhi Virulence[P SEP]*Yale J Biol Med,* 90**,** 283-90.
- COHEN, E. J., FERREIRA, J. L., LADINSKY, M. S., BEEBY, M. & HUGHES, K. T. 2017. Nanoscale-length control of the flagellar driveshaft requires hitting the tethered outer membrane. *Science,* 356**,** 197-200.
- COLDHAM, N. G., WEBBER, M., WOODWARD, M. J. & PIDDOCK, L. J. 2010. A 96-well plate fluorescence assay for assessment of cellular permeability and active efflux in *Salmonella enterica* serovar Typhimurium and *Escherichia coli*. *J Antimicrob Chemother,* 65**,** 1655-63.

- CONNOLLY, J. P., GOLDSTONE, R. J., BURGESS, K., COGDELL, R. J., BEATSON, S. A., VOLLMER, W., SMITH, D. G. & ROE, A. J. 2015. The host metabolite D-serine contributes to bacterial niche specificity through gene selection. *ISME J,* 9**,** 1052.
- COUSSENS, N. P. & DAINES, D. A. 2016. Wake me when it's over – Bacterial toxin–antitoxin proteins and induced dormancy. *Exp Biol Med (Maywood),* 241**,** 1332-42.
- CUI, P., NIU, H., SHI, W., ZHANG, S., ZHANG, W. & ZHANG, Y. 2018. Identification of Genes Involved in Bacteriostatic Antibiotic-Induced Persister Formation. *Front Microbiol,* 9**,** 413.
- DANDEKAR, T., FIESELMANN, A., FISCHER, E., POPP, J., HENSEL, M. & NOSTER, J. 2014. *Salmonella*-how a metabolic generalist adopts an intracellular lifestyle during infection. *Front Cell Infect Microbiol,* 4**,** 191.
- DATSENKO, K. A. & WANNER, B. L. 2000. One-step inactivation of chromosomal genes in *Escherichia coli* K-12 using PCR products. *Proc Natl Acad Sci U S A,* 97**,** 6640-5.
- DATTA, S., COSTANTINO, N., ZHOU, X. & COURT, D. L. 2008. Identification and analysis of recombineering functions from Gram-negative and Gram-positive bacteria and their phages. *Proc Natl Acad Sci U S A,* 105**,** 1626-31.
- DAURY, L., ORANGE, F., TAVEAU, J. C., VERCHERE, A., MONLEZUN, L., GOUNOU, C., MARREDDY, R. K., PICARD, M., BROUTIN, I., POS, K. M. & LAMBERT, O. 2016. Tripartite assembly of RND multidrug efflux pumps. *Nat Commun,* 7**,** 10731.
- DE FILIPPI, L., FOURNIER, M., CAMERONI, E., LINDER, P., DE VIRGILIO, C., FOTI, M. & DELOCHE, O. 2007. Membrane stress is coupled to a rapid translational control of gene expression in chlorpromazine-treated cells. *Curr Genet,* 52**,** 171-85.
- DE LA CRUZ, M. A., ZHAO, W., FARENC, C., GIMENEZ, G., RAOULT, D., CAMBILLAU, C., GORVEL, J.-P. & MÉRESSE, S. 2013. A Toxin-Antitoxin Module of Salmonella Promotes Virulence in Mice. *PLoS Pathog,* 9**,** e1003827.
- DE PEDRO, M. A. & CAVA, F. 2015. Structural constraints and dynamics of bacterial cell wall architecture. *Front Microbiol,* 6**,** 449.
- DELMAR, J. A. & YU, E. W. 2016. The AbgT family: A novel class of antimetabolite transporters. *Protein Sci,* 25**,** 322-37.
- DINH, T., PAULSEN, I. T. & SAIER, M. H., JR. 1994. A family of extracytoplasmic proteins that allow transport of large molecules across the outer membranes of gram-negative bacteria. *J Bacteriol,* 176**,** 3825-31.
- DOWD, S. E., KILLINGER-MANN, K., BLANTON, J., SAN FRANCISCO, M. & BRASHEARS, M. 2007. Positive adaptive state: microarray evaluation of gene expression in *Salmonella enterica* Typhimurium exposed to nalidixic acid. *Foodborne Pathog Dis,* 4**,** 187-200.
- DU, D., VOSS, J., WANG, Z., CHIU, W. & LUISI, B. F. 2015. The pseudo-atomic structure of an RND-type tripartite multidrug efflux pump. *Biol Chem,* 396**,** 1073-82.
- DU, D., WANG-KAN, X., NEUBERGER, A., VAN VEEN, H. W., POS, K. M., PIDDOCK, L. J. V. & LUISI, B. F. 2018. Multidrug efflux pumps: structure, function and regulation. *Nat Rev Microbiol,* 16**,** 523-539.
- DU, D., WANG, Z., JAMES, N. R., VOSS, J. E., KLIMONT, E., OHENE-AGYEI, T., VENTER, H., CHIU, W. & LUISI, B. F. 2014. Structure of the AcrAB-TolC multidrug efflux pump. *Nature,* 509**,** 512-5.
- DUERR, C. U., ZENK, S. F., CHASSIN, C., POTT, J., GUTLE, D., HENSEL, M. & HORNEF, M. W. 2009. O-antigen delays lipopolysaccharide recognition and impairs antibacterial host defense in murine intestinal epithelial cells. *PLoS Pathog,* 5**,** e1000567.
- DUFOUR, N. & RAO, R. P. 2011. Secondary metabolites and other small molecules as intercellular pathogenic signals. *FEMS Microbiol Lett,* 314**,** 10-7.
- DURFEE, T., NELSON, R., BALDWIN, S., PLUNKETT, G., 3RD, BURLAND, V., MAU, B., PETROSINO, J. F., QIN, X., MUZNY, D. M., AYELE, M., GIBBS, R. A., CSORGO, B., POSFAI, G., WEINSTOCK, G. M. & BLATTNER, F. R. 2008. The complete genome sequence of *Escherichia coli* DH10B: insights into the biology of a laboratory workhorse. *J Bacteriol,* 190**,** 2597-606.

- *E. COLI* GENOME PROJECT. 2002-2018. *Resources: Strain information* [Online]. https://www.genome.wisc.edu/resources/strains.htm. [Accessed 31/05 2018].
- EAVES, D. J., RICCI, V. & PIDDOCK, L. J. 2004. Expression of *acrB*, *acrF*, *acrD*, *marA*, and *soxS* in *Salmonella enterica* serovar Typhimurium: role in multiple antibiotic resistance. *Antimicrob Agents Chemother,* 48**,** 1145-50.
- EBERL, L. & RIEDEL, K. 2011. Mining quorum sensing regulated proteins - Role of bacterial cell-to-cell communication in global gene regulation as assessed by proteomics. *Proteomics,* 11**,** 3070-85.
- EICHER, T., SEEGER, M. A., ANSELMI, C., ZHOU, W., BRANDSTÄTTER, L., VERREY, F., DIEDERICHS, K., FARALDO-GÓMEZ, J. D. & POS, K. M. 2014. Coupling of remote alternating-access transport mechanisms for protons and substrates in the multidrug efflux pump AcrB. *eLife,* 3**,** e03145.
- EISELE, N. A., RUBY, T., JACOBSON, A., MANZANILLO, P. S., COX, J. S., LAM, L., MUKUNDAN, L., CHAWLA, A. & MONACK, D. M. 2013. *Salmonella* require the fatty acid regulator PPARδ for the establishment of a metabolic environment essential for long term persistence. *Cell Host Microbe,* 14**,** 171-182.
- ELBOURNE, L. D., TETU, S. G., HASSAN, K. A. & PAULSEN, I. T. 2017. TransportDB 2.0: a database for exploring membrane transporters in sequenced genomes from all domains of life. *Nucleic Acids Res,* 45**,** D320-d324.
- ENG, R. H., PADBERG, F. T., SMITH, S. M., TAN, E. N. & CHERUBIN, C. E. 1991. Bactericidal effects of antibiotics on slowly growing and nongrowing bacteria. *Antimicrob Agents Chemother,* 35**,** 1824-1828.
- EVANS, K., PASSADOR, L., SRIKUMAR, R., TSANG, E., NEZEZON, J. & POOLE, K. 1998. Influence of the MexAB-OprM multidrug efflux system on quorum sensing in *Pseudomonas aeruginosa*. *J Bacteriol,* 180**,** 5443-7.
- FAN, Y., EVANS, C. R. & LING, J. 2016. Reduced Protein Synthesis Fidelity Inhibits Flagellar Biosynthesis and Motility. *Sci Rep,* 6**,** 30960.
- FEASEY, N. A., MASESA, C., JASSI, C., FARAGHER, E. B., MALLEWA, J., MALLEWA, M., MACLENNAN, C. A., MSEFULA, C., HEYDERMAN, R. S. & GORDON, M. A. 2015. Three Epidemics of Invasive Multidrug-Resistant *Salmonella* Bloodstream Infection in Blantyre, Malawi, 1998-2014. *Clin Infect Dis,* 61 Suppl 4**,** S363-71.
- FENG, Z., HOU, T. & LI, Y. 2012. Unidirectional peristaltic movement in multisite drug binding pockets of AcrB from molecular dynamics simulations. *Mol Biosyst,* 8**,** 2699-709.
- FISHER, R. A., GOLLAN, B. & HELAINE, S. 2017. Persistent bacterial infections and persister cells. *Nat Rev Microbiol,* 15**,** 453-464.
- FITZPATRICK, T. B., AMRHEIN, N., KAPPES, B., MACHEROUX, P., TEWS, I. & RASCHLE, T. 2007. Two independent routes of *de novo* vitamin B6 biosynthesis: not that different after all. *Biochem J,* 407**,** 1-13.
- FRIEDLANDER, R. S., VLAMAKIS, H., KIM, P., KHAN, M., KOLTER, R. & AIZENBERG, J. 2013. Bacterial flagella explore microscale hummocks and hollows to increase adhesion. *Proc Natl Acad Sci U S A,* 110**,** 5624-9.
- FUX, C. A., SHIRTLIFF, M., STOODLEY, P. & COSTERTON, J. W. 2005. Can laboratory reference strains mirror "real-world" pathogenesis? *Trends Microbiol,* 13**,** 58-63.
- GAL-MOR, O., BOYLE, E. C. & GRASSL, G. A. 2014. Same species, different diseases: how and why typhoidal and non-typhoidal *Salmonella enterica* serovars differ. *Front Microbiol,* 5**,** 391.
- GARCIA-ANGULO, V. A. 2017. Overlapping riboflavin supply pathways in bacteria. *Crit Rev Microbiol,* 43**,** 196-209.
- GIBSON, D. G., YOUNG, L., CHUANG, R. Y., VENTER, J. C., HUTCHISON, C. A., 3RD & SMITH, H. O. 2009. Enzymatic assembly of DNA molecules up to several hundred kilobases. *Nat Methods,* 6**,** 343-5.
- GIL-CRUZ, C., BOBAT, S., MARSHALL, J. L., KINGSLEY, R. A., ROSS, E. A., HENDERSON, I. R., LEYTON, D. L., COUGHLAN, R. E., KHAN, M., JENSEN, K. T., BUCKLEY, C. D., DOUGAN, G., MACLENNAN, I. C., LOPEZ-MACIAS, C. &

CUNNINGHAM, A. F. 2009. The porin OmpD from nontyphoidal *Salmonella* is a key target for a protective B1b cell antibody response. *Proc Natl Acad Sci U S A,* 106**,** 9803-8.
- GOO, E., AN, J. H., KANG, Y. & HWANG, I. 2015. Control of bacterial metabolism by quorum sensing. *Trends Microbiol,* 23**,** 567-76.
- GRANT, C. L. & PRAMER, D. 1962. Minor element composition of yeast extract. *J Bacteriol,* 84**,** 869-70.
- GREENBERG, E. P., HASTINGS, J. W. & ULITZUR, S. 1979. Induction of luciferase synthesis in *Beneckea harveyi* by other marine bacteria. *Arch Microbiol,* 120**,** 87-91.
- GU, H., ZHAO, C., ZHANG, T., LIANG, H., WANG, X. M., PAN, Y., CHEN, X., ZHAO, Q., LI, D., LIU, F., ZHANG, C. Y. & ZEN, K. 2017. *Salmonella* produce microRNA-like RNA fragment Sal-1 in the infected cells to facilitate intracellular survival. *Sci Rep,* 7**,** 2392.
- GUAN, L. & NAKAE, T. 2001. Identification of Essential Charged Residues in Transmembrane Segments of the Multidrug Transporter MexB of *Pseudomonas aeruginosa*. *J Bacteriol,* 183**,** 1734-9.
- GUNN, J. S., MARSHALL, J. M., BAKER, S., DONGOL, S., CHARLES, R. C. & RYAN, E. T. 2014. *Salmonella* chronic carriage: epidemiology, diagnosis and gallbladder persistence. *Trends Microbiol,* 22**,** 648-55.
- GUPTA, A., BERBARI, E. F., OSMON, D. R. & VIRK, A. 2014. Prosthetic joint infection due to *Salmonella* species: a case series. *BMC Infect Dis,* 14**,** 633.
- HARA-KUDO, Y. & TAKATORI, K. 2011. Contamination level and ingestion dose of foodborne pathogens associated with infections. *Epidemiol Infect,* 139**,** 1505-10.
- HARSHEY, R. M. & MATSUYAMA, T. 1994. Dimorphic transition in *Escherichia coli* and *Salmonella typhimurium*: surface-induced differentiation into hyperflagellate swarmer cells. *Proc Natl Acad Sci U S A,* 91**,** 8631-5.
- HASELBECK, A. H., PANZNER, U., IM, J., BAKER, S., MEYER, C. G. & MARKS, F. 2017. Current perspectives on invasive nontyphoidal *Salmonella* disease. *Curr Opin Infect Dis,* 30**,** 498-503.
- HASSAN, K. A., ELBOURNE, L. D., LI, L., GAMAGE, H. K., LIU, Q., JACKSON, S. M., SHARPLES, D., KOLSTO, A. B., HENDERSON, P. J. & PAULSEN, I. T. 2015. An ace up their sleeve: a transcriptomic approach exposes the AceI efflux protein of *Acinetobacter baumannii* and reveals the drug efflux potential hidden in many microbial pathogens. *Front Microbiol,* 6**,** 333.
- HAVELAAR, A. H., KIRK, M. D., TORGERSON, P. R., GIBB, H. J., HALD, T., LAKE, R. J., PRAET, N., BELLINGER, D. C., DE SILVA, N. R., GARGOURI, N., SPEYBROECK, N., CAWTHORNE, A., MATHERS, C., STEIN, C., ANGULO, F. J. & DEVLEESSCHAUWER, B. 2015. World Health Organization Global Estimates and Regional Comparisons of the Burden of Foodborne Disease in 2010. *PLoS Med,* 12**,** e1001923.
- HAZEN, T. H., DAUGHERTY, S. C., SHETTY, A., MAHURKAR, A. A., WHITE, O., KAPER, J. B. & RASKO, D. A. 2015. RNA-Seq analysis of isolate- and growth phase-specific differences in the global transcriptomes of enteropathogenic *Escherichia coli* prototype isolates. *Front Microbiol,* 6**,** 569-569.
- HELAINE, S., CHEVERTON, A. M., WATSON, K. G., FAURE, L. M., MATTHEWS, S. A. & HOLDEN, D. W. 2014. Internalization of *Salmonella* by macrophages induces formation of nonreplicating persisters. *Science,* 343**,** 204-8.
- HELAINE, S., THOMPSON, J. A., WATSON, K. G., LIU, M., BOYLE, C. & HOLDEN, D. W. 2010. Dynamics of intracellular bacterial replication at the single cell level. *Proc Natl Acad Sci U S A,* 107**,** 3746-51.
- HELLING, R. B., JANES, B. K., KIMBALL, H., TRAN, T., BUNDESMANN, M., CHECK, P., PHELAN, D. & MILLER, C. 2002. Toxic waste disposal in *Escherichia coli*. *J Bacteriol,* 184**,** 3699-703.
- HERRERO-FRESNO, A. & OLSEN, J. E. 2018. *Salmonella* Typhimurium metabolism affects virulence in the host - A mini-review. *Food Microbiol,* 71**,** 98-110.
- HIBBERD, M. C., WU, M., RODIONOV, D. A., LI, X., CHENG, J., GRIFFIN, N. W., BARRATT, M. J., GIANNONE, R. J., HETTICH, R. L., OSTERMAN, A. L. & GORDON, J.

I. 2017. The effects of micronutrient deficiencies on bacterial species from the human gut microbiota. *Sci Transl Med,* 9.
- HIRAKATA, Y., SRIKUMAR, R., POOLE, K., GOTOH, N., SUEMATSU, T., KOHNO, S., KAMIHIRA, S., HANCOCK, R. E. & SPEERT, D. P. 2002. Multidrug efflux systems play an important role in the invasiveness of *Pseudomonas aeruginosa*. *J Exp Med,* 196**,** 109-18.
- HIRAKAWA, H., TAKUMI-KOBAYASHI, A., THEISEN, U., HIRATA, T., NISHINO, K. & YAMAGUCHI, A. 2008. AcrS/EnvR represses expression of the *acrAB* multidrug efflux genes in *Escherichia coli*. *J Bacteriol,* 190**,** 6276-9.
- HOBBS, E. C., YIN, X., PAUL, B. J., ASTARITA, J. L. & STORZ, G. 2012. Conserved small protein associates with the multidrug efflux pump AcrB and differentially affects antibiotic resistance. *Proc Natl Acad Sci U S A,* 109**,** 16696-701.
- HOGBERG, L. D., HEDDINI, A. & CARS, O. 2010. The global need for effective antibiotics: challenges and recent advances. *Trends Pharmacol Sci,* 31**,** 509-15.
- HOLDEN, V. I. & BACHMAN, M. A. 2015. Diverging roles of bacterial siderophores during infection. *Metallomics,* 7**,** 986-95.
- HORIYAMA, T. & NISHINO, K. 2014. AcrB, AcrD, and MdtABC multidrug efflux systems are involved in enterobactin export in *Escherichia coli*. *PLoS One,* 9**,** e108642.
- HOTLING, S., HABERLAG, B., TAMM, M., COLLATZ, J., MACK, P., STEIDLE, J. L., VENCES, M. & SCHULZ, S. 2014. Identification and synthesis of macrolide pheromones of the grain beetle *Oryzaephilus surinamensis* and the frog *Spinomantis aglavei*. *Chemistry,* 20**,** 3183-91.
- HOU, J.-H., CHEN, H.-W., GAO, Z.-J. & CAI, K. 2010. Molecular Evolutionary Analysis of Enterobacteriaceae AcrAB Multidrug Efflux Pump. *Biotechnology,* 20**,** 18-21.
- HUR, J., JAWALE, C. & LEE, J. H. 2012. Antimicrobial resistance of *Salmonella* isolated from food animals: A review. *Food Res Int,* 45**,** 819-830.
- ILYAS, B., TSAI, C. N. & COOMBES, B. K. 2017. Evolution of *Salmonella*-Host Cell Interactions through a Dynamic Bacterial Genome. *Front Cell Infect Microbiol,* 7**,** 428.
- JANGANAN, T. K., BAVRO, V. N., ZHANG, L., MATAK-VINKOVIC, D., BARRERA, N. P., VENIEN-BRYAN, C., ROBINSON, C. V., BORGES-WALMSLEY, M. I. & WALMSLEY, A. R. 2011. Evidence for the assembly of a bacterial tripartite multidrug pump with a stoichiometry of 3:6:3. *J Biol Chem,* 286**,** 26900-12.
- JAUFFRAIS, T., KILCOYNE, J., SECHET, V., HERRENKNECHT, C., TRUQUET, P., HERVE, F., BERARD, J. B., NULTY, C., TAYLOR, S., TILLMANN, U., MILES, C. O. & HESS, P. 2012. Production and isolation of azaspiracid-1 and -2 from *Azadinium spinosum* culture in pilot scale photobioreactors. *Mar Drugs,* 10**,** 1360-82.
- JENNINGS, E., THURSTON, T. L. M. & HOLDEN, D. W. 2017. *Salmonella* SPI-2 Type III Secretion System Effectors: Molecular Mechanisms And Physiological Consequences. *Cell Host Microbe,* 22**,** 217-231.
- JERSE, A. E., SHARMA, N. D., SIMMS, A. N., CROW, E. T., SNYDER, L. A. & SHAFER, W. M. 2003. A gonococcal efflux pump system enhances bacterial survival in a female mouse model of genital tract infection. *Infect Immun,* 71**,** 5576-82.
- JIANG, L., FENG, L., YANG, B., ZHANG, W., WANG, P., JIANG, X. & WANG, L. 2017. Signal transduction pathway mediated by the novel regulator LoiA for low oxygen tension induced *Salmonella* Typhimurium invasion. *PLoS Pathog,* 13**,** e1006429.
- KARIUKI, S., GORDON, M. A., FEASEY, N. & PARRY, C. M. 2015. Antimicrobial resistance and management of invasive *Salmonella* disease. *Vaccine,* 33 Suppl 3**,** C21-9.
- KEARNS, D. B. 2010. A field guide to bacterial swarming motility. *Nat Rev Microbiol,* 8**,** 634-44.
- KIM, J., WEBB, A. M., KERSHNER, J. P., BLASKOWSKI, S. & COPLEY, S. D. 2014. A versatile and highly efficient method for scarless genome editing in *Escherichia coli* and *Salmonella enterica*. *BMC Biotechnol,* 14**,** 84.
- KIM, S. R., MAENHAUT-MICHEL, G., YAMADA, M., YAMAMOTO, Y., MATSUI, K., SOFUNI, T., NOHMI, T. & OHMORI, H. 1997. Multiple pathways for SOS-induced mutagenesis in *Escherichia coli*: an overexpression of dinB/dinP results in strongly

enhancing mutagenesis in the absence of any exogenous treatment to damage DNA. *Proc Natl Acad Sci U S A,* 94**,** 13792-7.
- KIM, W. & SURETTE, M. G. 2005. Prevalence of Surface Swarming Behavior in *Salmonella*. *J Bacteriol,* 187**,** 6580-3.
- KINCADE, J. M. & DEHASETH, P. L. 1991. Bacteriophage lambda promoters *p*L and *p*R: sequence determinants of in vivo activity and of sensitivity to the DNA gyrase inhibitor, coumermycin. *Gene,* 97**,** 7-12.
- KINGSLEY, R. A., HUMPHRIES, A. D., WEENING, E. H., DE ZOETE, M. R., WINTER, S., PAPACONSTANTINOPOULOU, A., DOUGAN, G. & BAUMLER, A. J. 2003. Molecular and phenotypic analysis of the CS54 island of *Salmonella enterica* serotype Typhimurium: identification of intestinal colonization and persistence determinants. *Infect Immun,* 71**,** 629-40.
- KLOCKGETHER, J., MUNDER, A., NEUGEBAUER, J., DAVENPORT, C. F., STANKE, F., LARBIG, K. D., HEEB, S., SCHÖCK, U., POHL, T. M. & WIEHLMANN, L. 2010. Genome diversity of *Pseudomonas aeruginosa* PAO1 laboratory strains. *J Bacteriol,* 192**,** 1113-1121.
- KNODLER, L. A. 2015. *Salmonella enterica*: living a double life in epithelial cells. *Curr Opin Microbiol,* 23**,** 23-31.
- KNUFF, K. & FINLAY, B. B. 2017. What the SIF Is Happening-The Role of Intracellular *Salmonella*-Induced Filaments. *Front Cell Infect Microbiol,* 7**,** 335.
- KOHLI, N., CRISP, Z., RIORDAN, R., LI, M., ALANIZ, R. C. & JAYARAMAN, A. 2018. The microbiota metabolite indole inhibits *Salmonella* virulence: Involvement of the PhoPQ two-component system. *PLoS One,* 13**,** e0190613.
- KOIRALA, S., MEARS, P., SIM, M., GOLDING, I., CHEMLA, Y. R., ALDRIDGE, P. D. & RAO, C. V. 2014. A nutrient-tunable bistable switch controls motility in *Salmonella enterica* serovar Typhimurium. *MBio,* 5**,** e01611-14.
- KOTHARY, M. H. & BABU, U. S. 2001. Infective dose of foodborne pathogens in volunteers: A review. *J Food Saf,* 21**,** 49-68.
- KRISHNAMOORTHY, G., TIKHONOVA, E. B., DHAMDHERE, G. & ZGURSKAYA, H. I. 2013. On the role of TolC in multidrug efflux: the function and assembly of AcrAB-TolC tolerate significant depletion of intracellular TolC protein. *Mol Microbiol,* 87**,** 982-97.
- KRÖGER, C., COLGAN, A., SRIKUMAR, S., HÄNDLER, K., SIVASANKARAN, SATHESH K., HAMMARLÖF, DISA L., CANALS, R., GRISSOM, JOE E., CONWAY, T., HOKAMP, K. & HINTON, JAY C. D. 2013. An Infection-Relevant Transcriptomic Compendium for *Salmonella enterica* Serovar Typhimurium. *Cell Host Microbe,* 14**,** 683-695.
- KUAN, Y. D. & LEE, C. H. 2016. *Salmonella* overcomes tumor immune tolerance by inhibition of tumor indoleamine 2, 3-dioxygenase 1 expression. *Oncotarget,* 7**,** 374-85.
- KUMAR, S. 2018. Introduction to secondary metabolites. *Secondary Metabolite and Functional Food Components: Role in Health and Disease.*
- KUNKLE, D. E., BINA, X. R. & BINA, J. E. 2017. The *Vibrio cholerae* VexGH RND Efflux System Maintains Cellular Homeostasis by Effluxing Vibriobactin. *MBio,* 8.
- KWAMBANA-ADAMS, B., DARBOE, S., NABWERA, H., FOSTER-NYARKO, E., IKUMAPAYI, U. N., SECKA, O., BETTS, M., BRADBURY, R., WEGMULLER, R., LAWAL, B., SAHA, D., HOSSAIN, M. J., PRENTICE, A. M., KAMPMANN, B., ANDERSON, S., DALESSANDRO, U. & ANTONIO, M. 2015. *Salmonella* Infections in The Gambia, 2005-2015. *Clin Infect Dis,* 61 Suppl 4**,** S354-62.
- LACROIX, F. J., CLOECKAERT, A., GREPINET, O., PINAULT, C., POPOFF, M. Y., WAXIN, H. & PARDON, P. 1996. *Salmonella typhimurium acrB*-like gene: identification and role in resistance to biliary salts and detergents and in murine infection. *FEMS Microbiol Lett,* 135**,** 161-7.
- LAMARCHE, M. G. & DÉZIEL, E. 2011. MexEF-OprN Efflux Pump Exports the *Pseudomonas* Quinolone Signal (PQS) Precursor HHQ (4-hydroxy-2-heptylquinoline). *PLoS One,* 6.

- LAMAS, A., MIRANDA, J. M., REGAL, P., VAZQUEZ, B., FRANCO, C. M. & CEPEDA, A. 2018. A comprehensive review of non-*enterica* subspecies of *Salmonella enterica*. *Microbiol Res,* 206**,** 60-73.
- LAMERS, R. P., CAVALLARI, J. F. & BURROWS, L. L. 2013. The efflux inhibitor phenylalanine-arginine beta-naphthylamide (PAbetaN) permeabilizes the outer membrane of Gram-negative bacteria. *PLoS One,* 8**,** e60666.
- LAWLER, A. J., RICCI, V., BUSBY, S. J. W. & PIDDOCK, L. J. V. 2013. Genetic inactivation of *acrAB* or inhibition of efflux induces expression of *ramA*. *J Antimicrob Chemother,* 68**,** 1551-7.
- LEE, D. J., BINGLE, L. E., HEURLIER, K., PALLEN, M. J., PENN, C. W., BUSBY, S. J. & HOBMAN, J. L. 2009a. Gene doctoring: a method for recombineering in laboratory and pathogenic *Escherichia coli* strains. *BMC Microbiol,* 9**,** 1-14.
- LEE, S.-C., WANG, W. & LIU, P. 2009b. Construction of Gene Targeting Vectors by Recombineering. *Methods Mol Biol,* 530**,** 15-27.
- LENNEN, R. M., POLITZ, M. G., KRUZIKI, M. A. & PFLEGER, B. F. 2013. Identification of transport proteins involved in free fatty acid efflux in *Escherichia coli*. *J Bacteriol,* 195**,** 135-44.
- LESCHNER, S., WESTPHAL, K., DIETRICH, N., VIEGAS, N., JABLONSKA, J., LYSZKIEWICZ, M., LIENENKLAUS, S., FALK, W., GEKARA, N., LOESSNER, H. & WEISS, S. 2009. Tumor Invasion of *Salmonella enterica* Serovar Typhimurium Is Accompanied by Strong Hemorrhage Promoted by TNF-α. *PLoS ONE,* 4**,** e6692.
- LEUS, I. V., WEEKS, J. W., BONIFAY, V., SMITH, L., RICHARDSON, S. & ZGURSKAYA, H. I. 2018. Substrate specificities and efflux efficiencies of RND efflux pumps of *Acinetobacter baumannii*. *J Bacteriol*.
- LI, G., YAN, C., XU, Y., FENG, Y., WU, Q., LV, X., YANG, B., WANG, X. & XIA, X. 2014. Punicalagin inhibits *Salmonella* virulence factors and has anti-quorum-sensing potential. *Appl Environ Microbiol,* 80**,** 6204-11.
- LI, X. T., THOMASON, L. C., SAWITZKE, J. A., COSTANTINO, N. & COURT, D. L. 2013. Positive and negative selection using the *tetA-sacB* cassette: recombineering and P1 transduction in *Escherichia coli*. *Nucleic Acids Res,* 41**,** e204.
- LI, X. Z., PLESIAT, P. & NIKAIDO, H. 2015. The challenge of efflux-mediated antibiotic resistance in Gram-negative bacteria. *Clin Microbiol Rev,* 28**,** 337-418.
- LOBATO-MARQUEZ, D., MORENO-CORDOBA, I., FIGUEROA, V., DIAZ-OREJAS, R. & GARCIA-DEL PORTILLO, F. 2015. Distinct type I and type II toxin-antitoxin modules control *Salmonella* lifestyle inside eukaryotic cells. *Sci Rep,* 5**,** 9374.
- LOBO, M. C. & MANDELL, G. L. 1973. The effect of antibiotics on *Escherichia coli* ingested by macrophages. *Proc Soc Exp Biol Med,* 142**,** 1048-50.
- LONG, T., TU, K. C., WANG, Y., MEHTA, P., ONG, N. P., BASSLER, B. L. & WINGREEN, N. S. 2009. Quantifying the integration of quorum-sensing signals with single-cell resolution. *PLoS Biol,* 7**,** e68.
- LOPEZ, C. A., RIVERA-CHAVEZ, F., BYNDLOSS, M. X. & BAUMLER, A. J. 2015. The Periplasmic Nitrate Reductase NapABC Supports Luminal Growth of *Salmonella enterica* Serovar Typhimurium during Colitis. *Infect Immun,* 83**,** 3470-8.
- LÓPEZ, F. E., DE LAS MERCEDES PESCARETTI, M., MORERO, R. & DELGADO, M. A. 2012. *Salmonella* Typhimurium general virulence factors: A battle of David against Goliath? *Food Res Int,* 45**,** 842-851.
- LORKOWSKI, M., FELIPE-LOPEZ, A., DANZER, C. A., HANSMEIER, N. & HENSEL, M. 2014. *Salmonella enterica* invasion of polarized epithelial cells is a highly cooperative effort. *Infect Immun,* 82**,** 2657-67.
- MA, D., ALBERTI, M., LYNCH, C., NIKAIDO, H. & HEARST, J. E. 1996. The local repressor AcrR plays a modulating role in the regulation of *acrAB* genes of *Escherichia coli* by global stress signals. *Mol Microbiol,* 19**,** 101-12.

- MA, D., COOK, D. N., ALBERTI, M., PON, N. G., NIKAIDO, H. & HEARST, J. E. 1993. Molecular cloning and characterization of *acrA* and *acrE* genes of *Escherichia coli*. *J Bacteriol,* 175**,** 6299-313.
- MA, D., COOK, D. N., ALBERTI, M., PON, N. G., NIKAIDO, H. & HEARST, J. E. 1995. Genes *acrA* and *acrB* encode a stress-induced efflux system of *Escherichia coli*. *Mol Microbiol,* 16**,** 45-55.
- MALDONADO, R. F., SA-CORREIA, I. & VALVANO, M. A. 2016. Lipopolysaccharide modification in Gram-negative bacteria during chronic infection. *FEMS Microbiol Rev,* 40**,** 480-93.
- MALIK-KALE, P., WINFREE, S. & STEELE-MORTIMER, O. 2012. The bimodal lifestyle of intracellular *Salmonella* in epithelial cells: replication in the cytosol obscures defects in vacuolar replication. *PLoS One,* 7**,** e38732.
- MARKS, F., VON KALCKREUTH, V., AABY, P., ADU-SARKODIE, Y., EL TAYEB, M. A., ALI, M., ASEFFA, A., BAKER, S., BIGGS, H. M., BJERREGAARD-ANDERSEN, M., BREIMAN, R. F., CAMPBELL, J. I., COSMAS, L., CRUMP, J. A., ESPINOZA, L. M., DEERIN, J. F., DEKKER, D. M., FIELDS, B. S., GASMELSEED, N., HERTZ, J. T., VAN MINH HOANG, N., IM, J., JAEGER, A., JEON, H. J., KABORE, L. P., KEDDY, K. H., KONINGS, F., KRUMKAMP, R., LEY, B., LOFBERG, S. V., MAY, J., MEYER, C. G., MINTZ, E. D., MONTGOMERY, J. M., NIANG, A. A., NICHOLS, C., OLACK, B., PAK, G. D., PANZNER, U., PARK, J. K., PARK, S. E., RABEZANAHARY, H., RAKOTOZANDRINDRAINY, R., RAMINOSOA, T. M., RAZAFINDRABE, T. J., SAMPO, E., SCHUTT-GEROWITT, H., SOW, A. G., SARPONG, N., SEO, H. J., SOOKA, A., SOURA, A. B., TALL, A., TEFERI, M., THRIEMER, K., WARREN, M. R., YESHITELA, B., CLEMENS, J. D. & WIERZBA, T. F. 2017. Incidence of invasive *Salmonella* disease in sub-Saharan Africa: a multicentre population-based surveillance study. *Lancet Glob Health,* 5**,** e310-e323.
- MARSHALL, R. L. 2017. *Interactions within the tripartite drug-efflux pumps of Gram-negative bacteria.* Doctor of Philosophy, University Of Birmingham
- MARZEL, A., DESAI, P. T., GOREN, A., SCHORR, Y. I., NISSAN, I., PORWOLLIK, S., VALINSKY, L., MCCLELLAND, M., RAHAV, G. & GAL-MOR, O. 2016. Persistent Infections by Nontyphoidal *Salmonella* in Humans: Epidemiology and Genetics. *Clin Infect Dis,* 62**,** 879-886.
- MASI, M. & PAGÈS, J. M. 2013. Structure, Function and Regulation of Outer Membrane Proteins Involved in Drug Transport in Enterobactericeae: the OmpF/C – TolC Case. *Open Microbiol J,* 7**,** 22-33.
- MATIAS, V. R., AL-AMOUDI, A., DUBOCHET, J. & BEVERIDGE, T. J. 2003. Cryo-transmission electron microscopy of frozen-hydrated sections of *Escherichia coli* and *Pseudomonas aeruginosa*. *J Bacteriol,* 185**,** 6112-8.
- MAY, K. L. & SILHAVY, T. J. 2017. Making a membrane on the other side of the wall. *Biochim Biophys Acta,* 1862**,** 1386-1393.
- MEHTA, P. K., YADAV, A. K. & KUMAR, D. 2018. Secondary metabolites from microorganisms. *Secondary Metabolite and Functional Food Components: Role in Health and Disease.*
- MELTON, T., HARTMAN, P. E., STRATIS, J. P., LEE, T. L. & DAVIS, A. T. 1978. Chemotaxis of *Salmonella typhimurium* to Amino Acids and Some Sugars. *J Bacteriol,* 133**,** 708-16.
- MERCK. 2018. *92411 - Yeast Extract* [Online]. Merck. Available: https://www.sigmaaldrich.com/catalog/product/sial/92144?lang=en&region=GB [Accessed 11/08 2018].
- MIKKOLA, R. & KURLAND, C. 1992. Selection of laboratory wild-type phenotype from natural isolates of *Escherichia coli* in chemostats. *Mol Biol Evol,* 9**,** 394-402.
- MILES, A. A., MISRA, S. S. & IRWIN, J. O. 1938. The estimation of the bactericidal power of the blood. *J Hyg (Lond),* 38**,** 732-49.

- MILLER, C. P. & BOHNHOFF, M. 1950. The development of bacterial resistance to chemotherapeutic agents. *Annu Rev Microbiol,* 4**,** 210-22.
- MILLER, M. B., SKORUPSKI, K., LENZ, D. H., TAYLOR, R. K. & BASSLER, B. L. 2002. Parallel quorum sensing systems converge to regulate virulence in *Vibrio cholerae*. *Cell,* 110**,** 303-14.
- MINAGAWA, S., INAMI, H., KATO, T., SAWADA, S., YASUKI, T., MIYAIRI, S., HORIKAWA, M., OKUDA, J. & GOTOH, N. 2012. RND type efflux pump system MexAB-OprM of *Pseudomonas aeruginosa* selects bacterial languages, 3-oxo-acyl-homoserine lactones, for cell-to-cell communication. *BMC Microbiol,* 12**,** 70.
- MONSIEURS, P., DE KEERSMAECKER, S., NAVARRE, W. W., BADER, M. W., DE SMET, F., MCCLELLAND, M., FANG, F. C., DE MOOR, B., VANDERLEYDEN, J. & MARCHAL, K. 2005. Comparison of the PhoPQ regulon in *Escherichia coli* and *Salmonella typhimurium*. *J Mol Evol,* 60**,** 462-74.
- MUNITA, J. M. & ARIAS, C. A. 2016. Mechanisms of Antibiotic Resistance. *Microbiol Spectr,* 4.
- MURAKAMI, S., NAKASHIMA, R., YAMASHITA, E., MATSUMOTO, T. & YAMAGUCHI, A. 2006. Crystal structures of a multidrug transporter reveal a functionally rotating mechanism. *Nature,* 443**,** 173-9.
- NAKAMURA, H. 1965. Gene-Controlled Resistance to Acriflavine and Other Basic Dyes in *Escherichia coli*. *J Bacteriol,* 90**,** 8-14.
- NAKAMURA, H. 1968. Genetic determination of resistance to acriflavine, phenethyl alcohol, and sodium dodecyl sulfate in *Escherichia coli*. *J Bacteriol,* 96**,** 987-96.
- NAKAMURA, H. 1974. Plasmid-instability in *acrA* mutants of *Escherichia coli* K12. *J Gen Microbiol,* 84**,** 85-93.
- NAKAMURA, H., HACHIYA, N. & TOJO, T. 1978. Second acriflavine sensitivity mutation, *acrB*, in *Escherichia coli* K-12. *J Bacteriol,* 134**,** 1184-7.
- NIKAIDO, E., GIRAUD, E., BAUCHERON, S., YAMASAKI, S., WIEDEMANN, A., OKAMOTO, K., TAKAGI, T., YAMAGUCHI, A., CLOECKAERT, A. & NISHINO, K. 2012. Effects of indole on drug resistance and virulence of *Salmonella enterica* serovar Typhimurium revealed by genome-wide analyses. *Gut Pathog,* 4**,** 5-5.
- NIKAIDO, H. 2003. Molecular basis of bacterial outer membrane permeability revisited. *Microbiol Mol Biol Rev,* 67**,** 593-656.
- NIKAIDO, H. 2009. Multidrug resistance in bacteria. *Annu Rev Biochem,* 78**,** 119-46.
- NISHINO, K., HAYASHI-NISHINO, M. & YAMAGUCHI, A. 2009. H-NS modulates multidrug resistance of *Salmonella enterica* serovar Typhimurium by repressing multidrug efflux genes acrEF. *Antimicrob Agents Chemother,* 53**,** 3541-3.
- NISHINO, K., LATIFI, T. & GROISMAN, E. A. 2006. Virulence and drug resistance roles of multidrug efflux systems of *Salmonella enterica* serovar Typhimurium. *Mol Microbiol,* 59**,** 126-41.
- NISHINO, K. & YAMAGUCHI, A. 2001. Analysis of a complete library of putative drug transporter genes in *Escherichia coli*. *J Bacteriol,* 183**,** 5803-12.
- NTSOGO ENGUENE, V. Y., VERCHERE, A., PHAN, G., BROUTIN, I. & PICARD, M. 2015. Catch me if you can: a biotinylated proteoliposome affinity assay for the investigation of assembly of the MexA-MexB-OprM efflux pump from *Pseudomonas aeruginosa*. *Front Microbiol,* 6**,** 541.
- OLMSTED, J., 3RD & KEARNS, D. R. 1977. Mechanism of ethidium bromide fluorescence enhancement on binding to nucleic acids. *Biochemistry,* 16**,** 3647-54.
- PADILLA, E., LLOBET, E., DOMÉNECH-SÁNCHEZ, A., MARTÍNEZ-MARTÍNEZ, L., BENGOECHEA, J. A. & ALBERTÍ, S. 2010. *Klebsiella pneumoniae* AcrAB efflux pump contributes to antimicrobial resistance and virulence. *Antimicrob Agents Chemother,* 54**,** 177-183.
- PAWELEK, J. M., LOW, K. B. & BERMUDES, D. 1997. Tumor-targeted *Salmonella* as a novel anticancer vector. *Cancer Res,* 57**,** 4537-44.

- PEDROLLI, D., LANGER, S., HOBL, B., SCHWARZ, J., HASHIMOTO, M. & MACK, M. 2015. The *ribB* FMN riboswitch from *Escherichia coli* operates at the transcriptional and translational level and regulates riboflavin biosynthesis. *FEBS J,* 282**,** 3230-42.
- PEREZ, A., POZA, M., FERNANDEZ, A., FERNANDEZ MDEL, C., MALLO, S., MERINO, M., RUMBO-FEAL, S., CABRAL, M. P. & BOU, G. 2012. Involvement of the AcrAB-TolC efflux pump in the resistance, fitness, and virulence of *Enterobacter cloacae*. *Antimicrob Agents Chemother,* 56**,** 2084-90.
- PERRETT, C. A., KARAVOLOS, M. H., HUMPHREY, S., MASTROENI, P., MARTINEZ-ARGUDO, I., SPENCER, H., BULMER, D., WINZER, K., MCGHIE, E. & KORONAKIS, V. 2009. LuxS-based quorum sensing does not affect the ability of Salmonella enterica serovar Typhimurium to express the SPI-1 type 3 secretion system, induce membrane ruffles, or invade epithelial cells. *J Bacteriol,* 191**,** 7253-7259.
- PFAFFL, M. W. 2001. A new mathematical model for relative quantification in real-time RT-PCR. *Nucleic Acids Res,* 29**,** e45.
- PIDDOCK, L. J. 2006. Multidrug-resistance efflux pumps - not just for resistance. *Nat Rev Microbiol,* 4**,** 629-36.
- POPP, J., NOSTER, J., BUSCH, K., KEHL, A., ZUR HELLEN, G. & HENSEL, M. 2015. Role of host cell-derived amino acids in nutrition of intracellular *Salmonella enterica*. *Infect Immun,* 83**,** 4466-75.
- POS, K. M. 2009. Trinity revealed: Stoichiometric complex assembly of a bacterial multidrug efflux pump. *Proc Natl Acad Sci U S A,* 106**,** 6893-4.
- PUBLIC HEALTH ENGLAND 2017. *Salmonella* data 2006 to 2015. https://www.gov.uk/government/publications/salmonella-national-laboratory-data.
- RAETZ, C. R. & WHITFIELD, C. 2002. Lipopolysaccharide endotoxins. *Annu Rev Biochem,* 71**,** 635-700.
- RAVNSKJAER, K., FRIGERIO, F., BOERGESEN, M., NIELSEN, T., MAECHLER, P. & MANDRUP, S. 2010. PPARδ is a fatty acid sensor that enhances mitochondrial oxidation in insulin-secreting cells and protects against fatty acid-induced dysfunction. *J Lipid Res,* 51**,** 1370-9.
- RAYNER, M. H., SADLER, P. J. & SCAWEN, M. D. 1990. NMR studies of a bacterial cell culture medium (LB broth): cyclic nucleotides in yeast extracts. *FEMS Microbiol Lett,* 56**,** 217-21.
- REENS, A. L., CROOKS, A. L., SU, C. C., NAGY, T. A., REENS, D. L., PODOLL, J. D., EDWARDS, M. E., YU, E. W. & DETWEILER, C. S. 2018. A cell-based infection assay identifies efflux pump modulators that reduce bacterial intracellular load. *PLoS Pathog,* 14**,** e1007115.
- REICHARDT, C. & WELTON, T. 2010. Appendix A. Properties, Purification and Use of Organic Solvents. *Solvents and Solvent Effects in Organic Chemistry.* Fourth ed.: Wiley-VCH.
- RICCI, V., ATTAH, V., OVERTON, T., GRAINGER, D. C. & PIDDOCK, L. J. V. 2017. CsrA maximizes expression of the AcrAB multidrug resistance transporter. *Nucleic Acids Res,* 45**,** 12798-12807.
- RICCI, V., LOMAN, N., PALLEN, M., IVENS, A., FOOKES, M., LANGRIDGE, G. C., WAIN, J. & PIDDOCK, L. J. 2012. The TCA cycle is not required for selection or survival of multidrug-resistant Salmonella. *J Antimicrob Chemother,* 67**,** 589-599.
- RITCHIE, M. E., PHIPSON, B., WU, D., HU, Y., LAW, C. W., SHI, W. & SMYTH, G. K. 2015. *limma* powers differential expression analyses for RNA-sequencing and microarray studies. *Nucleic acids research,* 43**,** e47-e47.
- ROCHA, D. J., SANTOS, C. S. & PACHECO, L. G. 2015. Bacterial reference genes for gene expression studies by RT-qPCR: survey and analysis. *Antonie Van Leeuwenhoek,* 108**,** 685-93.
- RODRÍGUEZ-CARRIO, J., SALAZAR, N., MARGOLLES, A., GONZÁLEZ, S., GUEIMONDE, M., DE LOS REYES-GAVILÁN, C. G. & SUÁREZ, A. 2017. Free Fatty Acids

Profiles Are Related to Gut Microbiota Signatures and Short-Chain Fatty Acids. *Front Immunol,* 8**,** 823.
- ROMEO, T. 1998. Global regulation by the small RNA-binding protein CsrA and the non-coding RNA molecule CsrB. *Mol Microbiol,* 29**,** 1321-30.
- ROSNER, J. L. & MARTIN, R. G. 2009. An excretory function for the *Escherichia coli* outer membrane pore TolC: upregulation of *marA* and *soxS* transcription and Rob activity due to metabolites accumulated in *tolC* mutants. *J Bacteriol,* 191**,** 5283-92.
- RUHE, Z. C., LOW, D. A. & HAYES, C. S. 2013a. Bacterial contact-dependent growth inhibition (CDI). *Trends Microbiol,* 21**,** 230-7.
- RUHE, Z. C., WALLACE, A. B., LOW, D. A. & HAYES, C. S. 2013b. Receptor polymorphism restricts contact-dependent growth inhibition to members of the same species. *MBio,* 4.
- RUIZ, C. & LEVY, S. B. 2014. Regulation of *acrAB* expression by cellular metabolites in *Escherichia coli*. *J Antimicrob Chemother,* 69**,** 390-9.
- RYCROFT, J. A., GOLLAN, B., GRABE, G. J., HALL, A., CHEVERTON, A. M., LARROUY-MAUMUS, G., HARE, S. A. & HELAINE, S. 2018. Activity of acetyltransferase toxins involved in *Salmonella* persister formation during macrophage infection. *Nat Commun,* 9**,** 1993.
- SAIER, M. H., JR., TAM, R., REIZER, A. & REIZER, J. 1994. Two novel families of bacterial membrane proteins concerned with nodulation, cell division and transport. *Mol Microbiol,* 11**,** 841-7.
- SANA, T. G., FLAUGNATTI, N., LUGO, K. A., LAM, L. H., JACOBSON, A., BAYLOT, V., DURAND, E., JOURNET, L., CASCALES, E. & MONACK, D. M. 2016. *Salmonella* Typhimurium utilizes a T6SS-mediated antibacterial weapon to establish in the host gut. *Proc Natl Acad Sci U S A,* 113**,** E5044-51.
- SANDER, L. E., DAVIS, M. J., BOEKSCHOTEN, M. V., AMSEN, D., DASCHER, C. C., RYFFEL, B., SWANSON, J. A., MULLER, M. & BLANDER, J. M. 2011. Detection of prokaryotic mRNA signifies microbial viability and promotes immunity. *Nature,* 474**,** 385-9.
- SANTOS, R. L., RAFFATELLU, M., BEVINS, C. L., ADAMS, L. G., TUKEL, C., TSOLIS, R. M. & BAUMLER, A. J. 2009. Life in the inflamed intestine, *Salmonella* style. *Trends Microbiol,* 17**,** 498-506.
- SARGO, C. R., CAMPANI, G., SILVA, G. G., GIORDANO, R. C., DA SILVA, A. J., ZANGIROLAMI, T. C., CORREIA, D. M., FERREIRA, E. C. & ROCHA, I. 2015. *Salmonella typhimurium* and *Escherichia coli* dissimilarity: Closely related bacteria with distinct metabolic profiles. *Biotechnol Prog,* 31**,** 1217-25.
- SAURO, H. M. 2017. Control and regulation of pathways via negative feedback. *J R Soc Interface,* 14.
- SCHAUDER, S., SHOKAT, K., SURETTE, M. G. & BASSLER, B. L. 2001. The LuxS family of bacterial autoinducers: biosynthesis of a novel quorum-sensing signal molecule. *Mol Microbiol,* 41**,** 463-76.
- SCHMIDT, T. H., RAUNEST, M., FISCHER, N., REITH, D. & KANDT, C. 2016. Computer simulations suggest direct and stable tip to tip interaction between the outer membrane channel TolC and the isolated docking domain of the multidrug RND efflux transporter AcrB. *Biochim Biophys Acta,* 1858**,** 1419-26.
- SEEGER, M. A., DIEDERICHS, K., EICHER, T., BRANDSTATTER, L., SCHIEFNER, A., VERREY, F. & POS, K. M. 2008. The AcrB efflux pump: conformational cycling and peristalsis lead to multidrug resistance. *Curr Drug Targets,* 9**,** 729-49.
- SEEGER, M. A., SCHIEFNER, A., EICHER, T., VERREY, F., DIEDERICHS, K. & POS, K. M. 2006. Structural asymmetry of AcrB trimer suggests a peristaltic pump mechanism. *Science,* 313**,** 1295-8.
- SEEGER, M. A., VON BALLMOOS, C., VERREY, F. & POS, K. M. 2009. Crucial role of Asp408 in the proton translocation pathway of multidrug transporter AcrB: evidence from site-directed mutagenesis and carbodiimide labeling. *Biochemistry,* 48**,** 5801-12.

- SEO, J.-H., BAEK, S.-W., LEE, J. & PARK, J.-B. 2017. Engineering *Escherichia coli* BL21 genome to improve the heptanoic acid tolerance by using CRISPR-Cas9 system. *Biotechnol Bioproc E,* 22**,** 231-238.
- SILHAVY, T. J., KAHNE, D. & WALKER, S. 2010. The Bacterial Cell Envelope. *Cold Spring Harb Perspect Biol,* 2.
- SIMMONS, L. A., FOTI, J. J., COHEN, S. E. & WALKER, G. C. 2008. The SOS Regulatory Network. *Ecosal Plus,* 2008.
- SIRINAVIN, S., POKAWATTANA, L. & BANGTRAKULNONDH, A. 2004. Duration of nontyphoidal *Salmonella* carriage in asymptomatic adults. *Clin Infect Dis,* 38**,** 1644-5.
- SJUTS, H., VARGIU, A. V., KWASNY, S. M., NGUYEN, S. T., KIM, H. S., DING, X., ORNIK, A. R., RUGGERONE, P., BOWLIN, T. L., NIKAIDO, H., POS, K. M. & OPPERMAN, T. J. 2016. Molecular basis for inhibition of AcrB multidrug efflux pump by novel and powerful pyranopyridine derivatives. *Proc Natl Acad Sci U S A,* 113**,** 3509-14.
- SLAUCH, J. M., LEE, A. A., MAHAN, M. J. & MEKALANOS, J. J. 1996. Molecular characterization of the *oafA* locus responsible for acetylation of *Salmonella typhimurium* O-antigen: *oafA* is a member of a family of integral membrane trans-acylases. *J Bacteriol,* 178**,** 5904-9.
- SOLABIA GROUP BIOTECH. 2018. *Yeast Extract - A1202* [Online]. Solabia Group. Available: http://www.solabia.com/Produto_313,4/Peptones--Hydrolysates/Yeast-Extract.html [Accessed 11/08 2018].
- SONG, J., GAO, X. & GALAN, J. E. 2013. Structure and function of the *Salmonella* Typhi chimaeric A(2)B(5) typhoid toxin. *Nature,* 499**,** 350-4.
- SOPARKAR, K., KINANA, A. D., WEEKS, J. W., MORRISON, K. D., NIKAIDO, H. & MISRA, R. 2015. Reversal of the Drug Binding Pocket Defects of the AcrB Multidrug Efflux Pump Protein of Escherichia coli. *J Bacteriol,* 197**,** 3255-64.
- SPANIOL, V., BERNHARD, S. & AEBI, C. 2015. *Moraxella catarrhalis* AcrAB-OprM efflux pump contributes to antimicrobial resistance and is enhanced during cold shock response. *Antimicrob Agents Chemother,* 59**,** 1886-94.
- SPARACINO-WATKINS, C., STOLZ, J. F. & BASU, P. 2014. Nitrate and periplasmic nitrate reductases. *Chem Soc Rev,* 43**,** 676-706.
- STEEB, B., CLAUDI, B., BURTON, N. A., TIENZ, P., SCHMIDT, A., FARHAN, H., MAZE, A. & BUMANN, D. 2013. Parallel exploitation of diverse host nutrients enhances *Salmonella* virulence. *PLoS Pathog,* 9**,** e1003301.
- STEELE, J. H. 1963. Epidemiology of salmonellosis: Symposium. *Public Health Rep,* 78**,** 1065-88.
- STEWART, M. K. & COOKSON, B. T. 2012. Non-genetic diversity shapes infectious capacity and host resistance. *Trends Microbiol,* 20**,** 461-6.
- STOREK, K. M., AUERBACH, M. R., SHI, H., GARCIA, N. K., SUN, D., NICKERSON, N. N., VIJ, R., LIN, Z., CHIANG, N., SCHNEIDER, K., WECKSLER, A. T., SKIPPINGTON, E., NAKAMURA, G., SESHASAYEE, D., KOERBER, J. T., PAYANDEH, J., SMITH, P. A. & RUTHERFORD, S. T. 2018. Monoclonal antibody targeting the β-barrel assembly machine of *Escherichia coli* is bactericidal. *Proc Natl Acad Sci U S A,* 115**,** 3692-7.
- STROBER, W. 2001. Trypan blue exclusion test of cell viability. *Curr Protoc Immunol,* Appendix 3**,** Appendix 3B.
- SU, C. C., LI, M., GU, R., TAKATSUKA, Y., MCDERMOTT, G., NIKAIDO, H. & YU, E. W. 2006. Conformation of the AcrB multidrug efflux pump in mutants of the putative proton relay pathway. *J Bacteriol,* 188**,** 7290-6.
- SULAVIK, M. C., HOUSEWEART, C., CRAMER, C., JIWANI, N., MURGOLO, N., GREENE, J., DIDOMENICO, B., SHAW, K. J., MILLER, G. H., HARE, R. & SHIMER, G. 2001. Antibiotic susceptibility profiles of *Escherichia coli* strains lacking multidrug efflux pump genes. *Antimicrob Agents Chemother,* 45**,** 1126-36.
- SUN, J., DENG, Z. & YAN, A. 2014. Bacterial multidrug efflux pumps: mechanisms, physiology and pharmacological exploitations. *Biochem Biophys Res Commun,* 453**,** 254-67.

- SURETTE, M. G. & BASSLER, B. L. 1998. Quorum sensing in *Escherichia coli* and *Salmonella typhimurium*. *Proc Natl Acad Sci U S A,* 95**,** 7046-50.
- SUZUKI, K., WANG, X., WEILBACHER, T., PERNESTIG, A. K., MELEFORS, O., GEORGELLIS, D., BABITZKE, P. & ROMEO, T. 2002. Regulatory circuitry of the CsrA/CsrB and BarA/UvrY systems of *Escherichia coli*. *J Bacteriol,* 184**,** 5130-40.
- SYMMONS, M. F., BOKMA, E., KORONAKIS, E., HUGHES, C. & KORONAKIS, V. 2009. The assembled structure of a complete tripartite bacterial multidrug efflux pump. *Proc Natl Acad Sci U S A,* 106**,** 7173-8.
- TAGA, M. E., MILLER, S. T. & BASSLER, B. L. 2003. Lsr-mediated transport and processing of AI-2 in *Salmonella typhimurium*. *Mol Microbiol,* 50**,** 1411-27.
- TAKATSUKA, Y., CHEN, C. & NIKAIDO, H. 2010. Mechanism of recognition of compounds of diverse structures by the multidrug efflux pump AcrB of *Escherichia coli*. *Proc Natl Acad Sci U S A,* 107**,** 6559-65.
- TAKATSUKA, Y. & NIKAIDO, H. 2006. Threonine-978 in the Transmembrane Segment of the Multidrug Efflux Pump AcrB of *Escherichia coli* Is Crucial for Drug Transport as a Probable Component of the Proton Relay Network. *J Bacteriol,* 188**,** 7284-9.
- TAKATSUKA, Y. & NIKAIDO, H. 2009. Covalently linked trimer of the AcrB multidrug efflux pump provides support for the functional rotating mechanism. *J Bacteriol,* 191**,** 1729-37.
- TOGUCHI, A., SIANO, M., BURKART, M. & HARSHEY, R. M. 2000. Genetics of Swarming Motility in *Salmonella enterica* Serovar Typhimurium: Critical Role for Lipopolysaccharide. *J Bacteriol,* 182**,** 6308-21.
- TOUZE, T., ESWARAN, J., BOKMA, E., KORONAKIS, E., HUGHES, C. & KORONAKIS, V. 2004. Interactions underlying assembly of the *Escherichia coli* AcrAB-TolC multidrug efflux system. *Mol Microbiol,* 53**,** 697-706.
- TSUCHIDO, T. & TAKANO, M. 1988. Sensitization by heat treatment of *Escherichia coli* K-12 cells to hydrophobic antibacterial compounds. *Antimicrob Agents Chemother,* 32**,** 1680-3.
- UNIPROT CONSORTIUM 2014. UniProt: a hub for protein information. *Nucleic Acids Res,* 43**,** D204-D212.
- VARELA, C., RITTMANN, D., SINGH, A., KRUMBACH, K., BHATT, K., EGGELING, L., BESRA, G. S. & BHATT, A. 2012. MmpL genes are associated with mycolic acid metabolism in mycobacteria and corynebacteria. *Chem Biol,* 19**,** 498-506.
- VARGIU, A. V. & NIKAIDO, H. 2012. Multidrug binding properties of the AcrB efflux pump characterized by molecular dynamics simulations. *Proc Natl Acad Sci U S A,* 109**,** 20637-42.
- VÁZQUEZ-RIVERA, D., GONZÁLEZ, O., GUZMÁN-RODRÍGUEZ, J., DÍAZ-PÉREZ, A. L., OCHOA-ZARZOSA, A., LÓPEZ-BUCIO, J., MEZA-CARMEN, V. & CAMPOS-GARCÍA, J. 2015. Cytotoxicity of Cyclodipeptides from *Pseudomonas aeruginosa* PAO1 Leads to Apoptosis in Human Cancer Cell Lines. *Biomed Res Int,* 2015.
- VAZQUEZ-TORRES, A., JONES-CARSON, J., BAUMLER, A. J., FALKOW, S., VALDIVIA, R., BROWN, W., LE, M., BERGGREN, R., PARKS, W. T. & FANG, F. C. 1999. Extraintestinal dissemination of *Salmonella* by CD18-expressing phagocytes. *Nature,* 401**,** 804-8.
- VEAL, W. L. & SHAFER, W. M. 2003. Identification of a cell envelope protein (MtrF) involved in hydrophobic antimicrobial resistance in Neisseria gonorrhoeae. *J Antimicrob Chemother,* 51**,** 27-37.
- VERCHERE, A., DEZI, M., ADRIEN, V., BROUTIN, I. & PICARD, M. 2015. In vitro transport activity of the fully assembled MexAB-OprM efflux pump from Pseudomonas aeruginosa. *Nat Commun,* 6**,** 6890.
- WADDINGTON, C. S., DARTON, T. C. & POLLARD, A. J. 2014. The challenge of enteric fever. *J Infect,* 68 Suppl 1**,** S38-50.
- WALSH, A. G., MATEWISH, M. J., BURROWS, L. L., MONTEIRO, M. A., PERRY, M. B. & LAM, J. S. 2000. Lipopolysaccharide core phosphates are required for viability and intrinsic drug resistance in *Pseudomonas aeruginosa*. *Mol Microbiol,* 35**,** 718-27.

- WANG, Z., FAN, G., HRYC, C. F., BLAZA, J. N., SERYSHEVA, II, SCHMID, M. F., CHIU, W., LUISI, B. F. & DU, D. 2017. An allosteric transport mechanism for the AcrAB-TolC multidrug efflux pump. *eLife,* 6.
- WARNER, D. M. & LEVY, S. B. 2010. Different effects of transcriptional regulators MarA, SoxS and Rob on susceptibility of *Escherichia coli* to cationic antimicrobial peptides (CAMPs): Rob-dependent CAMP induction of the *marRAB* operon. *Microbiology,* 156**,** 570-8.
- WATTANAVANITCHAKORN, S., PRAKITCHAIWATTANA, C. & THAMYONGKIT, P. 2014. Rapid and simple colorimetric method for the quantification of AI-2 produced from *Salmonella* Typhimurium. *J Microbiol Methods,* 99**,** 15-21.
- WEATHERSPOON-GRIFFIN, N., YANG, D., KONG, W., HUA, Z. & SHI, Y. 2014. The CpxR/CpxA two-component regulatory system up-regulates the multidrug resistance cascade to facilitate *Escherichia coli* resistance to a model antimicrobial peptide. *J Biol Chem,* 289**,** 32571-82.
- WEBBER, M. A., BAILEY, A. M., BLAIR, J. M., MORGAN, E., STEVENS, M. P., HINTON, J. C., IVENS, A., WAIN, J. & PIDDOCK, L. J. 2009. The global consequence of disruption of the AcrAB-TolC efflux pump in *Salmonella enterica* includes reduced expression of SPI-1 and other attributes required to infect the host. *J Bacteriol,* 191**,** 4276-85.
- WEBBER, M. A., TALUKDER, A. & PIDDOCK, L. J. 2005. Contribution of mutation at amino acid 45 of AcrR to *acrB* expression and ciprofloxacin resistance in clinical and veterinary *Escherichia coli isolates*. *Antimicrob Agents Chemother,* 49**,** 4390-2.
- WEN, S. C., BEST, E. & NOURSE, C. 2017. Non-typhoidal *Salmonella* infections in children: Review of literature and recommendations for management. *J Paediatr Child Health,* 53**,** 936-941.
- WESTERMANN, A. J., FORSTNER, K. U., AMMAN, F., BARQUIST, L., CHAO, Y., SCHULTE, L. N., MULLER, L., REINHARDT, R., STADLER, P. F. & VOGEL, J. 2016. Dual RNA-seq unveils noncoding RNA functions in host-pathogen interactions. *Nature,* 529**,** 496-501.
- WESTON, N., SHARMA, P., RICCI, V. & PIDDOCK, L. J. V. 2017. Regulation of the AcrAB-TolC efflux pump in Enterobacteriaceae. *Res Microbiol*.
- WHITELEY, M., DIGGLE, S. P. & GREENBERG, E. P. 2017. Progress in and promise of bacterial quorum sensing research. *Nature,* 551**,** 313-320.
- WIEDEMANN, A., VIRLOGEUX-PAYANT, I., CHAUSSE, A. M., SCHIKORA, A. & VELGE, P. 2014. Interactions of *Salmonella* with animals and plants. *Front Microbiol,* 5**,** 791.
- WILLIAMSON, D. A., LANE, C. R., EASTON, M., VALCANIS, M., STRACHAN, J., VEITCH, M. G., KIRK, M. D. & HOWDEN, B. P. 2017. Increasing antimicrobial resistance in non-typhoidal *Salmonella* in Australia, 1979 - 2015. *Antimicrob Agents Chemother*.
- WINDER, C. L., DUNN, W. B., SCHULER, S., BROADHURST, D., JARVIS, R., STEPHENS, G. M. & GOODACRE, R. 2008. Global metabolic profiling of *Escherichia coli* cultures: an evaluation of methods for quenching and extraction of intracellular metabolites. *Anal Chem,* 80**,** 2939-48.
- WINTHER, K. S. & GERDES, K. 2011. Enteric virulence associated protein VapC inhibits translation by cleavage of initiator tRNA. *Proc Natl Acad Sci U S A,* 108**,** 7403-7.
- WOLSKA, K. I., GRUDNIAK, A. M., RUDNICKA, Z. & MARKOWSKA, K. 2016. Genetic control of bacterial biofilms. *J Appl Genet,* 57**,** 225-38.
- WORLD HEALTH ORGANIZATION. 2017a. *Antibiotic resistance* [Online]. http://www.who.int/mediacentre/factsheets/antibiotic-resistance/en/. [Accessed 20/12 2017].
- WORLD HEALTH ORGANIZATION. 2017b. *Global priority list of antibiotic-resistant bacteria to guide research, discovery, and development of new antibiotics* [Online]. http://www.who.int/medicines/publications/WHO-PPL-Short_Summary_25Feb-ET_NM_WHO.pdf. [Accessed 12/09 2018].
- WORLD HEALTH ORGANIZATION. 2017c. *Salmonella (non-typhoidal)* [Online]. http://www.who.int/mediacentre/factsheets/fs139/en/. [Accessed 20/12 2017].

- WRAY, C. & SOJKA, W. J. 1978. Experimental *Salmonella typhimurium* infection in calves. *Res Vet Sci,* 25**,** 139-43.
- WYATT, M. A., WANG, W., ROUX, C. M., BEASLEY, F. C., HEINRICHS, D. E., DUNMAN, P. M. & MAGARVEY, N. A. 2010. *Staphylococcus aureus* nonribosomal peptide secondary metabolites regulate virulence. *Science,* 329**,** 294-6.
- YAMAGUCHI, A., NAKASHIMA, R. & SAKURAI, K. 2015. Structural basis of RND-type multidrug exporters. *Front Microbiol,* 6**,** 327.
- YANG, S., LOPEZ, C. R. & ZECHIEDRICH, E. L. 2006. Quorum sensing and multidrug transporters in *Escherichia coli*. *Proc Natl Acad Sci U S A,* 103**,** 2386-91.
- YAO, X.-Q., KENZAKI, H., MURAKAMI, S. & TAKADA, S. 2010. Drug export and allosteric coupling in a multidrug transporter revealed by molecular simulations. *Nat Commun,* 1**,** 117.
- YIZHAK, K., GABAY, O., COHEN, H. & RUPPIN, E. 2013. Model-based identification of drug targets that revert disrupted metabolism and its application to ageing. *Nat Commun,* 4**,** 2632.
- YOSHIMURA, M., OSHIMA, T. & OGASAWARA, N. 2007. Involvement of the YneS/YgiH and PlsX proteins in phospholipid biosynthesis in both *Bacillus subtilis* and *Escherichia coli*. *BMC Microbiol,* 7**,** 69.
- YU, E. W., AIRES, J. R., MCDERMOTT, G. & NIKAIDO, H. 2005. A periplasmic drug-binding site of the AcrB multidrug efflux pump: a crystallographic and site-directed mutagenesis study. *J Bacteriol,* 187**,** 6804-15.
- ZAJC-SATLER, J. & GRAGAS, A. Z. 1977. Xylose lysine deoxycholate agar for the isolation of Salmonella and Shigella from clinical specimens. *Zentralbl Bakteriol Orig A,* 237**,** 196-200.
- ZAMPIERI, M., ENKE, T., CHUBUKOV, V., RICCI, V., PIDDOCK, L. & SAUER, U. 2017. Metabolic constraints on the evolution of antibiotic resistance. *Mol Syst Biol,* 13.
- ZGURSKAYA, H. I., KRISHNAMOORTHY, G., NTREH, A. & LU, S. 2011. Mechanism and Function of the Outer Membrane Channel TolC in Multidrug Resistance and Physiology of Enterobacteria. *Front Microbiol,* 2**,** 189.
- ZHANG, P., KHURSIGARA, C. M., HARTNELL, L. M. & SUBRAMANIAM, S. 2007. Direct visualization of *Escherichia coli* chemotaxis receptor arrays using cryo-electron microscopy. *Proc Natl Acad Sci U S A,* 104**,** 3777-3781.
- ZWAMA, M., YAMASAKI, S., NAKASHIMA, R., SAKURAI, K., NISHINO, K. & YAMAGUCHI, A. 2018. Multiple entry pathways within the efflux transporter AcrB contribute to multidrug recognition. *Nat Commun,* 9**,** 124.

APPENDIX I. Composition of buffers and media

A. 10X Tris-buffered saline (TBS)

Component	Brand	Cat. no.	Amount
Tris base (TRIZMA® base)	Sigma, USA	T1503	24.2g
NaCl	Sigma, USA	S6191	80g

Add 800mL of distilled water and adjust pH to 7.6 with HCl. Make up to 1L.
To prepare 1X TBS, add 100mL of 10X solution to 900mL of distilled water.
To make washing buffer, add 0.1% of Tween® 20 (Sigma, USA, cat. no. P9416).

B. 1M potassium phosphate buffer (PPB)

For making 100mL of 1M PPB:

Component	Brand	Cat. no.	Amount
1M K_2HPO_4	Sigma, USA	P5504	61.5mL
1M KH_2PO_4	BDH Chemicals, UK	296084J	38.5mL

To make 1L of 0.1M PPB, add 100mL of 1M PPB to 900mL of distilled water. Filter-sterilise in a 0.22μm pore, Stericup® Filtration Unit before use.

C. SOC medium

Component	Brand	Cat. no.	Amount
Tryptone	Oxoid, UK	LP0042	20g
Yeast extract	Oxoid, UK	LP0021	5g
NaCl 5M	Sigma, USA	S6191	2mL
KCl 1M	Sigma, USA	P5405	2.5mL
$MgCl_2$ 1M	Sigma, USA	M4880	10mL
$MgSO_4$ 1M	Sigma, USA	M7506-M	10mL
Glucose 1M	Sigma, USA	G8270	20mL

Add distilled water to make 1L of medium. Autoclave medium to sterilise.

D. MgMES minimal medium

Component	Brand	Cat. no.	Concentration
2-[N-morpholino] ethane-sulphonic acid (MES)*	Sigma, USA	M3058	170mM
KCl	Sigma, USA	P5405	5mM
$(NH_4)_2SO_4$	Sigma, USA	A3920	7.5mM
KH_2PO_4	Sigma, USA	P8541	0.5mM
K_2SO_4	Sigma, USA	P5655	1mM
$MgCl_2$	Sigma, USA	M4880	10mM
Glycerol	Sigma, USA	G5516	38mM
Casamino acids	BD Biosciences, USA	223050	0.1%

(*) adjust to a pH of 5.0 with HCl or KOH if needed.

Mix all the components of the medium and filter-sterilise. Store prepared media at 4°C.

E. Autoinducer bioassay (AB) medium

The base for this medium is prepared as follows:

Component	Brand	Cat. no.	Amount
NaCl	Sigma, USA	S6191	17.5g
$MgSO_4$	Sigma, USA	M7506-M	12.3g
Casamino acids	BD Biosciences, USA	223050	2.0g

Add ingredients to 970mL of distilled water and adjust pH to 7.5 with KOH. Add more distilled water to make 1L of base medium. Autoclave at 121°C and add the rest of the components to the medium:

Component	Brand	Cat. no.	Amount
1M Potassium Phosphate buffer pH 7.0*	*	*	10mL
0.1M L-arginine	Sigma, USA	A5006-100G	10mL
Glycerol	Sigma, USA	G5516-100L	10mL

(*) see Appendix I, section A.

Filter-sterilise all components and add to room temperature, autoclaved base medium.

F. MOPS minimal medium

This medium was purchased from TEKNOVA (USA, cat. no. M2106)

Component	Concentration
MOPS (MW 209.3)	40mM
Tricine (MW 179.2)	4.0mM
Iron sulfate stock	0.01mM
Ammonium chloride	9.5mM
Potassium sulfate	0.276mM
Calcium chloride	0.0005mM
Magnesium chloride	0.525mM
Sodium chloride	50mM
Ammonium molybdate	$3x10^{-9}$ M
Boric acid	$4x10^{-7}$ M
Cobalt chloride	$3x10^{-8}$ M
Cupric sulfate	10^{-8} M
Manganese chloride	$8x10^{-8}$ M
Zinc sulfate	10^{-8} M
Potassium phosphate dibasic	1.32mM
Glucose	0.2%

Make up to 1L in distilled water and filter-sterilise. Store at 4°C for up to one month.

G. EZ rich defined medium

This medium was purchased from TEKNOVA (USA, cat. no. 2105). The medium uses MOPS minimal medium as a base and is supplemented with:

Component	Concentration
Potassium hydroxide	1.5mM
Adenine	0.2mM
Cytosine	0.2mM
Uracil	0.2mM
Guanine	0.2mM
L-Alanine	0.8mM
L-Arginine HCl	5.2mM
L-Asparagine	0.4mM
L-Aspartic acid, potassium salt	0.4mM
L-Glutamic acid, potassium salt	0.6mM
L-Glutamine	0.6mM
L-Glycine	0.8mM
L-Histidine HCl H_2O	0.2mM
L-Isoleucine	0.4mM

L-Proline	0.4mM
L-Serine	10mM
L-Threonine	0.4mM
L-Tryptophan	0.1mM
L-Valine	0.6mM
L-Leucine	0.8mM
L-Lysine	0.4mM
L-Methionine	0.2mM
L-Phenylalinine	0.4mM
L-Cysteine HCl	0.1mM
L-Tyrosine	0.2mM
Thiamine	0.01mM
Calcium pantothenate	0.01mM
Para-Amino benzoic acid	0.01mM
Para-Hydroxy benzoic acid	0.01mM
Di hydroxy benzoic acid	0.01mM

Make up to 1L in distilled water and filter-sterilise. Store at 4°C for up to one month.

APPENDIX II. Preparation of antibiotics for agar-dilution MICs (20mL agar plates)

Stock concentration (μg/mL)	Volume of stock to use (μL)	Final concentration of antibiotic in 20mL of agar (μg/mL)
10,000	4,096	2,048
	2,048	1,024
	1,024	512
	512	256
	256	128
	128	64
	64	32
1,000	320	16
	160	8
	80	4
	40	2
	20	1
100	100	0.5
	50	0.25
	25	0.125
	13	0.063
10	60	0.031
	30	0.015
	15	0.008

APPENDIX III. Phenotype of *S.* Typhimurium and *E. coli* on XLD agar.

Figure A. Growth of *S.* Typhimurium SL1344, *E. coli* K-12 MG1655 and their respective *acrB* mutants on XLD agar.

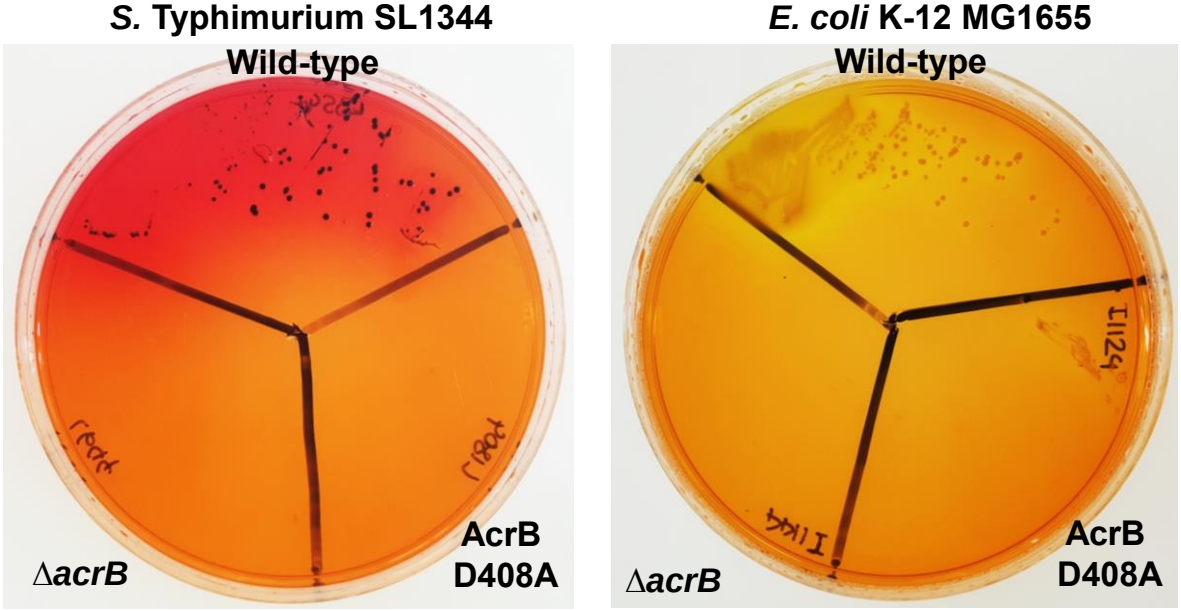

Deoxycholate, a bile salt and a substrate of AcrB, inhibits growth of *acrB* mutants on XLD agar. Mutants can sometimes grow on the first streak. *S.* Typhimurium forms translucent colonies with black centres and a bright pink halo around the colonies. *E. coli* forms opaque, pale yellow colonies with a yellow halo.

APPENDIX IV. Comparison of RND transporters in *E. coli* K-12MG1655 and *S.* Typhimurium SL1344.

Gene encoding RND transporter	Protein code	
	***Salmonella* Typhimurium SL1344**	***Escherichia coli* MG1655**
mdsB (Not annotated)	SL1344_0346	-
secD	SL1344_0402	b0408
acrB	SL1344_0468	b0462
cusA	-	b0575
ydhJ	SL1344_1374	b1644
mdtB (*yegN*)	SL1344_2104	b2075
mdtC (*yegO*)	SL1344_2105	b2076
acrD	SL1344_2444	b2470
aaeA (*yhcQ*)	SL1344_3337	b3241
acrF	SL1344_3364	b3266
mdtF (*yhiV*)	-	b3514

Information obtained from TransportDB Elbourne *et al.* (2017), available at: http://www.membranetransport.org/transportDB2/index.html

APPENDIX V. Measuring bacterial replication by flow cytometry

Figure A. Assessment of changes in replication dynamics of *S.* Typhimurium SL1344 using pDiGi.

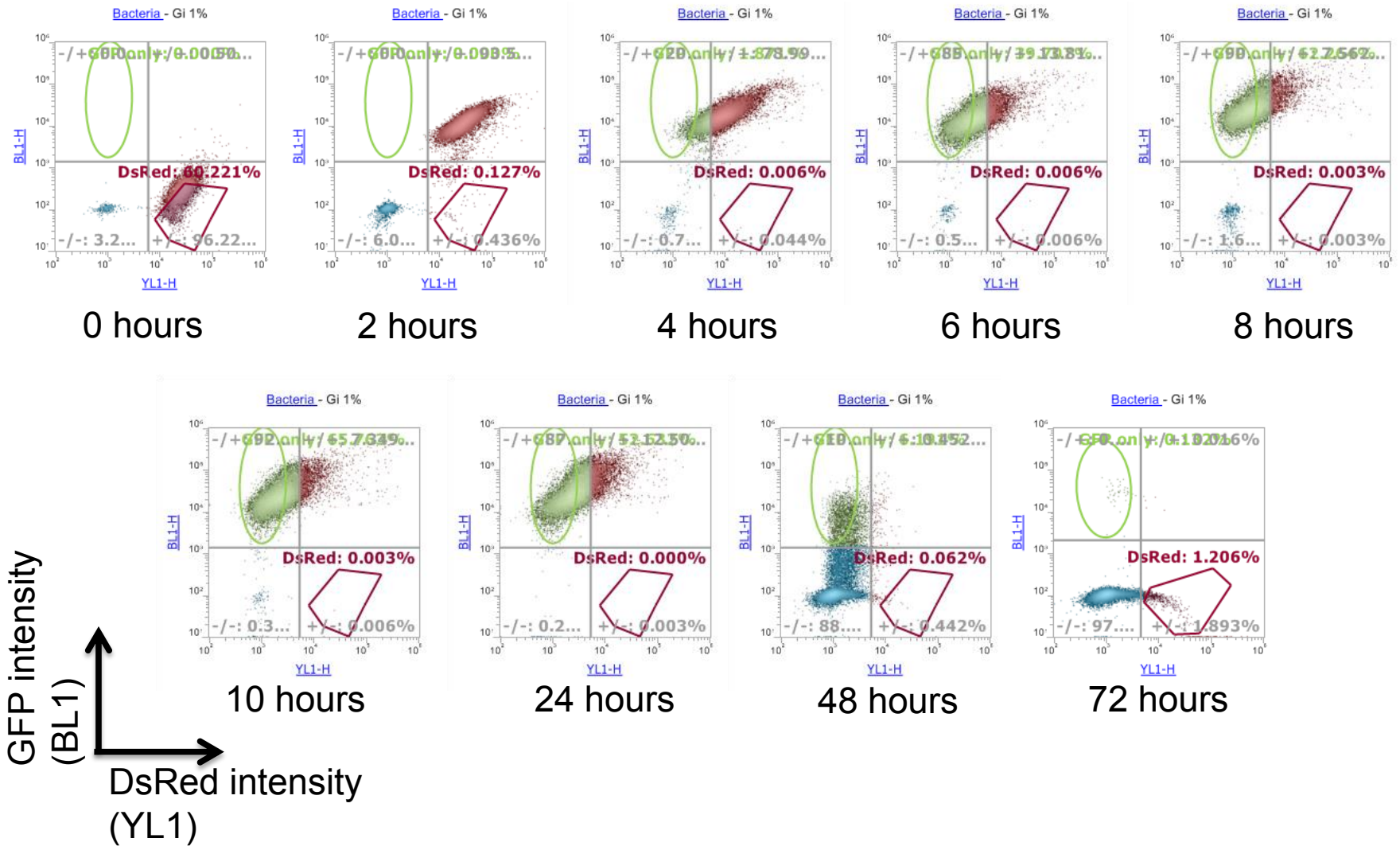

A representative plot of each time point from six experiments is shown. Similar to Figure A(6), plots of BL1 against YL1 are shown. Fresh, prewarmed, MgMES with glucose and IPTG was inoculated with an overnight culture of SL1344 or its AcrB D408A mutant expressing only DsRed. At 2 hours post-inoculation, almost all bacteria from the initial inoculum expressed GFP causing the population to shift towards a higher fluorescence intensity on the BL1 channel. Eventually, as *S.* Typhimurium replicates, the DsRed signal was completely diluted giving rise to a population that only expressed GFP. As the population entered death phase and IPTG was depleted from the media, the GFP fluorescence signal decreased until a non-fluorescent population was observed.

Figure B. Controls and gating strategy.

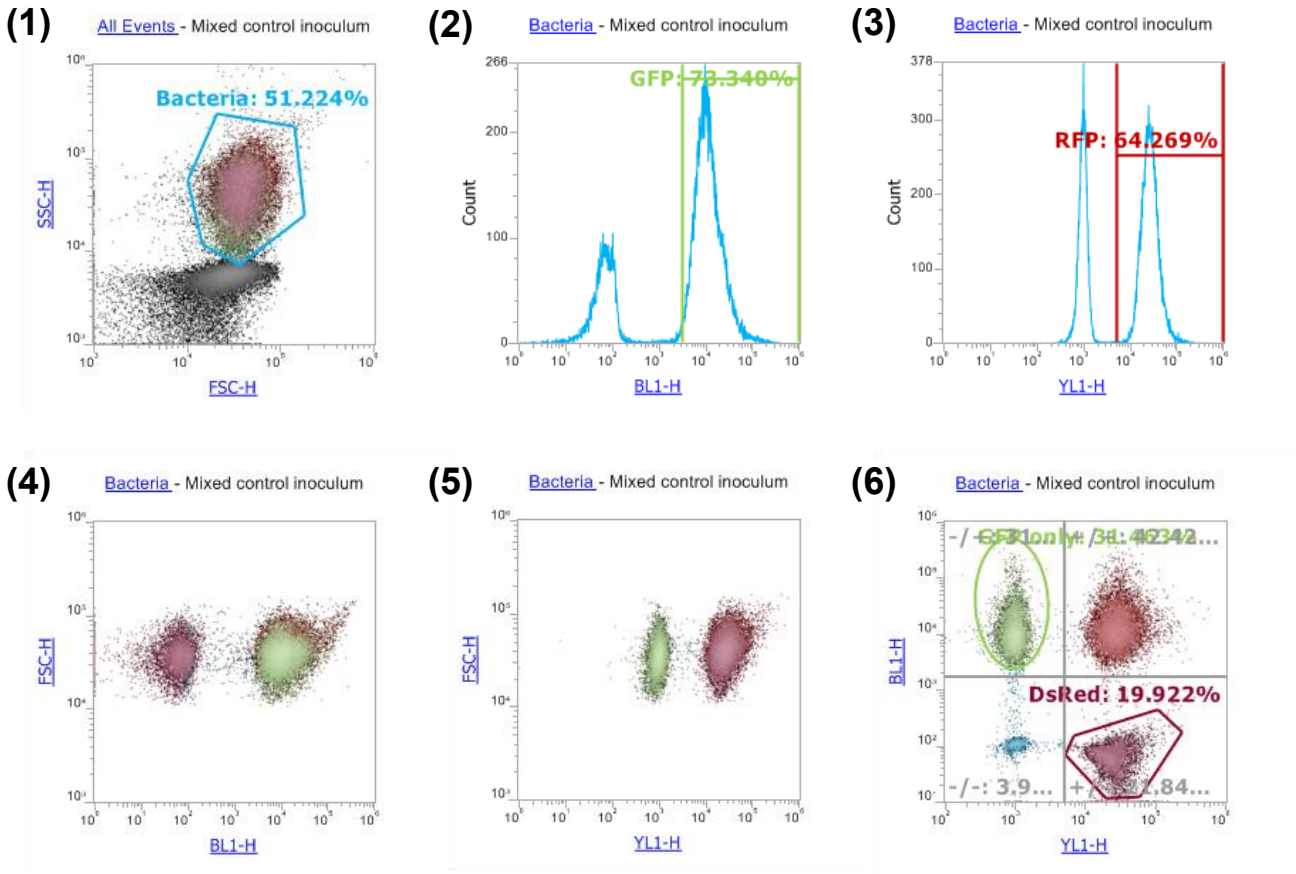

much bacteria as possible without including debris. Only counts within the "Bacteria" gate were considered for the experiments. (2) GFP fluorescence was identified in the BL1 channel and DsRed fluorescence was identified in the YL1 channel (3). To determine if bacteria expressing GFP could be separated from those expressing DsRed, a mixture of bacteria expressing solely GFP or DsRed and bacteria expressing both fluorescent proteins was used. Results for the BL1 channel are plotted in (4), where two distinct groups were observed: a population with high GFP fluorescence on the right of the plot and a second population with low GFP fluorescence on the left. The same trend is observed in channel YL1 (5), where a population with high DsRed fluorescence intensity is observed on the right of the plot and a low fluorescence intensity population, on the left. When BL1 was plotted against YL1 (6), four populations were observed: a GFP-only population on the top left quadrant, a population that expressed both fluorescent proteins on the top right qudrant, a small population of non-fluorescent bacteria on the bottom left quadrant and, on the bottom right quadrant, a population that only expressed DsRed. Bacteria expressing only GFP or DsRed were gated. Controls and gates were adjusted for each individual experiment.

APPENDIX VI. Data previously generated in the Piddock group (unpublished data)

Figure A. Toxicity of 3X SL1344 ExM on INT-407 cells.

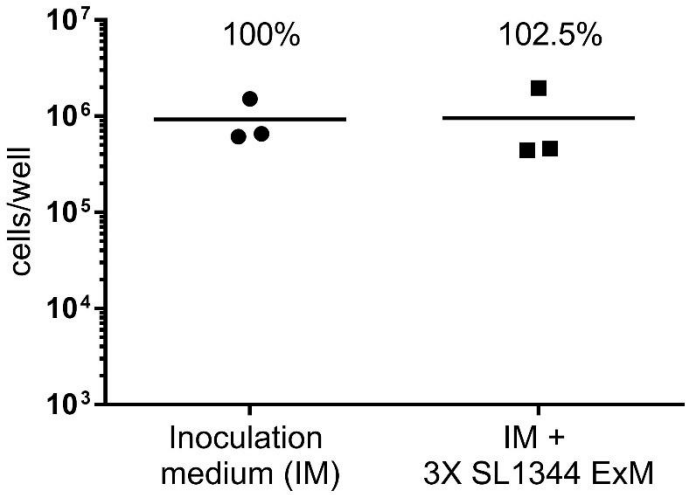

INT-407 cells were exposed to inoculation medium (IM) or IM with 3X SL1344 ExM for 2 hours. Cells were recovered and viable counting was carried out by trypan blue exclusion. A total of three replicates was carried out. Each dot represent a replicate and the line in the middle of the dots indicate the average. Data generated between Dr. Jessica Blair and Dr. Michelle Buckner.

Figure B. Effect of SL1344 ExM concentration on restoration of virulence of a Δ*acrB* mutant.

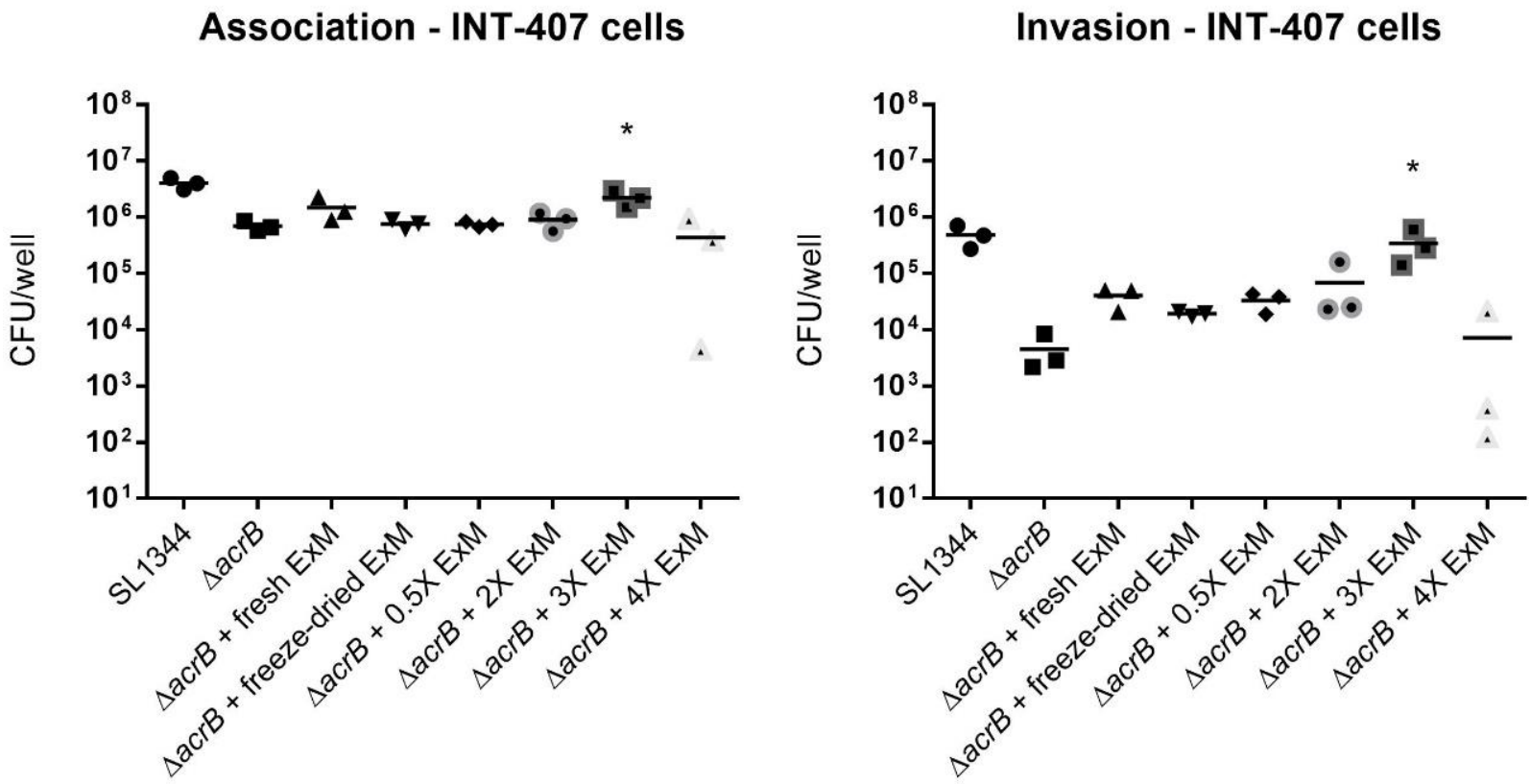

Association (2 hours) and invasion (4 hours) of a *S.* Typhimurium SL1344 Δ*acrB* mutant exposed to different concentrations of SL1344 ExM is shown. Each dot indicates an experimental replicate, the average of all replicates is shown by a black line. An (*) in this case indicates that there is no significant difference between the condition and SL1344 ($P>0.05$) as tested by a Student's t-test with Welch's corrections. All other conditions were significantly different from SL1344 ($P<0.05$). Data generated by Dr. Jessica Blair.

Figure C. Restoration kinetics of 3X SL1344 ExM.

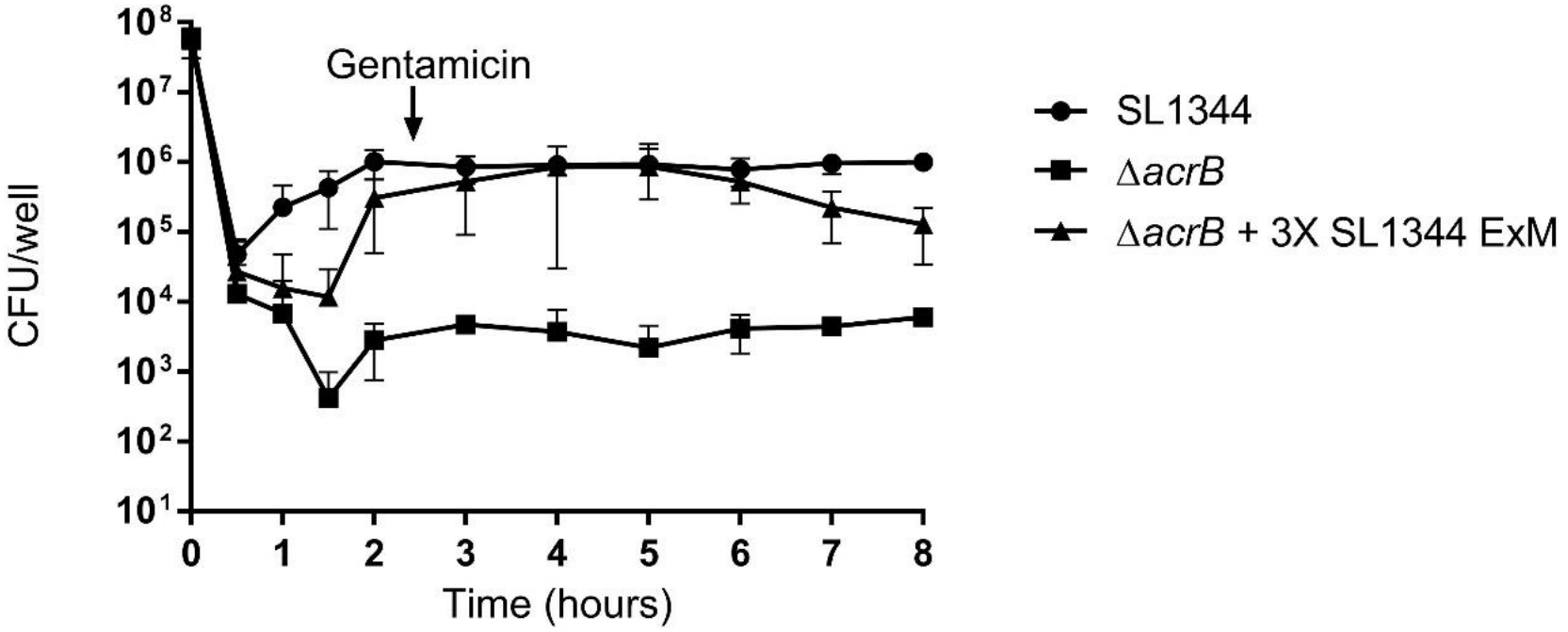

The average of a three replicates with its standard deviation is shown. *S.* Typhimurium SL1344 and its Δ*acrB* mutant with and without exposure to 3X SL1344 ExM were added to confluent INT-407 cells. Bacteria were recovered every 30 minutes for the first 2 hours. Gentamicin was added at 2.5 hours post-infection and amount of intracellular *S.* Typhimurium was measured every hour for 8 hours. Data generated by Dr. Michelle Buckner.

Figure D. Virulence-restoration effect of SL1344 ExM pretreated with proteinase K (1), heat-treated (2) and filtered through a 5kDa filter (3).

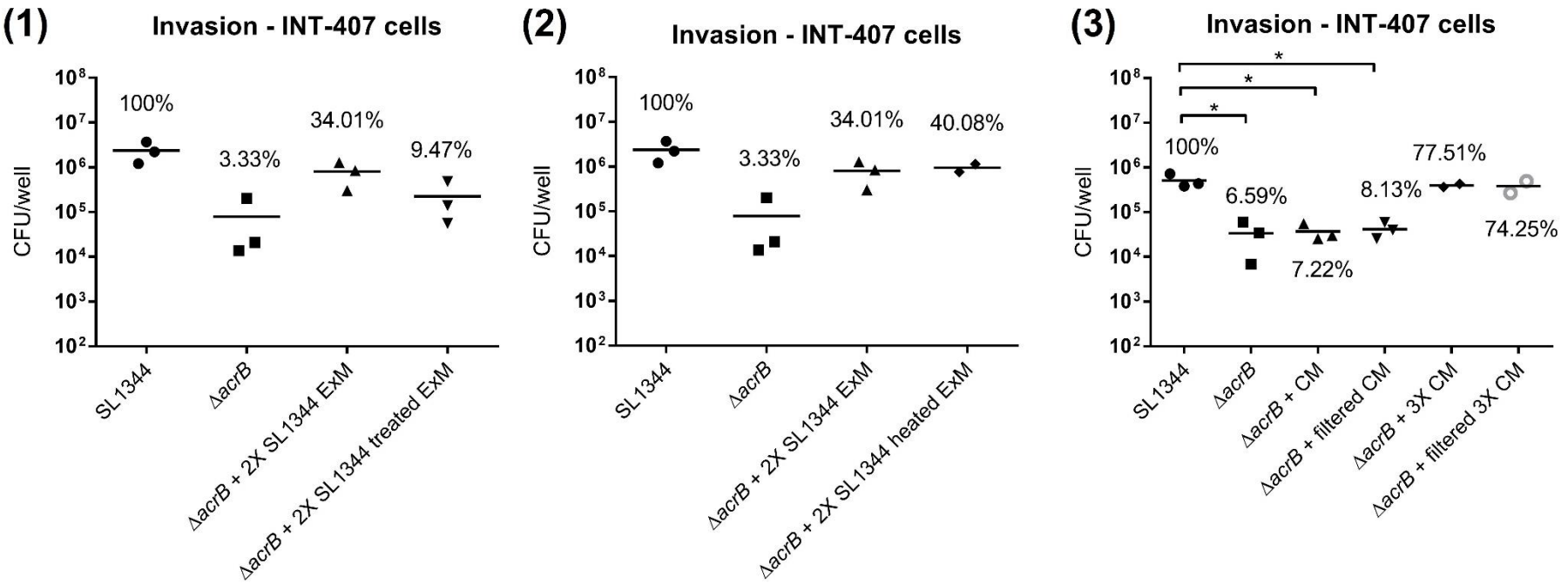

The virulence-restoration effect of SL1344 ExM after proteinase K treatment (1), 70°C heat treatment for an hour (2) or filtered through a 5kDa filter (3) was tested on a SL1344 Δ*acrB* mutant during infection of INT-407 cells. Invasion was measured at 4 hours post-infection (2 hours after addition of 100μg/mL of gentamicin). Each dot represents an experimental replicate. The line in the middle of the dots shows the average of all experiments. An (*) indicates a statistically significant difference between two groups ($P<0.05$) as determined by a Student's t-test with Welch's corrections. Data generated between Dr. Jessica Blair, Dr. Michelle Buckner and Amelia Lawler.

Figure E. Effect of 3X SL1344 ExM on restoration of virulence of a Δ*acrB* mutant in J774A.1 murine macrophages.

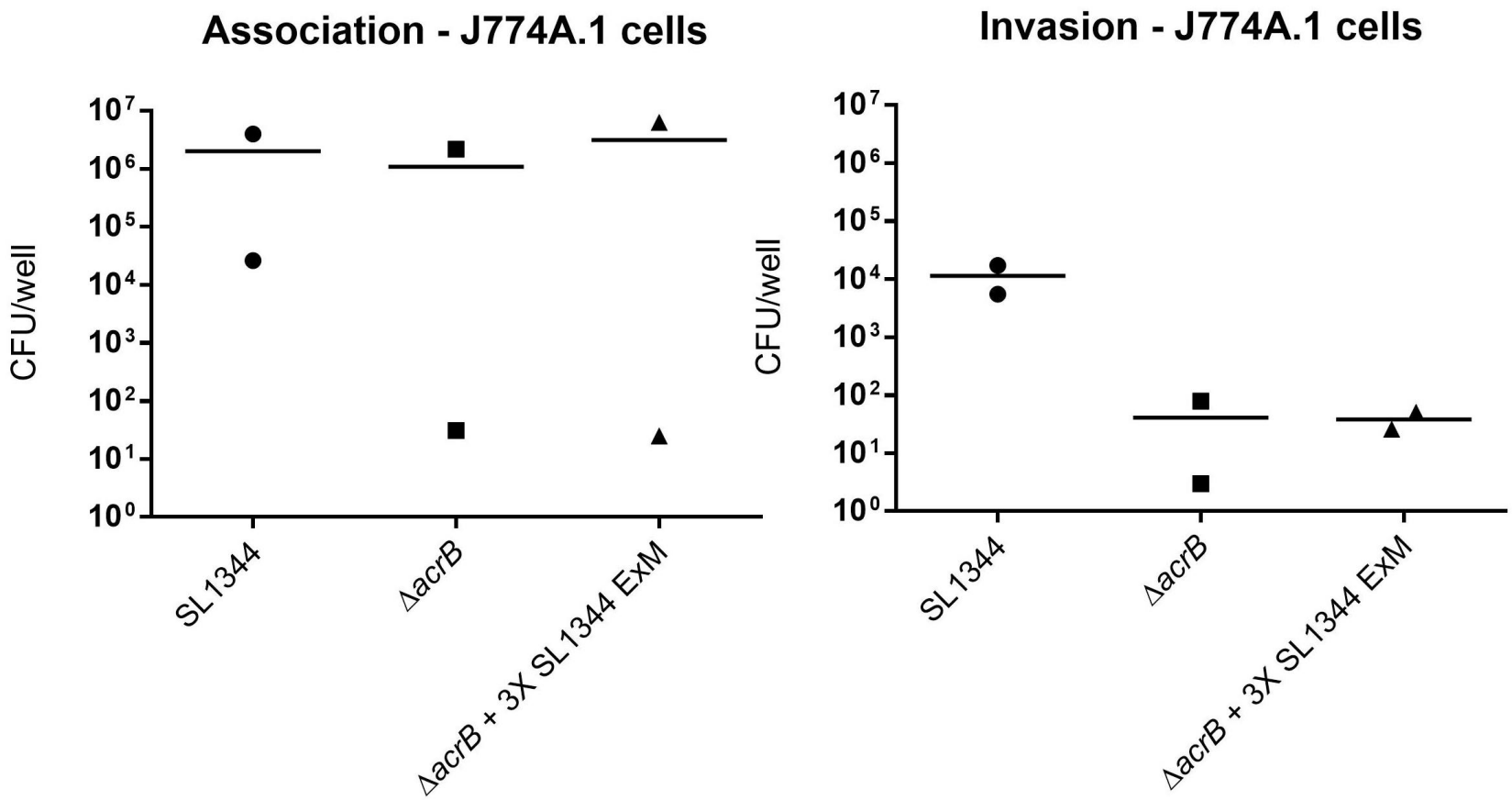

Association (2 hours) and invasion (4 hours) of a *S.* Typhimurium SL1344 Δ*acrB* mutant exposed to different concentrations of SL1344 ExM is shown. Each dot indicates an experimental replicate, the average of all replicates is shown by a black line.

Figure F. Effect of hexane, chloroform and methanol extracts of SL1344 ExM on restoration of virulence of an Δ*acrB* mutant.

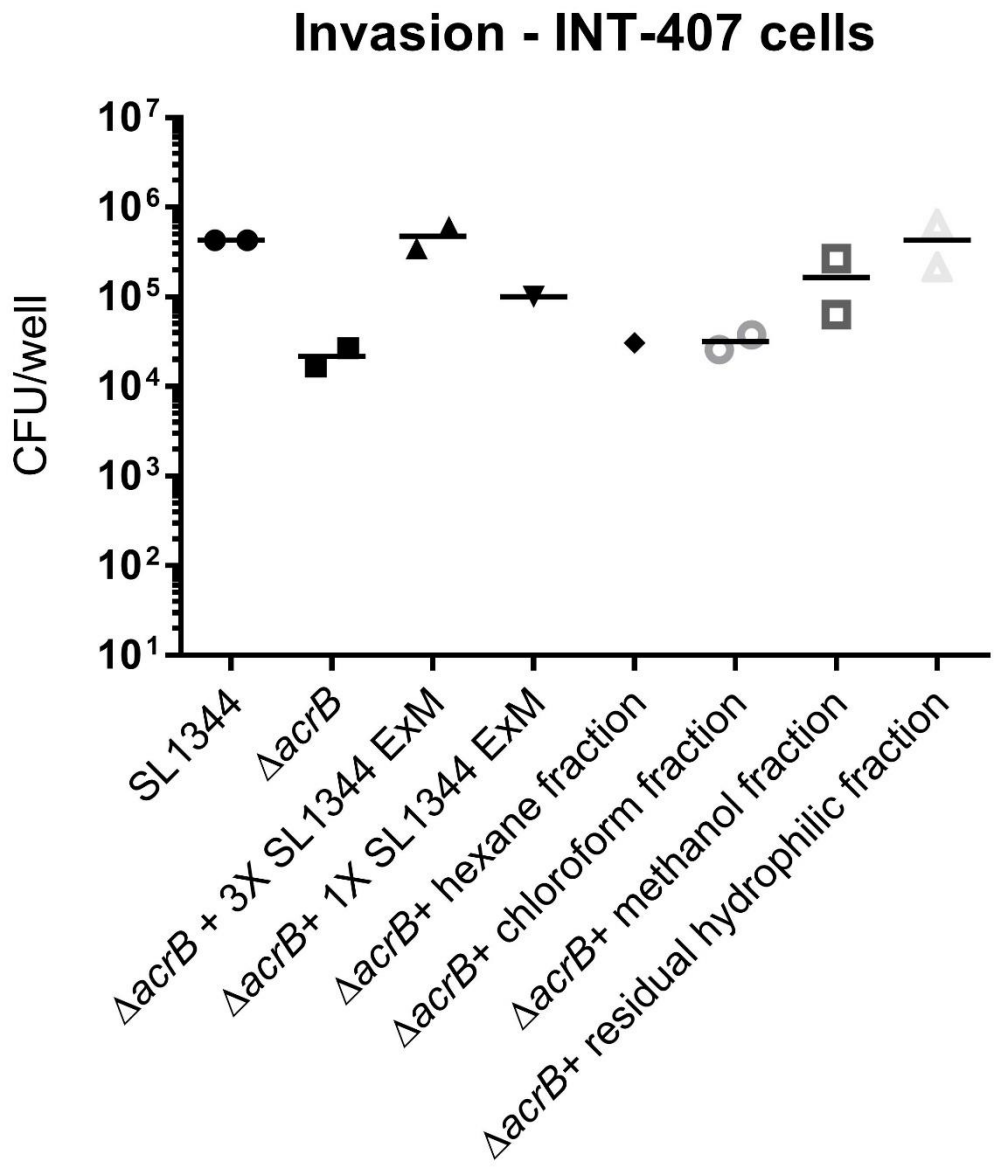

SL1344 ExM was sent to Professor Simon Gibbons (University College London, United Kingdom) for chemical fractionation. Each point indicates a biological replica. A line indicates the mean of all replicates. Data was generated by Dr. Jessica Blair.

APPENDIX VII. ExM analyses

Table A. Metabolites identified by LC-MS in the ExM of *S.* Typhimurium SL1344 compared against its *acrB* mutants.

Assay	Mass	Retention time	Metabolite putative ID	Fold-change			*P*-value	
				SL1344/ Δ*acrB*	SL1344/ AcrB D408A	SL1344/ LB	SL1344/ Δ*acrB*	SL1344/ AcrB D408A
Acyl-carnitines and degradation products								
HILIC NEG	258.0732521	445.171953	Propenoylcarnitine	3.28	2.86	1.90	1.12E-07	2.17E-03
HILIC NEG	292.1402204	450.196686	Hydroxybutyrylcarnitine	2.97	3.29	2.82	3.10E-04	3.98E-04
HILIC POS	348.1187439	323.811762	3-Methylglutarylcarnitine	3.85	3.28	2.94	3.35E-11	2.11E-12
HILIC POS	360.1340239	193.58106	Octenoylcarnitine	7.81	5.29	2.74	3.77E-08	4.59E-08
RP NEG	492.2128004	73.086789	Tetradecadiencarnitine	2.15	2.34	3.21	1.85E-05	2.98E-06
HILIC POS	302.1328395	51.455442	Hexenoylcarnitine;Serinyl-Lysine	3.38	3.45	1.70	1.65E-03	1.72E-03
HILIC POS	161.0784486	34.2596097	Trimethylaminoacetone	2.99	2.4	26.79	4.80E-08	1.21E-07
Acyl glycines								
HILIC POS	160.0965484	34.42764	Methylbutyrylglycine;Dehydrocarnitine; Isovalerylglycine;Acetylvaline; Valerylglycine	3.06	2.43	54.73	5.10E-08	1.26E-07
HILIC POS	232.0917143	39.5436798	Heptanoylglycine	3.6	3.3	3.23	3.30E-07	5.54E-07
Aromatic compounds and degradation products								
HILIC NEG	247.0700526	245.524542	Amino-3-(4-aminophenyl)propanoic acid;Tyrosinamide	3.05	2.42	2.78	1.82E-07	1.60E-07
HILIC NEG	251.0307655	176.03811	Benzylsuccinate;D-4-O-Methyl-myo-inositol	5.77	4.86	3.09	1.50E-06	2.96E-06
HILIC POS	259.0646416	371.76504	Dimethyl-ethylazulene	2.62	2.42	4.45	3.12E-09	1.73E-09
HILIC POS	391.101902	234.24063	3-O-Feruloylquinic acid	2.77	2.28	1.72	2.51E-08	1.49E-07

RP NEG	546.1365963	233.23221	Gravacridonediol glucoside	2.25	2.26	2.37	1.29E-10	1.92E-11
Biosynthesis of arginine								
HILIC POS	213.0634243	41.0311578	Glycyl-Valine;N-Acetylornithine	3.28	3.35	2.05	5.83E-07	2.62E-06
HILIC POS	260.0634923	369.169008	Argininic acid;Citrulline	3.91	3.19	0.50	3.89E-11	3.80E-08
Fatty acids and alcohols								
HILIC NEG	161.0005871	85.781022	Heptadiynediol;heptatrienoic acid	2.38	2.25	5.61	1.50E-06	1.12E-04
HILIC NEG	217.0727432	301.574838	Isoputreanine;N(6)-Methyllysine;octenedioic acid;Isopropenylpentanedioic acid	4.24	2.58	2.29	6.07E-05	6.75E-05
HILIC NEG	229.0616456	51.7106058	Tridecatrienediynol;methyl-oxooctanoic acid	23.78	15.83	3.96	1.15E-06	1.69E-06
HILIC NEG	235.0338791	147.26013	Methoxy-heptanethiol;Diaminosalicylic acid	1.98	2.6	4.26	1.13E-04	3.07E-05
HILIC POS	253.0580762	51.780753	Pyridoxamine;Octadienol	37.54	23.26	4.45	9.15E-08	1.26E-07
HILIC POS	507.2806926	169.481586	6-bromo-heptacosadienoic acid	3.24	2.39	2.80	5.42E-10	5.45E-10
HILIC POS	521.2962622	144.010764	6-bromo-octacosadienoic acid	2.04	2.2	1.92	3.93E-08	1.30E-08
RP NEG	507.2822155	309.295308	Hydroxynervonic acid	2.24	2.08	2.91	8.89E-09	1.14E-07
Peptides								
HILIC NEG	305.0738808	315.828969	Threoninyl-Proline	2.54	2.44	2.42	1.03E-05	1.14E-05
HILIC NEG	325.0886776	84.647397	Methionyl-Methionine	3.95	4.71	19.14	1.32E-06	2.19E-07
HILIC NEG	354.0871382	294.628926	Hydroxyprolyl-Tryptophan	2.09	2.29	2.06	4.00E-05	2.02E-05
HILIC POS	320.1252048	295.83276	Aspartyl-Tryptophan	4.07	3.17	2.34	4.70E-09	1.43E-08
HILIC POS	334.0780381	98.399466	Gamma-Glutamyl Glutamine	3.25	2.72	1.21	5.60E-08	6.88E-08
RP NEG	292.140411	76.03977	Arginyl-Proline	2.28	2.3	4.81	5.20E-10	1.50E-08
HILIC POS	302.1328395	51.455442	Hexenoylcarnitine;Serinyl-Lysine	3.38	3.45	1.70	1.65E-03	1.72E-03
HILIC POS	213.0634243	41.0311578	Glycyl-Valine;N-Acetylornithine	3.28	3.35	2.05	5.83E-07	2.62E-06
RP NEG	355.1363503	76.50735	Arginyl-Asparagine	2.38	2.21	6.66	8.25E-07	3.94E-06
HILIC NEG	355.1358	447.598872	Aspidospermidine;Arginyl-Asparagine	3.38	3.75	NDM	1.47E-03	1.36E-03

Phospholipids								
HILIC POS	484.1509792	172.426503	PC[12:4]	2.89	2.75	2.62	6.86E-07	9.00E-07
HILIC POS	505.3462169	242.807634	PC(O-16:0/0:0);PC(O-8:0/O-8:0)	2.34	2.14	2.35	4.56E-10	7.74E-09
RP NEG	633.2252304	269.93487	Lactodifucotetraose;PI[14:0]	2.27	2.06	2.43	9.80E-13	2.35E-12
RP NEG	762.3537815	245.209146	PS[29:2]	2.25	2.1	2.05	8.29E-09	1.90E-08
Sulfur metabolism								
HILIC NEG	199.9691243	420.953532	Cysteine-S-sulfate	2.11	2.13	0.61	4.51E-04	4.31E-04
HILIC POS	286.0895123	85.915542	Homocystine;Tetrahydrobiopterin	4.6	4.96	NDM	9.63E-10	1.35E-11
Tryptophan degradation products								
HILIC NEG	188.0350862	174.963696	Kynurenic acid	4.65	4.21	2.83	4.26E-06	7.92E-06
HILIC NEG	235.0722472	372.204723	6-Hydroxy-1H-indole-3-acetamide	2.79	2.44	2.67	5.27E-06	1.49E-05
HILIC POS	175.0865767	242.65002	Indole-3-acetamide	2.19	2.11	2.46	3.11E-08	7.83E-08
HILIC POS	197.0683914	242.60394	1H-Indole-3-acetamide	2.93	2.64	1.91	3.97E-08	7.79E-10
HILIC POS	203.0800026	390.270726	5-Hydroxykynurenamine	2.35	2.08	0.95	5.89E-09	3.68E-08
RP NEG	235.0724742	131.446632	N'-Formylkynurenine	3.12	2.58	4.08	1.27E-09	3.50E-08
RP POS	146.0602319	283.353345	1H-Indole-3-carboxaldehyde	2.57	2.43	1.98	2.40E-09	3.58E-09
RP POS	161.0801954	126.978843	Indoleacetaldehyde	5.88	3.01	12.10	4.30E-16	1.77E-11
HILIC POS	174.054775	109.519884	Quinaldic acid	9.57	7.42	3.38	3.52E-09	5.03E-09
RP NEG	164.0360592	271.164708	Pyridoxolactone;Formylanthranilic acid	3.88	3.25	1.90	2.10E-08	5.06E-08
HILIC POS	193.0969989	126.6984	Cotinine N-oxide;Hydroxycotinine;5-Hydroxyindoleacetaldehyde	3.8	3.39	2.15	4.80E-13	7.25E-11
Others								
HILIC NEG	268.9476175	232.581666	2-Phosphoglyceric acid;3-Phosphoglyceric acid	2.39	2	1.68	1.76E-06	2.70E-05
HILIC NEG	487.2197627	73.242414	sn-3-O-(geranylgeranyl)glycerol 1-phosphate	2.34	2.65	2.57	1.15E-06	1.88E-06

HILIC POS	193.101794	248.888241	Epithiomenthane;Menthenethiol; Thiogeraniol	2.46	2.1	1.58	3.72E-09	3.47E-09
HILIC POS	219.0875002	302.118372	Isoputreanine;Methyllysine	4.91	2.84	2.74	5.83E-08	2.39E-07
HILIC POS	364.1448486	91.062954	N-(2-Hydroxyisobutyl)-2,4,8,10,12-tetradecapentaenamide	3.65	4.25	2.51	1.91E-08	9.65E-09
HILIC POS	376.1288616	123.763314	Pantetheine 4'-phosphate	3.57	4.67	1.35	1.01E-05	5.68E-06
HILIC NEG	355.1358	447.598872	Aspidospermidine;Arginyl-Asparagine	3.38	3.75	NDM	1.47E-03	1.36E-03
HILIC NEG	251.0307655	176.03811	Benzylsuccinate;D-4-O-Methyl-myo-inositol	5.77	4.86	3.09	1.50E-06	2.96E-06

NDM indicates that the metabolite was not found in LB. Where more than one putative ID was assigned, the metabolite that belongs to the indicated class is shown in red.

Table B. Metabolites identified by LC-MS in the ExM of *E. coli* MG1655 and its AcrB D408A mutant.

Assay	Mass	Retention time	Metabolite putative ID	Classification of metabolite	Count MG1655	Count AcrB D408A
RP POS	256.13516	226.55747	4'-Methoxychalcone; cinnamyl benzoate	Aromatic compounds	9	1
HILIC POS	233.09535	95.23062	1,3-Diphenyl-1-propanone;1,3-Diphenyl-2-propanone;Lactaroviolin;p-methoxystilbene;(±)-Myrtenyl acetate;2-Acetoxy-p-mentha-1,8-diene;4-Hydroxypropofol;8-Ocimenyl acetate;Cucujolide IV;Cucujolide IX;Ethyl - Decatrienoate;Hexylresorcinol;Lyratol acetate;Neolyratyl acetate;p-Mentha-1,8-dien-10-yl acetate;p-Mentha-1(7),5-dien-2-ol acetate;Perillyl acetate	Aromatic compounds; fatty acids/alcohols	9	0
HILIC POS	332.23706	513.08261	Hexanal hexyl isoamyl acetal;iso-1,2-heptadecanediol	Fatty acids/alcohols	8	2
HILIC POS	345.24947	474.61652	11-methyl-1,2-heptadecanediol; anteiso-1,2-octadecanediol; hexanal dihexyl acetal; iso-1,2-octadecanediol	Fatty acids/alcohols	8	2
HILIC NEG	264.0003	54.021506	4-Amino-2-methylenebutanoic acid; D-Proline; L-Proline	Fatty acids/alcohols; others (amino acids)	10	2
HILIC POS	278.13485	500.03193	L-alpha-glutamyl-L-hydroxyproline; Lauric acid(d3); n-decanohydroxamic acid	Others (glutamine metabolism); fatty acids/alcohols	8	1
HILIC NEG	285.10269	467.31401	O-Phospho-4-hydroxy-L-threonine; 2-Amino-3-phosphonopropionic acid; D-Aspartic acid;Iminodiacetic acid; L-Aspartic acid	Others (vitamin B_6 metabolism, amino acids); fatty acids/alcohols	9	1
HILIC POS	166.04973	501.83192	4-Pyridoxolactone; 5-Pyridoxolactone; Formylanthranilic acid	Others (vitamin B_6 metabolism);	9	0

				tryptophan metabolism		
RP POS	148.07997	50.331454	Alanylglycine;D-Glutamine;L-Glutamine; 1,5-Octadien-3-one; 2,3-Dimethyl-2-cyclohexen-1-one; 2,4-Octadienal; 6-Methyl-3,5-heptadien-2-one; trans, trans-3,5-Octadien-2-one; 1-Hexanol;2-Ethoxybutane;3-Hexanol	Peptides; others (amino acids); fatty acids	8	1
HILIC NEG	879.36187	38.673168	Evasterioside E;(3b,16a,25-Acetoxy-3,16,20,22-tetrahydroxy-5-cucurbiten-11-one 3-glucoside;PG[29:0];Ginsenoside Rh6;Monensin A;PA[34:6];20,23-cis-Bullatalicinone;27-Hydroxybullatacin;9-Hydroxyasimicinone;Annoglaucin;Annonin XIV;Bullatetrocin;Glabracin A;Mucocin;Muricatin C;Purpurenin;Rollidecin A;Rollimusin;Rollitacin	Phospholipids	9	2
HILIC POS	918.49757	468.22191	26-Desglucoavenacoside A;Fistuloside B;PS[42:8];PS[40:7];PC[37:6];PE(P-18:0/22:6(14OH));PE[40:6]	Phospholipids	9	2
HILIC POS	181.09687	45.868967	(4-Ethoxyphenyl)urea;5-Hydroxykynurenamine;L-2-Amino-3-(4-aminophenyl)propanoic acid;Tyrosinamide;Butadiene-styrene rubber;(±)-2,6-Dimethyl-6-hepten-1-ol;1-Nonen-3-ol;2-Methyl-4-heptanone;2-Methyloctanal;2-Nonanone;2-Nonen-1-ol;3-Nonanone;3-Nonen-1-ol;6-Nonen-1-ol;Amyl propyl ketone;Dihydroisophorol;3-Methyldioxyindole;4-(3-Pyridyl)-3-butenoic acid;(-)-3-Thujene;(-)-4(10)-Thujene;(-)-7,7-Dimethyl-2-methylenebicyclo[2.2.1]heptane;(-)-alpha-Carene;(-)-alpha-Pinene;(-)-alpha-thujene;(-)-beta-Pinene;(+)-4(10)-Thujene;(+)-a-Pinene;(+)-alpha-Carene;(+)-alpha-	Tryptophan metabolism; fatty acids/alcohols; others (hidrocarbons); aromatic compounds	8	1

			Pinene;(+)-alpha-thujene;(+)-Comphene;3,7-Dimethyl-1,3,7-octatriene;5-Isosylveterpinolene;alpha-Carene;alpha-ocimene;alpha-Phellandrene;alpha-Terpinene;Artemisiatriene;beta-Phellandrene;beta-Pinene;cis-Ocimene;D-Limonene;Polylimonene;Sylveterpinolene;Terpinolene;trans-Ocimen			
HILIC POS	255.1125	40.326308	Melatonin;Valyl-Valine;(+)-Anhydro-beta-rotunol;1,2-Dehydro-alpha-cyperone;1,3,5,11-Bisabolatetraen-10-one;10-Hydroxy-isolaurene;2-Hexyl-3-phenyl-2-propenal;5beta-1,3,7(11)-Eudesmatrien-8-one;ar-Turmerone;Furanodiene;Furodysin;Furodysinin;iso-Debromo-laurinterol;Mutisianthol;(-)-Bornyl acetate;(+)-Bornyl acetate;4-Hydroxy-6-dodecenoic acid lactone;Aleprylic acid;Allyl 3-cyclohexylpropionate;alpha-Campholene acetate;alpha-Terpineol acetate;Artemisia alcohol acetate;beta-Terpinyl acetate;Buibuilactone;cis-3-Hexenyl cis-3-hexenoate;cis-3-Hexenyl trans-2-hexenoate;cis-3-Hexenyl trans-4-hexenoate;cis,cis-dodeca-3,6-dienoic acid;Cucujolide II;Cucujolide VIII;Dihydro-5-(2-octenyl)-2(3H)-furanone;Dihydrocarveol acetate;Ethyl-decadienoic acid;gamma-Terpinyl acetate;Geranyl acetate;Isopulegol acetate;Linalyl acetate;Methyl 2-undecynoate;p-Menth-1-en-9-ol acetate;S-Cucujolide II;Santolina acetate;1,2,3,4-Tetrahydro-2-methyl-b-carboline;2,2,3,4-Tetramethylpentane;2,3,4-Trimethylhexane;3,4-Dimethylheptane;Isononane;Nonane	Tryptophan metabolism; peptides; fatty acids/alcohols; others (hidrocarbons)	8	1

HILIC NEG	400.25675	492.67748	Urothion	Unknown (not a bacterial metabolite)	8	2
HILIC POS	446.27694	522.05348	PGF2alpha-EA(d4)	Unknown (not a bacterial metabolite)	8	2
HILIC POS	579.35296	502.74869	Ginsenoyne A linoleate	Unknown (not a bacterial metabolite)	8	1
HILIC POS	86.751898	511.03425	Unidentified	Unknown	9	1
HILIC POS	347.69734	501.79559	Unidentified	Unknown	10	2
HILIC POS	389.2954	560.43464	Isotope	Unknown	8	0

An arbitratry count was assigned to each feature (putative metabolite) to identify those metabolites that were in a high concentration in the wild-type strain and low in the mutant strain. Where more than one putative ID was assigned, the metabolites that belong to the designated classes are shown in red.